ERDC/CRREL TR-08-16

US Army Corps
of Engineers®
Engineer Research and
Development Center

Opportune Landing Site Program

Suitability Measurement and Analysis for Fort Bliss Naval Air Facility OLS

Rosa T. Affleck, Charles C. Ryerson,
Lynette A. Barna, and Keran J. Claffey

September 2008



Cold Regions Research
and Engineering Laboratory

Approved for public release; distribution is unlimited.

COVER: Ground truth measurements at Fort Bliss Opportune Landing Site.

ERDC/CRREL TR-08-16
September 2008

Suitability Measurement and Analysis for Fort Bliss Naval Air Facility OLS

Rosa T. Affleck, Charles C. Ryerson, Lynette A. Barna, and Keran J. Claffey

US Army Engineer Research and Development Center
Cold Regions Research and Engineering Laboratory
72 Lyme Road
Hanover, New Hampshire 03755-1290

Approved for public release; distribution is unlimited.

Prepared for US Air Force Research Laboratory Air Vehicles Directorate

Under Customer Order Number GWRVA00472412

Abstract: The Army relies on agility and speed, including the ability to conduct air transport operations where no runways exist, and where engineers cannot be pre-positioned. One of the most difficult problems is locating large, smooth, flat, and obstruction-free areas that are sufficiently firm to support at least one aircraft operation, and preferably many. The Opportune Landing Site (OLS) program demonstrated the use of remote sensing technology and state-of-the-ground forecast tools to accelerate the process of selecting OLSs. To evaluate the quality of the selected OLSs, ground truth measurements were conducted at Fort Bliss in New Mexico. Before conducting field measurements, several sites identified by OLS software were visually inspected to evaluate and select a suitable OLS for field testing. Evaluation procedures were based on Air Force Civil Engineer Support Agency (AFCESA) recommendations for evaluating airfield pavements. Soil strength and moisture measurements were made at several locations along the OLS, and overall quality was evaluated during three seasons. Assessment software was able to predict an OLS adequate for landing a C-130, but not capable for a C-17. This was true for all three field assessments at Fort Bliss.

DISCLAIMER: The contents of this report are not to be used for advertising, publication, or promotional purposes. Citation of trade names does not constitute an official endorsement or approval of the use of such commercial products. All product names and trademarks cited are the property of their respective owners. The findings of this report are not to be construed as an official Department of the Army position unless so designated by other authorized documents.

DESTROY THIS REPORT WHEN NO LONGER NEEDED. DO NOT RETURN IT TO THE ORIGINATOR.

Contents

Figures and Tables v

Nomenclature viii

Preface x

1 Introduction 1

2 Background 4

2.1 OLS Software 5
2.2 Site Selection 6

3 Runway Assessment Site (RAS) Analysis Criteria 12

3.1 Introduction 12
3.1.1 Geometric Evaluation of RAS (Smooth, Level, Flat, Obstruction) 12
3.1.2 Field Test Overview 17
3.1.3 Aircraft Operational Requirements 18
3.1.4 Compile Data 18
3.1.5 Estimates of Allowable Gross Loads/Allowable Passes 19
3.1.6 Surface Characteristics 20
3.2 Overall OLS Rating 26

4 Runway Assessment Site (RAS) Evaluation 28

4.1 Evaluation Procedure, Measurement Technique, and Methodology 28
4.1.1 Weather Monitoring Instrumentation 28
4.2 Non-Seasonal Impacts 28
4.2.1 Surface Profile (Topography, Flatness, and Smoothness Measurements) 28
4.2.2 Soil Characterization (Surface Soil Color, Soil Type, Density, Organics) 29
4.3 Seasonal Impacts 33
4.3.1 Surface Conditions 33
4.3.2 Vegetation 34
4.3.3 Soil Moisture 34
4.3.4 Soil Strength 36
4.4 Site Description of Systematic Imagery Runway Assessment Site (SI-RAS) 40
4.4.1 Location 40
4.4.2 Field Visits and Sampling at Systematic Imagery Runway Assessment Site (SI-RAS) 40
4.4.3 Weather Information 42
4.4.4 Topography 45

5 Analysis and Results on Systematic Imagery Runway Assessment Site (SI-RAS) 49

5.1 Soil Characterization 49
5.1.1 Soil Type and Texture Profile 49

5.1.2 Munsell *58*
5.1.3 Density *58*
5.1.4 Organics *60*
5.1.5 Natural Resources Conservation Service (NRCS) Soils Information *60*
5.1.6 Soil Characterization Discussion and Summary *61*
5.2 Seasonal Impacts 63
5.2.1 Surface Conditions *63*
5.2.2 Soil Moisture *82*
5.2.3 Soil Strength *88*

6 Conditions at Precision Corrected Imagery Runway Assessment Site (PCI-RAS) 109
6.1 Surface Condition at Precision Corrected Imagery Imagery RAS (PCI-RAS) 109
6.2 Soil Condition at Precision Corrected Imagery Imagery RAS (PCI-RAS) 115

7 OLS Software Seasonal Analysis 116
7.1 OLS Software Seasonal Consistency 117
7.2 OLS Software Seasonal Accuracy 119

8 Overall OLS Rating 126

9 Conclusion and Recommendations 130

References 132

Appendix A1: CEERD-RS Trip Report, 17 March 2005 135

Appendix A2: CEERD Trip Report, Rosa Affleck and Lynette Barna, 6 June 2005 155

Appendix B: Description of Terrain Features at Fort Bliss 181

Appendix C: Calibration of Soil Moisture Measuring Instruments 213

Appendix D: Compilation of DCP Profiles from OLS at Fort Bliss 237

Report Documentation Page 349

Figures and Tables

Figures

Figure 1. General location of and driving to the OLS at Fort Bliss 7
Figure 2. OLSs evaluated during the reconnaissance visit in June 2005 8
Figure 3. Close-up of area 6 with 270- x 4000-ft OLS, which were visited in June 2005 9
Figure 4. OLS software analysis using 200- by 3000-ft runway dimensions found many more runways 10
Figure 5. Fort Bliss OLS showing the RAS and fenced area where the weather station was located 11
Figure 6. Procedures for determining the suitability of an OLS, modified from practice established by AFCESA in ETL 2002-19 13
Figure 7. Sampling grid used to evaluate the RAS at Fort Bliss OLS 14
Figure 8. Soil strength on semi-prepared airfield for the C-17 and the C-130H 21
Figure 9. Sample evaluation of surface strength on semi-prepared airfield for C-17 operations 22
Figure 10. Picture taken from ETL 97-9 for severity rating of localized loose aggregate 26
Figure 11. Air temperature data taken before, during, and after each IOP at Fort Bliss RAS weather observation station 42
Figure 12. Precipitation data from the observation station near the RAS 44
Figure 13. Wind speed observed from the weather station near the RAS averaged every five minutes for the entire monitored time 45
Figure 14. Contour map of the entire Fort Bliss RAS 46
Figure 15. Elevation profile along RAS center line 46
Figure 16. Typical lateral profiles of the RAS at Fort Bliss, slope slightly to the south 48
Figure 17. Soil on the surface before digging the soil pits 49
Figure 18. Soil profile at Station 1+70 51
Figure 19. Soil profile at station 5+50 2S 53
Figure 20. Soil profile at 8+50 CL 54
Figure 21. Soil pit at 10+10 CL down to 0.38 m 55
Figure 22. Soil profile at 2+50 10S, caliche layer 56
Figure 23. Soil pit at the weather station area 57
Figure 24. Soil density profiles taken using a nuclear density gage at five locations on Fort Bliss RAS 59
Figure 25. Symbolic representation of surface features from the visual survey along the RAS in sections 64
Figure 26. Surface features such as mounds, animal burrows, and caliche pieces observed on the RAS at Fort Blis 68
Figure 27. Typical vegetation types on Fort Bliss RAS and the surrounding area 70
Figure 28. Vegetation cover calculated from the photos taken at six locations 75

Figure 29. Variation in vegetation greenness during three IOPs at Fort Bliss OLS 79
Figure 30. Moisture profiles taken from Dynamax ML2 probes during IOP #1 84
Figure 31. Average soil moisture profiles from the Dynamax ML2 probes taken during IOP #1 85
Figure 32. Profiles of soil moisture contents in % volumetric from the Dynamax ML2 taken in October 2005, as shown in contours 85
Figure 33. Precipitation observed from the weather station installed near the RAS 86
Figure 34. Surface soil moisture for three field visits at Fort Bliss RAS 86
Figure 35. Soil moisture profiles using the gravimetric method from samples taken in July 2005 (IOP #1) and in October (IOP #2) 87
Figure 36. Gravimetric moisture contents converted to percent volume along with soil moisture profiles measured using the Dynamax ML2 88
Figure 37. Soil strength contours measured using the Dynamic Cone Penetrometer for all IOPs on Fort Bliss RAS 90
Figure 38. CBR profiles at sampling location 2+10 2N taken during the three IOPs at Fort Bliss 95
Figure 39. CBR profiles at sampling location 8+50 CL taken during the three IOPs at Fort Bliss with higher soil strength at 300-mm depth 96
Figure 40. Profile of the topmost part of the caliche layer detected from the DCP data 97
Figure 41. Soil strength for top 0.3 m measured from the light Clegg impact hammer expressed in CBR for the Fort Bliss RAS 99
Figure 42. Calculated force indicating the surface soil strength throughout the RAS during the three IOPs 100
Figure 43. Selected CBR profiles showing layers with weak soil strength taken during IOP #1 at the Fort Bliss RAS 102
Figure 44. Selected CBR profiles showing layers with weak soil strength taken during IOP #2 at the Fort Bliss RAS 103
Figure 45. Selected CBR profiles showing layers with weak soil strength taken during IOP #3 at the Fort Bliss RAS 104
Figure 46. CBR values at each depth range at RAS 106
Figure 47. Shift on RAS location due to georectification level of imagery 110
Figure 48. Area west, north, northwest, and northeast of the SI-RAS location 111
Figure 49. Number of OLSs located seasonally, by software version 118
Figure 50. Fort Bliss RAS Precision georeferenced in white outline, and Systematic georeferenced in green outline 121
Figure 51. 18 May 2003 Landsat USGS Systematic georeferenced image with Version 7 of the OLS software 121
Figure 52. 2 July 2005 Landsat USGS Precision georeferenced image with Version 7 OLS software 122
Figure 53. 22 October 2005 Landsat USGS Precision georeferenced image with Version 7 OLS software 123
Figure 54. 16 April 2006 Landsat USGS Precision georeferenced image with Version 7 OLS software 123
Figure 55. 18 May 2003 Landsat USGS Systematic georeferenced image with Version 10 of the OLS software 124

Figure 56. 16 April 2006 Landsat USGS Precision georeferenced image with Version 10 of the OLS software locating the red OLSs 125

Tables

Table 1. Runways for landing zone guidelines developed for C-130 and C-17 15
Table 2. OLS geometric evaluation rating used on the RAS 17
Table 3. Surface characteristics used to evaluate the OLS 25
Table 4. An estimation for the overall rating of the entire OLS for C-17 and C-130 27
Table 5. Intensive operational periods (IOPs) at Fort Bliss 36
Table 6. Soil field measurements taken at Fort Bliss OLS during each IOP 41
Table 7. Munsell color of the in-situ soil next to the surface 58
Table 8. Laboratory analysis of density for caliche samples 60
Table 9. Soil information published by Soil Survey Geographic (SSURGO) Database, NRCS map unit number 63 (Jerag very fine sandy loam, 1 to 5 percent slopes) 62
Table 10. Summary of the soils on the RAS at Fort Bliss 62
Table 11. Vegetation cover summary from the photos taken during IOP #2 at selected sampling locations 75
Table 12. OLS rating for surface condition for all seasons 81
Table 13. CBR distribution calculated from DCP profiles and CIH_L (0.5-kg hammer) at Fort Bliss RAS during all IOPs 93
Table 14. Examples of CIH_L datasets with decreasing readings 98
Table 15. PCASE loading capacity results for three seasons based on *estimated* DCP CBR 108
Table 16. Number of OLSs located seasonally by software 118
Table 17. Seasonal overall rating for Fort Bliss OLS 129
Table 18. The overall rating of the entire OLS 129

Nomenclature

AFCESA	Air Force Civil Engineer Support Agency
AFRL-VA	Air Force Research Laboratory Air Vehicles Directorate
AGL	Allowable Gross Load
AMC	Air Mobility Command
ASTM	American Society for Testing Materials
ATT	Advanced Theater Transport
ATT SSTOL	Advanced Theater Transport Super Short Takeoff and Landing
BLM	Bureau of Land Management
BOLS	Boeing Opportune Landing Site
CBR	California Bearing Ratio
CIH	Clegg Impact Hammer
CIH_L	Light Clegg Impact Hammer (0.5-kg-mass hammer)
CIV	Clegg Impact Value
CIV\L	Clegg Impact Value for 0.5-kg-mass hammer
CONUS	Conterminous United States
CORS	Continuously Operated Reference Stations
CRREL	Cold Regions Research and Engineering Laboratory
DCP	Dynamic Cone Penetrometer
DoD	Department of Defense
ERDC	Engineer Research and Development Center

ETL	Engineering Technical Letter
FCS	Future Combat System
FOD	Foreign Object Damage
GIS	Geographic Information System
GPS	Global Positioning System
IOP	Intensive Operational Period
LZ	Landing Zone
NAF	Naval Air Facility
NRCS	Natural Resources Conservation Service
OLS	Opportune Landing Site
RAS	Runway Assessment Site
RMS	Root Mean Square
SAS	Soil Assessment Site
SSURGO	Soil Survey Geographic
TRANSCOM	US Transportation Command
USCS	Unified Soil Classification System
USDA	United States Department of Agriculture
UTM	Universal Transverse Mercator
WGS	World Geodetic System

Preface

This report was prepared by Rosa T. Affleck, Research Civil Engineer, Force Projection and Sustainment Branch; Dr. Charles C. Ryerson, Research Physical Scientist, Terrestrial and Cryospheric Sciences Branch; Lynette A. Barna, Research Civil Engineer, Force Projection and Sustainment Branch; and by Keran J. Claffey, Research Scientist, Terrestrial and Cryospheric Sciences Branch, US Army Engineer Research and Development Center (ERDC), Cold Regions Research and Engineering Laboratory (CRREL), Hanover, New Hampshire.

Funding for this research was provided by the US Transportation Command (TRANSCOM) through Air Mobility Command (AMC), Air Force Research Laboratory Vehicles Directorate (AFRL-VA), and the OLS Program at Engineer Research and Development Center, Cold Regions Research and Engineering Laboratory (ERDC-CRREL). The authors thank J. McDowell and K. Eizenga, Air Force Research Laboratory Air Vehicles Directorate (AFRL-VA) Opportune Landing Site (OLS) Program Manager for his support and guidance. The OLS program is managed by AFRL/VA at Wright-Patterson Air Force Base, in partnership with ERDC-CRREL and The Boeing Company.

The authors gratefully acknowledge US Army Garrison Command, Installation Management Agency, Fort Bliss, for allowing field work on their training land. The authors thank the following personnel at US Fort Bliss, Directorate of Environment: S. Offutt, and C. Carrig for showing the site, coordinating their schedule with the fieldwork, and providing logistic and safety support for field reconnaissance and field work; and D. Dodge and D. Duran for providing logistic and shipping support.

Several CRREL engineers, scientists, and technicians assisted with extensive field work and the authors acknowledge their hard work and significant contribution to the project: C. Berini, G. Gooch, L. Danyluk, and P. Seman. The authors appreciate the effort done by R. Lichvar, botanist at the Remote Sensing/Geographic Information System Center in Hanover, New Hampshire, for vegetation identifications. The authors recognize other CRREL personnel, including E. Ochs for running the Boeing Opportune Landing Site (BOLS) software and for providing spatial data and in-

formation about the OLS for the Runway Assessment Site (RAS); S. Orchino and C. Smith for laboratory soil analyses, equipment help, and logistics support; F. Scott for support on data quality assurance; and J. Quimby for shipping and receiving our field supplies and equipment.

The authors acknowledge the following for their significant technical contribution to the field program and providing technical review for this report: S. Shoop of ERDC-CRREL, senior research civil engineer; R. Rollings of Rollings Consulting, LLC; and Captain J. Kost of the United States Air Force Academy.

This report was prepared under the general supervision of Dr. Justin B. Berman, Chief, Research and Engineering Division, CRREL; and Dr. Robert E. Davis, Director, CRREL.

At the time this work was performed, Colonel Richard B. Jenkins was Commander and Executive Director of ERDC. Dr. James R. Houston was Director.

1 Introduction

Effectiveness in modern warfare requires response to a wide variety of adversaries rapidly, lethally, and oftentimes stealthily. This requires, in part, the ability to conduct air transport operations to locations without existing runways, and where engineers cannot be pre-positioned because of time constraints and the need for surprise. One of the most difficult problems is locating large, smooth, flat, obstruction-free areas that are also sufficiently firm to support at least one aircraft operation, and preferably many. Today, locating adequate opportune landing sites requires skilled image analysts and days of work, augmented by site survey teams visiting candidate locations and assessing the proposed site or landing zone (LZ).

Several new approaches have been taken to improve the capability of rapidly locating OLSs from the use of satellite imagery (Manley 2001, Ryerson and McDowell 2007, Vincent and Jennings 2004). Using the approaches described by these authors, the OLS Program is demonstrating and improving upon the capability of current technology for locating satisfactory sites, with the future goal of landing airplanes without first placing "boots on the ground."

The OLS Program evolved from a capability developed by The Boeing Company to demonstrate that transport aircraft can operate out of many more locations than are available using prepared runways. That is, larger numbers of unimproved OLS sites should be available in any area than improved runways . Using software developed at Bowling Green State University (Vincent and Jennings 2004), The Boeing Company demonstrated that transports could be operated out of hundreds of austere runways.

Utilizing 30-m resolution LANDSAT imagery, Dr. Robert Vincent from BGSU developed techniques using five of the LANDSAT bands to exclude areas of dense, woody vegetation, freestanding water, sloping and undulating ground, and obstructions (Manley 2001, Vincent and Jennings 2004). LANDSAT pixels were provided with a score, the Boeing Landing Suitability Index, BLSI, which indicated the relative quality of a pixel for landing aircraft. Smaller BLSI numbers related to higher quality surfaces. When adjacent pixels of less than a threshold BLSI number equating to an ac-

ceptable surface were combined to form a contiguous surface of minimum specified size and direction, an OLS was plotted on the LANDSAT image. Boeing and BGSU evaluated the OLS software at a number of field sites (Alvin 2000, Manley 2001, Vincent and Jennings 2004) in California, New Mexico, South Dakota, and Louisiana, and found that the software did locate sites with the attributes sought. Also, all sites were considered firm to support aircraft. Even though an explicit methodology was not created in the software to locate firm locations, OLSs located were, fortuitously, firm.

The OLS program is intended to demonstrate how existing technologies can rapidly accelerate the process of selecting OLSs using remote sensing technology and state-of-the-ground forecast tools (Ryerson and McDowell 2007). However, in the process of demonstration, techniques within the program are being improved and made more robust. The OLS program, started in mid-2004 and scheduled for completion in September 2007, consists of eight fundamental tasks. The Boeing Company will 1) provide software allowing the selection of OLS locations using satellite imagery, 2) provide a capability of predicting soil type, 3) provide a military utility study, and 4) integrate products from all partners into a coherent software package. The ERDC will 5) evaluate the capability of Boeing OLS software for reliably locating suitable OLSs and determine the ability of the software to locate smooth, flat, and obstruction-free landing sites seasonally, 6) provide the capability to predict soil moisture with depth, and 7) provide the capability of predicting soil strength. The capability of all partners will be evaluated in 8) a demonstration (blind test) during 2007. Though the end state in 2007 will not be a full operational capability, it will demonstrate the capabilities of current technology in a semi-integrated functional demonstration package.

This report primarily describes work addressing ERDC task 5 and portions of tasks 6 and 7. This was accomplished by conducting field work at CONUS locations selected by the Boeing OLS software according to criteria described in Section 2 of this report. Specifically, ERDC's goals were to establish whether OLSs selected by the software met criteria established by the AFCESA for contingency airfields, but modified by ERDC for OLS. The criteria modified for OLS to assess the surface conditions include vegetation (type and height), Foreign Object Damage (loose granular materials), flatness, roughness (undulations), mounds, standing water, surface debris and organic materials, surface drainage, and animals burrows.

ERDC also examined the seasonal conditions of the OLS, including OLS loading capacity. The AFCESA criteria, created jointly by the Air Force and the USACE, provide requirements for paved and unpaved runways regarding suitability for various types of aircraft, loadings, and number of operations (AFCESA 2002a, 2002b; UFC 3-260-02).

Ultimately, ERDC conducted field work at four locations: El Centro Naval Air Facility in southern California (Affleck et al. 2008), at Fort Bliss in New Mexico (this report), and at two locations in southern Indiana (Barna et al. 2008). This report describes field work conducted at Fort Bliss, and provides a seasonal assessment of the suitability of the software-selected OLS to be used as a viable landing site.

2 Background

A runway assessment site (RAS) consists of entire OLS runways as predicted by the Boeing software. The main objective of RAS is to evaluate the quality of OLSs selected by the Boeing software, and to develop a knowledge base about OLS software indicators for "greenness" and "flatness" coefficients used to select the runways. The RAS also will be used to evaluate soil properties and the software's ability to select OLSs in any season.

The Air Force uses the following considerations when selecting permanent airfields: topography, vegetative cover, existing construction, weather elements, wind direction, soil conditions, flood hazard, natural and man-made obstructions, adjacent land use, availability of usable airspace, accessibility of roads and utilities, and potential for expansion capability. Potential for encroachment and effects of noise on the local community also must be considered (AFCESA 2004). In addition to several criteria mentioned above, AFCESA Engineering Technical Letter (ETL) 04-7 provides dimensional, marking, and lighting criteria and guidance for planning, design, construction, and evaluation of landing zones used for aircrew training and contingency operations of C-130 and C-17 aircraft.

Other factors that would affect the runway dimensions have to be considered, e.g., altitude and temperature (more takeoff distance is required in hot desert or high mountain locations because air is less dense). The runway dimensions are typically selected by the flyers and are never selected by the civil engineer. The OLS software is not designed to consider all of the criteria desired by the Air Force for permanent airfields. It is designed to select candidate locations for contingency operations, specifically areas that are smooth, flat, level, and free of obstructions and woody vegetation that would harm aircraft. It does not consider wind direction and speed, flood hazard, accessibility to roads and utilities, noise, or potential for expansion, nor does it consider approach and departure corridor clearances. Therefore, RAS characteristics were evaluated based only on what the software can be expected to predict. OLS dimensions were based on minimum requirement 20 by 914 m (60 by 3000 ft) and 30 by 1067 m (90 by 3500 ft) for C-130 and C-17 assault landing zones, respectively (ETL 04-7), for semi-prepared runways. However, wider and longer (i.e., 80 by 1200

m) runway dimensions were also examined in order to account for clearance and overrun. These dimensions are for the study, and actual dimensions will vary for location, mission, and aircraft.

2.1 OLS Software

The Being OLS software uses the method developed by Dr. Robert Vincent, in which each pixel on a LANDSAT image is assigned with a BLSI value relating to the quality of a pixel. A pixel with small BLSI number corresponds to a high quality surface. An OLS is composed of adjacent pixels with BLSI numbers below a threshold value, forming a continuous area of specified length and width. Being OLS software version 7 (OLS-MS), used to select the OLS for the fieldwork, requires vegetation and flatness (gradient) indices. These thresholds for vegetation and gradient are based on the selected pixels from areas in the four field sites that Dr. Robert Vincent and team identified as good based on their field observation and verification. The selected pixels fell within vegetation values of 1.8 and gradients of 0.02 and found excellent correlation with the regions identified as acceptable landing sites by Dr. Robert Vincent and team (Blake, personal communication). The software also requires input for OLS dimensions (length and width), but the OLS results can sometimes have longer lengths than the minimum length specified.

For Fort Bliss, the software was run on two of LANDSAT's images. The first run used LANDSAT imagery (frame 033_038) for 13 June 01 with a flatness index of 0.02 and a vegetation index of 1.8. OLS results from this run were used during the initial visual evaluation at Fort Bliss in March 2005 (Appendix A). A following run using version 7 of the software was performed on LANDSAT imagery (frame 033_037) taken on 18 May 2003 with systematic georectification. The software was run with a flatness index of 0.02 and a vegetation index of 1.8 for 30- by 900-m (90- by 3000-ft) and 80- by 1200-m (270- by 4000-ft) runway dimensions. Results from this run and the corresponding visual assessment from the site visit in June 2005 are listed in Appendix A. The 18 May 2003 imagery was rerun for 60- by 914-m (200- by 3000-ft) runway dimensions since there were limited number of 80- by 1200-m (270- by 4000-ft) OLSs at Fort Bliss. The OLSs were mapped on an orthophotograph to use in site selection and fieldwork.

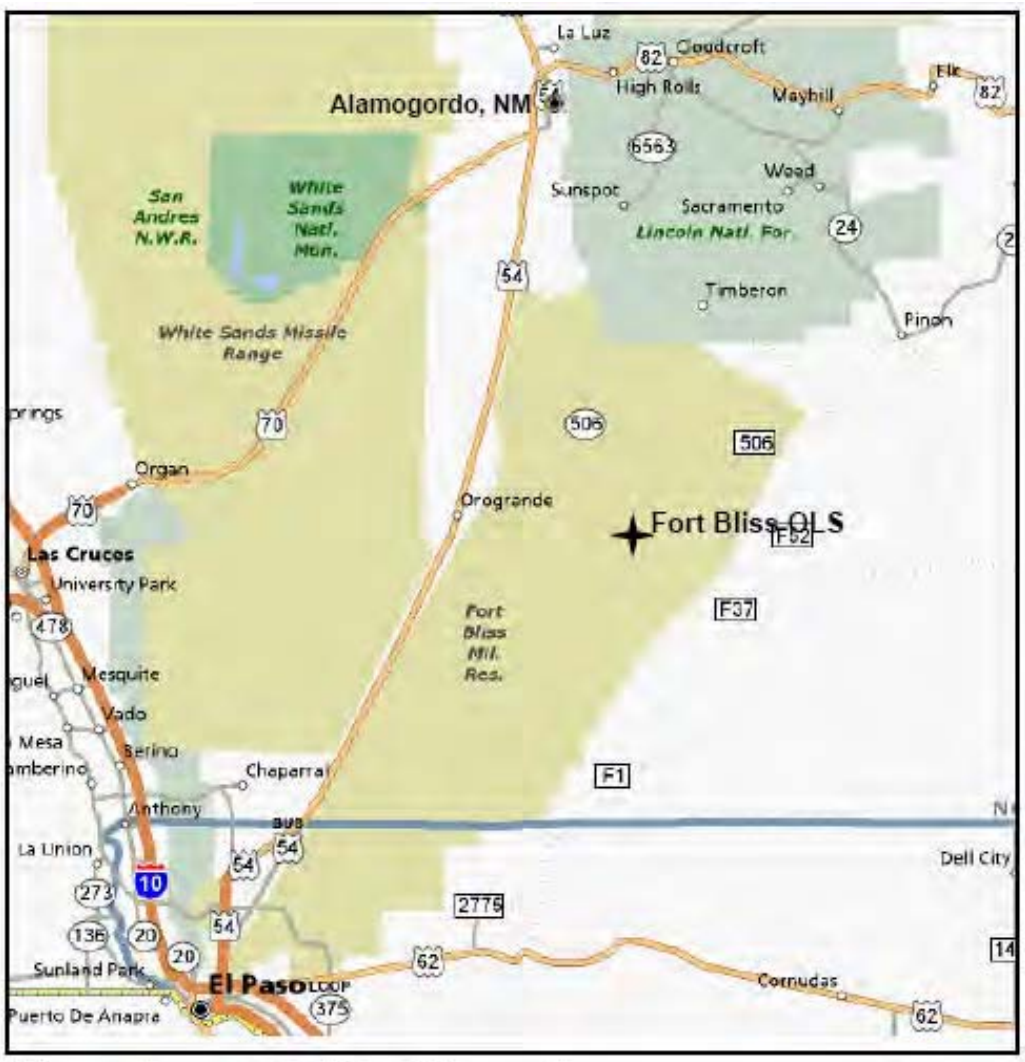
The field site (location where CRREL took the measurements) is off by 233 m to the west and 97 m to the north. This is because the LANDSAT imagery used to locate OLS was at systematic georectification or basic level only. A LANDSAT image is georeferenced at various degrees of geoprocessing precision (Ryerson et al. in prep.). The basic level is called "systematic." Another degree of georeferencing a LANDSAT imagery is based on precision-corrected level using an orthophoto. The level of geoprocessing in the LANDSAT imagery resulted in the misplacement of the RAS location. A detailed discussion on the georeferencing of the imagery including the offset determination is reported in Section 7.2. The runway assessment site (RAS) describing the OLS using the systematic imagery is referred to in this report as SI-RAS, and the OLS using precision-corrected imagery is assigned as PCI-RAS. Comparison of the sites is presented in Section 6.

2.2 Site Selection

The chosen RAS is at Fort Bliss on the US Army military reservation on Otero Mesa, in south-central New Mexico (Fig. 1). The area is generally flat and is leased by ranchers for cattle grazing. Otero Mesa is rock-controlled upland dissected by many drainageways (Soil Survey 1981). The Sacramento Mountains are to the north. The climate is arid to semiarid continental. Precipitation varies greatly from year to year and from month to month. As reported by the USDA, annual precipitation ranges from 0.3 to 0.5 m (12 to 18 in.) in the higher elevations. The main source of moisture in the rainy season (summer) is moist air from over the Gulf of Mexico. Prolonged rainy periods are practically unknown, but occasional heavy thunderstorms with flash flooding do occur. The main source of moisture in the winter is eastward-moving storms from over the Pacific Ocean. The temperature is relatively hot most days from mid-May to mid-September and can be 32 °C (90°F) or higher. Winter months (mid-November to mid-March) can be cold, and average number of days below freezing ranges from 80 to 100 per year (USDA Soil Survey 1981).

Initial reconnaissance to evaluate several OLSs were made during our initial site visits of the area (see Appendix A for trip reports). First reconnaissance of the area was in March 2005, and a second site visit was made in June 2005. The purpose of the visits was to visually evaluate OLSs identified by the Boeing software and to select an OLS suitable for field testing from the extensive list. Because of the extent of the area to survey, ERDC-CRREL personnel were escorted by the Fort Bliss Range Control Officers

during the visits. (Access to the site is available only with permission of the Fort Bliss Range Control Officers because live fire occurs in the area.) The primary considerations for RAS at this site were mainly access for field work activities and safety of the field personnel.



This map is generated from Mapquest.

Direction to the OLS: From Alamogordo, NM take Highway 54 South, turn left (East) onto State Highway 506, across the escarpment, right onto the gravel access road to Centennial Bombing Range, pass the Mesa Horse Camp and continue heading East for approximately 3 km.

Figure 1. General location of and driving to the OLS at Fort Bliss.

The OLSs assessed during the second reconnaissance trip, in June 2005, were based on the LANDSAT imagery taken on 18 May 2003 for 30- by 900-m (90- by 3000-ft) and 80- by 1200-m (270- by 4000-ft) runway dimensions. During this visit, the general area containing OLSs suitable for field evaluation was in Maneuver Area 18 (Fig. 2, area 6). The Boeing software detected no OLSs using the LANDSAT imagery for 13 June 2001. Figure 3 is the close-up of Enclosed Area 6. Because of the limited number of OLSs with 80- by 1200-m (270- by 4000-ft) dimension in the area, software analysis was conducted using the 18 May 2003 LANDSAT imagery for 60- by 914-m (200- by 3000-ft) runway dimensions. Resulting OLSs for the same area (Enclosed Area 6) are shown in Figure 4.

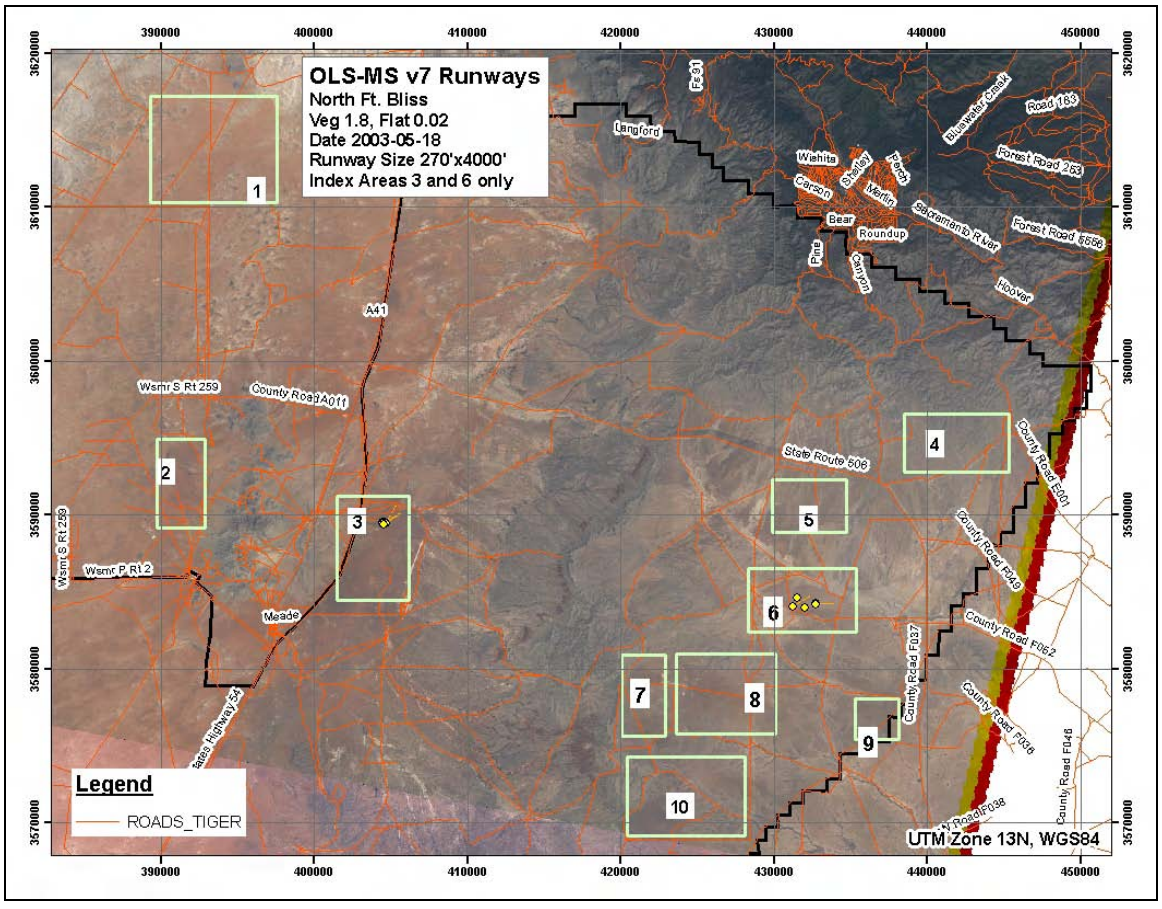


Figure 2. OLSs evaluated during the reconnaissance visit in June 2005 (areas 3 and 6).

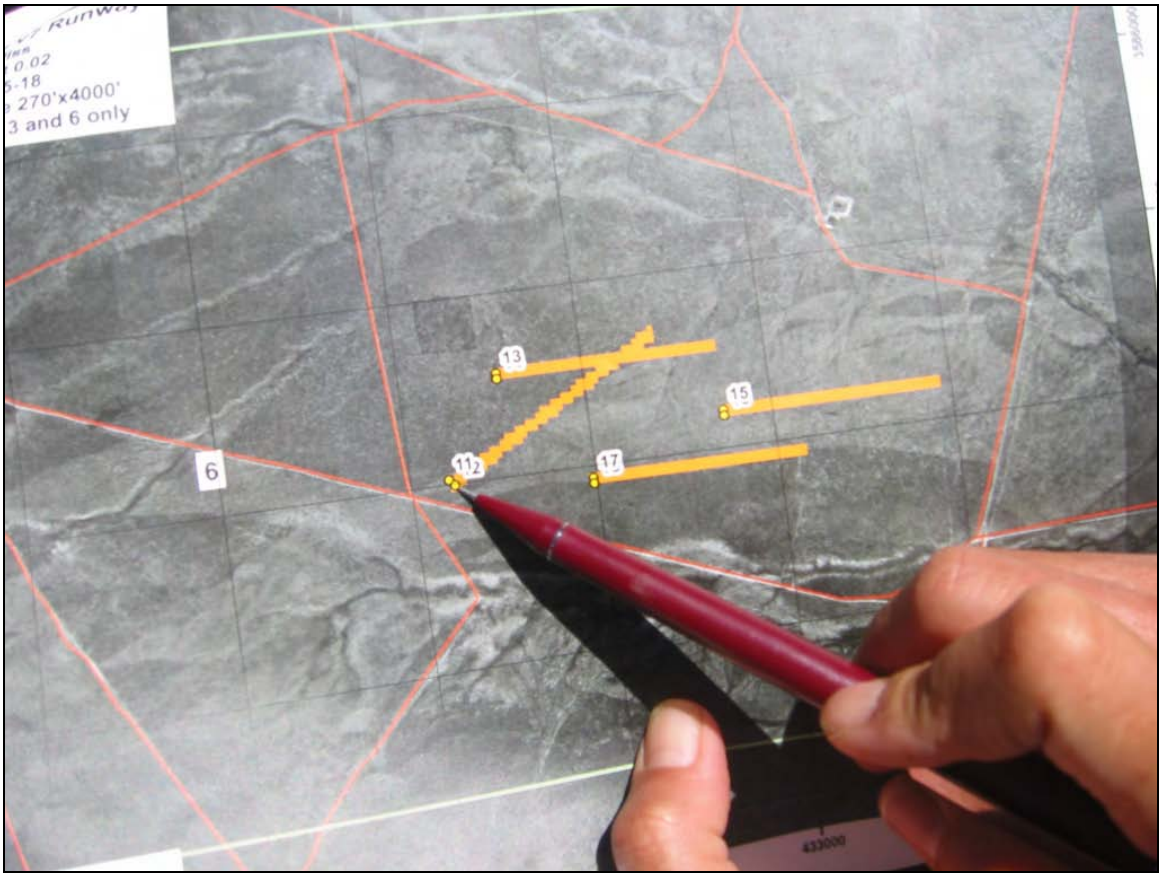


Figure 3. Close-up of area 6 with 270- x 4000-ft OLS, which were visited in June 2005 (18 May 2003 LANDSAT imagery).

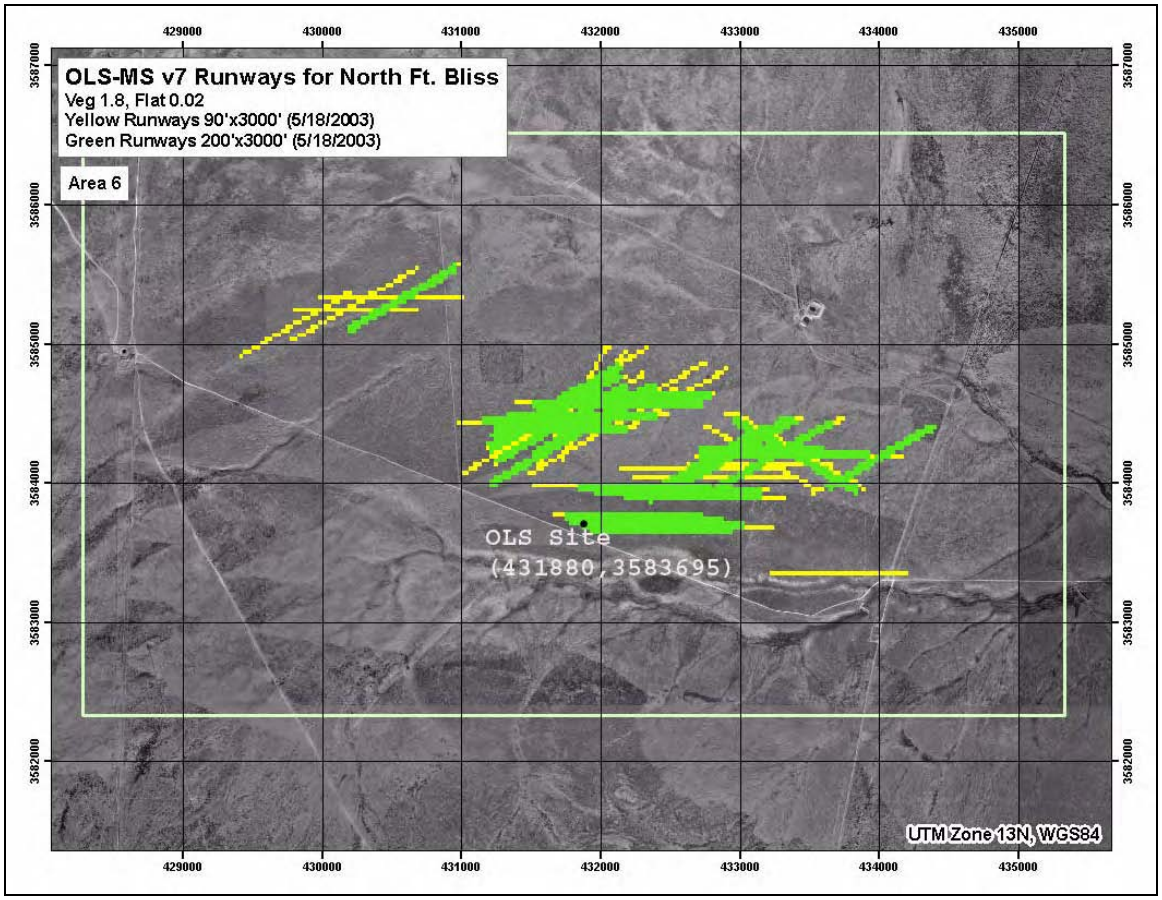


Figure 4. OLS software analysis using 200- by 3000-ft runway dimensions found many more runways (LANDSAT imagery, 18 May 2003).

We were permitted to park the vehicles only along the side of the road. Because no off-road driving is allowed, potential RAS locations need to be located close to the road. This is also critical for logistics, hauling the instruments, and safety during field work. The area is used for training exercises and is near an active bombing range. Permission was obtained prior to the start of each field visit. The selected RAS is shown in Figure 5.

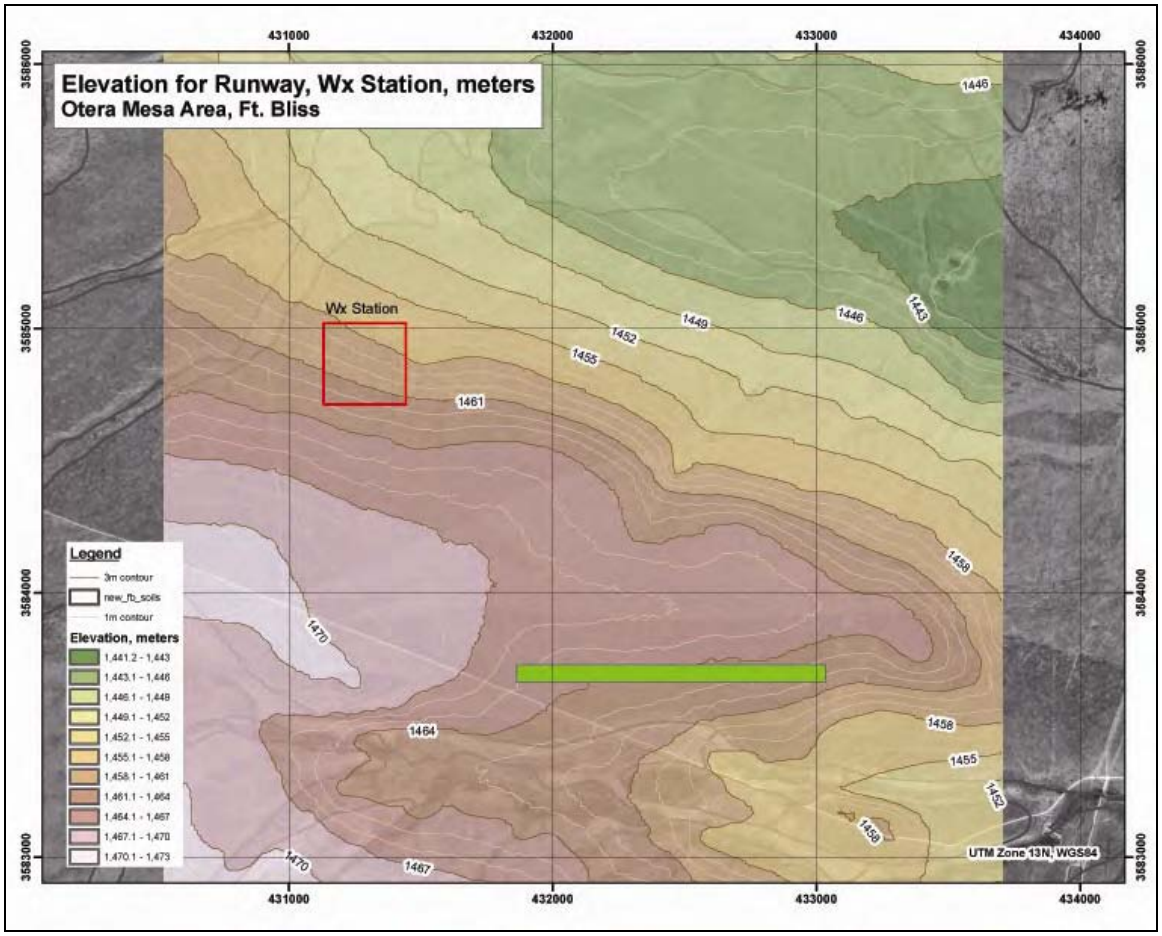


Figure 5. Fort Bliss OLS showing the RAS and fenced area where the weather station was located.

3 Runway Assessment Site (RAS) Analysis Criteria

3.1 Introduction

Field work at Fort Bliss was done to determine whether the OLS software identified suitable landing sites that met both geometric and strength requirements to land an aircraft. This field program, therefore, provided a "ground truth" assessment of the adequacy of the OLS software. Currently, there is no standard method of evaluating an OLS. For this reason, a prime component of the field techniques used are based on existing Air Force procedures published in ETL 2002-19, *Airfield Pavement Evaluation Standards and Procedure* (AFCESA 2002a). Other sources drawn on to provide field measurements that would assist in evaluating an OLS came from vehicle mobility, pavement engineering, and ASTM standards. Figure 6 was modified from the Air Force pavement evaluation method to describe the process used to determine whether the software located a suitable landing site. Each step of the process is described in more detail.

3.1.1 Geometric Evaluation of RAS (Smooth, Level, Flat, Obstruction)

The first step of the field evaluation was to locate and mark the center end points using the OLS coordinates with the aid of a GPS. By locating the runway end points, sampling locations then could be marked or flagged for specific intervals (stationing) along the OLS. ETL 2002-19 (AFCESA 2002a) guidelines for determining sampling locations for semi-prepared runways can be used for prioritizing to assess the critical locations of the runway. For the RAS, we adopted similar procedures. However; the sampling layout was established to allow sampling of the entire RAS using a regular grid spacing (Fig. 7). Field teams performed as many tests as time permitted, and prioritized test locations by focusing on weak soil areas first and to cover each feature or aspect of the runway.

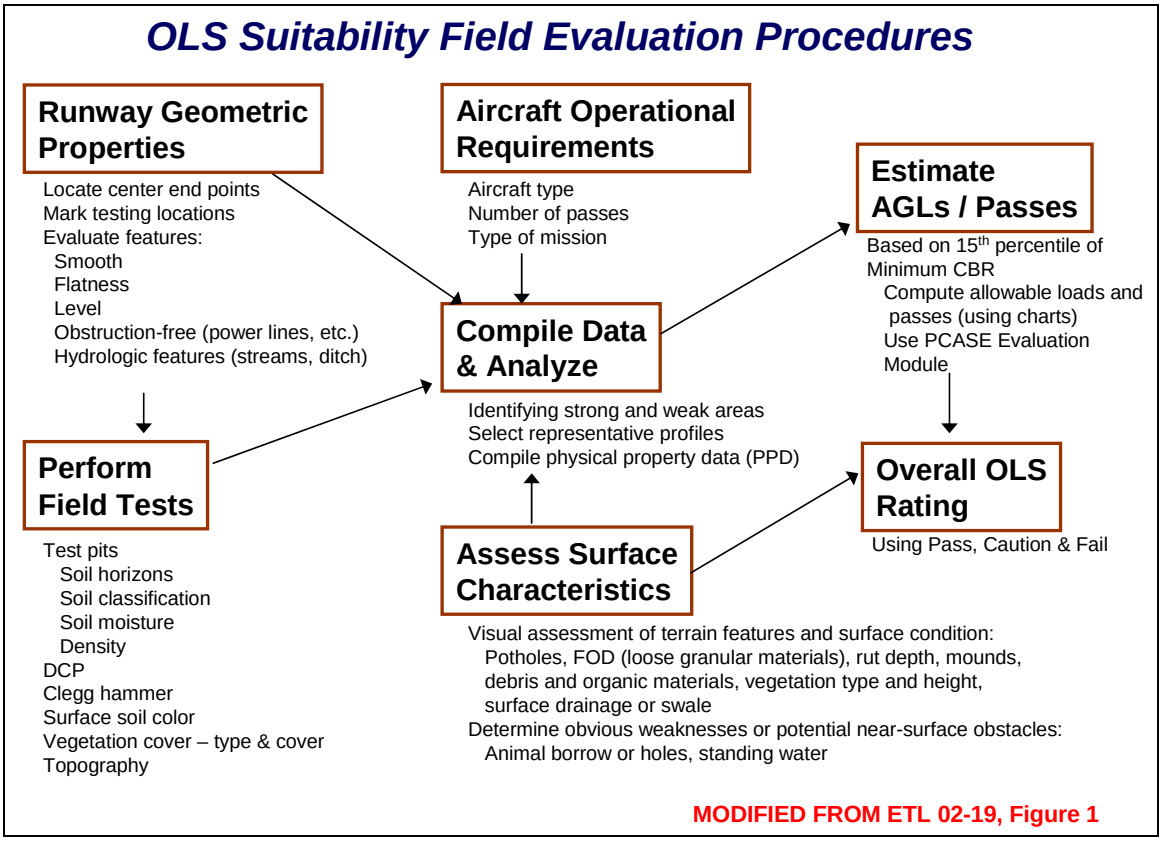


Figure 6. Procedures for determining the suitability of an OLS, modified from practice established by AFCESA in ETL 2002-19 (AFCESA 2002a).

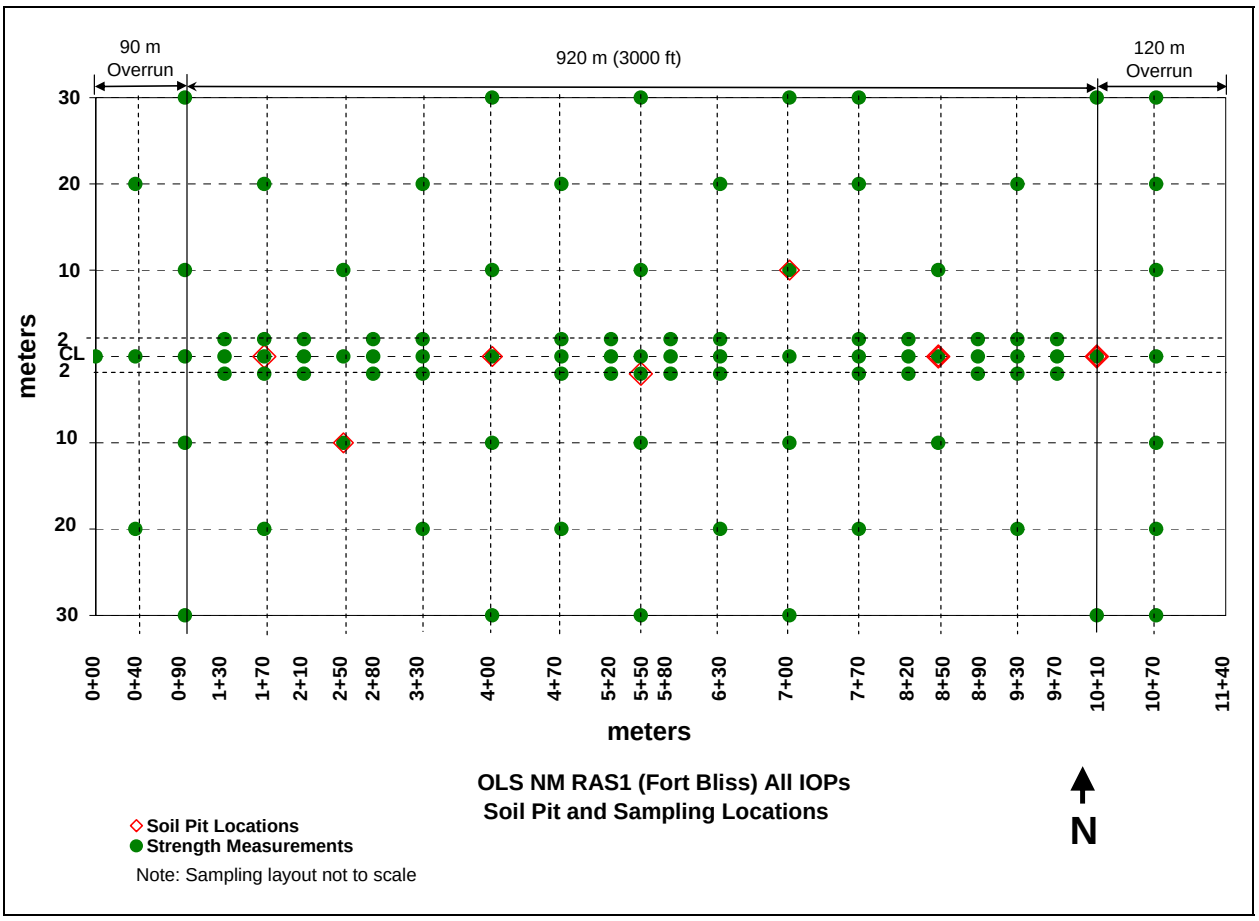


Figure 7. Sampling grid used to evaluate the RAS at Fort Bliss OLS. (Not drawn to scale.)

Smoothness and flatness of the runway were noted and defined in terms of undulation, gradient, or slope. Undulation and slope were measured typically using a level instrument. Vertical obstructions, such as power lines and power poles near the OLS, dense vegetation, and vegetation greater than 1 m (3 ft) in height, were noted: if they exist in an area, the runway is not suitable. Hydrologic features such as standing water, ditches, and streams may not have been present on an OLS during the initial visit but may have occurred during one of the RAS visits because of the climatic effects of the area. These features, if present, should be noted in terms of the length and width of any standing water areas.

The slope of the runway should follow the design guidelines for runway design. Table 1 provides landing zone criteria and requirements in terms of dimensions and slope gradients for transverse and longitudinal directions from ETL 04-7. The criterion for the longitudinal grade is 3% maximum slope for landing zones. Minimum distance between grade changes is 61 m

(200 ft). Grade changes cannot exceed 1.5% measured at 61-m (200-ft) intervals. ETL 04-7 also states that grade changes should be held to a minimum and should be gradual. The required transverse grade is 1.5 to 5.0%. For specification of the longitudinal and transverse grades, we developed "green" and "red" ratings for the OLS evaluation. A rating of green was assigned for longitudinal grades of less than 3% and for transverse grades of less than 5%. Red was assigned for greater than 3% and 5% for longitudinal grade and transverse grades, respectively. Abrupt grade changes of greater than 1.5% with less than 61 m were considered red.

Table 1. Runways for landing zone guidelines developed for C-130 and C-17 (adopted from AFCESA 2004).

Item No.	Item description	Paved		Semi-Prepared		Remarks
		C-130	C-17	C-130	C-17	
1	Length	As required	As required	As required	As required	
2	Width	As required	As required	As required	As required	
3	Width of shoulders	Min. 3 m (10 ft)				Remove all tree stumps and loose rocks in shoulder areas. Shoulders for paved LZs shall be paved. Shoulders for semi-prepared LZs should be stabilized to prevent erosion by jet blast. Where adequate sod cover cannot be established, shoulders should be chemically stabilized.
4	Longitudinal grades of runway and shoulders	Max. 3%				Hold to minimum practicable. Grades may be both positive and negative but must not exceed specified limit.
5	Longitudinal runway grade change	Max. 1.5% per 61 m (200 ft)				Grade changes should be held to a minimum and should be gradual. Minimum distance between grade changes is 61 m (200 ft). Grade changes cannot exceed 1.5% measured at 61-m (200-ft) intervals.

Table 1 (cont'd). Runways for landing zone guidelines developed for C-130 and C-17 (adopted from AFCESA 2004).

Item No.	Item description	Paved		Semi-Prepared		Remarks
		C-130	C-17	C-130	C-17	
6	Transverse grade of runway	0.5% minimum 3.0% maximum				Transverse grades should slope down from the runway centerline. The intent of the transverse grade limit is to provide adequate cross slope to facilitate drainage without adversely affecting aircraft operations
7	Transverse grade of runway shoulders	1.5% minimum 5.0% maximum				Transverse grades should slope down from the runway edge. The intent of the transverse grade limit is to facilitate drainage.
8	Width of graded area	10.5 m (35 ft)				Cut trees flush with the ground and remove rocks larger than 100 mm (4 in.) in diameter. Remove vegetation (excluding grass) to within 150 mm (6 in.) of the ground. Jet blast may cause erosion of the graded area. For paved LZs where adequate vegetation cannot be established to prevent erosion, the graded area can be covered with a thin 38- to 51-mm (1.5- to 2.0-in.) asphalt layer.
9	Transverse grade of graded area	2.0% minimum 5.0% maximum				Grades may slope up or down to provide drainage, but may not penetrate the primary surface.
10	Width of maintained area	18.5 m (60 ft)	21.5 m (70 ft)	18.5 m (60 ft)	21.5 m (70 ft)	Remove obstructions: cut trees flush with ground. Remove rocks that project more than 150 mm (6 in.) above grade. Remove vegetation (excluding grass) to within 150 mm (6 in.) of the ground.
11	Maintained area: Transverse grade	Maximum range: +10.0% to –20.0%				Grades may slope up or down to provide drainage, but may not exceed +10.0% nor –20.0% slope.

The summary for the criteria used to evaluate the RAS in terms of its smoothness, flatness, obstruction, and hydrologic features is listed in Table 2.

Table 2. OLS geometric evaluation rating used on the RAS.

Geometric criteria	Ratings	
	Green	Red
Flatness	Slope: < 3% for longitudinal direction < 5% for transverse direction	Slope: > 3% for longitudinal direction > 5% for transverse direction
Smoothness	Undulation (grade change, wavelength): < 1.5% in ≥ less 61-m distance	Undulation (grade change, wavelength): > 1.5% in < less 61-m distance
Obstacles	No power lines in the vicinity, no trees or vegetation < 1 m (3 ft)	Power line 200 m near the OLS, trees or vegetation > 1 m (3 ft)
Hydrologic features	None	If present

3.1.2 Field Test Overview

Using the sampling layout (Fig. 7), several soil pits were excavated to determine the stratigraphy of the soil horizons, soil texture, soil density, and soil moisture profiles. Soil texture was determined by collecting samples for laboratory analysis to determine the soil classification. Surface soil color was determined using the Munsell color chart and was not used in the analysis, but was intended to be used for another task under the OLS program. Soil density was measured primarily using a nuclear density gage and drive cylinders, which were found be unsuitable for granular soils. Soil moisture content was measured at various depths using several methods (sensors in volumetric and gravimetric). Soil strength was measured for surface and subsurface layers using several instruments. Soil strength profiles were collected using the Dynamic Cone Penetrometer (DCP). The DCP is the standard instrument and is recommended by AFCESA to assess a runway's soil strength profile. Because of lack of confinement in soil near the surface, the actual strength of the surface layer using the DCP is at some depth depending on the soil type (Webster et al. 1994). Surface soil strength was measured using the Clegg Impact Hammer (CIH), the Static Cone Penetrometer, and a Drop cone. Both the DCP and CIH are commonly used to assess strength of mechanically compacted soils for roads and airfields. The Static Cone Penetrometer is used to assess soil strength

for vehicle mobility applications on cross-country terrain (i.e., natural soils) or trails. The Drop cone is used to assess soil compaction and was designed for agricultural soils. Because the OLSs are on natural soil (not mechanically constructed soils), both the Static Cone Penetrometer and the Drop cone would provide useful information to complement the DCP and CIH. The Static Cone Penetrometer didn't work well at Fort Bliss and El Centro OLSs because of caliche or granular materials present in the soil.

Vegetation type was identified by collecting samples and taking photos along the RAS. Photos also were taken to estimate the amount of vegetation cover as described in Section 6.1.

The topography of the runway was determined from survey elevations at each marked location on the sampling map, as described in Section 4. Lateral and longitudinal profiles of the runway were derived from the survey data to examine runway flatness and smoothness. A more detailed laser-level profile of the runway centerline also was measured to provide information that can be used to determine surface roughness or undulation.

3.1.3 Aircraft Operational Requirements

Knowledge of aircraft type, gross loads, and traffic volume are necessary when evaluating an OLS and its potential capacity, because the capability of the structure will dictate the allowable gross weight of the aircraft and the overall number of operations that may be conducted. In this investigation, the RAS was evaluated as an unsurfaced runway suitable for C-130 and C-17 aircraft.

3.1.4 Compile Data

All of the data collected to characterize the RAS were compiled and analyzed to assist in identifying stronger or weaker areas and any other limitations. The RAS was then separated into representative areas based on thickness and type of the soil layers, soil strength, and surface characteristics. The representative soil strength profile then was used to estimate the aircraft allowable gross load and/or the number of aircraft passes using the standard methodology briefly discussed below.

3.1.5 Estimates of Allowable Gross Loads/Allowable Passes

All information obtained to characterize the RAS was used in conjunction with the evaluation curves established in ETL 2002-19 (AFCESA 2002a) primarily to determine the allowable gross load (AGL) and allowable number of passes for the C-130 and C-17. For a semi-prepared airfield, two steps are required to manually evaluate the runway: first, evaluate for surface layer strength; second, evaluate for surface layer thickness and strengths and thicknesses of underlying layers. AFCESA developed the strength charts for specific aircraft as shown in Figure 8. Using the chart, the maximum number of passes can be determined by projecting horizontally the measured CBR value (y-axis) for the soil layer to intersect with the appropriate aircraft weight, and then project vertically to determine the number of passes (Fig. 9). This process is repeated for all subsurface soil layers and the layer that produces the lowest allowable number of passes is the controlling layer for the evaluation. Normally in airfield design, the number of passes is translated to loading type (i.e., channelized traffic for unsurfaced runway) to determine the runway coverage (e.g., a bell-shape distribution of passes along the runway as a function of traffic types). However, the loading type or runway coverage of the RAS is not included in this analysis.

The structural capacity (aircraft load and number of passes) of the OLS was determined in layers of 0.15-m (6-in.) increments from the surface down to 1 m (3 ft). For airfield design, CBR value for the specific soil tested should be selected near the lower part of the range (UFC 3-260-02). Because of the scatter in CBR values where soil conditions vary substantially, take the representative CBR profile collected in test area by obtaining the 85^{th} percentile of the maximum (or 15^{th} percentile of the minimum) CBR values based on airfield design for subgrade soils. The scatter that can be expected with normal control procedures will vary with soil type. The CBR profile used to determine maximum number of passes is based on the 15^{th} percentile of the minimum CBR values collected on the OLS for each layer in 0.15-m (6-in.) increment.

PCASE (Pavement Design and Evaluation Software) (www.pcase.com) is another source for evaluating suitability of OLS for aircraft loading capacity. The software and documents can be downloaded through the Web site. The OLS loading capacity can be analyzed using PCASE evaluation module for unsurfaced runways. The module contains unsurfaced layer, subgrade,

and unbound material types, which are appropriate for natural soil conditions. The thickness of the layers and the corresponding CBR values can be imported into the module. The software is run for specific aircraft and will determine the aircraft load and number of passes.

3.1.6 Surface Characteristics

Assessment of terrain characteristics involved a visual survey of the surface characteristics of the RAS to record the near-surface terrain conditions in greater detail and to identify hazard areas to aircraft operations. This step identifies inhomogeneity within the RAS by evaluating the RAS either for areas where the structure is potentially too weak (such as areas of ponding surface water) to support aircraft operations without resulting in excessive damage to the surface of the landing zone, or areas where aircraft operations may result in the OLS structure causing damage to the aircraft (e.g., small, loose surface material being ingested into aircraft engines). Potentially weak areas would lessen either the number of landing and takeoff operations, or the allowable gross weight of the aircraft that the structure will support. The near surface is considered to be within approximately 12 inches above or below (e.g., a drainage ditch) the horizontal plane of the natural terrain.

Procedures for evaluating and rating either semi-prepared or unsurfaced pavements are described in ETL 2002-19 (AFCESA 2002a) and provided the basis for characterizing RAS surface characteristics. The existing rating system for classifying the distress level on semi-prepared airfields for C-17 Contingency and Training Operations (ETL 97-9) consists of seven distress levels (potholes, loose aggregate, ruts, rolling resistance material [RRM], dust, jet blast erosion, and stabilized failure). These distress levels are coded as green, amber, and red. Green means low risk to aircraft operations, Amber indicates a medium risk, and Red designates high-risk operations and identifies areas that should be repaired before subsequent aircraft operations. The ETL 97-9 rating system was used and amended to generate criteria for assessing the condition of the RAS. Table 3 contains the criteria based on the impact of surface distresses for the C-17 (ETL 97-9), along with other features particular to aircraft operations on OLS.

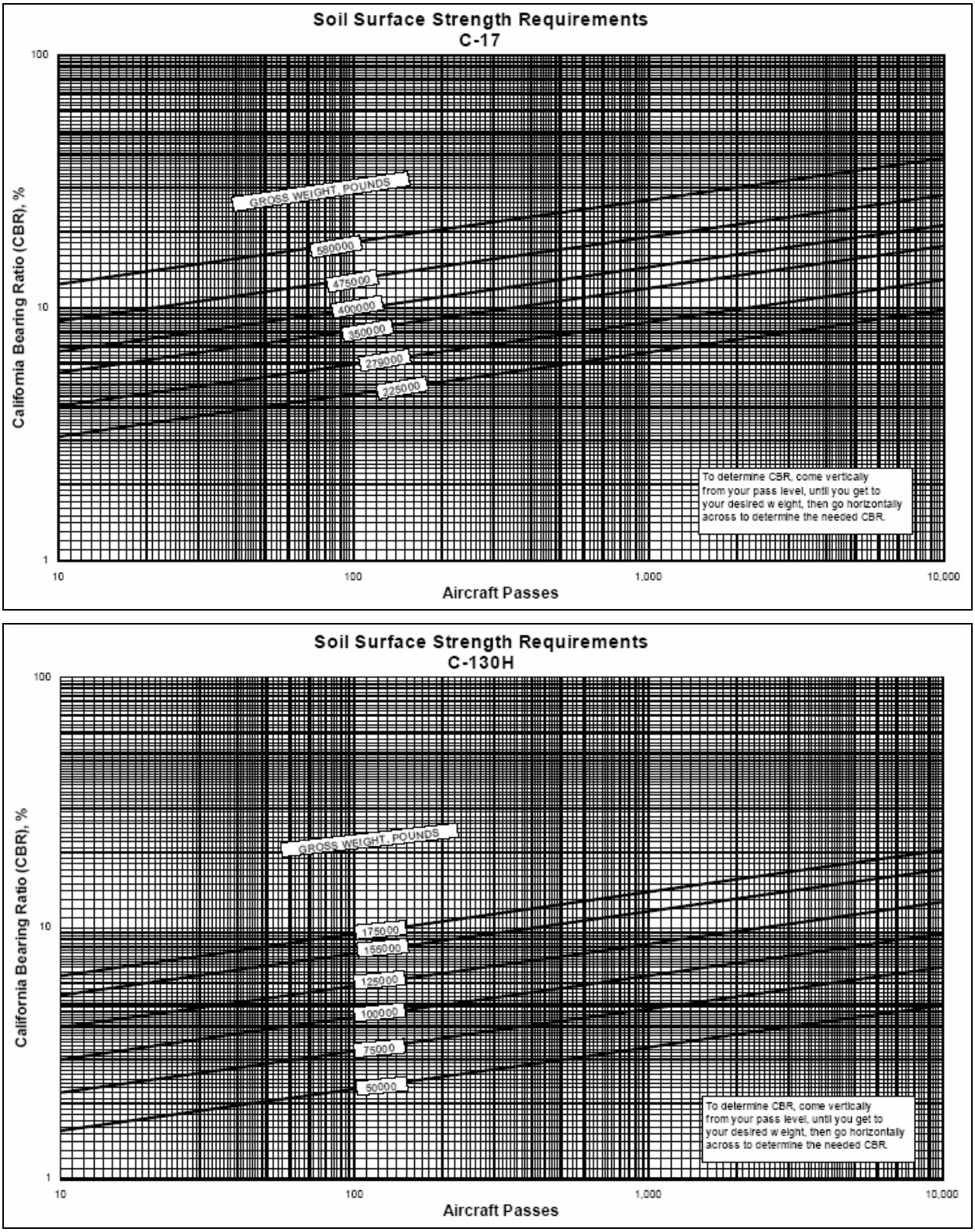


Figure 8. Soil strength on semi-prepared airfield for the C-17 and the C-130H.

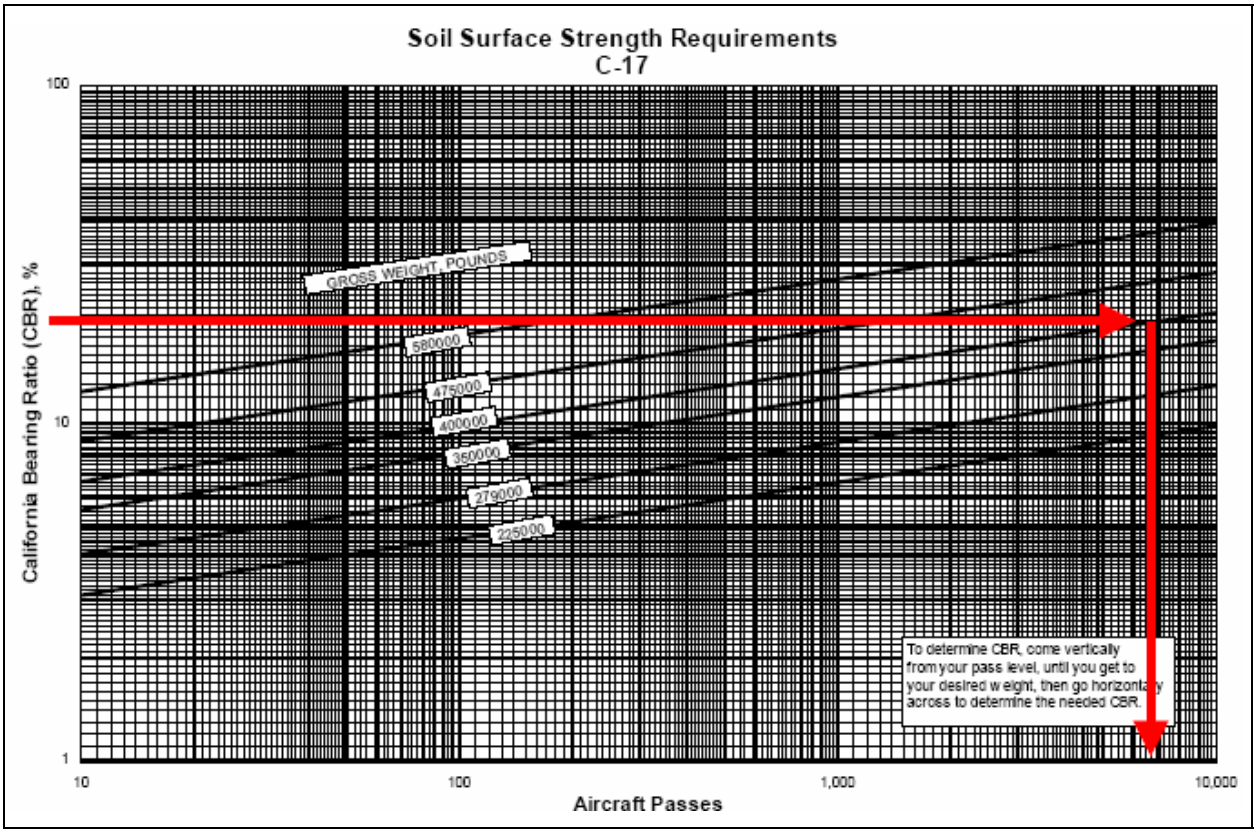


Figure 9. Sample evaluation of surface strength on semi-prepared airfield for C-17 operations.

The features of the RAS were documented during a "walk-through" conducted during three visits in summer, fall, and spring. A walk-through entails examining the entire area of the RAS and documenting the physical characteristics. Each of the features was quantified in order to determine the rating representing the entire RAS (Table 3). The types of OLS features documented and evaluated included but were not limited to

1. Potholes or depressions: Typically well defined bowl-shaped depressions in the airfield surface. The number, location, and depth of potholes can be critical to aircraft operations.

2. Loose aggregate: Rock outcrop and loose aggregates (Fig. 10) including small stones 6 mm (0.25 in.) or larger on the surface can create problems such as FOD (Foreign Object Damage) and ingestion that could damage the engine and other parts of the aircraft. (FOD varies with plane and engine type.) Loose aggregate on the OLS surface can cause roughness of slippery conditions when wet.

AFCESA recommended that rocks more than 100 mm (4 in.) in diameter be removed from the operational surface.

3. Rut depths: Surface depressions of 12 inches or less made from mechanical equipment, such as farm equipment or motorized vehicles, particularly within or across the aircraft wheel path area.

4. Rolling resistance material: Loose fine-grained surface material, such as from tilling, that increases drag (friction) upon takeoff, requiring a longer takeoff distance for the aircraft.

5. Dust: Loose material that becomes airboane when disturbed. The natural material on unsurfaced airfields and the multiple passes of the aircraft cause these fine materials to separate from the soil binder and become a significant problem for personnel, trailing aircraft, and the environment. ETL 97-9 suggested measuring dust by having a vehicle drive at 60 mph down the runway; if the vehicle cannot be seen because of the dust cloud, then the rating is Red. This method was not performed on the OLS, but was noted on the nearby trails as a vehicle drove.

6. Jet blast erosion: Areas where soil is blown, stripped away by engine blast. Jet blast erosion is uncommon on the OLS unless the area was previously used as a landing zone.

7. Stabilized layer failure: Failure of a stabilized surface layer occurs. Desert areas can have a naturally stabilized layer such as duricrust and desert deposits. The desert forms evaporite deposits: as water with minerals evaporates, the minerals are left behind to cement soil and aggregate particles together. These often are called duricrusts or pedecretes. Often termed by constituent, calcium carbonate deposits become caliche or calcrete, dolomite becomes dolocrete, gypsum becomes gypcrete, silica becomes silicrete, etc. Duricrusts can be weakly or strongly cemented, can be discontinuous or massive. Desert pavement, on the other hand, is a process of ablation. A desert pavement has boulders and cobbles/aggregates and soil has the sand and fines progressively removed by wind. As sand and fines are removed, rocks accumulate on the surface until

they form an almost continuous layer of rock, and only scattered rock in a sandy soil matrix is typically found below the layer.

8. Animal burrows: Animal holes, surface scouring, and surface irregularities caused by wildlife or farm animals are signs that the soil structure has been disrupted and would weaken the support of the soil for aircraft operations. Some of the burrows are connected in a series of subsurface small tunnels, creating pockets or voids in the soil strata. A measurement consisting of the size of the animal holes, number of holes, and extent of the area with holes is critical because soil will collapse when subjected to loading.

9. Mounds: Soil accumulation typically around the lower part of bushes. Mounds are measured based on their surface profile (height and he base diameter of the mounds). Mounds can be translated as inverted potholes. The size of the mounds was characterized similarly to the severity used for potholes.

10. Vegetation: Type and area of coverage of plant material found on the RAS. Vegetation of certain types, such as bushes or a field of corn, may impede aircraft operations.

11. Standing water/wet areas: Ponding of surface water indicates poorly draining soils resulting in weak areas. Areas are noted and characterized by depth and approximate diameter.

12. Surface drainage paths: Patterns of flow from runoff that cause surface roughness, including natural and man-made ditches.

13. Surface debris and organic materials: Loose materials present on the surface that can damage the aircraft, e.g., logs, tree branches, organic litter from agricultural plants, and natural vegetation. The bulkiness and amount should be examined and quantified because these materials could puncture the aircraft's tires or be ingested into the engine.

14. Snow depth: In areas of seasonal change, the presence of a snow layer is noted.

Table 3. Surface characteristics used to evaluate the OLS.

	Surface categories	Green	Amber	Red
	Potholes depth diameter	< 100 mm (4 in.) and/or < 380 mm (15 in.)	100 - 230 mm (4–9 in.) and > 380 mm (15 in.)	>230 mm (9 in.) and > 380 mm (15 in.)
2	Loose aggregate, coverage	< 10%	10 to 50%	> 50%
3	Rut depths	< 100 mm (4 in.)	100–230 mm (4–9 in.)	> 230 mm (9 in.)
4	Rolling resistance material, depth	< 90 mm (3.5 in.)	90–195 mm (3.5 –7.75 in.)	> 195 mm (7.75 in.)
5	Dust	Does not obstruct visibility	Partially obstructs visibility, appr. 400 m (¼ mile)	Thick; obstructs visibility
6	Jet blast erosion, depth	< 25 mm (1 in.)	25–75 mm (1–3 in.)	> 75 mm (3 in.)
7	Stabilized layer, depth	< 25 mm (1 in.)	25–50 mm (1–2 in.)	> 50 mm (2 in.)
8	Animal burrows*			
	Number of holes	< 3 with	3 to 6 with	>6 with
	Average holes	< 25 m (1 in.) and	25 m (1 in.) and	> 25 m (1 in.) and
	Diameter Area coverage and spacing	10 by 10 m area for every 200 m	10 by 10 m area, at every 100 m.	10 by 10 m area or bigger, at every 100 m or less.
9	Mounds*			
	Height	< 100 mm (4 in.) and/or	100–230 mm (4–9 in.) and	>230 mm (9 in.)
	Base diameter	< 380 mm (15 in.)	> 380 mm (15 in.)	> 380 mm (15 in.)
10	Vegetation*			
	Height	< 0.5 m (1.5 ft)	< 0.5 m (1.5 ft)	> 0.5 m (1.5 ft)
	Stem or branch diameter	no branches or bushes and tall grass	< 1-in. diameter	> 1 in.
11	Standing water*			
	Depth	zero	0.25 mm (1 in.) and	> 50 mm (2 in.) and
	Diameter		> 380 mm (15 in.)	> 380 mm (15 in.)
12	Surface drainage paths,* depth	< 100 mm (4 in.)	100 to 230 mm (4 to 9 in.)	> 230 mm (9 in.)
13	Surface debris and organics materials*			
	Amount of organics	<5% and	5 to 20% and	>20% and
	Diameter of logs or debris	< 50 mm (2 in.)	> 50 – 100 mm (2 to 4 in.)	> 100 mm
14	Snow depths*	zero	25 to 50 mm (1 to 2 in.)	> 50 mm (2 in.)

* Additional evaluation features added specifically to evaluate RASs using similar approach to that for C-17 semi-prepared runways. These additional distress types are rated subjectively and further.



Figure 10. Picture taken from ETL 97-9 for severity rating of localized loose aggregate.

3.2 Overall OLS Rating

The overall rating of the entire OLS is determined based on approximation from the total analysis of the surface characteristics based on Table 3, the geometry properties (smoothness, flatness) using Table 2 and the soil strength for calculating the loading capacity of the natural soil structure. Table 4 is the culmination of all the ratings for each category representing the entire OLS from the evaluation information and analysis. An "excellent" OLS must have greater than or equal to 80% (11 out of 14) Green, 20% (3 out of 14) Amber ratings, and zero Red ratings for all surface categories for surface characteristics. It has 100% for geometric properties and the aircrafts (C-130H or C-17) should have loading capacity between minimum and maximum gross load at 10 passes. A "marginal" OLS should exhibit 50% Green, 50% Amber, and no Red ratings for surface characteristics; 100% for geometric properties; and the aircrafts (C-130H or C-17) should have assigned allowable loads between minimum and maximum weights of the aircrafts with number of passes between three and 10. An "unacceptable" or a "fail" rating will contain greater than 50% Red rating

of surface characteristics and fewer than two passes at minimum aircraft load or less.

Table 4. An estimation for the overall rating of the entire OLS for C-17 and C-130.

Categories	Excellent or Pass	Marginal or Caution	Unacceptable or Fail
Surface characteristics	Green: ≥ 80% (11 out of 14), Amber: ≤ 20% (3 out of 14), Red: zero	Green: 50%, Amber: ≥ 50%, Red: zero	Green: zero, Amber: ≤ 50%, Red: ≥ 50%
Geometric properties	Green: 100%	Green: 100%	Green: <100%
Aircrafts loading capacity using charts or PCASE: Allow. gross load Number of passes	Between min. & max. weight ≥ 5 and ≤ 10	Between min. & max. weight ≥ 3 and < 5	Minimum weight or less < 2
Or using average CBR categories: C-17 CBR @ min. weight @ max. weight	> 6 < 10	> 2 & ≤ 6 > 4 & ≤ 10	≤ 2 ≤ 4
C-130 CBR @ min. weight @ max. weight	> 4 < 12	> 2 & ≤ 4 > 6 & ≤ 12	≤ 2 ≤ 6
C17: minimum weight = 126.6 metric ton (279,000 lb), maximum weight = 265 metric ton (585,000 lb) C130: minimum weight = 31 metric ton (69,000 lb), maximum weight = 79 metric ton (175,000 lb)			

4 Runway Assessment Site (RAS) Evaluation

4.1 Evaluation Procedure, Measurement Technique, and Methodology

4.1.1 Weather Monitoring Instrumentation

An existing fenced test area used for environmental monitoring by Fort Bliss personnel was used for the weather station. The weather station (UTM 0431172m E, 3584751m N, UTM Zone 13N, WGS 1984) is approximately 1.5 km from the starting point of the OLS. The weather station included instrumentation to measure air temperature, relative humidity, wind speed/direction, and rainfall, soil temperature, and soil moisture. The soil temperature probe contains seven thermistors spaced 10 cm apart, the top placed under the soil surface and the bottom thermistor located at 60 cm below the surface. The soil moisture probe had sensors located 5 , 15 , 25 , 35, 55 , and 95 cm below the soil surface. Data gathered from all the instrumentation will be used for the soil strength model, which is another task under the OLS program and not part of this report.

4.2 Non-Seasonal Impacts

4.2.1 Surface Profile (Topography, Flatness, and Smoothness Measurements)

During the first field visit, the runway ends and sampling points were marked along the RAS using a total station surveying instrument with a Trimble GPS (Global Positioning System) Pathfinder. The GPS system is designated as “map grade,” providing a positional accuracy to within 0.5 m (1.6 feet) when coupled with the Continuously Operated Reference Stations (CORS). The vertical datum was set using Delorme Topo USA digital map software (version 4.0) to determine the elevation of the sampling stations.

To capture the micro relief or undulation and surface roughness along the centerline of the RAS, a laser profile was collected every 1 m in areas that are noticeably rough and every 5 m in areas that are relatively smooth. The spacing for measuring the profile was solely on the perception of the data gatherer (i.e., 1-m profile readings for areas with mounds, depressions, or

swales). A surface roughness value along the center line of the RAS is calculated from the elevation data taken by laser level using the Root Mean Square (RMS), as follows

$$RMS = \sqrt{\frac{1}{n}\left(\sum f_i x_i^{\,2}\right)} \tag{1}$$

where n = number of data,

$$f_i x_i = \left(x_i - \bar{x} \right),$$

$\bar{x}$ = the mean of the data.

A profilometer also was used to illustrate the roughness and flatness of the surface. This instrument consists of rods spaced 2 cm apart, each marked vertically at 1-cm intervals. Photos were taken to detect the undulation of the ground.

4.2.2 Soil Characterization (Surface Soil Color, Soil Type, Density, Organics)

The physical properties of the RAS soils were characterized using several techniques to assess the suitability of the runway and to help in the implementation of the OLS moisture and soil strength algorithms. Assessment of the ability of the RAS to support aircraft operations required soil strength measurements to a depth of 1 m. The RAS field site also provided an opportunity to gather information that supported the ERDC OLS program for soil moisture and soil strength prediction tasks. Soil moisture with depth and soil physical characteristics such as texture, density, and plasticity were measured to support this work. Also, Boeing was tasked to identify soil type at OLS sites using satellite imagery and other terrain-related information. Therefore, surface soil color was identified with a Munsell chart, and surface soil samples were collected to assess mineralogy and organic matter content for Boeing hyperspectral analyses. All surface samples were taken and the organic matter analyses were completed. However, mineralogical analyses were not conducted because Boeing was forced to abandon the hyperspectral approach when the Hyperion satellite became unavailable.

Particle size distribution provides information about soil texture, which is one of the key properties for classifying soil type. The soil classification is directly related to the bearing capacity or strength of the soil. The process for determining soil classification on the RAS and characterizing soil profile is described below.

For the OLS project, soil density measurements at the RAS are valuable in understanding density values in natural soils and impact the soil strength. Frequently, "as-built" density values of engineered soils are reported in airfield studies. However, there is very limited information published for soil density values in natural soils, such as might be found at OLS sites. The measurements taken during the OLS project will add to the body of knowledge currently available. Another use for the density measurements, specifically the dry density, is that it is needed to convert the moisture content on a dry weight basis to a volumetric measurement. Using measured values provide a higher confidence for a model that uses inferred soil density values or values from the literature that may not fully represent the actual field conditions. From a practical standpoint, taking the measurements at the field site required equipment that is portable and easy to use (although some logistics are required for transportation of specialized equipment, such as the nuclear density gage).

A density test with nuclear gage consists of a radioactive source at the end of the rod and the detector at the rear of the machine housing. The source rod is extended at 50-mm (2-in.) increments into the soil to take density readings at each depth; the source rod can be extended down to 305 mm (12 in.). The density measured is the average density along a line between the source at depth and the sensor at the surface (i.e., reading at 305 mm [12 in.] is not the density at 305 mm ([12 in.] but rather is the average density from 305 mm [12 in.] to the surface). Unlike assessing the density of constructed or mechanically compacted soils, deploying the nuclear gage to measure the soil density on natural, dry, granular soils such as this site was troublesome. In these dry, granular soils, when the template rod was pulled out of the soil, the hole partly filled, allowing only a shallow depth for the source rod to penetrate. As a result, in most cases density measurements were achieved with readings at maximum depths shallower than 305 mm (12 in.) or until the source rod resisted further extension. Also, some error in the readings could have been caused by soil disturbance during digging and the process of setting up the gage. To compensate for these

errors, eliminating the top 100 mm readings was recommended because the longer the source rod is extended into the hole, the more soil is included in the measurement, and the more reliable are the results. Therefore, the density readings reported here are the average densities at depths from 150 mm (6 in.) to the surface, and below.

The section below describes soil field characteristics measured at the Fort Bliss RAS that are anticipated to be unaffected by seasonal change: soil texture, soil color identification, and soil density. Samples collected from the soil pits at varying depths were used to determine the soil texture with depth. The soil samples were sent back and analyzed for grainsize, Atterberg limits, and specific gravity tests at CRREL's soil laboratory.

4.2.2.1 Field Soil Sampling and Testing

Soil pits were dug at selected locations (see Fig. 7) to collect soil samples at various depths to characterize the soil profile. Before digging and disturbing the ground, photos were taken a full 360° around the flagged location of the ground surface. In most instances, the color of the soil on the surface was identified using the Munsell soil color chart (Munsell 2000). Surface soil samples were collected before digging the pits. The pits were large, approximately 2 by 2 m (6 by 6 ft), because of soil slumping back into the hole. The objective depth of soil pits was 1 m. Photos were taken of the soil profile, and distinct soil layers were noted. Soil samples were taken at various depths and were sent back to CRREL for laboratory analysis of grain size distribution, Atterberg limits, organic content, moisture, and specific gravity.

Concurrent with digging each soil pit, soil density measurements were made to determine the density profile using the Troxler Model 3440 surface moisture-density nuclear gage. The nuclear gage is used widely in the USAF since at least 1976 and is routine in almost all military construction (on mechanically compacted soils during construction projects). The procedures used for the equipment comply with ASTM D-2922 and ASTM D-3017. ASTM D-2922 states that acceptable precision using the nuclear gage for wet density readings are standard deviation of 5.4, 4.3, and 7.4 kg/m^3 (0.34, 0.27, and 0.46 lb/ft^3) for clay, poorly graded sand, and silt soils, respectively (for a single operator and direct transmission mode). The primary measurements from the gage are wet density (total density in units of grams per cubic centimeter or pounds per cubic foot) and soil

moisture (M in units of grams or pounds of water per cubic centimeter or feet of dry soil). Also, the nuclear gage displays the dry density value calculated from the difference between the wet density and M.

When the nuclear gage is positioned in a soil pit, density measurements can be made at 50-mm (2 in.) intervals from the base of the probe to a depth of 305 mm (12 in.) below the base. This is accomplished by driving a template rod into the soil from the surface, creating a hole into which a rod with a nuclear source is inserted. For measurements deeper than 305 mm (12 in.) from the base of the instrument, the soil pit was excavated down another 305 mm (12 inches) where the bottom of the pit is leveled to provide good contact and a base for the instrument. This process is repeated to the required depth. Density readings were attempted to a depth on 915 mm (36 in.). However, problems were encountered because of soil slumping, and hard and granular soil.

A total of six soil pits were conducted at Fort Bliss RAS. During IOP #1 on 18–21 July 2005, five pits were dug in the following locations:

1. 1+70 CL,
2. 5+50 2S,
3. 8+50 CL,
4. 10+10 CL, and
5. near the weather station.

An additional soil pit was excavated during the second IOP at station 2+50 10S. The reason for conducting a soil analysis near the weather station was to determine whether the soil type is similar to the RAS, because the location of the RAS is quite a distance away. This information was relevant for the soil strength model, a separate task under the OLS program. The pits varied in depth because of a caliche layer that varied in depth with location on the RAS. Pits were redug in undisturbed soil during IOP #2 at stations 8+50 CL and 10+10 CL because soil samples for these locations from IOP #1 were lost and sampling were conducted 1 m off the prior pits (normally

taken on the other side of sampling location). No additional soil samples were collected during the third IOP.

4.2.2.2 Laboratory Testing

Samples were analyzed in the laboratory using ASTM standards D 421-85, D 422-63, D 4318-00, D 854-02, and D 2487-00 (both textural and plasticity characteristics [Atterberg limits] and specific gravity test). The resulting soil classification is reported per the Unified Soil Classification System (USCS) (ASTM 2003).

Surface soil samples were tested for organic content by weight following ASTM 2974. Test method A was conducted to determine moisture content; method C, an accepted method used for geotechnical purposes, used a muffle furnace to determine ash content. Although ASTM 2974 test is for peat-type soils to determine whether a soil is organic or not (i.e., classifying the soil with an O [organic] to be either OL [organic silt] or OH [organic clay]) based on the ratio of the liquid limit run with and without oven drying, this method was used for RAS soils in order to calculate the organic content in the soil. Samples were tested in groups of ten. Replicates of tests were performed on samples taken at each location to examine the variation in results using each test method.

4.3 Seasonal Impacts

Seasonal effects can influence the suitability of an OLS by producing changes in moisture, snow, soil frost, and thaw, including changes in ground animal activity and vegetation cover with resulting impact in soil strength. Seasonal impacts on the Fort Bliss RAS were assessed by seasonal examination of the surface conditions, recording the types and height of vegetation, and measuring the soil moisture and soil strength profiles.

4.3.1 Surface Conditions

The surface conditions were examined to discern weak areas, obstructions, and drainage. For example, a mound with animal holes is a sign that the soil will collapse when a load is applied. Vegetation cover, greenness, species, and height were examined. The vegetation cover was captured using

photographs, and the types of vegetation species were identified by a CRREL botanist from the photographs.

4.3.2 Vegetation

4.3.2.1 Vegetation Type and Height

Vegetation identification was accomplished for dominant species by collecting samples and placing them in clear plastic bags. The vegetation samples and corresponding photos were then identified by botanist Robert Lichvar at CRREL. Minor species may have been missed. The representation vegetation height was noted for each plant.

4.3.2.2 Vegetation Cover and Greenness

Quantification of vegetation cover on the RAS is approximated using photos of the landscape taken from directly overhead at several sampling locations. Vegetation cover from the overhead photos are quantified by determining the total area covered by various plants. From the 3,072- by 2,304-pixel photos, the total area of the photo is 7,077,888 pixels square. Each of the photos was analyzed using ArcMap software (ArcGIS) by digitizing the polygons surrounding the plants, and the software calculated the total area of plant cover. Percent vegetation cover was calculated using the ratio of plant cover to total area multiplied by 100. This method of quantifying the vegetation cover is an approximation and does not include vegetation litter or organics such as dead grass or branches that were present on the surface. Also, extrapolation of the small photograph sample areas to the area of the RAS is also approximate. However, the photos are chosen to be representative of vegetation patterns observed. At six of these sampling locations, the vegetation cover was calculated from two oblique photos for the low-height plant species, then an average value was taken to represent the percent vegetation cover.

4.3.3 Soil Moisture

Soil moisture was measured with depth during every IOP. Several methods were used, including the Dynamax sensors (ML2 and PR2 probes) and gravimetric methods using the spoon and drive-cylinder samples (ASTM D 2216-98, ASTM D 2937-04). The Dynamax sensors provide moisture content in percent volume, whereas oven-dried samples are reported in percent by weight. The volumetric soil moisture content of the soil was meas-

ured using the Dynamax Theta probe ML2 sensors and the Dynamax Profile Probe, PR2. Volumetric soil moisture content is the ratio between the volume of water present and the total volume of the sample, and is expressed in %Vol. It is important to note that desert soils often have minerals such as calcium sulfate, which can be anhydrate, hemihydrate, or hydrate, depending on the amount of water bound in the mineral. The minerals can cause chaos with the moisture sensors used in the nuclear gage and for those dielectric constant moisture sensors as estimator for moisture content (Rollings, personal communication, 2007). This water in the mineral is not available to affect soil behavior but gets picked up by the sensors.

ML2 is a soil impedance-based measurement containing an electronics array of four sharpened stainless steel rods, or tines. Impedance is dependent almost solely on the soil apparent dielectric constant. Dielectric constant of soil is a function of its water content (http://www.dynamax.com/ or ftp://ftp.dynamax.com/Manuals/ml2x.pdf). To measure the soil moisture profile, the tines are inserted into the soil. ML2 readings were conducted on the surface and at various depths in the soil pits during IOP #1, by shoveling narrow holes during IOP #2, and measuring only at the surface during IOP #3.

The PR2 probe consists of a sealed polycarbonate rod, roughly 25 mm in diameter, with electronic sensors (pairs of stainless steel rings) arranged at fixed intervals along its length. The signal is applied to the pairs of stainless steel rings and an electromagnetic field is transmitted extending about 100 mm into the soil. The electromagnetic field is a function of the soil permittivity, which changes with water content in the soil (see PR2 User Manuals). PR2 sensors were installed during IOP #2; however, measurements were taken only during IOP #3.

The gravimetric soil moisture contents were obtained following standard procedures (ASTM D 2216-05) from specimens collected via spoon and drive-cylinder samples. For the spoon samples, soil specimens of 500 g or more were collected, placed in airtight plastic bags, and weighed. Soil density measurements were made using the drive-cylinder method, and soil moisture contents were taken from these samples. The gravimetric soil moisture contents, w, were derived from the oven-dried samples taken in the RAS using

$$w = \frac{M_w}{M_s} 100(\%) \quad (2)$$

where M_w = mass of water, and

M_s = mass of soil solids (dry soil).

4.3.4 Soil Strength

Soil strength is one of the critical parameters determining whether soil bearing capacity is sufficient for landing an aircraft, or if the OLS is suitable for multiple passes. Seasonal differences in surface and subsurface soil strength were measured at selected locations on the sampling grid (Fig. 7) during each IOP (Table 5). In-situ soil strength measurements on the RAS were estimated and obtained using the Dynamic Cone Penetrometer, the Clegg Impact Hammer and the Drop cone.

Table 5. Intensive operational periods (IOPs) at Fort Bliss.

	Seasons	Field visit dates
IOP #1	Summer	18–21 July 2005
IOP #2	Fall	24–28 October 2005
IOP #3	Spring	20–21 April 2006

4.3.4.1 Dynamic Cone Penetrometer (DCP)

The Dynamic Cone Penetrometer (DCP) was used to measure the soil strength profile for pavement and airfield applications (ASTM, 2003 D 6951-03; FM 5-430-00-2), including expedient assessment of airfield conditions in terms of evaluating the field soil strength. Information from the device is used to quantify the bearing capacity of the soil, and is translated into soil strength in terms of California Bearing Ratio (CBR) values ranging from 1 to 100% (where the 100% value is representative of the CBR or crushed limestone gravel). The DCP was used to a maximum depth of 1 m, the full depth capability of the instrument as configured for the OLS field work. Both manual and Digital Acquisition System (Vertek) methods were used to record the DCP values of cumulative penetration and number of blows.

The DCP consists of a steel rod with a 1.6-cm-diameter shaft and a 60° cone, which can be disposable. It can be fitted with either a 4.5- or 7.7-kg

(10- or 17.1-lb) hammer. As the whole device is held vertically, the cone is tapped into the soil by the drop of the hammer from a set distance. The number of hammer blows are counted, and penetration depth is measured for each set of hammer blows. CBR values are calculated using a relationship (eq. 2) developed for use in pavement design or evaluation (Webster et al. 1992)

$$CBR\% = \frac{292}{DCPindex^{1.12}} \tag{3}$$

where

CBR = soil strength

$DCPindex$ = average penetration caused by one hammer blow.

Because of lack of confinement on the soil surface, the DCP can measure strengths of thin layers below the surface for fine-grained plaster materials but requires thicker surface for the non-plastic coarse-grained materials. For silty sand (SM) soil, the average penetration depth required is 13 cm (5 in.) (Webster et al. 1994). One DCP profile was conducted at each sampling location on the RAS unless additional verification was needed or an incident occurred where the rod deviated from vertical.

4.3.4.2 Clegg Impact Hammer

Surface soil strength was measured using the Clegg Impact Hammer (CIH). The CIH is a nondestructive testing device for design and evaluation of pavements. The device consists of a cylindrical mass hammer (4.5-kg mass) dropped within a guide tube from a set height. The hammer is dropped four times at each location and the readings are recorded for each drop. The hammer is equipped with an accelerometer that measures the peak deceleration on impact. The readings are displayed as Clegg Impact Value (CIV) and the fourth reading is converted to CBR (ASTM, 2003 D 5874; Clegg 1980). The CIH was tried on the RAS and it was found that the instrument readings were out of range for the type of soil conditions encountered. Therefore a light CIH (CIH_L), with a 0.5-kg (1.1-lb) mass and 50-mm- (1.97-in.-) diameter hammer, which was developed for testing softer materials, was used to assess the surface soil strength on the RAS.

Similar to the CIH (standard 4.5-kg CIH), the CIH_L consists of a hammer, guide tube, and read-out unit. The hammer is equipped with an accelerometer and the instrument reads the peak deceleration on impact, which is the Clegg impact value (CIV) expressed in units of tenths of gravities (g). At a stationary location, the hammer is dropped four times, noting the CIV for each drop, and this corresponds to one dataset. The mechanism in soils may be described as compaction immediately under the impact area (increasing with blows), and penetration of this compacted zone into the body of the material with consequent lateral and vertical deformations. At higher blow numbers the resistance to deformation resulting from the confinement may be seen as reflecting the overall stiffness of the surrounding material (Clegg 1978). On mechanically constructed soils, the CIV readings generally increase for each subsequent drop. However, it is not always the case for natural soils. The recommended practice is to use the fourth blow reading to calculate the CBR. The CIH_L hammer is free falling at 0.3 m (12 in.) inside the guide tube, and the instrument displays a Clegg impact value (CIV/L) that can be converted to soil strength.

A correlation of CIV/L_4 (fourth Clegg Impact Value for the 0.5-kg hammer) with CBR was developed by Millar (1977). This correlation was developed from few data points. Additional tests were conducted to expand the range of data and further refine the existing algorithm from CIV/L_4 to CBR (Affleck et al. in prep.), as

$$CBR = 0.0121\left(\mathrm{CIV/L_4}\right)^2 + 0.1005\left(\mathrm{CIV/L_4}\right) \tag{4}$$

where

CBR = soil strength measured using a CBR test (ASTM 2003)

(CIV/L_4) = the fourth drop Clegg impact value for 0.5-kg mass hammer.

Replicates CIV/L datasets were taken at each sampling location. Equation 3 was applied to each dataset, and then an average was taken at each sampling location to represent the surface CBR value.

4.3.4.3 Other Tools

Surface strength also was measured using the Drop cone. The Drop cone, also called a Surface Damage Cone, was designed for measuring surface penetration resistance and soil compaction potential from vehicle traffic for agricultural applications (Godwin et al. 1991). The dynamic measurements taken by the Drop cone are based on work (kinetic energy) imparted to the soil and are reported as a force.

The Drop cone consists of a large 30° cone screwed to a rod weighing 2 kg, which is dropped from 1 m through a PVC guide tube. The combined weight of the rod and the cone is 4.5 kg. Penetration is measured for only a single drop and is generally taken for three measurements per location. Strength of the soil can be determined by calculating the force exerted by the cone needed to penetrate into the ground. Analyses using similar type of cones have been done by Abele (1990) and Vaz and Hopmans (2001), and other equations exist—Herrick and Jones (2002) and Stolf et al. (2005). The force applied is the work done on the soil divided by the penetration distance using the equation

$$R = \frac{Whn}{x} + W + Q \tag{5}$$

where

W = weight of drop hammer (kg);

h = height of drop (cm);

n = number of hammer blows;

x = difference in depth between blow sets (cm);

Q = weight of tool (w/o hammer) (kg);

R = force (kg_f).

4.4 Site Description of Systematic Imagery Runway Assessment Site (SI-RAS)

4.4.1 Location

The OLS selected for the fieldwork is 60 m (200 ft) wide and 1141 m (3740 ft) long, in Maneuver area 18, on Otero Mesa at Fort Bliss. Its orientation is exactly east-west. The western end of the OLS is close to the access road (Fig. 5) and was chosen as the starting point of the RAS. The area also is used for cattle grazing where cows roam freely in a large range with barbed-wire fencing. The Sacramento Mountains are visible to the north.

4.4.2 Field Visits and Sampling at Systematic Imagery Runway Assessment Site (SI-RAS)

To capture seasonal effects, three field visits or intensive operational periods (IOPs) were conducted for three seasons (Table 5): summer (IOP #1), fall (IOP #2), and spring (IOP #3). Field work was not conducted during the winter at Fort Bliss. To characterize the OLS site, surveys of surface and subsurface conditions were conducted for each IOP to examine the seasonal and non-seasonal conditions, including terrain and vegetation features and measurement of soil properties.

Prior to IOP #1, a sampling grid was created for the Fort Bliss OLS. The beginning point of the runway starts at station 0+00 (Fig. 7) with the easting and northing coordinates of 431880, 3583695, respectively. At station 0+00, grid points that are offset from the center line are denoted by its distance and whether they are located north or south of the centerline. For example, station 1+70 means it is located at 170 m (560 ft) from the RAS centerline start point, CL stands for the centerline, 10N means 10 m (33 ft) offset to north of the centerline, and 30S indicates 30 m (98 ft) offset from the center line to the south. The sampling grid was developed to sample the entire RAS and used to denote locations for measuring of surface and subsurface data, including vegetation type and cover, and excavating soil pits to identify soil type and measure density, soil strength and moisture (Fig. 7). The green dots in Figure 7 identify all of the sampling locations from all IOPs where at least one measurement was taken and also identify the locations where soil pits were excavated (symbolized by the red diamond). A complete summary of all measurements recorded during each IOP and at each sampling station is given in Table 6.

Table 6. Soil field measurements taken at Fort Bliss OLS during each IOP.

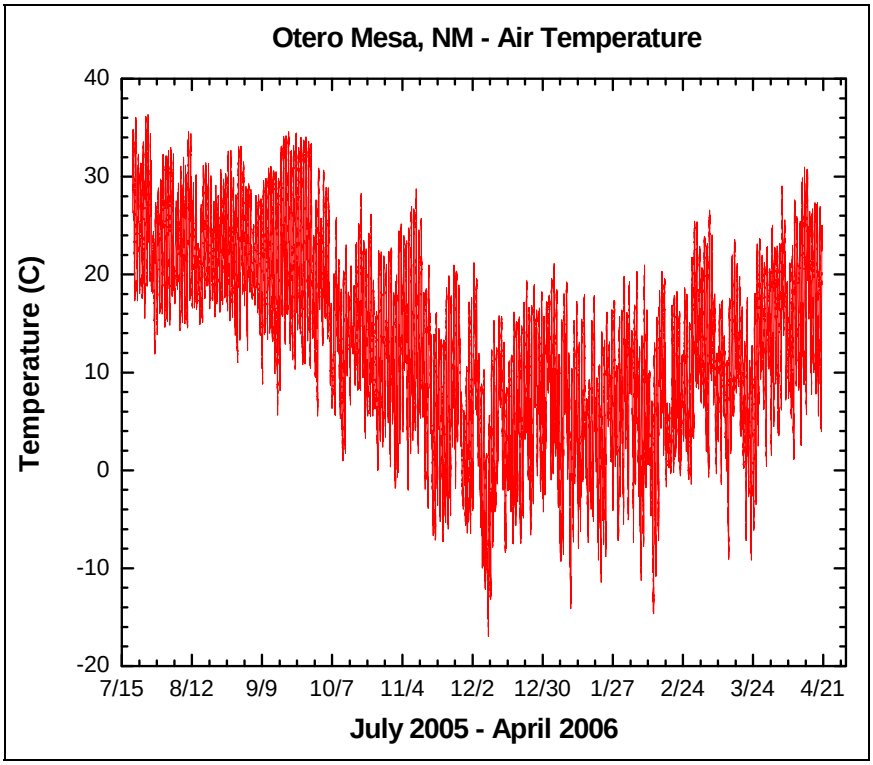
DCP = Dynamic Cone Penetrometer (Strength Profile) — x indicates that a measurement was taken
Clegg = Clegg Hammer (Surface Strength)
Army Cone = Cone Index (Strength Profile)
Dor Cone (Surface Strength)
Dynamax = Soil Moisture (Surface and/or with depth)
S = Soil sample(s) taken
D = Density (Density using Troxler and/or Density using drive cylinder)
V = Vegetation Cover (images)

	SUMMER, July 18-21, 2005								FALL, October 24-28, 2005								SPRING, April 20-21, 2006							
Sampling points	DCP	Clegg	Army Cone	Dor Cone	Dynamax	S	D	V	DCP	Clegg	Army Cone	Dor Cone	Dynamax	S	D	V	DCP	Clegg	Army Cone	Dor Cone	Dynamax	S	D	V
0+40 20N	x	x		x				x	x	x		x	x											
0+40 CL	x	x		x				x	x	x		x	x			x	x	x		x	x			x
0+40 20S	x	x		x				x	x	x		x	x											
0+90 30S	x	x		x				x	x	x		x	x				x	x			x			
0+90 10S	x	x		x				x	x	x		x	x				x	x			x			
0+90 CL	x	x		x				x	x	x	x	x	x			x	x	x		x	x			x
0+90 10N	x	x		x				x	x	x		x	x				x	x			x			
0+90 30N	x	x		x				x	x	x		x	x				x	x			x			
1+30 2N	x	x		x					x	x	x	x	x				x	x		x	x			
1+30 CL								x								x								
1+30 2S	x	x		x					x	x	x	x	x				x	x		x	x			
1+70 20S	x	x		x				x	x	x		x	x											
1+70 2S	x	x		x					x	x	x	x	x				x	x		x	x			
1+70 CL	x	x		x	x	x	x	x	x	x	x	x	x			x	x	x		x	x			x
1+70 2N	x	x		x					x	x	x	x	x				x	x		x	x			
1+70 20N	x	x		x				x	x	x		x	x											
2+10 2N	x	x		x					x	x	x	x	x				x	x		x	x			
2+10 CL								x								x								
2+10 2S	x	x		x					x	x	x	x	x				x	x		x	x			
2+50 10S	x	x		x				x	x	x		x	x	x	x	x	x	x			x			
2+50 CL	x	x		x				x	x	x	x	x	x			x	x	x		x	x			x
2+50 10N	x	x		x				x	x	x		x	x				x	x			x			
2+80 2N	x	x		x					x	x	x	x	x				x	x		x	x			
2+80 CL								x								x								
2+80 2S	x	x		x					x	x	x	x	x				x	x		x	x			
3+30 20S	x	x		x				x	x	x		x	x											
3+30 2S	x	x		x					x	x	x	x	x				x	x		x	x			
3+30 CL								x								x								
3+30 2N	x	x		x					x	x	x	x	x				x	x		x	x			
3+30 20N	x	x		x				x	x	x		x	x											
4+00 30N		x		x				x	x	x		x	x				x	x			x			
4+00 10N	x	x		x				x	x	x		x	x				x	x			x			
4+00 CL	x	x		x				x	x	x	x	x	x	x	x	x	x	x		x	x			x
4+00 10S	x	x		x				x	x	x		x	x				x	x			x			
4+00 30S		x		x				x	x	x		x	x				x	x			x			
4+70 20S	x	x		x					x	x		x	x											
4+70 2S	x	x		x					x	x	x	x	x				x	x		x	x			
4+70 CL								x								x								
4+70 2N	x	x		x					x	x	x	x	x				x	x		x	x			
4+70 20N	x	x		x					x	x		x	x											
5+20 2N	x	x		x					x	x	x	x	x				x	x		x	x			
5+20 CL								x								x								
5+20 2S	x	x		x					x	x	x	x	x				x	x		x	x			
5+50 30S	x	x		x					x	x		x	x				x	x			x			
5+50 10S	x	x		x				x	x			x	x				x	x			x			
5+50 2S					x	x	x	x																
5+50 CL	x	x		x					x	x	x	x	x			x	x	x		x	x			x
5+50 10N	x	x		x				x	x	x		x	x				x	x			x			
5+50 30N	x	x		x					x	x		x	x				x	x			x			
5+80 2N	x	x		x					x	x	x	x	x				x	x		x	x			
5+80 CL								x								x								
5+80 2S	x	x		x					x	x	x	x	x				x	x		x	x			
6+30 20S	x	x		x				x	x	x		x	x											
6+30 2S	x	x		x					x	x	x	x	x				x	x		x	x			
6+30 CL								x								x								
6+30 2N	x	x		x					x	x	x	x	x				x	x		x	x			
6+30 20N	x	x		x				x	x	x		x	x											
7+00 30N	x	x		x				x	x	x		x	x					x			x			
7+00 10N	x	x		x				x	x	x		x	x	x	x		x	x			x			
7+00 CL	x	x		x				x	x	x	x	x	x			x	x	x		x	x			x
7+00 10S	x	x		x				x	x	x		x	x				x	x			x			
7+00 30S	x	x		x				x	x	x		x	x				x	x			x			
7+70 20S	x	x		x				x	x	x		x	x											
7+70 2S	x	x		x					x	x	x	x	x				x	x		x	x			
7+70 CL		x						x								x								
7+70 2N	x			x					x	x	x	x	x				x	x		x	x			
7+70 20N	x	x		x				x	x	x		x	x											
7+70 30N																	x							
8+20 2N	x	x		x					x	x	x	x	x				x	x		x	x			
8+20 CL								x								x								
8+20 2S	x	x		x					x	x	x	x	x				x	x		x	x			
8+50 10S	x	x		x				x	x	x		x	x				x	x			x			
8+50 CL	x	x		x	x	x	x	x	x	x	x	x	x	x	x	x	x	x		x	x			x
8+50 10N	x	x		x				x	x	x		x	x				x	x			x			
8+90 2N	x	x		x					x	x	x	x	x				x	x		x	x			
8+90 CL								x								x								
8+90 2S	x	x		x					x	x	x	x	x				x	x		x	x			
9+30 20S	x	x		x				x	x	x		x	x											
9+30 2S	x	x		x					x	x	x	x	x				x	x		x	x			
9+30 CL	x	x		x				x	x	x	x	x	x			x	x	x		x	x			x
9+30 2N	x	x		x					x	x	x	x	x				x	x		x	x			
9+30 20N	x	x		x				x	x	x		x	x											
9+70 2N	x	x		x					x	x	x	x	x				x	x		x	x			
9+70 CL								x								x								
9+70 2S	x	x		x					x	x	x	x	x				x	x		x	x			
10+10 30S	x	x		x					x	x		x	x				x	x			x			
10+10 CL	x	x		x	x	x	x	x	x	x	x	x	x	x	x	x	x	x		x	x			x
10+10 30N	x	x		x					x	x		x	x				x	x			x			
10+70 30N																								
10+70 20N		x		x					x	x		x	x								x			
10+70 10N	x																							
10+70 CL	x	x		x				x	x	x	x	x	x			x	x	x			x			x
10+70 10S																		x						
10+70 20S	x	x		x					x	x		x	x								x			

4.4.3 Weather Information

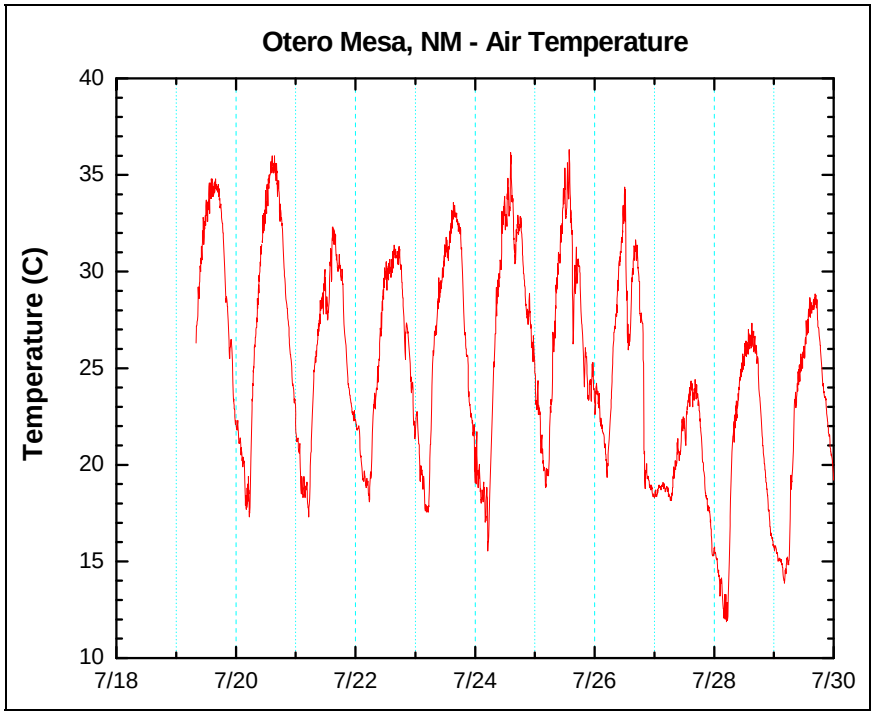
As expected, the Fort Bliss OLS at Otero Mesa was a warm, dry environment, with warmer temperatures in the summer and cooler temperatures in the winter. Air temperature was recorded every 10 seconds and averaged every 5 minutes from July 2005 to April 2006 as shown in Figure 11a. The graph shows that there were only a few days with temperatures near freezing. Contrary to what was reported by the UDSA (USDA Soil Survey 1981), this qualified as a relatively warm year. High temperatures reached near 38 °C (100 °F) in July, during IOP #1 (Fig. 11b). Cooling occurred around October 16, days before IOP #2 (Fig. 11c). The air temperature hovered around 30 °C (86 °F) during the middle of the day in the spring (Fig. 11d).

Precipitation data monitored near the RAS showed only a small amount of rain recorded during the nine months of monitoring. No rain events occurred during the IOPs (Fig. 12).

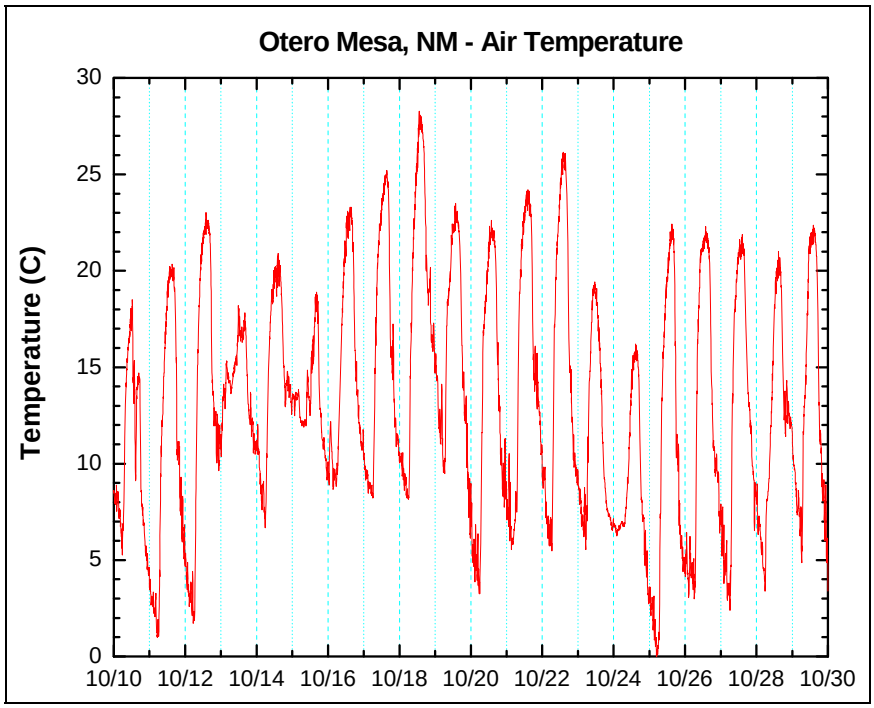


a. Continuous observation.

Figure 11. Air temperature data taken before, during, and after each IOP at Fort Bliss RAS weather observation station.

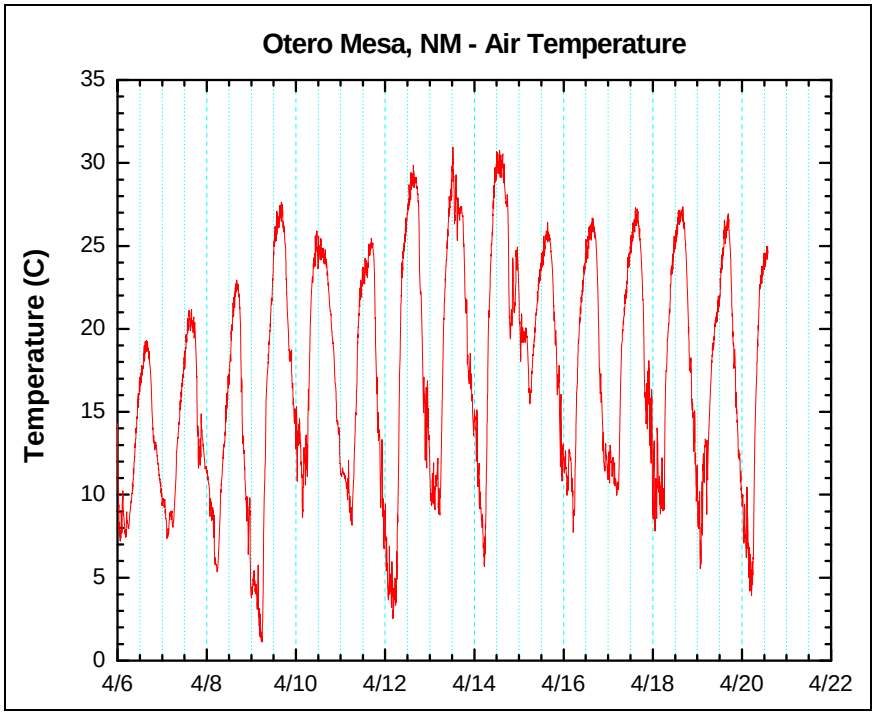


b. First intensive operational period (IOP #1) (18–21 July 2005).



c. Second intensive operational period (IOP #2) (24–28 October 2005).

Figure 11 (cont'd).



d. Third intensive operational period (IOP #3) (20–21 April 2006).

Figure 11 (cont'd). Air temperature data taken before, during, and after each IOP at Fort Bliss RAS weather observation station.

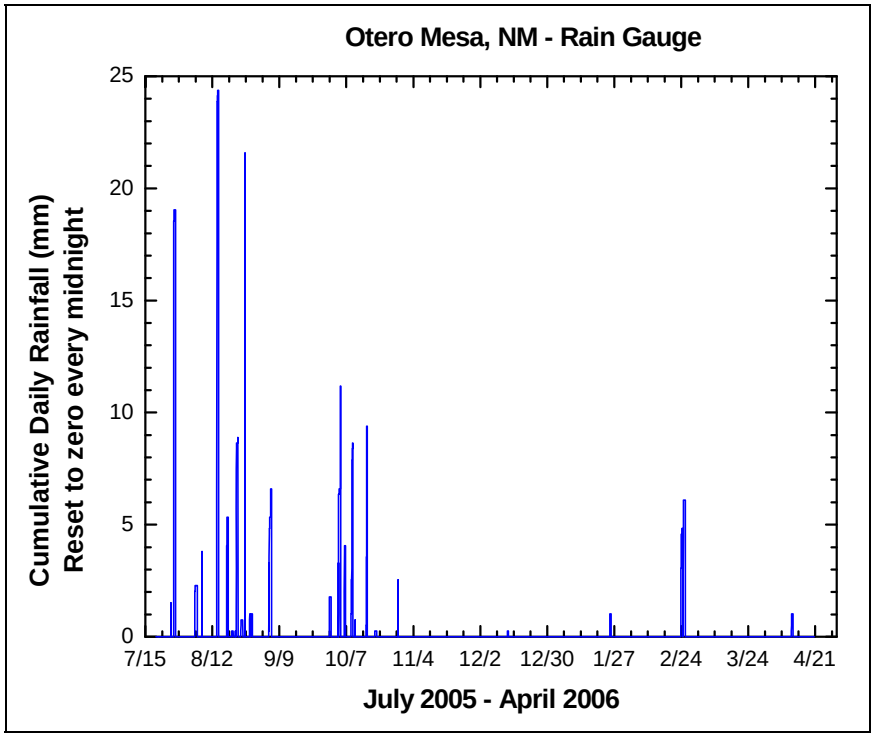


Figure 12. Precipitation data from the observation station near the RAS.

The weather station sampled the wind data every 10 seconds and output was averaged over a five-minute period (Fig. 13). The wind speed data suggested that very light wind (less than 3 m/sec) is common in the area. However, wind speeds of 12 m/sec (27 mph) or higher occasionally occur (Fig. 13). Wind tends to pick up during mid-day and normally originates in the west and northwest. Higher wind speeds can cause dust storms in semi-arid environments with dry soils, but light breezes can improve visibility by clearing dust after disturbance from vehicular or aircraft traffic.

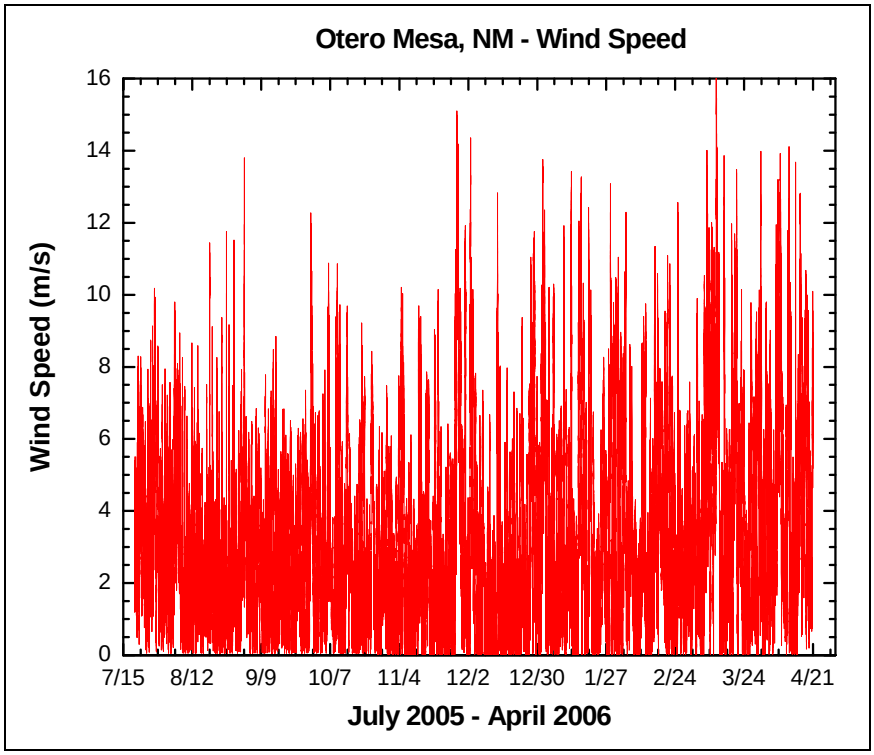


Figure 13. Wind speed observed from the weather station near the RAS averaged every five minutes for the entire monitored time.

4.4.4 Topography

The topography of the OLS is relatively flat but gently sloping to the southeast for most of the RAS (Fig. 14). The elevation of the RAS center line from the total station data showed a gradual decrease of 3.8 m from the beginning (west) to the end (east) (Fig. 15a). The overall grade of the center of the RAS from the beginning to the end is 0.33%, which is relatively flat. To capture the micro relief or undulation and surface roughness along the centerline of the RAS, a laser profile was collected every 1 m in areas that are noticeably rough and every 5 m in areas that are relatively smooth.

The spacing for measuring the profile was solely on the perception of the data gatherer (i.e., 1-m profile readings for areas with mounds, depressions, or swales). The laser level data in Figure 15b display the mounds and surface scouring from animals along the center of the RAS. Typical surface undulations of the RAS are illustrated using the profilometer as shown in Figure 15c. The natural ground undulation is in the range of 6 and 8 cm over spans between 0.5 and 1.5 m. Some of the undulations are caused by animal holes and bare ground between vegetated areas.

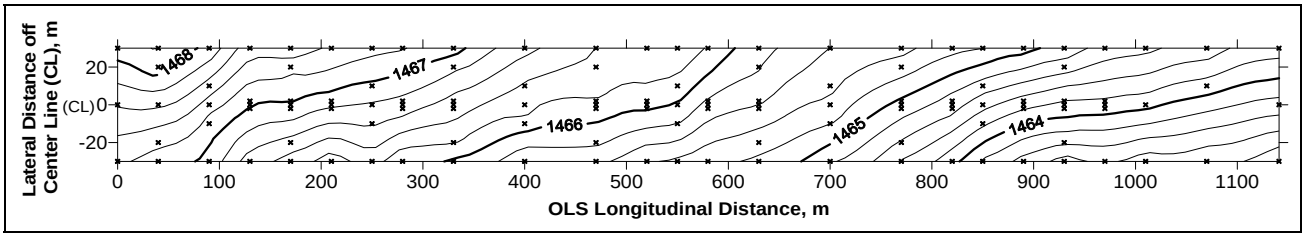
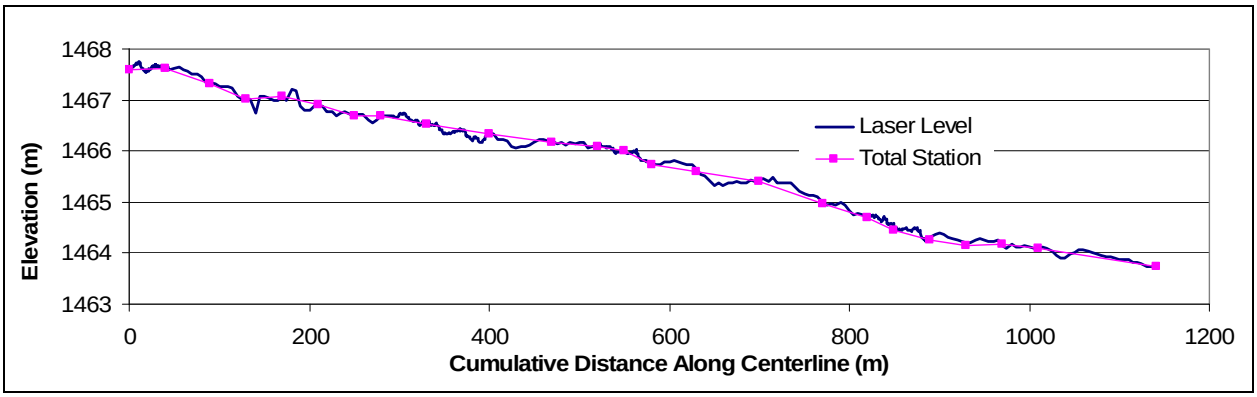


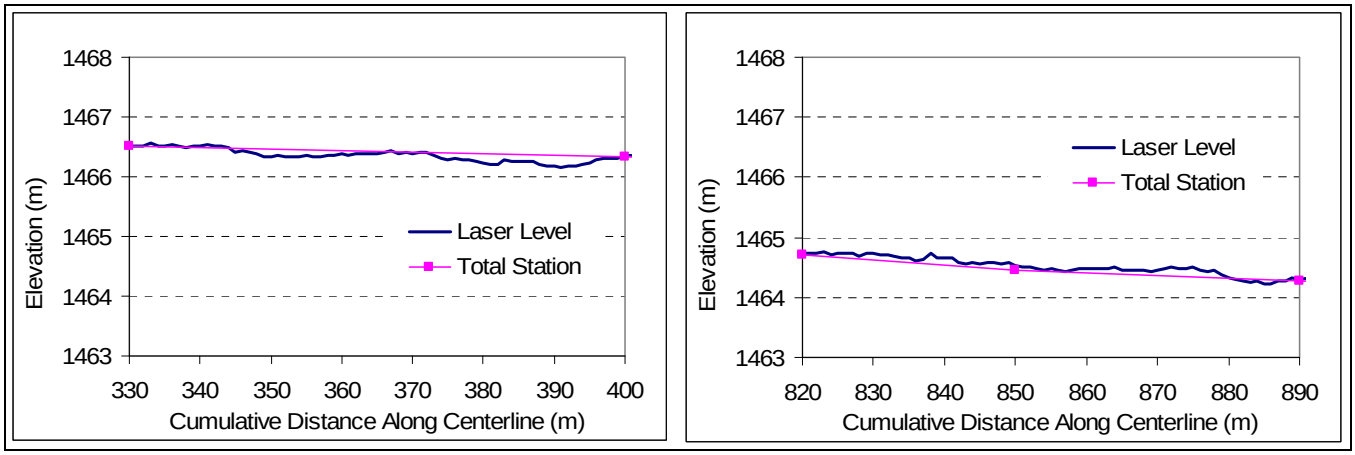
Figure 14. Contour map of the entire Fort Bliss RAS. The x symbols show where elevations (m) were taken.

Surface roughness along the center line of the RAS is calculated using the Root Mean Square (RMS), equation (1) from the elevation data taken by laser level. The RMS value is determined to be 1.13 m along the centerline for the entire OLS.



a. Elevation along the OLS centerline.

Figure 15. Elevation profile along RAS center line.



b. Surface roughness reflected from higher sampling using the laser level.



c. Surface undulation using the profilometer. The rods are horizontally spaced 2 cm apart and each rod is vertically marked at 1-cm intervals.

Figure 15 (cont'd).

The average lateral or transverse cross-sectional grade of the OLS ranges from 1.1% to 2.8 % slope. Typical transverse profiles of the OLS are shown in Figure 16.

The maximum allowable longitudinal grade of runways is 3% maximum slope (ETL 04-7). The longitudinal grade for the Fort Bliss RAS is less than the maximum allowable. Lateral or transverse grades on this RAS also are within the bounds of the ETL criteria.

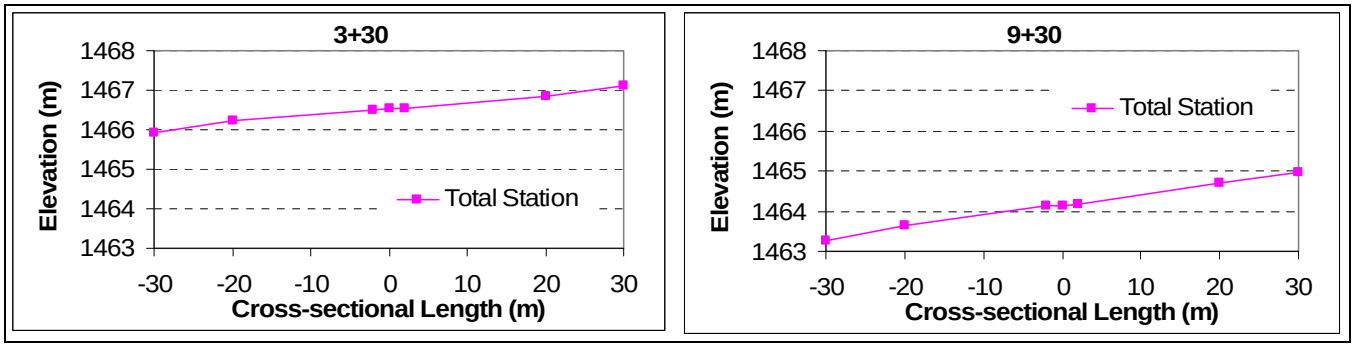


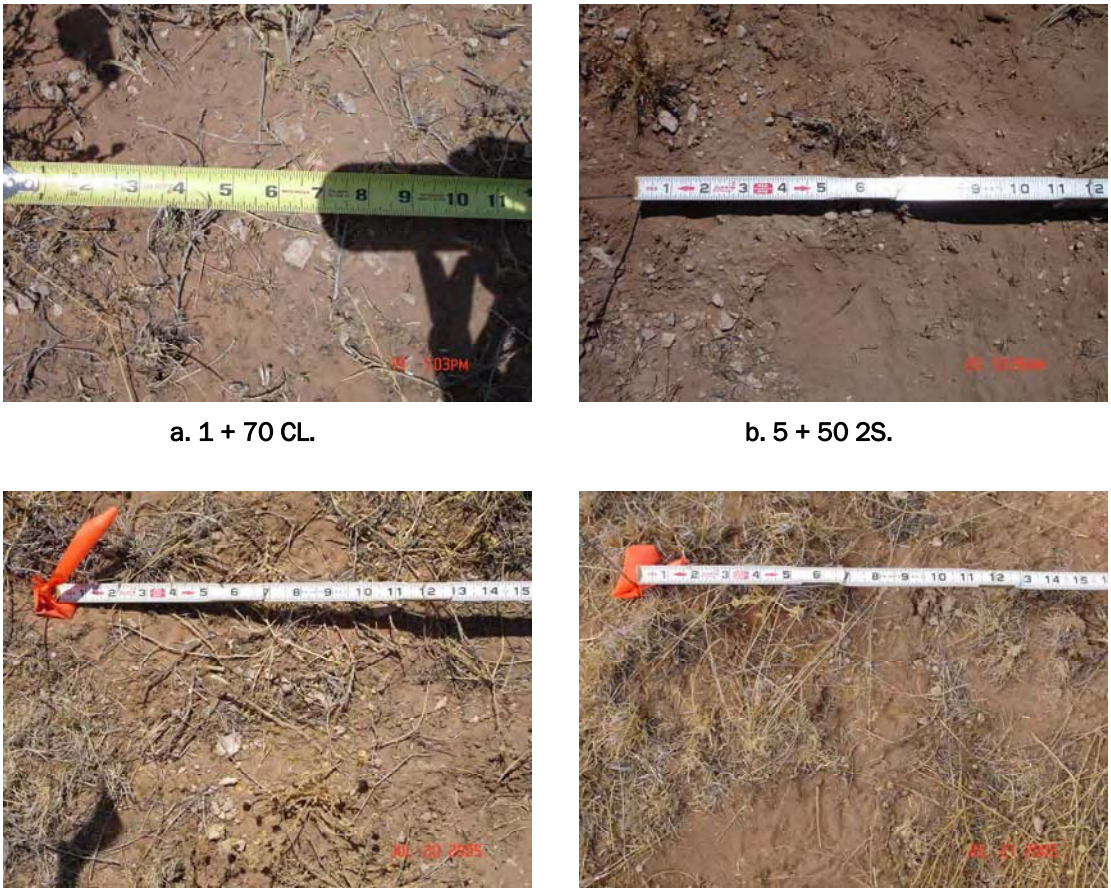
Figure 16. Typical lateral (transverse) profiles of the RAS at Fort Bliss, slope slightly to the south. Station 3+30 is 2% grade and station 9+30 is 2.8% grade.

5 Analysis and Results on Systematic Imagery Runway Assessment Site (SI-RAS)

5.1 Soil Characterization

5.1.1 Soil Type and Texture Profile

Figure 17 shows the soil exposed on the surface at five sampling points on the RAS and at the weather station. Significant amounts of exposed soil were observed on the RAS, including granular pieces of caliche materials. Some of the soil pits at a few sampling points were quite shallow because of the caliche layer, which was difficult to dig or pick through by hand.



a. 1 + 70 CL. b. 5 + 50 2S.

c. 8 + 50 CL. d. 10 + 10 CL.

Figure 17. Soil on the surface before digging the soil pits.



e. 2+50 10S.



f. Weather station.

Figure 17 (cont'd). Soil on the surface before digging the soil pits.

At station 1+70 CL, soil samples were taken near the surface and at 0.36 m (14 in.) below the surface (although the soil pit was dug down to 0.58 m [23 in.]). The soil profile at station 1+70 CL displays a finer soil in the upper 0.36 m, with pieces of caliche embedded in the soil immediately below it (Fig. 18a–c). The bottom of the pit was at 0.58 m, where the caliche layer was very well defined (Fig. 18b). The grain size distribution chart from the laboratory test results is shown in Figure 18d. The surface soil type based on USCS is classified as Silty Sand (SM) with a plasticity index of zero. The particle size distribution for the soil sample at a depth of 0.36 m (14 in.) contained 96.5% cobbles (materials greater than 50 mm or 2 in.) and the rest of the soil sample ranged from gravel to fine sand (Fig. 18d).

The pit at station 5+50 2S was dug to 0.914 m (36 in.) and a photo of the soil profile is shown in Figure 19a. The soil was observed to be relatively uniform and the caliche layer was not encountered throughout the depth. Soil samples were collected at the surface and at 0.15-, 0.30-, and 0.76-m (6-, 12-, and 30-in.) depths. The results from the grain size analysis of the soils collected at station 5+50 2S is shown in Figure 19b and is classified as Silty Sand (SM).

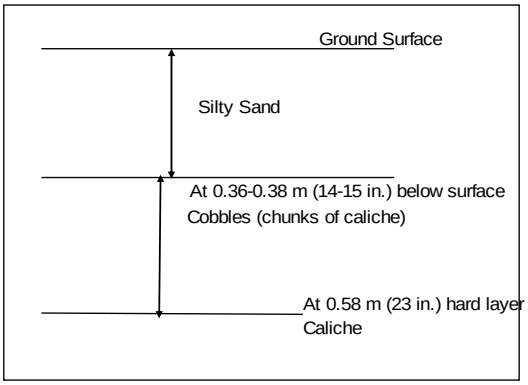
Figure 20a shows the soil profile of the entire pit dug at station 8+50 CL. Caliche chunks were encountered 0.5 m (20 in.) below the surface. Soil samples were collected at various depths including the surface. From the grain size analysis, the soil was relatively uniform and consistent from surface down to 0.30 m (12 in.) and the gradation indicated a Silty Sand (SM) soil. However, at 0.4 m (18 in.), the soil was a more uniform sand classified as Silty Sand, SM (Fig. 20b).



a. From the surface down to 0.686 m (27 in.).

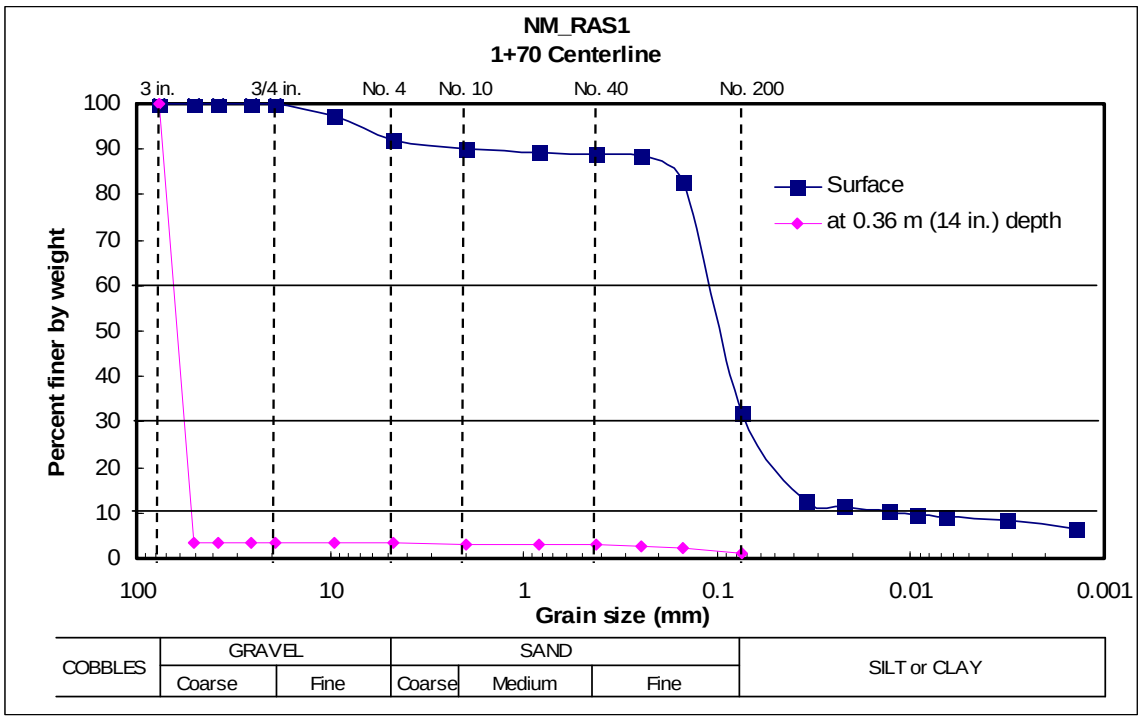


b. Caliche pieces at the bottom of the pit.



c. Soil profile in the field.

Figure 18. Soil profile at Station 1+70.



d. Results from the laboratory grain-size analysis of the soil samples.

Figure 18 (cont'd). Soil profile at Station 1+70.

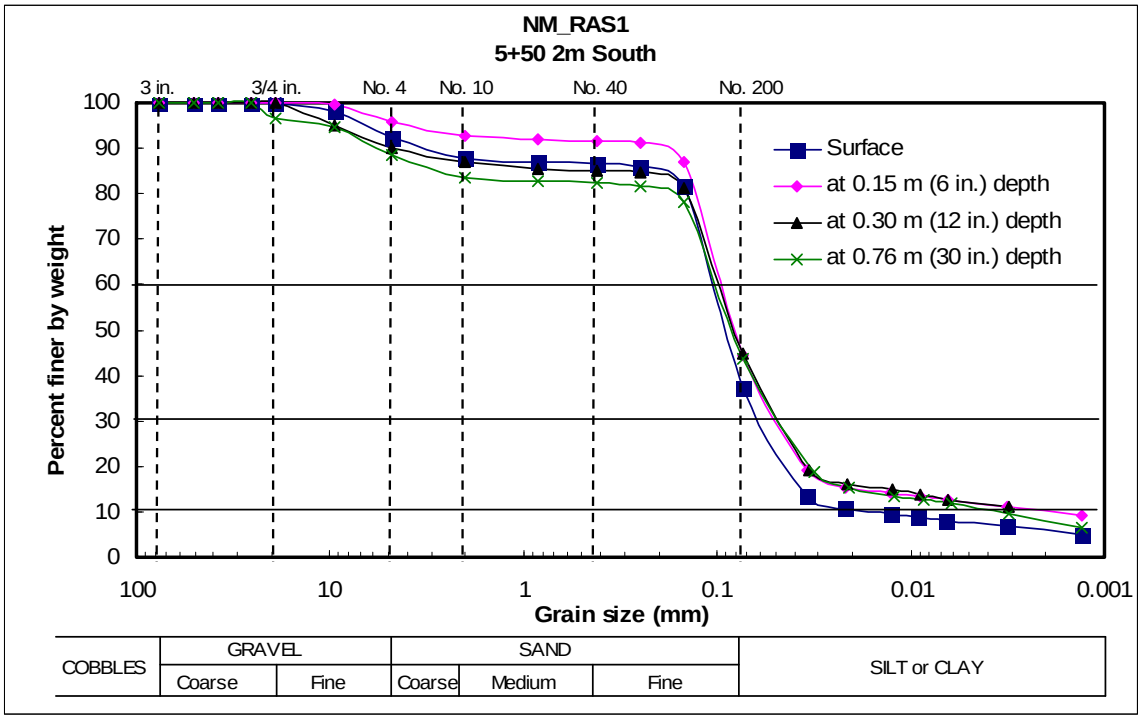
The soil pit at station 10+10 CL was dug to 0.38 m (15 in.) to the caliche layer (Fig. 21a). The grain size analysis identified the soil as a Silty Sand (SM) to 0.30-m (12-in.) depth (Fig. 21b).

Only a shallow soil pit was achieved at sampling point 2+50 10S. The caliche layer was encountered at 0.30 m (12 in.) deep, making it difficult to dig deeper (Fig. 22a). The soil from the surface to 0.3 m below is classified as Silty Sand (SM) as well (Fig. 22b).

The pit near the weather station was the shallowest of all of the soil pits. The caliche layer (chunks) was present near the surface at 0.076 m (3 in.), as shown in Figure 23a. The soil pit was difficult to dig deeper than 0.2 m (8 in.). The results from the grainsize analysis can be seen in Figure 23b. The soil type at the surface is a Silty Sand (SM). However, at depths where the soil was mixed with caliche pieces or chunks, the gradation became a Gravelly Silt (GM) with granular materials larger than 20 mm (0.75 in.) (Fig. 23b).



a. Soil pit down to 0.914-m (36-in.) depth.

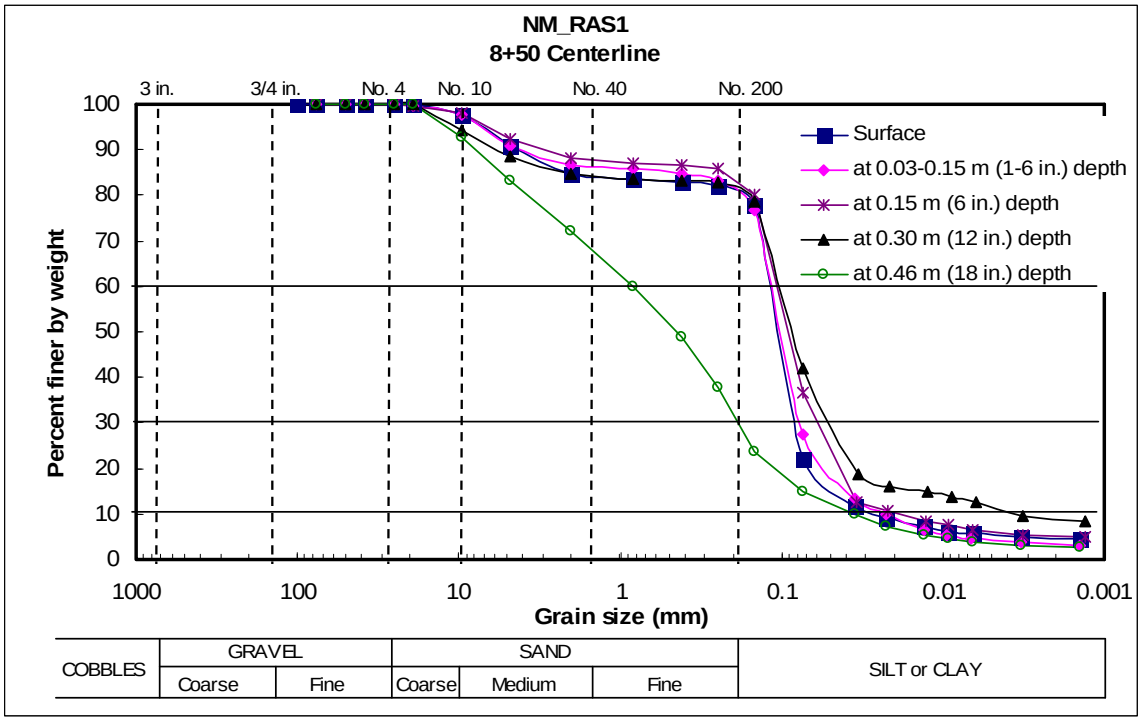


b. Results from the laboratory grain size analysis of the soil samples.

Figure 19. Soil profile at station 5+50 2S.



a. Entire soil pit where the bottom of the pit is located at 0.5 m (20 in.) below the surface.

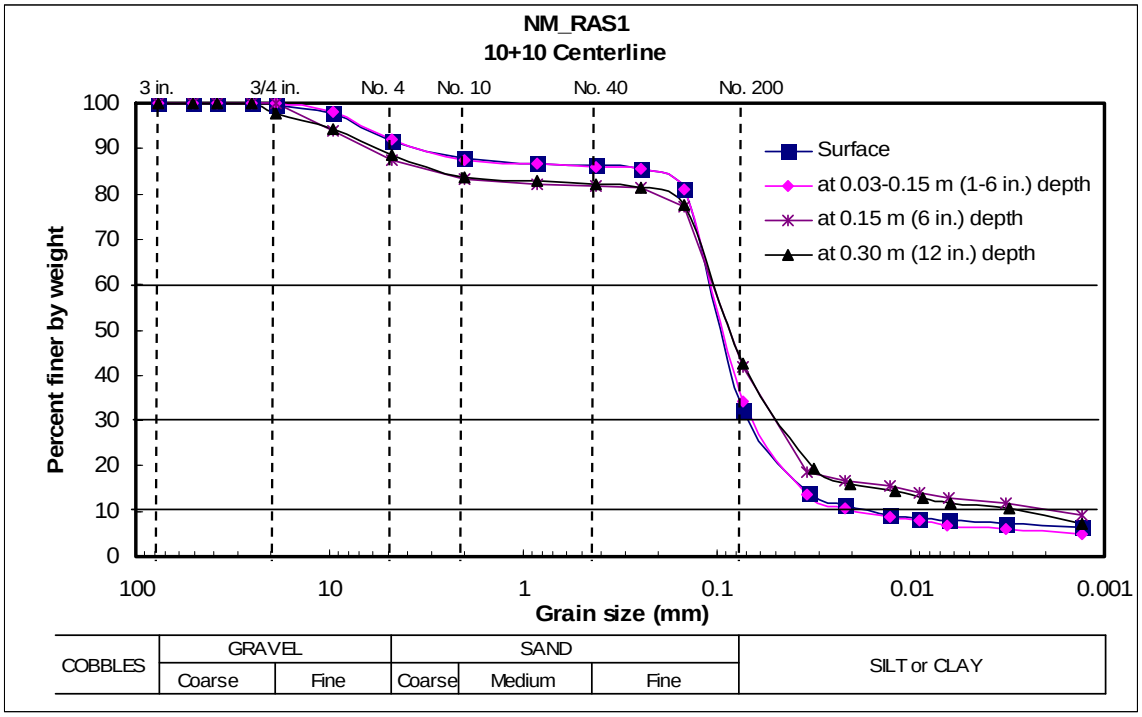


b. Results from the laboratory grain-size analysis of the soil samples.

Figure 20. Soil profile at 8+50 CL.



a. Entire profile and caliche at the bottom of the pit.

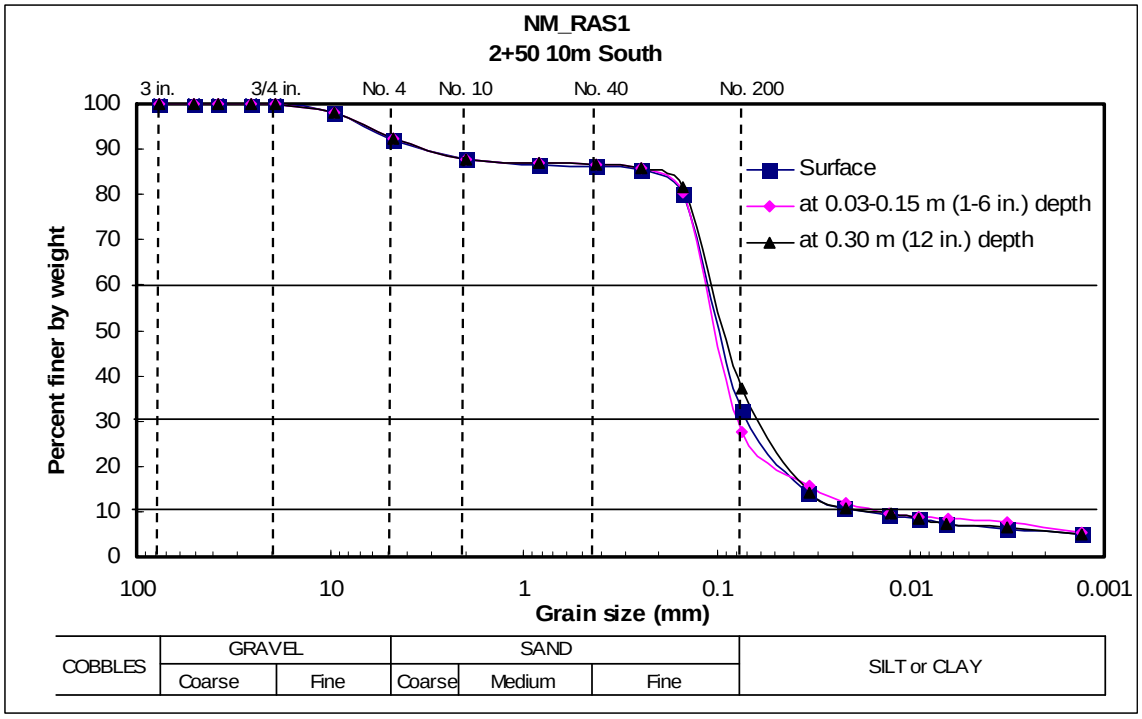


b. Results from the laboratory grain-size analysis of the soil samples.

Figure 21. Soil pit at 10+10 CL down to 0.38 m (15 in.).



a. Soil pit down to 0.3 m (12 in.) below the surface.

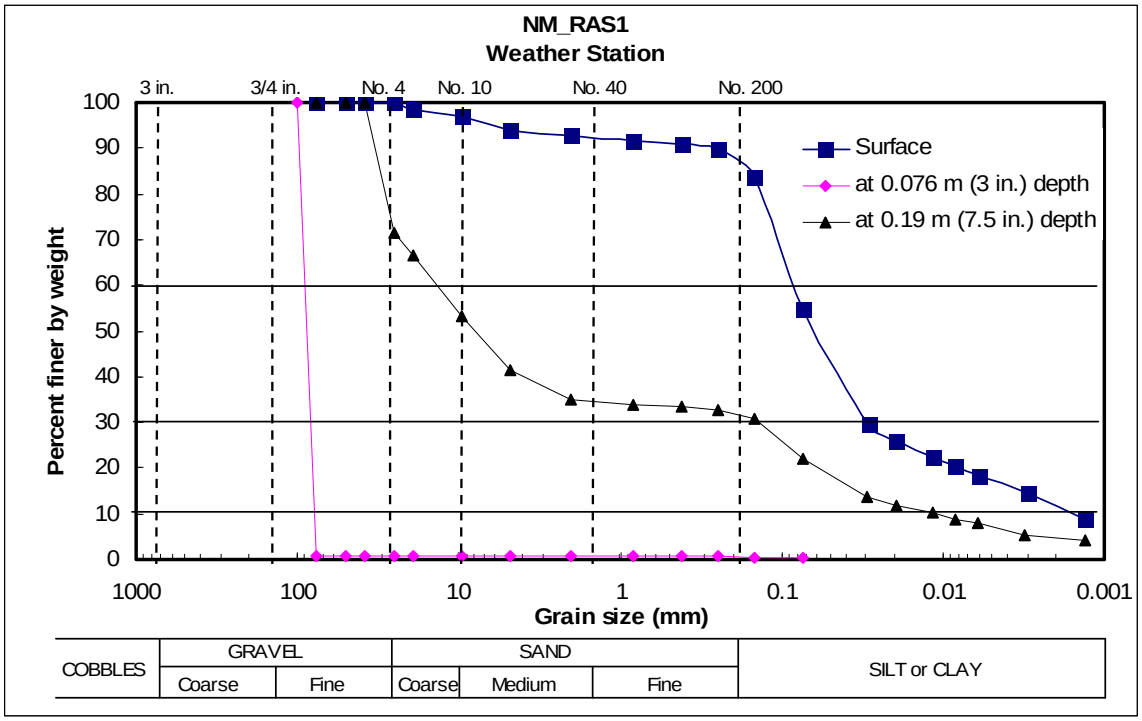


b. Results from the laboratory grain-size analysis of the soil samples.

Figure 22. Soil profile at 2+50 10S, caliche layer.



a. Caliche layer encountered very near the surface.



b. Results from the laboratory grain size analysis of the soil samples.

Figure 23. Soil pit at the weather station area.

5.1.2 Munsell

The summary of the surface soil color for this RAS is listed in Table 7 (Munsell 2000).

Table 7. Munsell color of the in-situ soil next to the surface.

Location	Color and description
1+70 CL	10YR 8/3 Very pale orange
5+50 2S	10YR 8/3 Very pale orange
8+50 CL	10YR 5/4
10+10 CL	10YR 6/6 Brownish yellow
Weather station	10YR 6/4 Yellowish brown to light brown
2+50 10S	10Y/R 5/4

5.1.3 Density

Soil density measurements were made with the Troxler nuclear gage at 1+70 CL, 5+50 2S, 8+50 CL, 10+10 CL, and near the weather station during the first IOP. During the second IOP, soil density measurements were performed at 2+50 10S, and retaken at locations 8+50 CL and 10+10 CL in undisturbed soil. Because we excluded shallow density readings (or readings above 100 mm), density measurements at 1+70 CL and 10+10 CL from IOP #1 and 2+50 10S from IOP #2 are not included in the analysis. Density profiles measured during IOPs #1 and #2 are summarized in Figure 24. The density ranged from 1496 to 1518 kg/m^3 (93.4 to 94.8 lb/ft^3), and from 1389 to 1445 kg/m^3 (86.7 to 90.2 lb/ft^3) at depths 0.15 and 0.41 m (6 and 16 in.), respectively. The density trend at these locations follows the same pattern with depth except for the density below 0.5 m (20 in.) (Fig. 24). This variation in soil density is typical for natural soils due to nonhomogenous layering and uneven depths of the caliche layer. This variation also may be caused from instrument or measurement error.

A compaction analysis on the Fort Bliss OLS soil sample was conducted by Danyluk et al. (2008), and the result showed that the soil has an optimum density of 1884 kg/m^3 (117.6 lb/ft^3) and a maximum moisture content of 12.6% following the modified proctor method (ASTM D1557-2). The in-situ dry density values measured on the OLS vary with depths and are significantly lower than the density from the modified proctor.

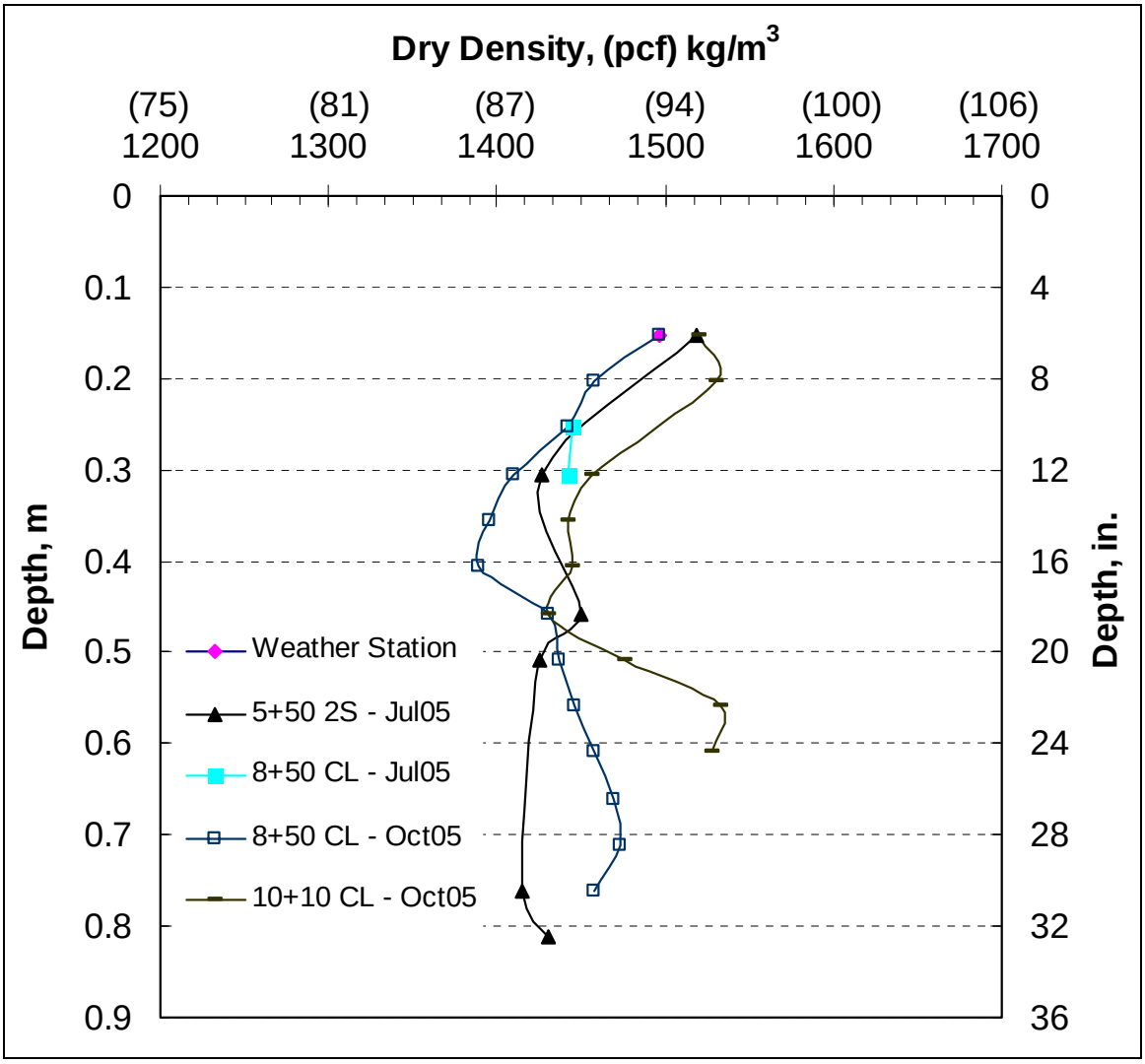


Figure 24. Soil density profiles taken using a nuclear density gage at five locations on Fort Bliss RAS.

Because it is difficult to measure the density of the caliche layer using the Troxler Nuclear Gage, samples of caliche pieces were brought to the laboratory. The density was measured following the volume displacement method as described in EM 1110-2-1906, Laboratory Soils Testing. The caliche density ranges from 1873 to 2033 kg/m^3 (116.9 to 126.9 lb/ft^3) as listed in Table 8.

Table 8. Laboratory analysis of density for caliche samples.

Sample		FB WX STN 3"-4"	FB WX STN 7.5"	FB 170m 14"
Wt. Sample + Paraffin in Air	gm	127.54	45.84	130.20
Wt. Sample in Air	gm	119.50	43.11	123.39
Wt. of Paraffin in Air	gm	8.04	2.73	6.81
Vol. of Paraffin	cc	8.93	3.03	7.57
Wt. Sample + Paraffin in Water	gm	57.87	22.61	61.79
Vol. of Sample + Paraffin	cc	69.67	23.23	68.41
Vol of Sample	cc	60.74	20.20	60.84
Wet Unit Wt of Sample	lb/ft^3	122.77	133.19	126.55
Moisture Content	%	4.18%	4.96%	8.21%
Dry Unit Wt of Sample	lb/ft^3	117.85	126.90	116.95
Dry Unit Wt of Sample	kg/m^3	1888	2033	1873

5.1.4 Organics

One test sample was taken to measure the organic content for station 1+70 and a test sample for the weather station, while three replicates were performed for station 5+50 2S. The results from replicate tests are reported here as average value. The organic contents found at stations 1+70 CL, 5+50 2S, and the weather Sstation were 0.86, 0.86 and 0.80 percent, respectively. Because this area has relatively little vegetation, a low organic content is to be expected.

5.1.5 Natural Resources Conservation Service (NRCS) Soils Information

The soils data reported in the Soil Survey Geographic (SSURGO) database do not quite match the soil type found on the RAS. The RAS soils information published on the SSURGO database produced by USDA, Natural Resources Conservation Service (NRCS), reported the soil type from various horizons described as well-drained very fine sandy loam, presented in Table 9. The OLS location is classified with a soil series called Jerag very fine sandy loam with 1- to 5-percent slopes and the USCS soil type ranges from clay (CL), clayey and silty sand (SC-SM), to gravelly clay (GC). Clay soils were not found on the RAS but possibly can be found on the playas (outside the RAS area).

Soil density information presented in Table 10 is from the SSURGO Database by USDA, NRCS, which measured density of natural soil samples (i.e., soil clods. The bulk density is typically estimated from laboratory measurements on selected functions, or algorithms based on pedotransfer functions. The soil density in the SSURGO data reported the representa-

tive soil bulk density of the area in the range between 1200 and 1400 kg/m^3 (75 and 87.4 lb/ft^3) with volume determined at water tension of 1/3 bar. Also, the representative values for soil bulk density reported for coated soil clod vary from 1440 to 1560 kg/m^3 (89.9 to 97.4 lb/ft3), which are within the range of our measured dry densities from the nuclear gage.

5.1.6 Soil Characterization Discussion and Summary

Table 10 shows the soil type profiles measured at the Fort Bliss RAS using the USCS method, along with the percentage of fines and density. Along the OLS, the upper layer, varying in depth, is mainly non-plastic silty sand (SM). However, based on the grain size results, most of the soil samples have fines portion (passing 0.1 mm) with almost 50% indicating that the soils are borderline ML. Then a transition zone of gravelly silt (caliche pieces with silt) material is typically found immediately above the caliche layer. Caliche is a deposit of calcium carbonate, which acts as a cement with other materials, including gravel, sand, clay, and silt. Caliche occurs worldwide, generally in arid or semi-arid regions (Rollings and Rollings 1996 [http://en.wikipedia.org/wiki/Caliche_%28Mineral%29]). Information from wikipedia.org indicated that caliche layers can vary from a few inches to feet thick, and multiple layers can exist in a single location. For this study, we recorded only the depth of the shallowest coherent caliche layer because mechanized excavation equipment was not available or desirable for use on the RAS.

The modified proctor result on the Fort Bliss OLS soil sample showed that the soil has an optimum density of 1884 kg/m^3 (117.6 lb/ft^3) with a corresponding maximum moisture content of 12.6% (Danyluk et al. 2008). The in-situ dry density values measured on the OLS are significantly lower than the density from the modified proctor, which is a density value of this particular soil for airfield design and construction. The in-situ soil density varies with depth, which is common on natural soils. Because soil density is one of the major parameters in soil strength, variability in soil density will result in inconsistent soil strength. Soil failure (i.e., sinkage resulting from soil compaction) can occur on soil with low density if subjected to loading by aircraft traffic.

Organic content was found to be insignificant and will not cause any harm to the aircraft.

Table 9. Soil information published by Soil Survey Geographic (SSURGO) Database, NRCS map unit number 63 (Jerag very fine sandy loam, 1 to 5 percent slopes).

Horizon Layer	Horizons	Distance from top of soil to upper bound of soil horizon cm	Distance from top of soil to base of soil horizon cm	Distance from top to bottom of soil horizon cm	The oven dry weight of the less than 2 mm soil material per unit volume of soil at a water tension of 1/3 bar. Low Value g/cc	Representative Value g/cc	High Value g/cc	The oven dry weight of the less than 2 mm soil material per unit volume of soil exclusive of the desication crack, measured on a coated clod. Representative Value, g/cc	USCS
A	A	0	8	8	1.35	1.4	1.45	1.46	CL, SC-SM
Bt	B	8	23	15	1.25	1.3	1.35	1.48	CL
Bk	B	23	48	25	1.25	1.3	1.35	1.56	CL, GC
Bkm	B	48	64	16					
2Bk	B	64	203	139	1.15	1.2	1.25	1.44	CL, GC

Table 10. Summary of the soils on the RAS at Fort Bliss.

Soil Properties	USCS Type [A]	Percent Fines	Specific Gravity	USCS Type [A]	Percent Fines	Specific Gravity	USCS Type [A]	Percent Fines	Specific Gravity	Dry Density kg/m^3	USCS Type [A]	Percent Fines	Specific Gravity	Dry Density kg/m^3	USCS Type [A]	Percent Fines	Specific Gravity	Dry Density kg/m^3	USCS Type [A]	Percent Fines	Specific Gravity	Dry Density kg/m^3
Sampling Station	**1+70 CL**			**2+50 10S**			**5+50 2S**				**8+50 CL**				**10+10 CL**				**Weather Station**			
Depth, m																						
Surface	SM	32.0	2.58	SM	32.2	2.63	SM	37.1	2.60	-	SM	22.2	2.60	-	SM	32.4	2.62	-	ML	54.7	2.57	
0.025-0.15 (1-6)				SM	28.4	2.62					SM	27.3	2.62	1496	SM	34.2	2.60	1520	Caliche	0.4	-	1496
0.15-0.2 (6-8)							SM	44.6	2.62	1518	SM	36.5	2.60	1458	SM	41.7	2.62	1530	GM	22.2	2.57	
030 (12)				SM	37.1	2.63	SM	44.9	2.63	1427	SM	42.1	2.63	1410	SM	42.5	2.6	1456				
0.36 (14)	Caliche	1.2	-											1395				1442				
0.46 (18)										1450	SM$^+$	14.9	2.62	1430				1430				
0.76 (30)							SM	43.8	2.63	1414				1458								

[A] Unified Soil Classification System Descriptions:

GM = Caliche with sand
ML = Sandy silt
SM = Silty sand
SM$^+$ = Silty sand with caliche chunks

All Non-plastic soils (Plasticity Index = 0)

5.2 Seasonal Impacts

5.2.1 Surface Conditions

5.2.1.1 Surface Condition and Features

A walk-through visual survey along the RAS was conducted to determine the surface condition of the runway during IOP #1. From the visual survey, the observer noted vegetation type, vegetation cover, tire tracks or ruts, drainage, soil scouring from water or animals, land marks, mounds, animal holes, artillery rounds, and anything else that could present a hazard to aircraft operations. A sketch was generated from the visual survey as shown in Figure 25. The sketch is a symbolic illustration of the surface features and is not drawn to precise scale. No additional visual survey was conducted in the subsequent visits because no significant changes were observed.There were areas of animal holes all over the RAS and in the area near the RAS. The holes ranged in size from 0.025 to 0.2 m (1 to 8 in.) in diameter and some had significant mounds of dirt adjacent to the holes (Fig. 26a). When we stepped on an animal burrow area, our shoes sunk in and created a depression under the footprint. The animal burrows consisted of connected animal holes with series of small tunnels creating soil voids. The depth of these burrows was difficult to survey and was not investigated, but we assumed that most burrows were above the caliche layer and may be into the caliche layer. Large pieces of caliche were often observed on the ground where mounds with animal holes were located (Fig. 26b). Another feature observed on the RAS was small holes in the middle of a cleared area, which seemed to be where ants were nesting (Fig. 26c). A more detailed compilation of photos taken during IOP #1 is shown in Appendix B. Although the thorough survey of the surface features was conducted during the first IOP (IOP #1) as illustrated in Figure 25, features such as the animal burrows and ant holes remained in the same vicinity based on the brief surveys conducted during IOP #2 and IOP #3.

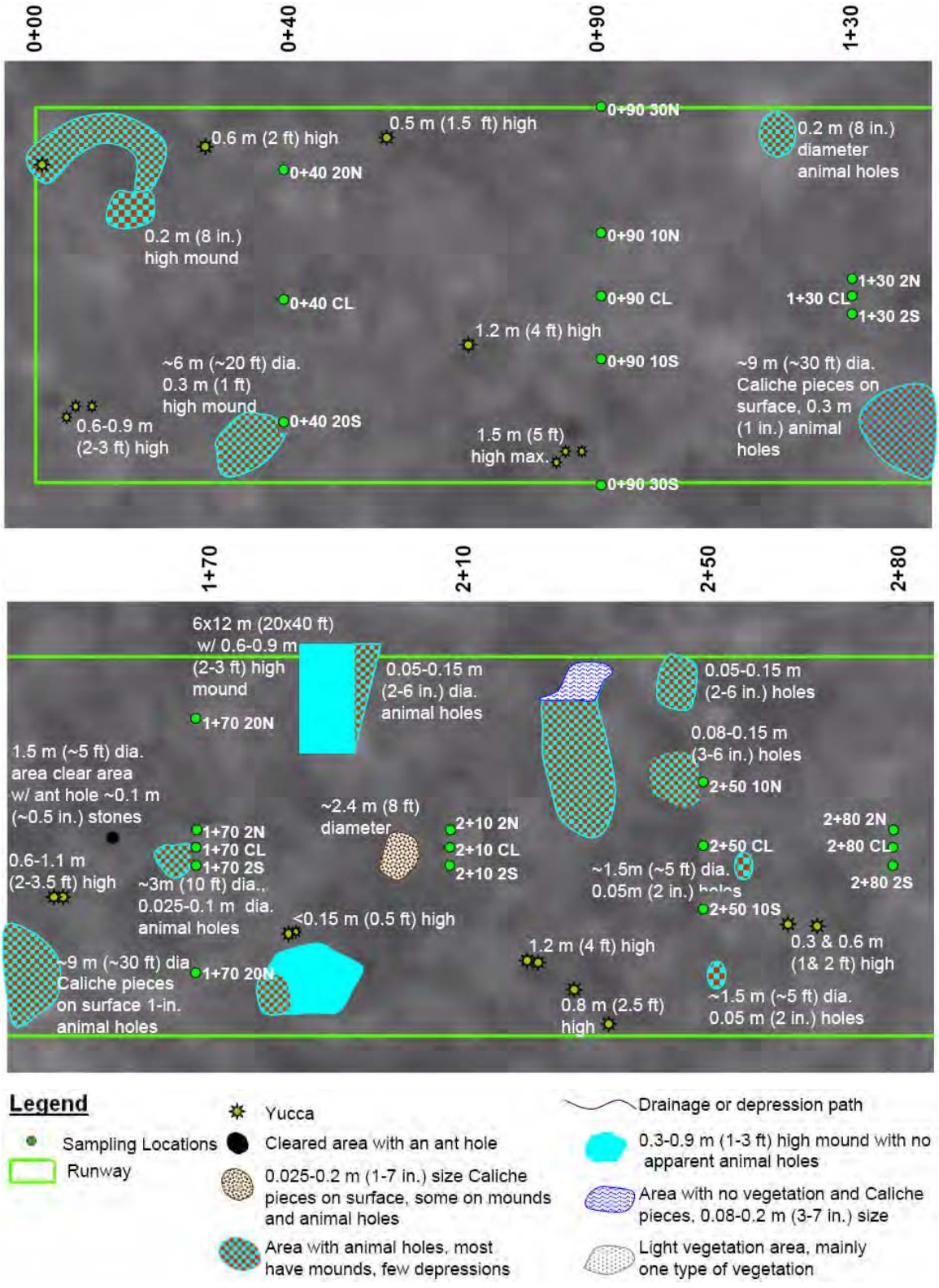


Figure 25. Symbolic representation of surface features from the visual survey along the RAS in sections.

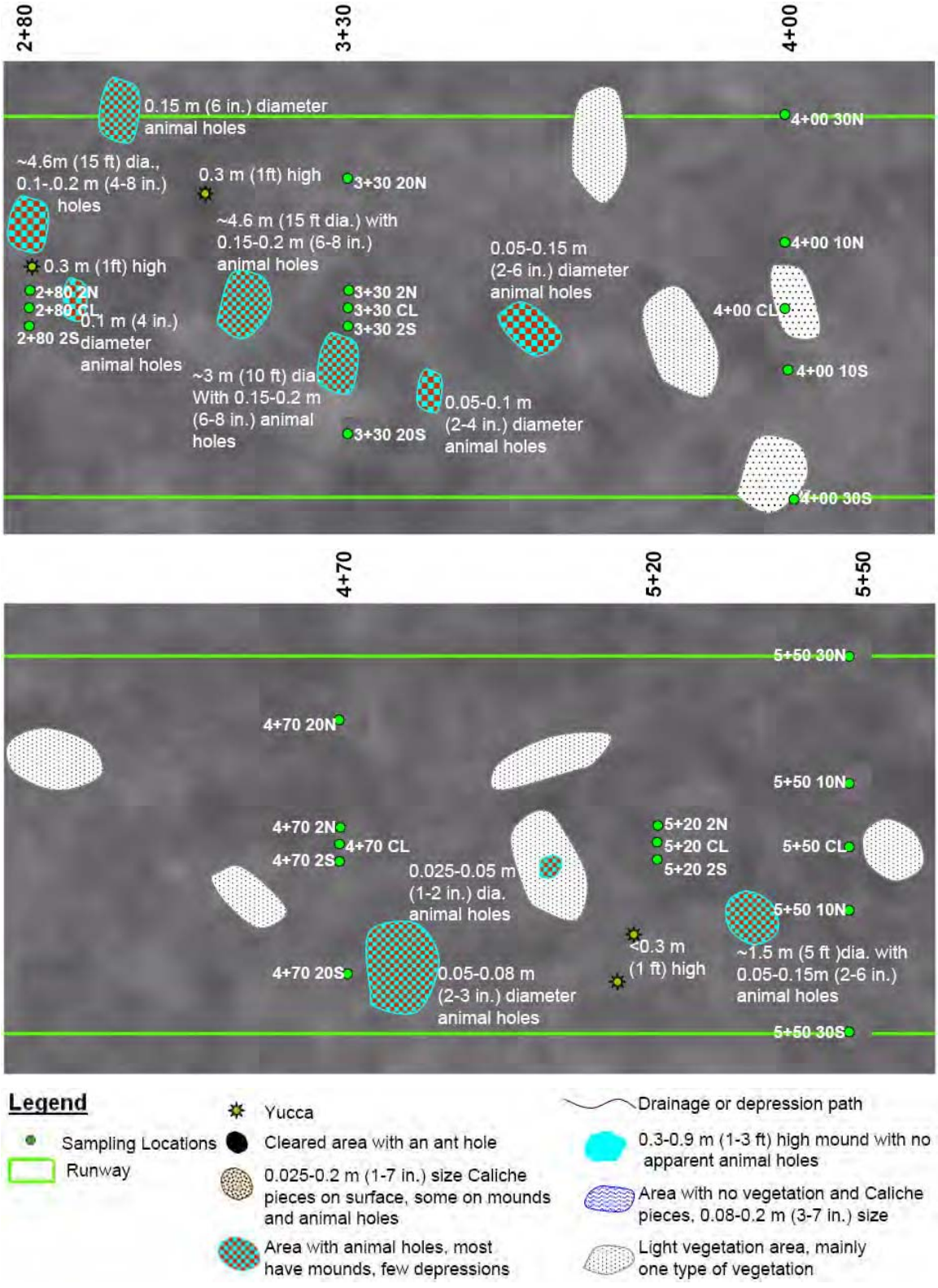


Figure 25 (cont'd).

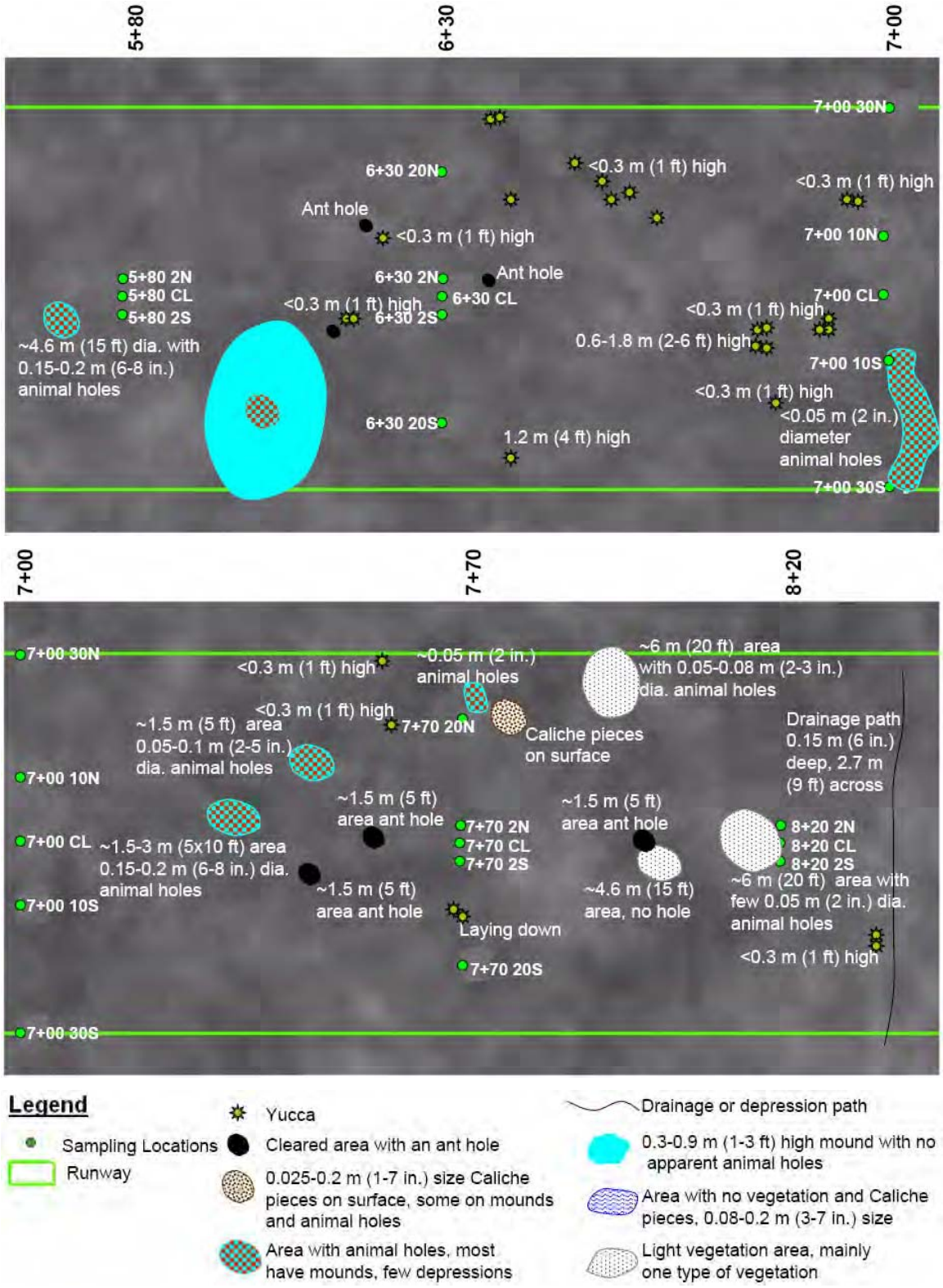


Figure 25 (cont'd). Symbolic representation of surface features from the visual survey along the RAS in sections.

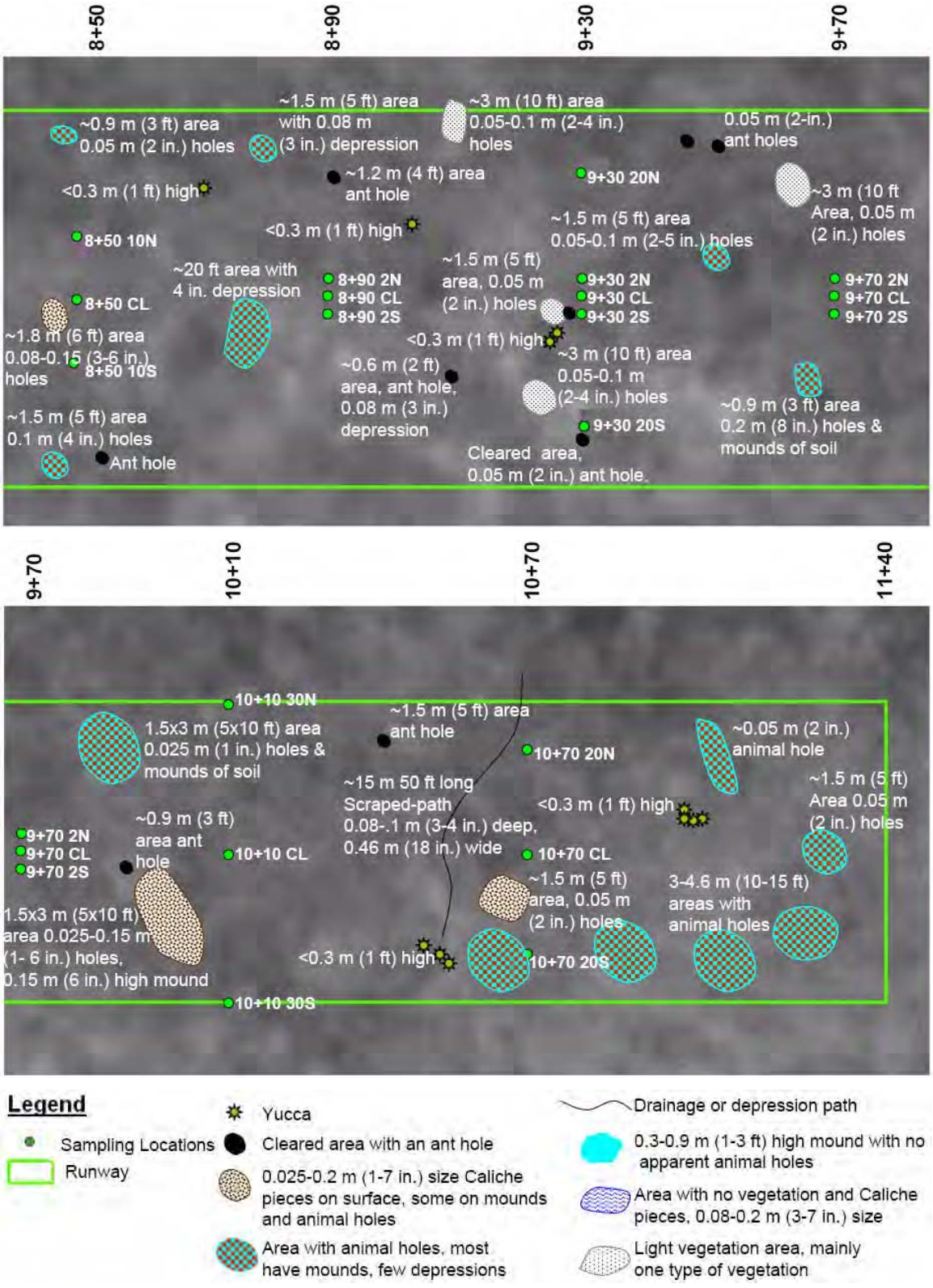


Figure 25 (cont'd).



a. Soil mounds with animal holes near Station 2+80. Photo taken during IOP #1.



b. Large mound with animal holes and gravelly (caliche pieces) materials on the surface near Station 3+30. Photo taken during IOP #1.

Figure 26. Surface features such as mounds, animal burrows, and caliche pieces observed on the RAS at Fort Bliss



c. Example of a clear area with small holes and small calicle particles on the surface. Photo taken near station 8+20 during IOP #3.

Figure 26 (cont'd).

5.2.1.2 Vegetation Type and Height

The primary vegetation types on the RAS and their distribution are described below in Figure 27. The vegetation types remained the same every season even though they went through a seasonal growing cycle.

The vegetation height of each plant is reflected in the photos in Figure 27. With the exception of the yucca trees and cholla, most of the vegetation on the RAS was less than 0.5 m in height.



a. Yucca baccata.[1]



b. Penstemon patens.[2]



c. Opuntia imbricata (cholla).[3]

Figure 27. Typical vegetation types on Fort Bliss RAS and the surrounding area.

[1] There are a few yucca trees on the RAS. This plant is strong and rugged and can reach 3 m (10 ft) in height with a 0.3-m- (12-in.-) diameter trunk.

[2] There are a limited number of penstemon patens on the RAS.

[3] There are a few of these bushes on the RAS.



d. Delphinium virescens.[4]



e. Nolina microcarpa.[5]



f. Lygodesmia exigua.[6]

Figure 27 (cont'd).

[4] There are a few of these plants along the RAS.

[5] There are a few nolinas on the RAS.

[6] This is a common plant in the area.



g. Salsola tragus.[7]



h. Verbesina enceloides.[7]



i. Guteriezia sarathoides.[8]

Figure 27 (cont'd). Typical vegetation types on Fort Bliss RAS and the surrounding area.

[7] This is one of the common plants on the RAS.

[8] There are a few guteriezia sarathoides in the area.



j. Croton wigginsii.[9]



k. Erioneuron pulchellum.[10]



l. Physalis.[11]

Figure 27 (cont'd).

[9] There are a limited number of these plants on the RAS.

[10] This is a common plant on the RAS.

[11] Physalis is one of the uncommon plants in the area.



m. Plantago eriopoda.[12]



n. Lappula medouskii.[12]



o. Pectis papposa.[13]

Figure 27 (cont'd). Typical vegetation types on Fort Bliss RAS and the surrounding area.

[12] There are a few of these plants on the RAS.

[13] This is a common plant along the RAS.

5.2.1.3 Vegetation Cover and Greenness

The variation in vegetation cover at this RAS may change from season to season, and also is dependent on disturbances generated from cattle grazing in the area. Analysis to determine the vegetation cover was conducted on photos taken during October IOP (IOP #2). A summary of the vegetation coverage is listed in Table 11. These photos were selected by dividing the RAS into six areas and a photo to represent each sectional area was randomly picked for the analysis. The vegetation cover varied throughout the RAS, as shown in Figure 28. Localized dense and sparse vegetation covers were observed on the entire RAS. Even in areas with dense vegetation cover, the ground surface was still visible between plants.

Table 11. Vegetation cover summary from the photos taken during IOP #2 at selected sampling locations.

Sampling locations	0+90 CL	2+10 CL	5+50 CL	7+00 CL	8+50 CL	10+10 CL
Vegetation cover, %	75	56	39	53	43	41



a. 0+90 CL

Figure 28. Vegetation cover calculated from the photos taken at six locations. Hatched polygons are digitized areas of plant cover along the RAS.



b. 5+50 CL



c. 2+10 CL

Figure 28 (cont'd). Vegetation cover calculated from the photos taken at six locations. Hatched polygons are digitized areas of plant cover along the RAS.



d. 7+00 CL



e. 8+50 CL.

Figure 28 (cont'd).



f. 10+10 CL

Figure 28 (cont'd). Vegetation cover calculated from the photos taken at six locations. Hatched polygons are digitized areas of plant cover along the RAS.

Seasonal changes in vegetation in terms of greenness and health of the various plants were observed during the summer, fall, and spring IOPs (Fig. 29). Some plant types (i.e., Guteriezia sarathiodes) remained green while others turned brown (Fig. 29a) during the summer IOP (in July). The vegetation is greener in October (IOP #2, Fig. 29b) than in July. During the third IOP (in April 2006), nearly all the vegetation was brown (Fig. 29c). This vegetation cycle is relatively typical in semi-arid environments, being tied more to moisture availability than to seasonal temperature changes.

5.2.1.4 Surface Water

No surface water was observed on the RAS during any of the IOPs.

5.2.1.5 Rutting

There was no evidence of vehicle tracks on the RAS because vehicles are not allowed to drive overland—they can park only off the side of the road. The main disturbance was tracks and footprints from the cattle, because the area is used for grazing.



a. July 2005 at station 5+50 CL looking west.



b. October 2005, at station 5+80 CL looking west.

Figure 29. Variation in vegetation greenness during three IOPs at Fort Bliss OLS.



c. April 2006, at station 5+50 CL looking west.

Figure 29 (cont'd). Variation in vegetation greenness during three IOPs at Fort Bliss OLS.

5.2.1.6 Dust

When the ground is disturbed, dust is quite common in the dry environment. There are enough fine particles in the soil, ranging from 22 to 55% of less than 0.075 mm (#200 sieve) in size to create dust clouds when the soil surface is disturbed. Dust was created while digging and filling soil pits, but it was not noted or quantified. Significant dust was observed when ranchers drove their vehicles on the dirt road near the RAS during all three IOPs. When we drove vehicles as a caravan, approximately 60 m (200 ft) of the road was visible in front of the trailing vehicle when the leading vehicle was at a distance of 150–250 m (500–800 ft). However, we have no photos of dust generated by digging or from vehicle traffic to illustrate the dispersion of particles and clearing.

5.2.1.7 Surface Conditions Discussion and Summary

A summary of the surface conditions and their ratings for the OLS is described in Table 12, which is based on Table 3 in Section 3. Some of the ratings are considered subjective and other distress types do not apply particularly for an OLS (i.e., jet blast erosion or stabilized layer failure).

Cemented layers such as the caliche could be considered as stabilized; however, its surface irregularity and unevenness can harm an aircraft (i.e., sinkage and tire punctures).

Table 12. OLS rating for surface condition for all seasons.

	Surface categories	Rating
1	Potholes	**Green and Amber**: < 100 to 230 mm (< 4 to 9 in.) deep and > 380 mm (15 in.) in diameter
2	Loose aggregate	**Amber**: Covers between 1/10 and 1/2 of RAS
3	Ruts	**Green:** No ruts
4	Rolling resistance material	**Amber**: > 195 mm (7.75 in.) deep
5	Dust	**Amber**: Partially obstructs visibility, appr. 400 m (¼ mile)
6	Jet blast erosion	Not applicable on the RAS because there is no scouring caused by jet blast erosion.
7	Stabilized layer failure	Not applicable on the RAS because of caliche layer.
8	Animal burrows	**Amber and Red**: Number of animal holes between 3 and more than 6 in some areas with 25-mm- (1-in.-) dia. holes, in a 10- by 10-m area, at every 100 m.
9	Mounds	**Green**: < 100 mm (4 in.) high and/or < 380-mm- (15-in.-) diameter base
10	Vegetation	**Green**: < 0.5-m (1.5-ft) high grass, no bushes or branches
11	Standing water	**Green**: No water ponding
12	Surface drainage paths	**Green**: Exists, but < 100 mm (4 in.) deep
13	Surface debris and organic materials	**Green:** Minimal organics on the RAS
14	Snow depth	**Green**: Zero snow cover

Potholes are normally caused by soil failure from vehicle loading. However, existing pothole-like shapes or depressions observed on the RAS are created from existing and abandoned animal burrows. These irregular bowl shapes on the surface are generated from natural compaction and settlement of soil into voids from the animal holes. The RAS is rated as "Amber," which is assigned to irregular bowl shapes between 100 and 230 mm (< 4 to 9 in.) deep, and greater than 380 mm (15 in.) in diameter.

Areas with animal burrows were prevalent on the RAS. If the RAS is subjected to aircraft loading, uneven compaction may take place and localized soil failure can occur. The number and size of the holes, and the area covering the animal burrows, are quantified for rating. A rating of "Red" indicates more than six holes of less than 25-m (1-in.) diameter, in an approximately 10- by 10-m area, every 100 m or less. With big holes in a

large area, it is likely that rutting and depression will result when an aircraft lands on the OLS. Using "Green, Amber, Red" criteria defined in Table 3 (Section 3) for surface category, the rating in terms of surface condition due to existing animal burrows can be rated as "Amber," and "Red" in some sections of the RAS.

Caliche pieces ranging in size from 0.025 to 0.2 m (1 to 7 in.), and a fair estimate of 10 to 20% coverage of loose caliche, were found on the ground surface. Rocks larger than 0.1 m (4 in.) must be removed from the operational surface according to AFCESA's criteria. Loose aggregate is considered to be a potential cause of Foreign Object Damage (FOD), which can damage aircraft components such as engines, tires, etc. Using "Green, Amber, Red" criteria, the OLS is rated as "Amber" because of loose aggregate between 1/10 and 1/2 of the RAS.

With the exception of a small number of yucca trees on the RAS, the vegetation will not limit landing aircraft. The yucca trees could be a significant obstruction, but there are very few and they are fairly small. Using the criteria listed in Table 3 for "Green, Amber, Red" criterion, the RAS is rated as "Green" for vegetation obstruction.

Dust is certainly an issue in the semi-arid environment. There are large amounts of fine particles in the soil ranging from 22 to 55% of less than 0.075 mm in size that can be airborne for a minute or two. Dust was observed to be thick and obstructed visibility. Using "Green, Amber, Red" criteria, the RAS is rated as "Amber," which is used when dust partially obstruct visibility.

5.2.2 Soil Moisture

Soil moisture was measured using several methods in both volumetric and gravimetric units with considerable variation among measurement methods (Appendix C). Sampling locations where soil moisture was measured at various depths during all IOPs are listed in Table 6.

5.2.2.1 Dynamax (ML2, PR2)

During IOP #1, soil moisture contents taken by the HH2 (ML2) probe were measured only in the soil pits. Soil moisture content readings were taken at least three or more times for replication. In order to capture the

moisture profile, soil moisture contents were measured at the surface and at various depths (e.g., 0.08, 0.15, 0.3, 0.6, 0.9 m [3, 6, 12, 24, 36 inches]). In most cases on this RAS at depths less than 0.9 m, the tines or rods had difficulty extending into the soil because of the granular soil or the caliche layer.

The soil moisture profiles from the replicate readings during the first IOP can be seen in Figure 30 and showed that the moisture is within 1-3% volume between readings. The soil moisture near the surface was less than 4% by volume throughout the RAS, and depending on the location the moisture gradually increased with depth, then slightly decreased below 0.3 m. The average soil moistures were calculated for each location (Fig. 31) and moisture profiles reflected the low values in July for dry summer condition in the area.

The soil moisture contents using the HH2 (ML2) probe taken during IOP #2 (October IOP) are shown in Figure 32. During this IOP, soil moisture measurements were taken at approximately 77 sampling locations shown as dots in the contour profile. The surface moisture in IOP #2 ranged from 5 to 10% volume near the surface. Moisture content gradually increased with depth, then slightly decreased below 0.3 m.

Weather records immediately prior to the October IOP show recent rainfall (Fig. 33). Two separate rain events occurred, with 9.5 mm of rainfall on October 16th and less than ¼ of mm on October 20th. These rainfall events explain some, if not all, of the soil moisture changes observed during the October IOP.

Only surface moisture was measured using the HH2 during IOP #3. The surface moisture contents from the three IOPs show a very dry summer, some moisture in the soil in the fall, and a dry spring (Fig. 34). During IOP #2 (October 2005), the vegetation was also much greener than during IOP #1 (July 2005) and IOP #3 (April 2006).

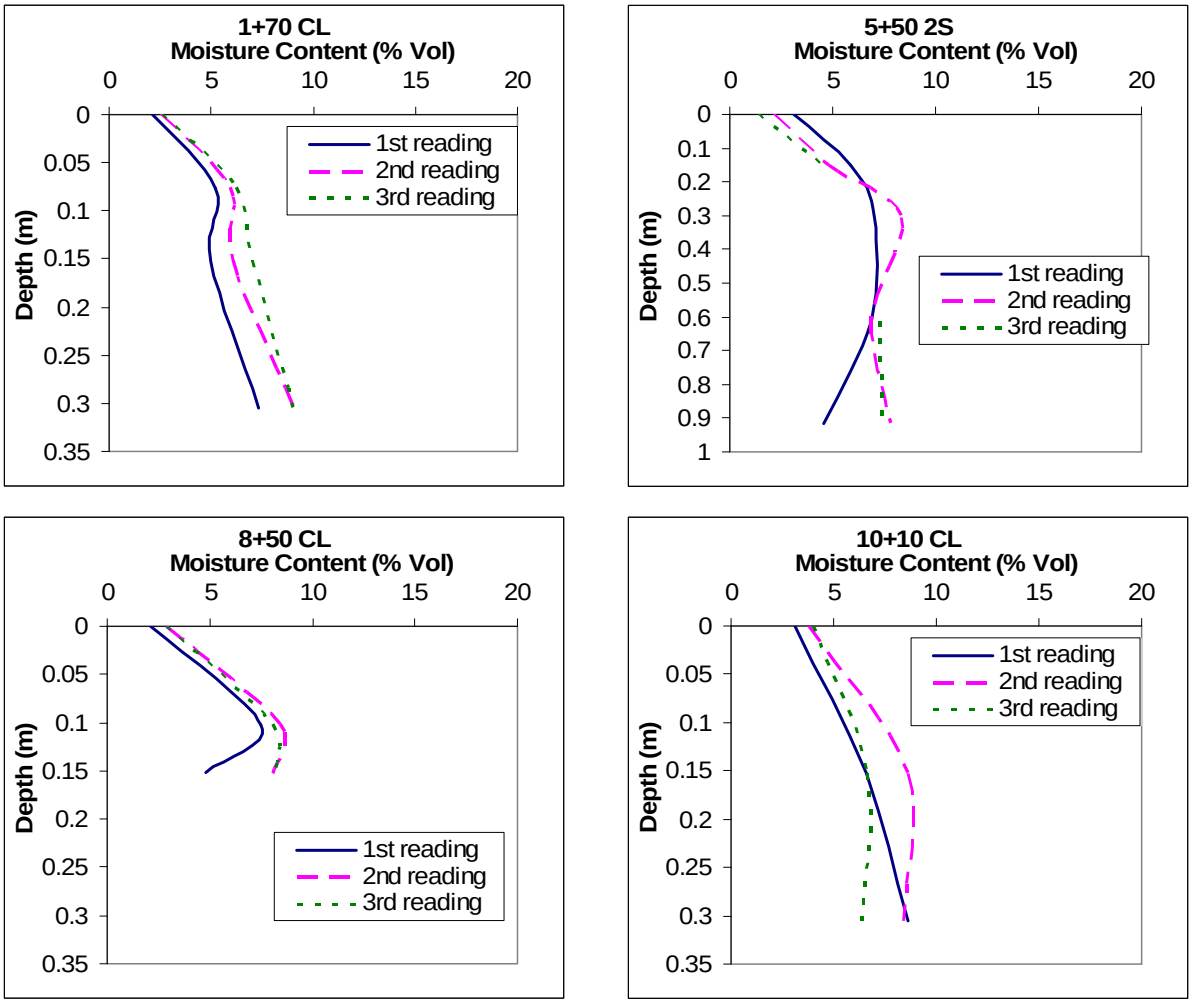


Figure 30. Moisture profiles taken from Dynamax ML2 probes during IOP #1.

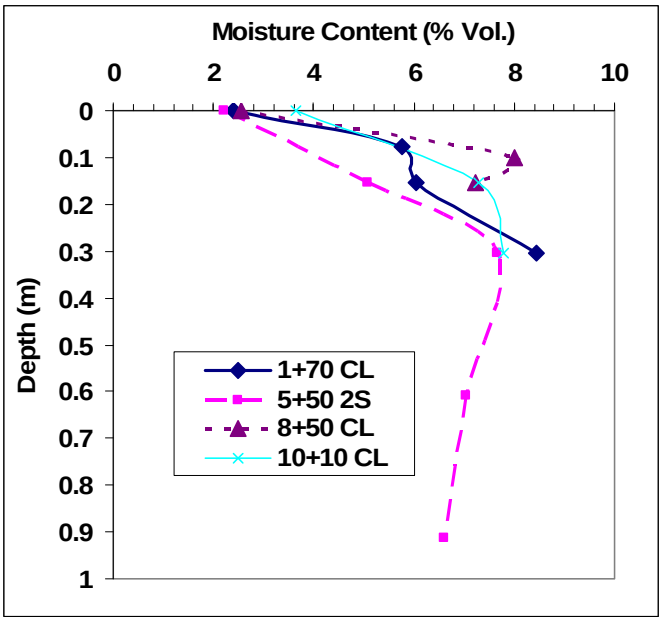


Figure 31. Average soil moisture profiles from the Dynamax ML2 probes taken during IOP #1 (July 2005)

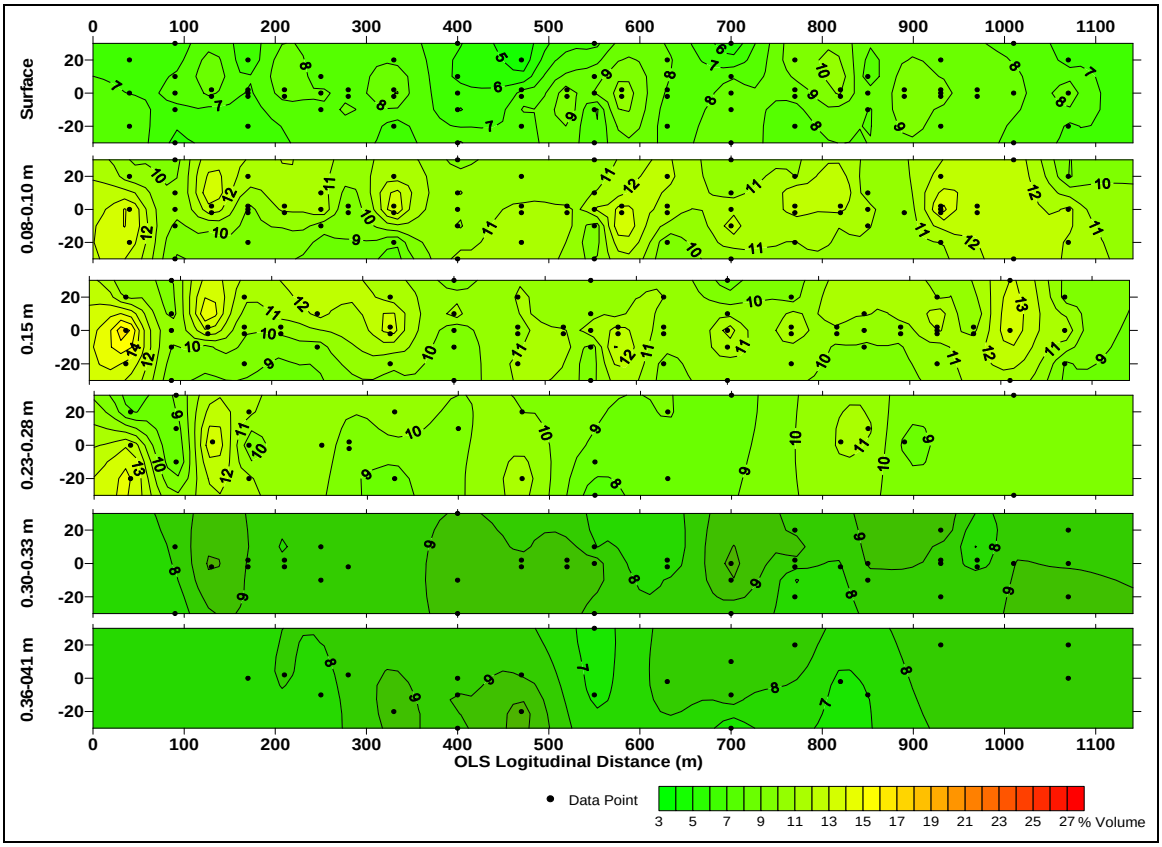


Figure 32. Profiles of soil moisture contents in % volumetric from the Dynamax ML2 taken in October 2005, as shown in contours. The dots are the sampling locations where soil moisture measurements were taken with depth in the soil.

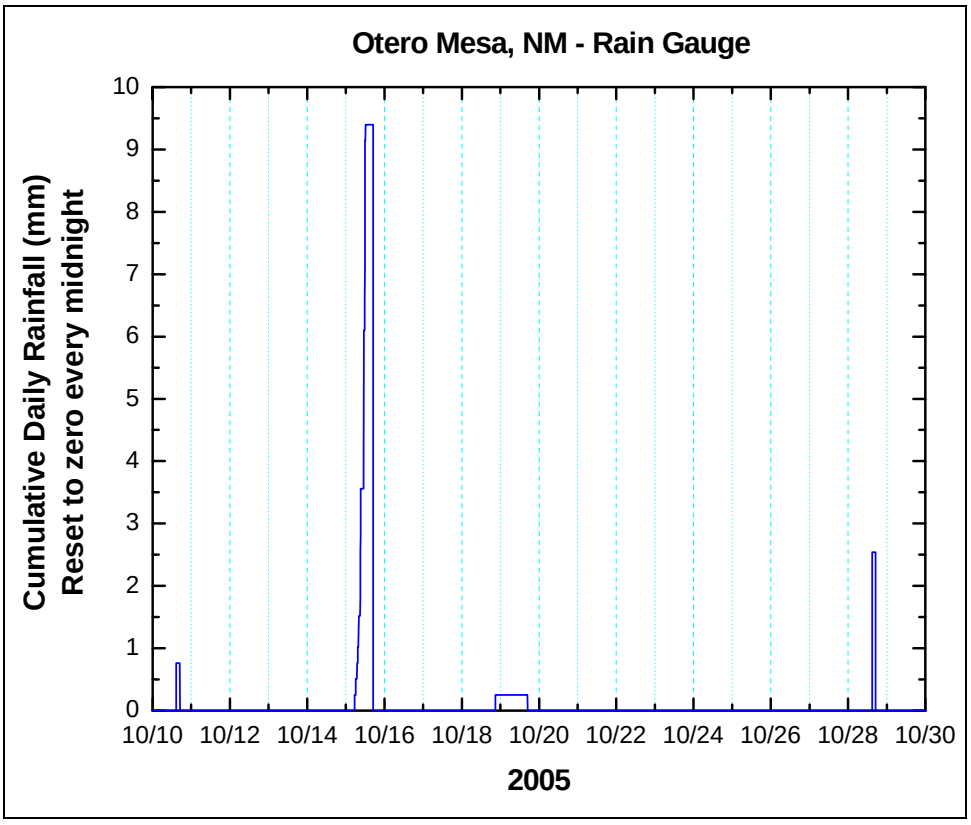


Figure 33. Precipitation observed from the weather station installed near the RAS.

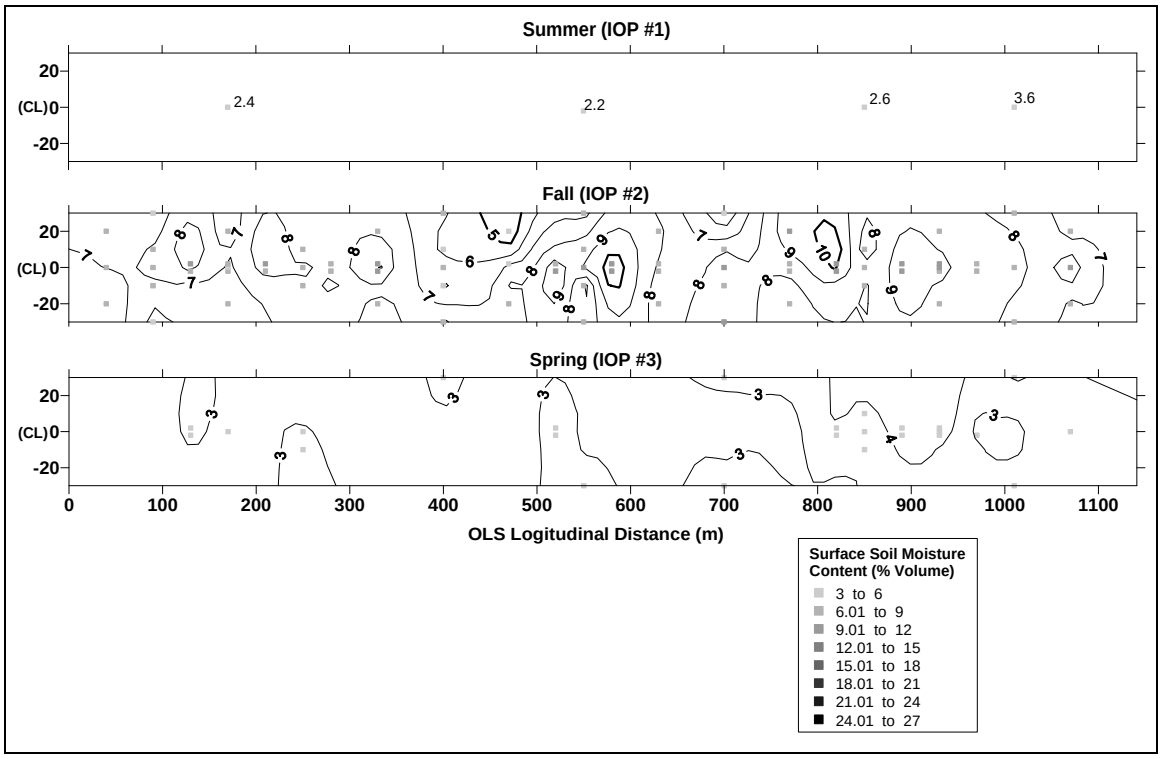


Figure 34. Surface soil moisture (in % volume) for three field visits at Fort Bliss RAS.

5.2.2.2 Gravimetric Soil Moisture Contents (Including Drive-Cylinder Soil Samples)

The profiles for soil moisture contents obtained from the gravimetric samples taken during summer and fall are reported in Figure 35. Soil moisture content profiles for IOP #1 (summer condition) were measured at 2.4% and 2.6% near the surface, then the soil moisture increased with depth, but the whole soil moisture profile was quite dry. During IOP #2, the soil was more moist, with soil moisture ranging from 3.8 to 11.4% throughout the profile.

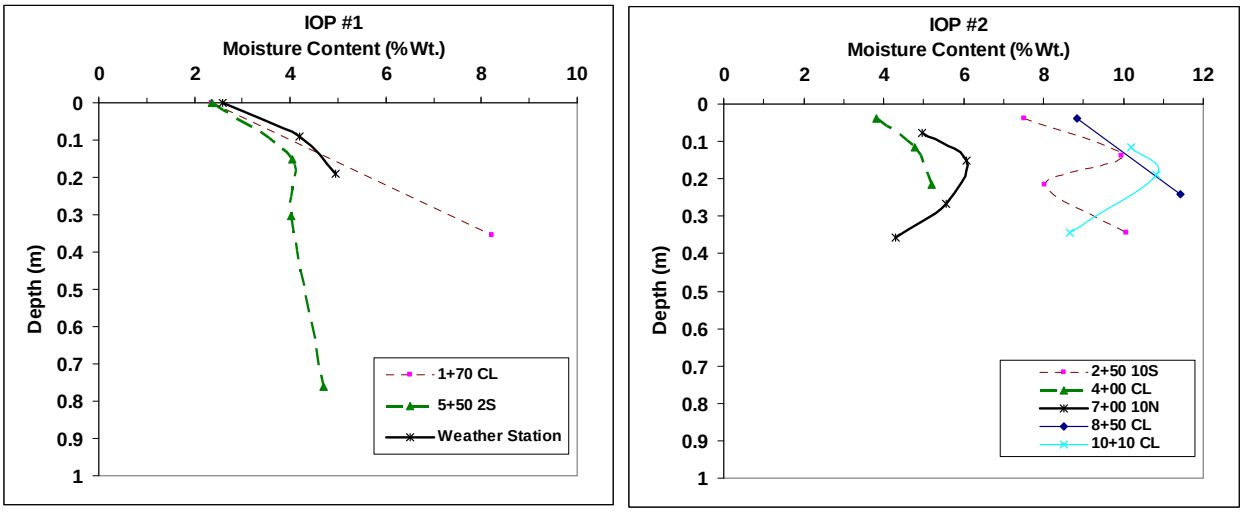
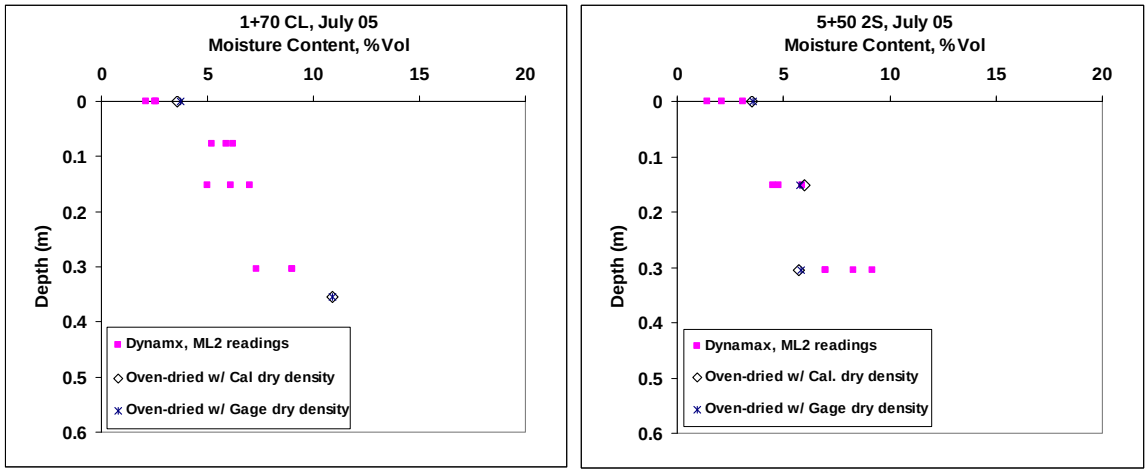
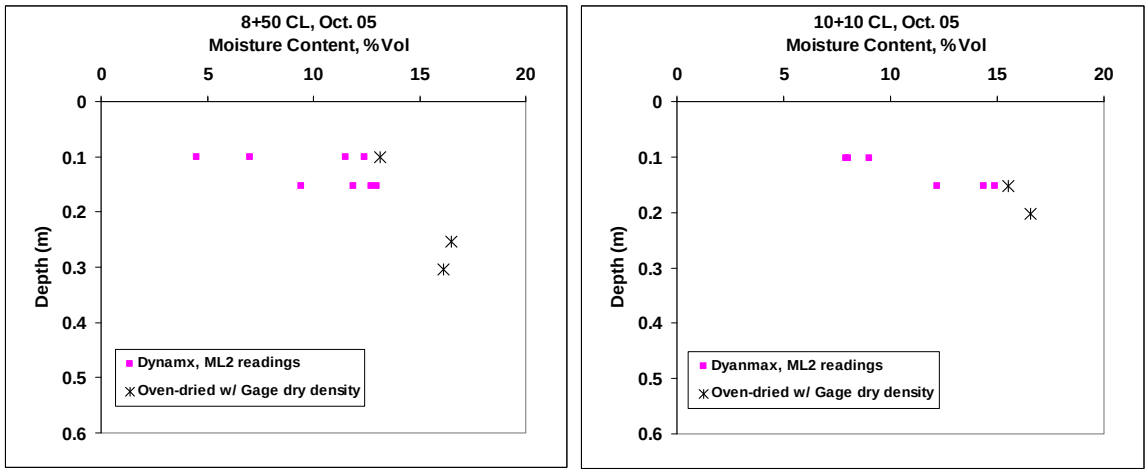


Figure 35. Soil moisture profiles using the gravimetric method from samples taken in July 2005 (IOP #1) and in October (IOP #2).

Soil moisture contents measured between the Dynamax ML2 and the gravimetric soil samples are found to be within 2 to 3 % water content of one another for IOP #1 (Fig. 36a). More scatter was observed in soil moisture measurements taken during IOP #2, as can be seen in Figure 36b.



a. IOP #1.



b. IOP #2.

Figure 36. Gravimetric moisture contents converted to percent volume along with soil moisture profiles measured using the Dynamax ML2.

5.2.3 Soil Strength

5.2.3.1 Dynamic Cone Penetrometer (DCP)

An Excel macro procedure was developed to average the CBR profiles for each sampling location within each of the following depth ranges:

a) 0 to 0.15 m (0 to 6 in.);

b) 0.15 to 0.30 m (6 to 12 in.);

c) 0.30 to 0.45 m (12 to 18 in.);

d) 0.45 to 0.6 m (18 to 24 in.);

e) 0.60 to 0.75 m (24 to 30 in.) and;

f) 0.75 to 0.9 m (30 to 36 in.).

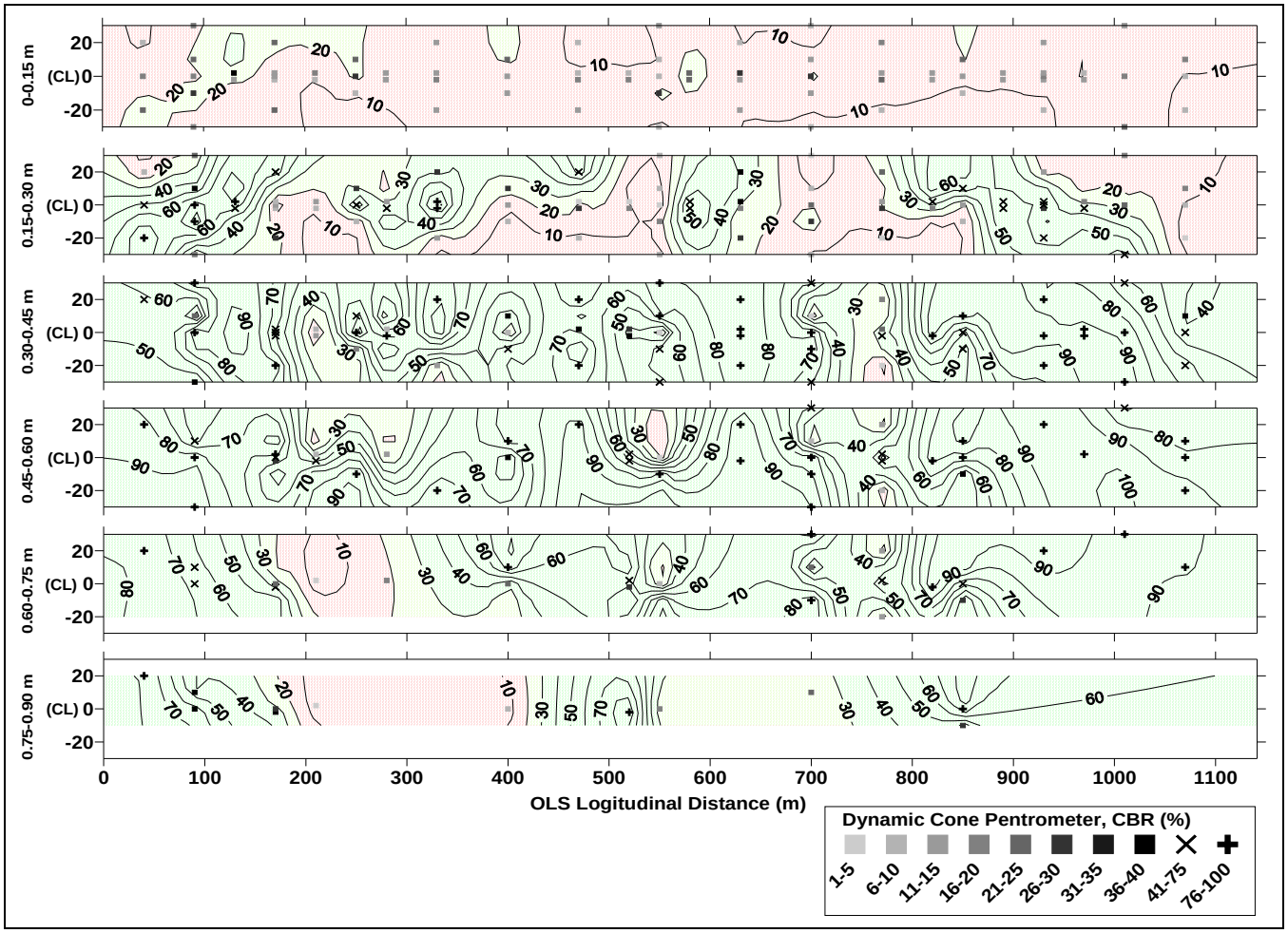
These groupings enable easy comparisons of the data. The CBR data for each IOP are graphed using contour plots, and the sampling locations are marked using shading and shapes denoting the CBR value (Fig. 37).The summary for the averages from CBR profiles are listed in Table 13 for IOP #1, IOP #2, and IOP #3.

As described in Section 5.1, a caliche layer was observed while pits were dug. Encountering the upper layer of the caliche was apparent when conducting the DCP tests if the rod would not penetrate further, and in some cases the device bounced as the DCP weight was being dropped. Hence the test was stopped at that depth. Although the ETL (AFCESA 2002a) recommended drilling through the hard layer and continuing the DCP testing past the hard layer primarily to look for a soft layer that might fail, this was unnecessary on the RAS due to geologic features (i.e., caliche layer). At deeper depth ranges, e.g., 0.60 to 0.75 m (24 to 30 in.) and 0.75 to 0.9 m (30 to 36 in.), the contours can be questionable because of missing data points.

During IOP #1 (in July 2005), an increasing trend of CBR with depth was typically found on the RAS. CBR values for the 0.15- to 0.3-m (6- to 12-in.) soil layer ranged from 3 to 92. At this layer, several sampling locations showed a well-defined area with CBR values less than 10 (1+70 2N, 4+70 2N, 5+50CL, and several others) see Table 13 (Fig. 37a). However, soil strength increased significantly in the 0.30-to 0.45-m (12- to 18-in.) depth range on most of the RAS, with few small pockets of soft areas (Fig. 37a). The caliche layer was the main source of the soil strength increase at this depth.

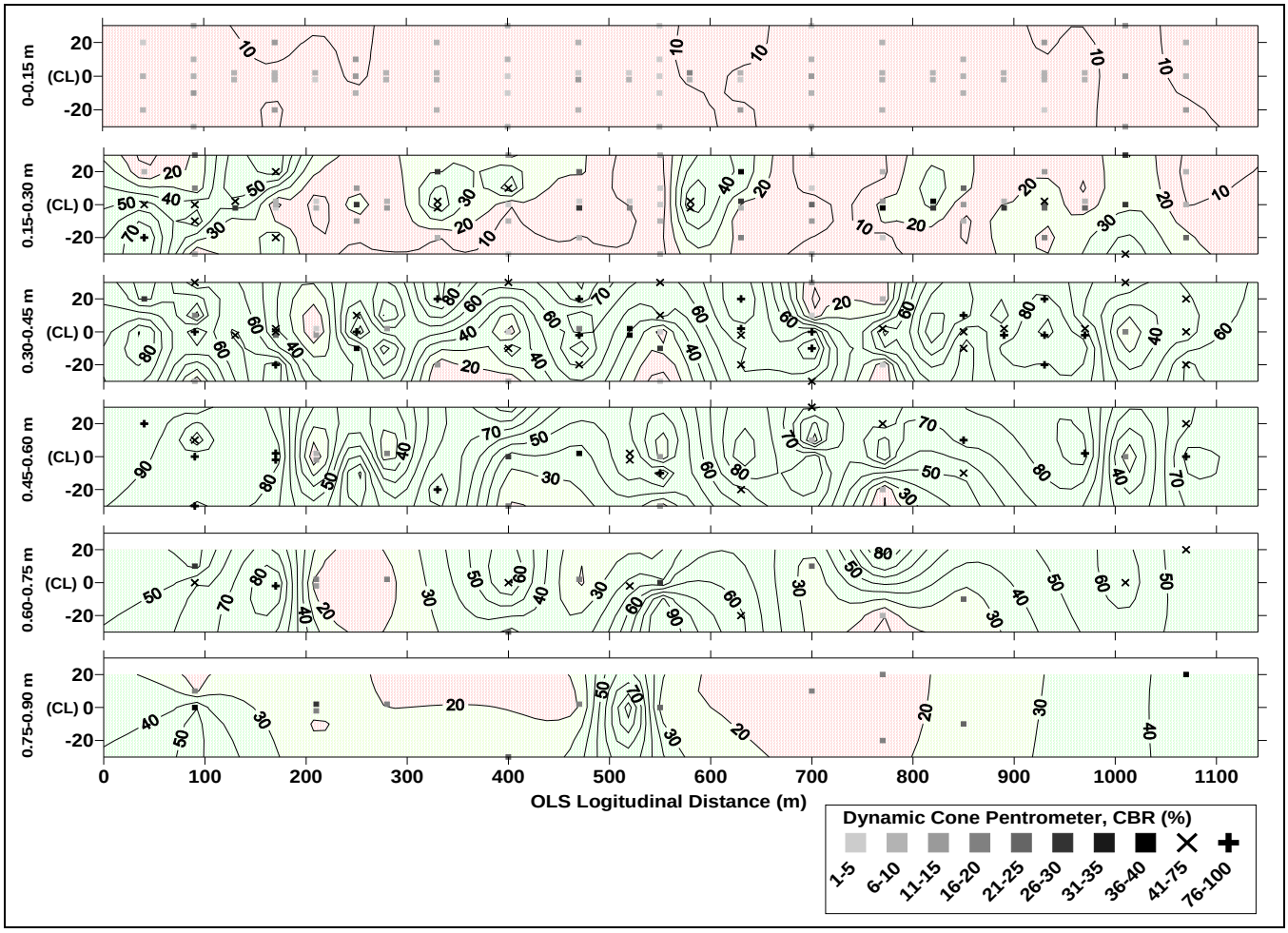
Figure 37b shows the CBR distribution as a contour plot during IOP #2 (October 2005). The distribution of CBR values for 0.15 to 0.3 m (6 to 12 in.) during IOP #2 is found to be different compared to the previous IOP, with significant sampling locations with CBR of 10 and below (Table 13). Soil strength significantly increased at the 0.30- to 0.45-m (12- to 18-in.) depth as shown in Figure 37b, which is influenced by the caliche layer.

Unlike during IOPs #1 and #2, DCP measurements during IOP #3 were fewer in number due to time constraints (Tables 6 and 13). However the CBR values observed during IOP #3 (April 2006) are almost similar to previous IOPs. The contours may not totally reflect the CBR of the entire OLS due to fewer samples (Fig. 37c).



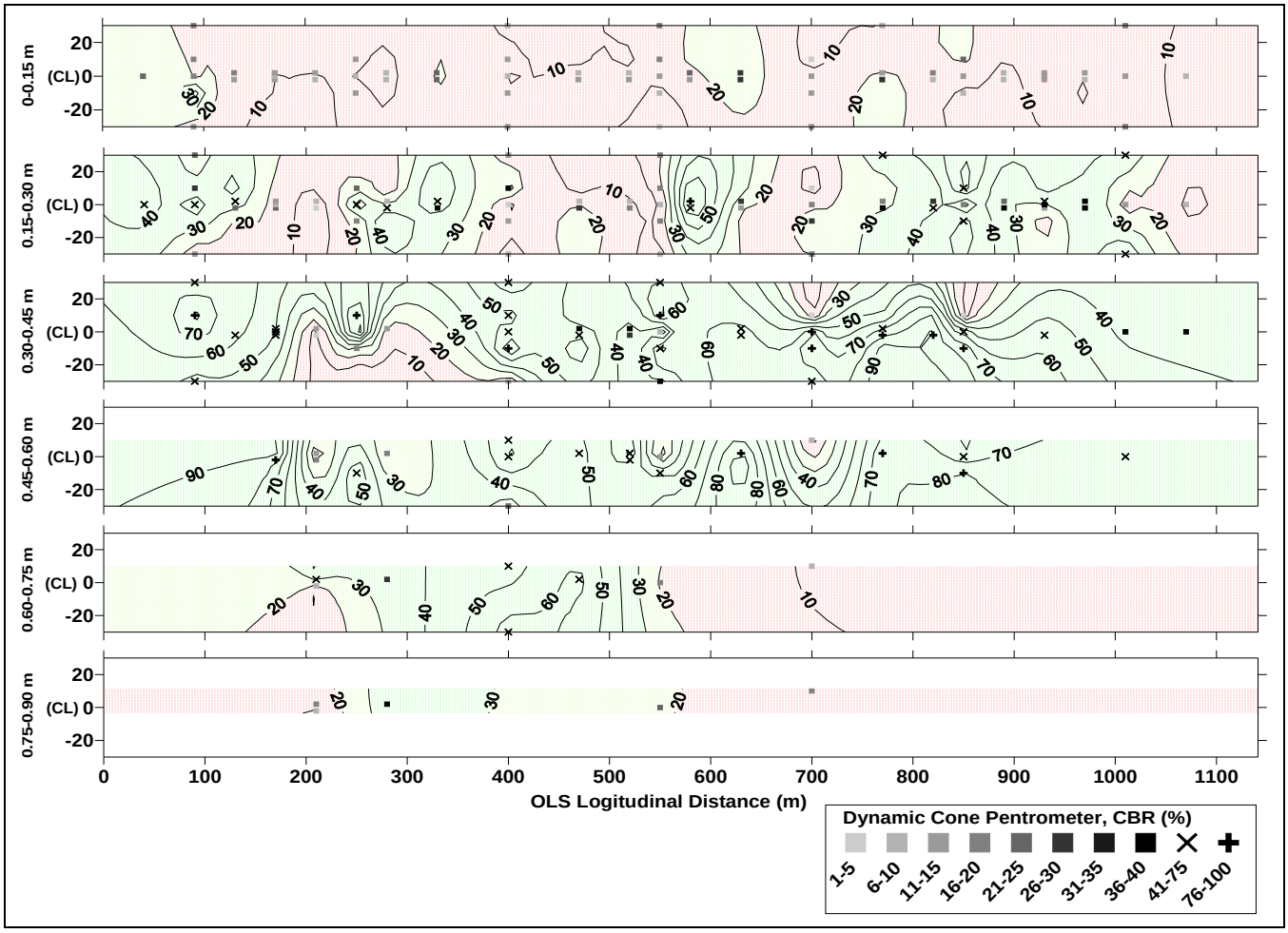
a. CBR contours for each depth range (July 2005).

Figure 37. Soil strength contours measured using the Dynamic Cone Penetrometer for all IOPs on Fort Bliss RAS. Red-shaded areas have CBR values of less than 20.



b. CBR contours for each depth range (October 2005).

Figure 37 (cont'd).



c. CBR contours for each depth range (April 2006).

Figure 37 (cont'd). Soil strength contours measured using the Dynamic Cone Penetrometer for all IOPs on Fort Bliss RAS. Red-shaded areas have CBR values of less than 20.

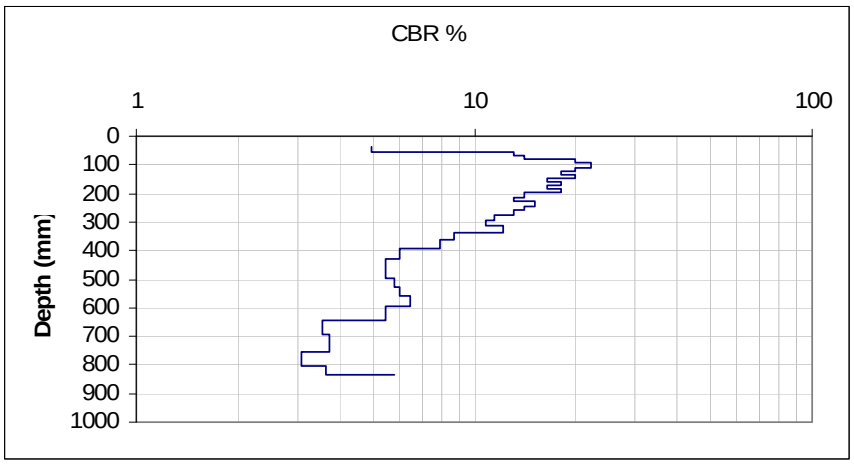
CBR profiles from all the DCP data for all IOPs are compiled in Appendix D. The profiles for each sampling location can be compared for seasonal changes mainly for the soil above the caliche layer. Typical DCP profiles taken at sampling locations 2+10 2N and 8+50 CL are shown in Figure 38 and 39, respectively. At sampling locations 2+10 2N, the caliche layer is discontinuous and shows weak soil strength below the surface. At 8+50 CL, the caliche layer can be detected easily from all the DCP profiles and shows weak soil strength at the surface. The soil above the caliche layer has relative low strength. Because of the non-homogeneous condition of the soil, variation of CBR values can be observed on the DCP profiles representing the soil strength on the RAS.

Table 13. CBR distribution calculated from DCP profiles and CIH_L (0.5-kg hammer) at Fort Bliss RAS during all IOPs. Shaded numbers are CBR values less than 5.

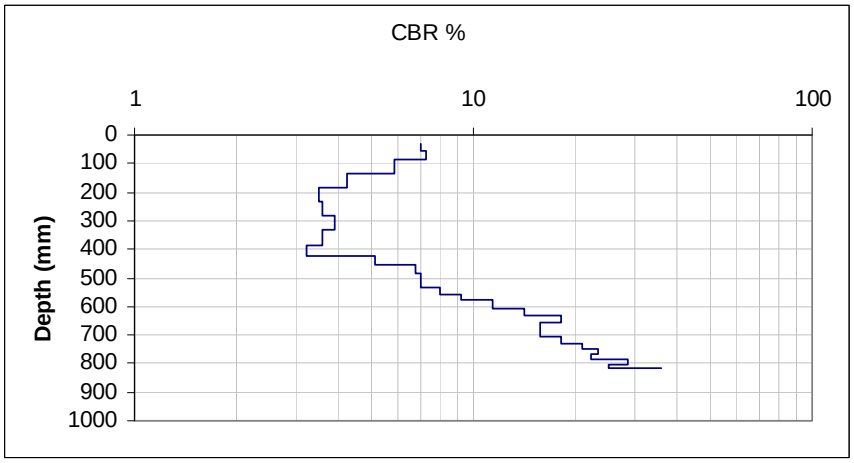
Sampling Locations	IOP#1, July 2005									IOP#2, October 2005									IOP#3, April 2006									CBR 0.5 kg Clegg Hammer		
	Avg. CBR within 15 cm bins						Avg. CBR within 30 cm bins			Avg. CBR within 15 cm bins						Avg. CBR within 30 cm bins			Avg. CBR within 15 cm bins						Avg. CBR within 30 cm bins					
	0-15	15-30	30-45	45-60	60-75	75-90	0-30	30-60	60-90	0-15	15-30	30-45	45-60	60-75	75-90	0-30	30-60	60-90	0-15	15-30	30-45	45-60	60-75	75-90	0-30	30-60	60-90	IOP#1	IOP#2	IOP#3
0+40 20N	8	7	58	83	79	79	8	66	79	5	6	30	96			5	54											6	5	
0+40 CL	15	53					41			6	57	100				41	100		24	45					17	62		4	4	5
0+40 20S	24	83					67			8	84					59												6	4	
0+90 30S	15	17	36	95			16	69		6	7	10	78			7	51		12	12	45				12	45		8	5	4
0+90 10S	26	92					55			10	62					42			49						13	66		5	4	4
0+90 CL	16	77	99	92	69	68	64	96	69	10	48	77	92	61	54	33	84	59	15	49					10	11	36	6	4	4
0+90 10N	23	40	22	55	62	39	31	44	59	10	20	16	57	34	15	15	41	26	19	32	84				6	13	8	5	4	4
0+90 30N	16	22	90				19	90		9	21	71	100			16	79		17	23	61				21	61		5	5	5
1+30 2N	37	88					59			8	62					37			18	47					46	100		6	5	6
1+30 2S	13	46	100				36	100		8	28	74				19	74		11	21	62				15	41		7	5	5
1+70 20S	21	26	89				24	89		12	40	94				28	94											7	6	
1+70 2S	6	6	46	33	58	40	6	43	53	7	3	20	85	93		6	53	93	11	21	52	78			7	17	35	4	5	4
1+70 CL	11	10	58	74	22	26	10	67	24	7	8	62				8	62		8	7	51				47			5	4	5
1+70 2N	12	5	69	99			10	79		8	8	42	90			8	51		11	15	51	100			18	78		6	5	6
1+70 20N	24	58					46			14	72					48												8	7	
2+10 2N	17	14	8	6	4	4	16	7	4	6	4	4	8	18	28	5	7	22	12	8	10	12	41	15	40			7	8	7
2+10 2S	6	9	13	73			8	49		3	6	13	10	12	17	6	12	14	7	1	3	15	8	7	7	56		2	3	5
2+50 10S	9	6	19	95			7	66		8	12	37	100			10	51		14	16	19	61			8	44	62	8	4	7
2+50 CL	26	68	99				55	99		13	35	97				26	97		8	56	100				27	74		4	6	6
2+50 10N	21	25	71				23	71		12	13	71				13	71		13	22	78				32	51	43	5	4	8
2+80 2N	13	10	8	14	18		12	12	18	6	9	12	15	17	20	8	14	18	7	7	15	19	34	36	8	56		6	4	6
2+80 2S	12	55	97				45	97		7	14	100				11	100		7	56					15	43		6	4	5
3+30 20S	13	10	12	78			11	53		8	7	11	89			7	58											5	4	
3+30 2S	17	75	100				62	100		8	48					31			21	35					38			9	8	5
3+30 2N	15	80	100				68	100		10	55					36			22	56					37			7	6	4
3+30 20N	12	33	89				27	89		7	27	96				19	96											7	5	
4+00 30N										9	14	68	100			12	76		7	10	68				9	68		7	6	4
4+00 10N	24	26	38	80	85		25	65	85	8	60					39			14	39	44	57	43		27	84		5	6	5
4+00 CL	11	11	9	36	23	6	11	28	21	4	2	4	33	75		4	22	75	9	3	49	64			30			4	3	6
4+00 10S	12	6	64				10	64		4	8	57				7	57		11	14	79				49			5	5	5
4+00 30S										6	4	6	19	24	25	5	14	25	10	6	7	22	65		8	18	65	6	5	4
4+70 20S	12	6	79	100			10	85		6	8	60				7	60											4	4	
4+70 2S	20	32	100				26	100		12	28	97				21	97		12	33	74				7	51		6	5	4
4+70 2N	8	4	39				6	39		3	4	17	35	17	16	4	26	17	10	6	39	47	62		17	62		5	5	3
4+70 20N	7	69	82	94			60	89		9	23	93				17	93											5	4	
5+20 2N	8	4	34	44	74		6	36	74	4	3	39	56			3	47		8	8	39	74			9	27		7	5	5
5+20 2S	18	17	40	71	30	91	18	51	63	7	16	40	62	44	100	12	51	58	14	15	32	55			13	59		8	5	8
5+50 30S	6	5	45				6	45		6	6	1	10	100		6	8	100	4	6	35				5	35		4	6	4
5+50 10S	26	19	68	95	100		22	79	100	4	6	26	82	100		5	54	100	9	15	71	55			17	81		6		4
5+50 CL	9	3	1	5	7	20	8	4	15	4	3	3	13	32	22	4	11	31	10	6	7	11	18	20	8	9	19	4	4	4
5+50 10N	9	7	78				8	78		5	3	59				4	59		16	18	81				7	6	24	5	4	4
5+50 30N	13	10	77				11	77		5	7	53				6	53		15	18	59				17	59		6	4	5
5+80 2N	25	53					38			17	63					38			21	78					56			8	4	6
5+80 2S	22	71					47			8	54					35			14	70					58			6	4	5

Table 13 (cont'd). CBR distribution calculated from DCP profiles and ClH_L (0.5-kg hammer) at Fort Bliss RAS during all IOPs. Shaded numbers are CBR values less than 5.

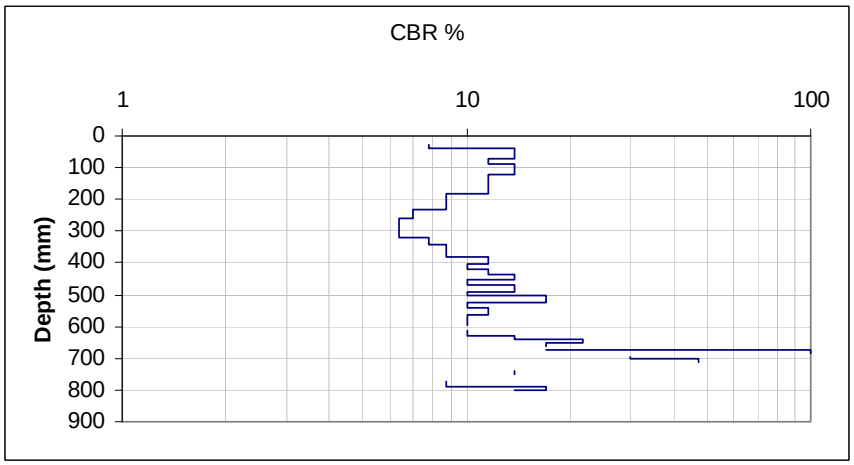
6+30 20S	11	26	91				21	91		12	17	73	65	62		15	70	62											8	5	
6+30 2S										5	7	65	100			6	76		25	14	69	100			19	70			5	3	6
6+30 2N	29	39	90				34	90		9	28	81				19	81		27	32	59	89			31	63			6	6	5
6+30 20N	8	40	88	98			32	92		15	39	93				27	93												9	5	
7+00 30N	6	3	67	53	79		5	64	79	4	2	13	65			3	42												7	5	4
7+00 10N	11	9	5	10	21	22	10	8	22	5	3	2	10	24	15	4	8	23	5	4	3	6	9	17	16	78			4	4	5
7+00 CL	26	20	80	90			23	84		11	20	83	100			15	89		15	17	78				24	82			6	6	6
7+00 10S	12	27	78	79	94		22	78	94	5	13	96				9	96		14	29	82				4	5	13		11	5	5
7+00 30S	8	7	60	92			8	76		5	7	56				6	56		12	19	59				16	59			6	6	5
7+70 20S	7	4	4	10	13		5	8	13	6	3	5	6	8	17	4	5	13											6	6	
7+70 2S	21	28	50	68			25	60		6	36	100				27	100		32	37	93				14	61			7	5	6
7+70 2N	12	13	25	63	67		13	49	67	9	15	49	100			12	55		13	15	56	79			35	93			6	6	6
7+70 20N	15	23	19	14	11		20	17	11	7	7	8	63	100	17	7	40	58	10	41					32				12	6	
8+20 2N	12	65	100				52	100		8	39	100				26	100		18	29	100				25	100			7	5	5
8+20 2S	12	16	91	86	98		14	90	98	6	26	100				20	100		10	42	81				33	81			8	7	5
8+50 10S	7	8	44	36	28	29	7	39	28	7	6	53	50	24	23	7	52	24	9	58	77	85			47	78			4	5	4
8+50 CL	13	14	55	80	62	86	14	70	76	6	15	64				11	64		11	16	62	59			57	0			5	5	4
8+50 10N	21	61	97	94	100		47	96	100	9	24	87	75			17	81		24	70					14	61			8	4	8
8+90 2N	14	52	100				41	100		6	9	62				8	62		8	25					19				7	5	5
8+90 2S	10	67	100				54	100		7	31	87				21	87		7	37					28				5	6	4
9+30 20S	9	50	80				39	80		3	17	79				14	79												4	4	
9+30 2S	11	29	94				23	94		9	24	87				16	87		14	11	58				12	58			7	6	5
9+30 CL	17	65	100				50	100		8	22	100				15	100		14	36					28				8	8	4
9+30 2N	11	67	100				55	100		9	41					30			15	43					31				5	5	5
9+30 20N	14	12	79	100	97		13	87	97	11	13	81				12	81												6	4	
9+70 2N	9	19	92	99			15	94		7	6	57	97			6	80		12	38					28				6	7	6
9+70 2S	11	44	93				35	93		7	21	91				17	91		9	38					28				5	7	6
10+10 30S	21	66	97				53	97		14	50					32			16	52					32				6	5	6
10+10 CL	18	21	88	100			19	91		15	27	16	19	66		20	18	66	14	12	37	74			13	44			8	5	6
10+10 30N	15	18	61	68	85		17	64	85	13	32	61				22	61		15	41					31				5	5	5
10+70 20N										7	7	49	67	41	43	7	57	42											8	5	
10+70 10N	15	17	39	76	88		16	55	88																						
10+70 CL	9	8	41	82			8	65		6	10	40	85			9	45		6	8	36				7	36			9	6	5
10+70 20S	5	5	65	94	100		5	75	100	12	23	74				17	74												5	8	
Total Count	74	74	67	41	27	12	74	67	27	77	77	66	35	20	14	77	66	20	61	60	42	21	8	5	61	44	9		77	76	61
Minimum	5	3	1	5	4	4	5	4	4	3	2	1	6	8	15	3	5	13	4	1	3	6	8	7	4	0	8		2	3	3
Maximum	37	92	100	100	100	91	68	100	100	17	84	100	100	100	100	59	100	100	49	78	100	100	65	36	58	100	65		12	8	8
15th percentile of Minimum	8	6	22	33	17	15	8	43	18	5	6	12	13	17	16	5	25	18	8	7	21	15	9	12	8	17	14		5	4	4
% w/ CBR <= 10	26	27	9	10	7	17	24	6	4	81	40	14	9	5	0	43	6	0	31	20	10	5	25	20	23	9	11		97	100	100
% w/ CBR <= 5	1	11	4	2	4	8	4	1	4	21	14	9	0	0	0	16	2	0	3	5	5	0	0	0	3	5	0		38	70	69
% w/ CBR <= 2	0	0	1	0	0	0	0	0	0	0	3	3	0	0	0	0	0	0	0	2	0	0	0	0	0	2	0		1	0	0



a. 2+10 2N IOP #1 (July 2005).

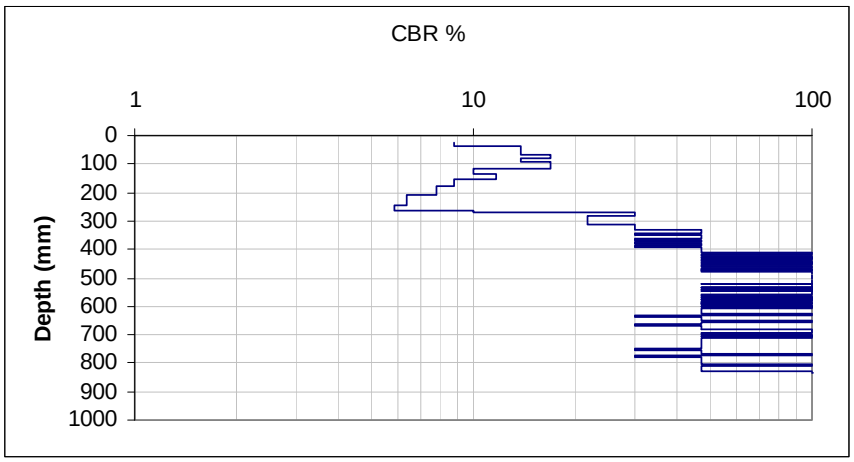


b. 2+10 2N IOP #2 (October 2005).

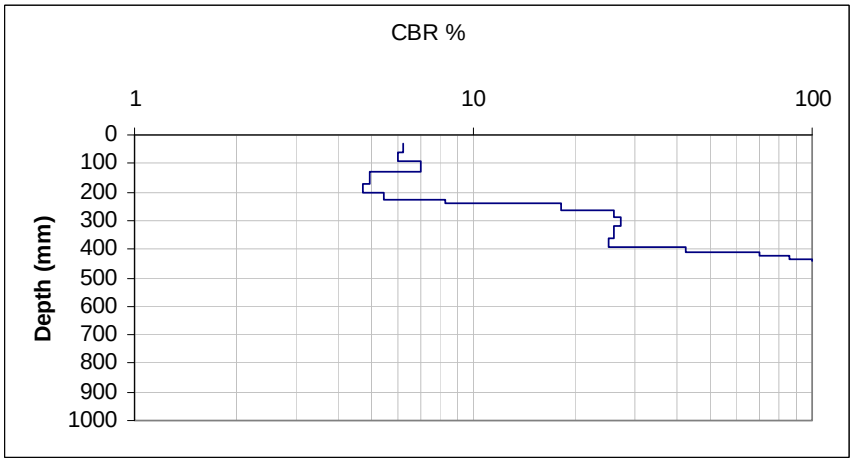


c. 2+10 2N IOP #3 (April 2006).

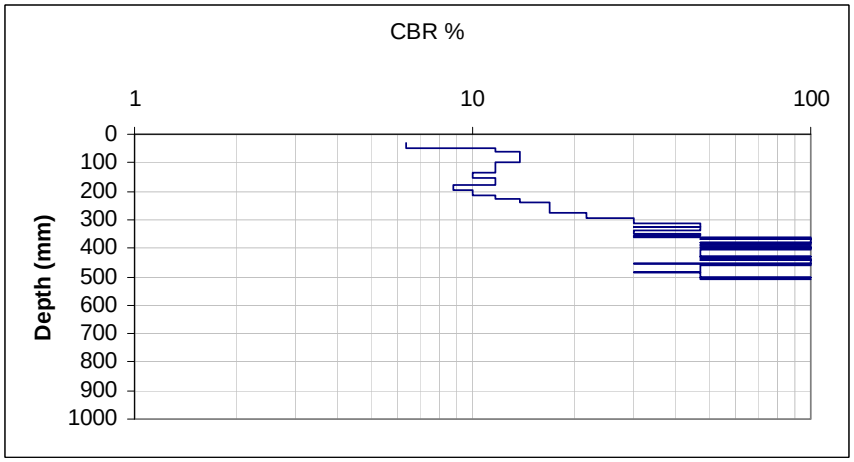
Figure 38. CBR profiles at sampling location 2+10 2N taken during the three IOPs at Fort Bliss.



a. 8+50 CL IOP #1 (July 2005).



b. 8+50 CL IOP #2 (October 2005).



c. 8+50 CL IOP #3 (April 2006).

Figure 39. CBR profiles at sampling location 8+50 CL taken during the three IOPs at Fort Bliss with higher soil strength at 300-mm depth.

Because caliche layer at various depths was found while digging the soil pits, the location of the upper bound of the caliche layer can be estimated using the DCP profiles. The soil strength CBR reached 100% as the tip of DCP was hitting the top of the caliche layer. The DCP profiles from all IOPs revealed caliche at depths from 117 to 774 mm. The depth to the top of the caliche layer relative to the RAS surface elevation is graphically shown in Figure 40.

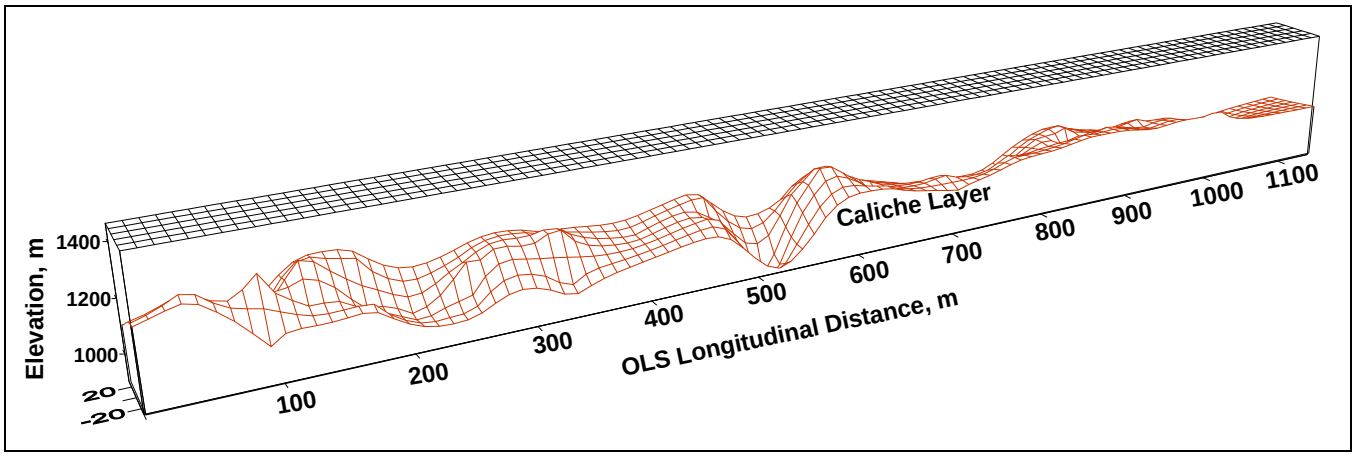


Figure 40. Profile of the topmost part of the caliche layer detected from the DCP data.

5.2.4.2 Clegg Hammer

CIV/L readings should increase for each subsequent drop, as a result of elastic rebound in the soil, as described in Section 4, and that was not always the case when the CIH_L (0.5-kg hammer) was used on the RAS. We discussed this issue with the equipment manufacturer and they stated that it is not uncommon to have the fourth reading lower than the third reading for certain soil conditions as a result of the effect of organic materials (Brown and Crandell, personal communication). In some cases, the first one or two blows flatten and and compact the soil; then the succeeding blows can pulverize and loosen the immediate surface or may continue to compact the material. On this RAS, we found compaction of soil with significant depth of hammer indentation after conducting tests, and on a surface with thin-crust layer where the soil was pulverized after the third and fourth drops. There also are several possibilities as to why the third blow reading is sometimes higher than the fourth blow (Crandell, personal communication). First, if loose material falls into the impact crater, this too can cause a downwards bias. Second, the material might begin to spring back (such as soils with organic materials), causing some cushioning which may be sufficient in effect to cause the readings to appear lower.

Lastly, it is possible then that subsequent blows are retarded sufficiently by hitting the rim of the crater formed by previous blows.

A few of those cases were observed at this RAS. Equation 3 was applied on datasets with decreasing readings, and in most cases showed insignificant differences in CBR values (Table 14). Nevertheless, Equation 3 was used to convert the fourth reading to CBR for all of the datasets, regardless of whether the values were increasing or decreasing. The CBR for each sampling location was computed by averaging the calculated CBR values from all the datasets for that sampling location. The distribution of the CBR values for each IOP is shown in Figure 41 and Table 13. The minimum and maximum CBR values are found to be 2 and 12 during the summer visit, and 3 and 8 during the fall and spring visits. The results showed no significant difference in soil strength for the three IOPs. The higher soil moisture during IOP #2 was not sufficient enough to influence the soil strength for that season.

Table 14. Examples of CIH_L datasets with decreasing readings.

	0.5 kg Clegg Hammer Readings:					CBR Values calculated using Equation 3				
Location, IOP	1st	2nd	3rd	4th		1st	2nd	3rd	4th	
0+40 20S, IOP#1	12.5	20.8	22.7	19.0	⇒⇒⇒	3	7	9	6	
	9.8	15.0	14.8	16.3		2	4	4	5	
	10.7	17.3	18.8	18.7		2	5	6	6	
						3	6	6	6	Average CBR
6+30 20S, IOP#2	8.1	10.7	12.0	12.7		2	2	3	3	
	11.3	14.4	16.0	16.2		3	4	5	5	
	10.4	16.1	19.0	17.8	⇒⇒⇒	2	5	6	6	
	11.5	17.9	19.9	21.6		3	6	7	8	
						2	4	5	5	Average CBR
5+20 2S, IOP #3	11.7	19.4	21.0	21.4		3	7	7	8	
	17.9	18.0	20.2	23.8		6	6	7	9	
	11.9	17.7	22.9	19.0	⇒⇒⇒	3	6	9	6	
	10.4	18.1	20.5	21.4		2	6	7	8	
						3	6	8	8	Average CBR

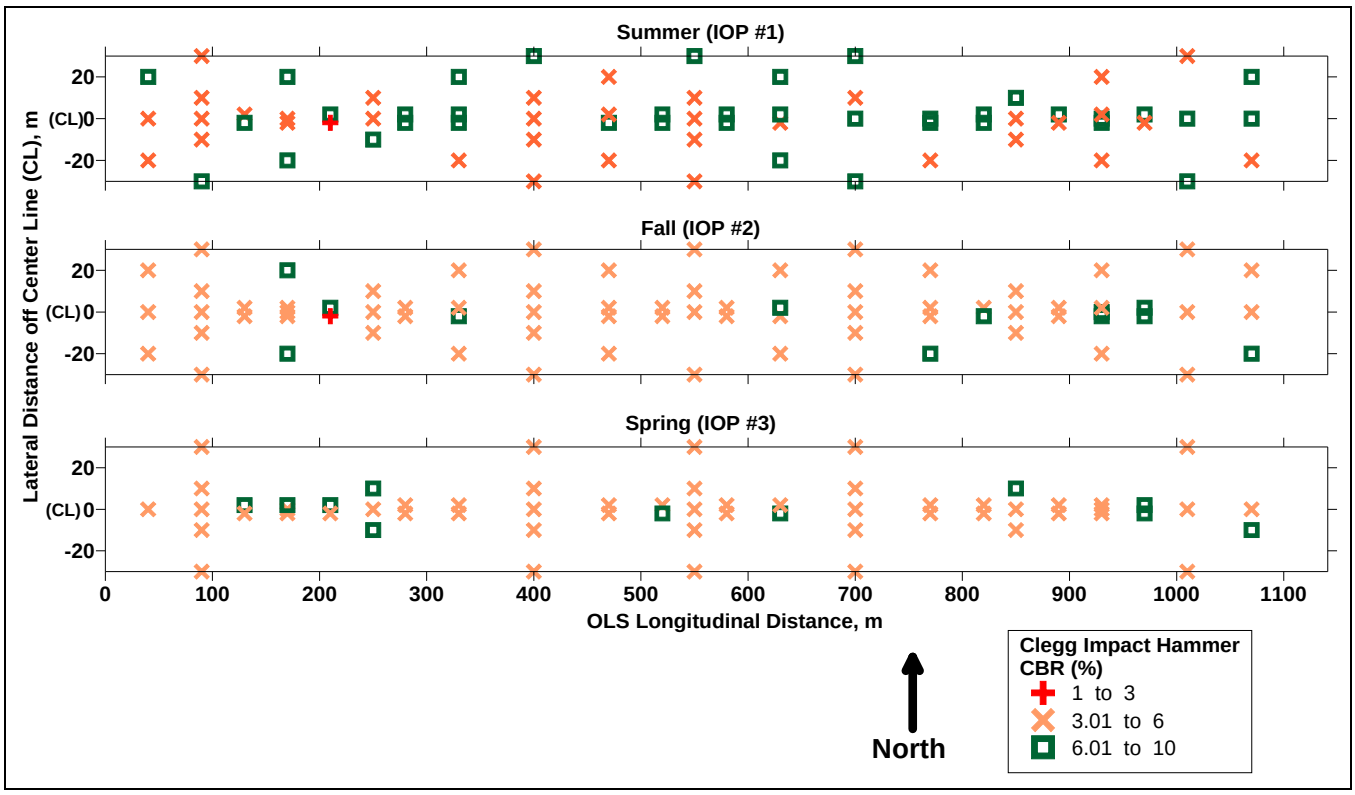


Figure 41. Soil strength for top 0.3 m (6 in.) measured from the light Clegg impact hammer expressed in CBR (%) for the Fort Bliss RAS.

5.2.3.3 Drop cone

The force calculated using equation 5 from the Drop cone measurements for the entire RAS for three IOPs can be seen in Figure 42. Most of the areas presented very little resistance, resulting in force values of 0.7 and 0.8 kN. One or two sampling locations displayed higher resistance, with force in the 1-kN range.

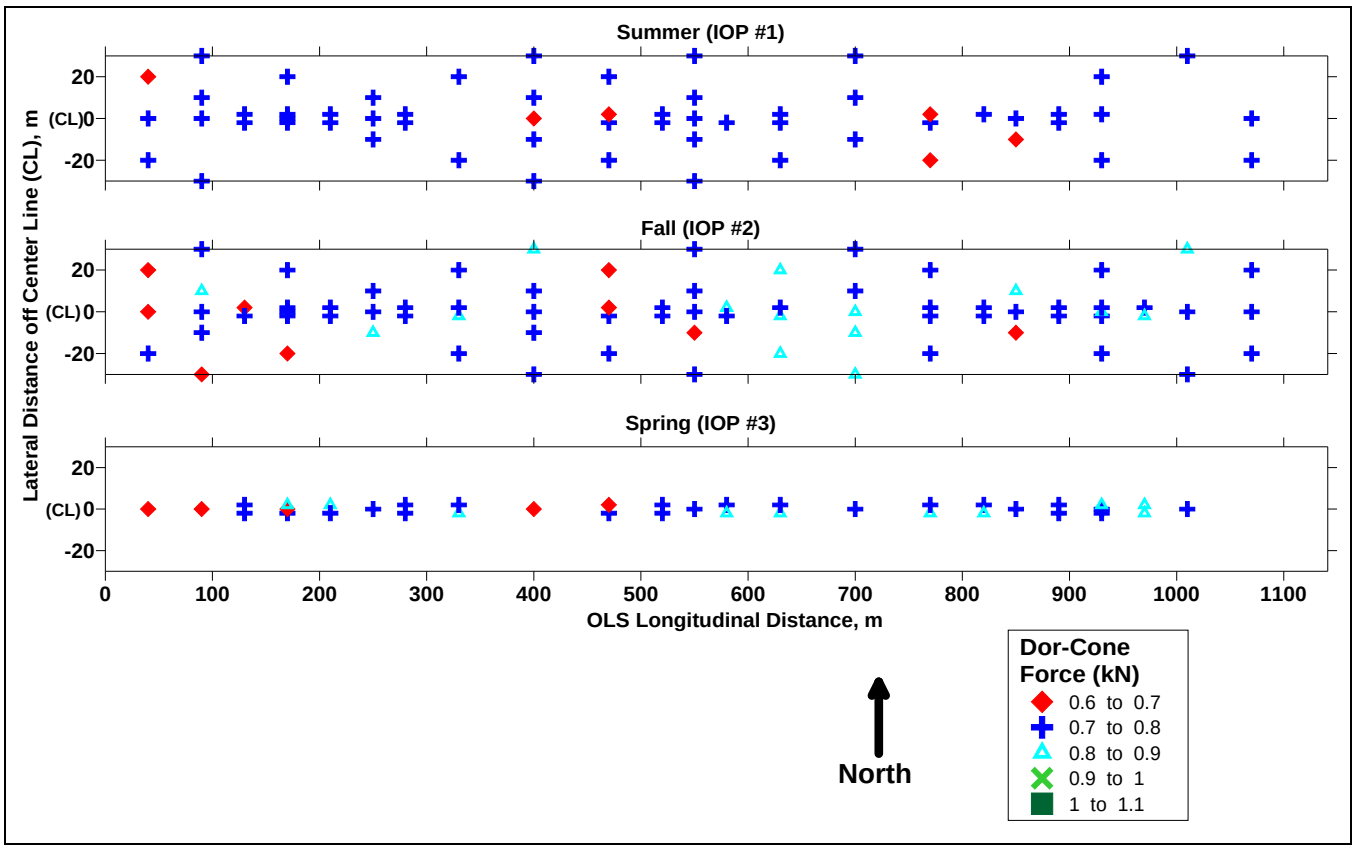


Figure 42. Calculated force indicating the surface soil strength throughout the RAS during the three IOPs.

5.2.3.4 Soil Strength Summary

The surface CBR values between the DCP and the 0.5-kg Clegg hammer showed significant differences. It is important to note that each instrument has a correlation to provide the CBR values as indices. The 0.5-kg Clegg hammer provides a CBR value only for the upper layer of the soil based on hammer dynamic impact onto the soil surface, whereas the DCP is based on penetration resistance and provides CBR values as far down as 1 m (3 ft) deep from the surface. Because of low confining at the upper portion of the soil layer, the DCP CBR values for the 0- to 0.15-m (0- to 6-in.) depths can be questionable. However, DCP is the standard tool for measuring soil strength by AFCESA for airfield design and evaluation. The CBR profiles of the weak areas on the OLS determine the suitability for specific aircraft and number of passes.

The 0.5-kg Clegg hammer CBR values do not match with the DCP data, and the percent of distribution from the CBR 0.5-kg Clegg hammer reflected a higher distribution for CBR values of five and less. Because the 0.5-kg Clegg hammer is not commonly used in constructed and natural

soils, further assessment and correlations, including sensitivity analysis, are needed between these instruments.

The typical process for evaluating a contingency airfield using the AFCESA is breaking a CBR profile in layers, because an existing runway normally consist of various subsurface structures (i.e., base, subbase, subgrade). The same procedure was applied to the selected DCP profiles in order to determine the various layers of CBR values on the OLS for natural soils. Figures 43, 44, and 45 are actual CBR profiles along with the average CBR values defining the layers for IOP #1, IOP #2, and IOP #3, respectively. These CBR profiles are representing the weakest soil layers indicated by low CBR values. At least one DCP profile during IOP #1 (in July 2005) contained a CBR value of one (i.e., sampling location 5+00 CL) as shown in Figure 43. Up to 14% of the DCP data at 0.15- to 0.3-m (6- to 12-in.) depth consisted of CBR values between 3 and 5. The low CBR values are located in specific limited areas and some of these locations are along the center line of the RAS. Figure 44 shows CBR profiles for sampling locations 4+00 CL and 5+50 30S, showing layers with weak soil strength taken in October 2005 (IOP #2). Similar pattern of layering was observed at sampling locations 2+10 2S and 4+00 CL during IOP #3 in April 2006 (Fig. 45).

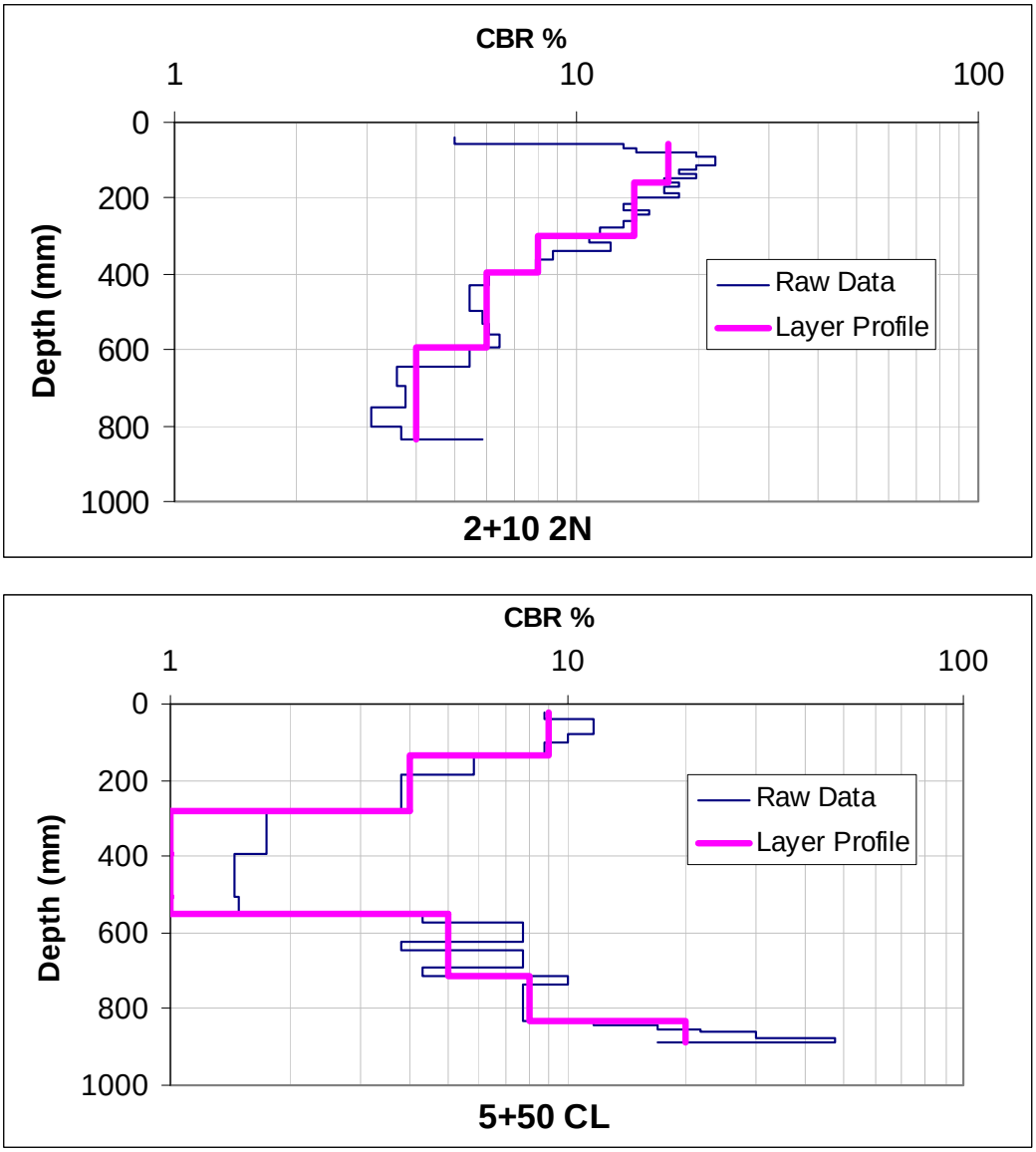


Figure 43. Selected CBR profiles showing layers with weak soil strength taken during IOP #1 at the Fort Bliss RAS.

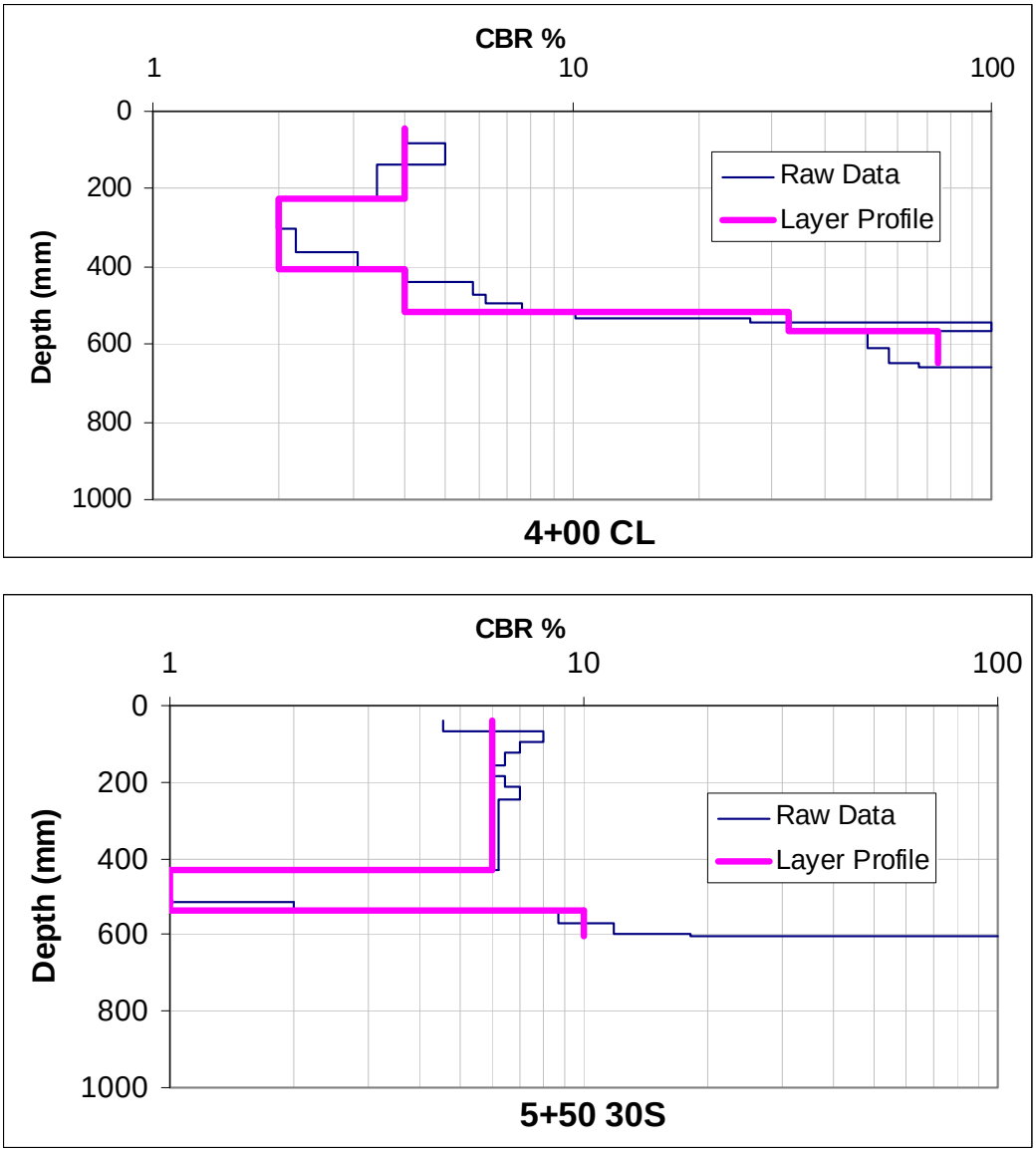


Figure 44. Selected CBR profiles showing layers with weak soil strength taken during IOP #2 at the Fort Bliss RAS.

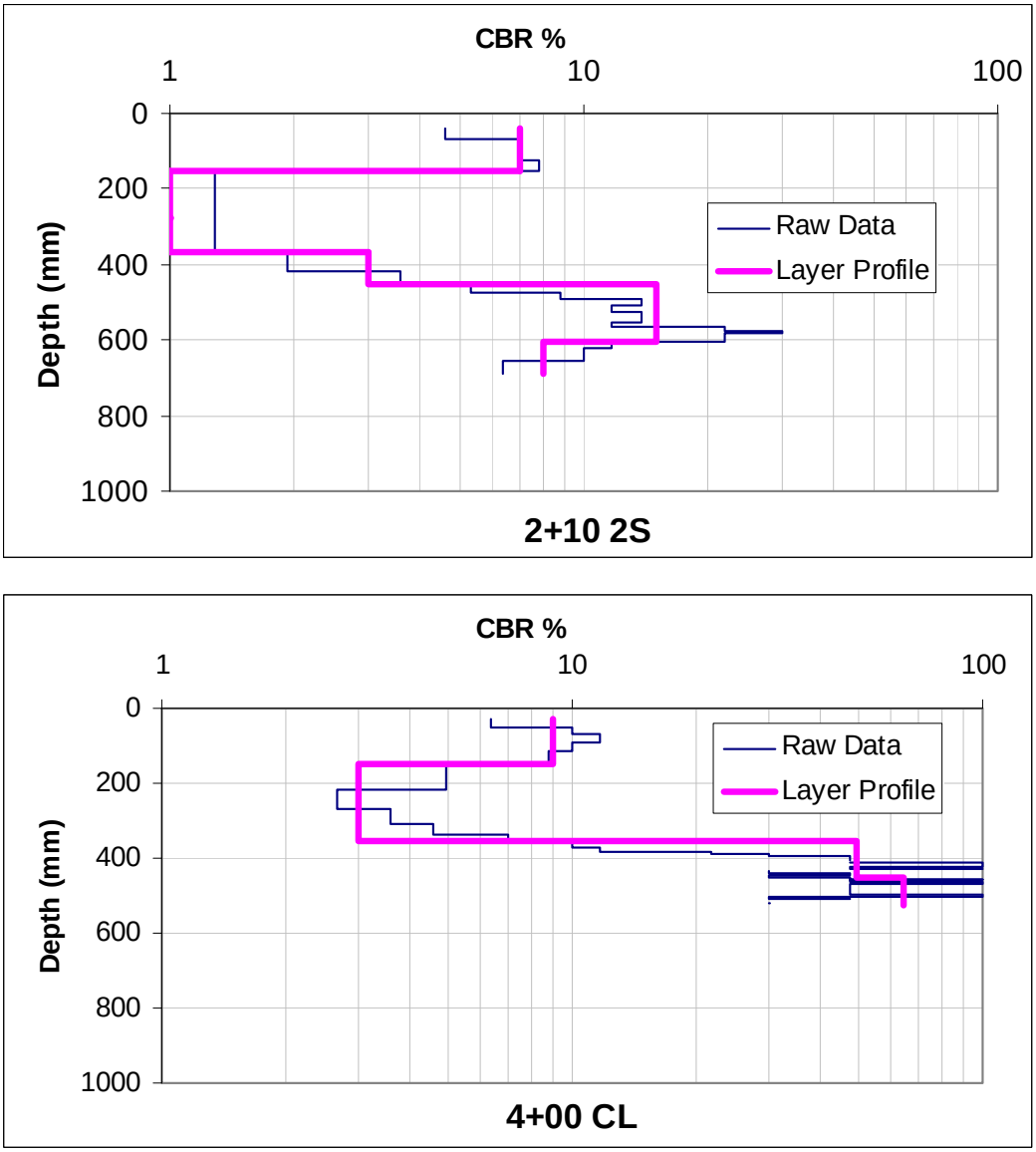


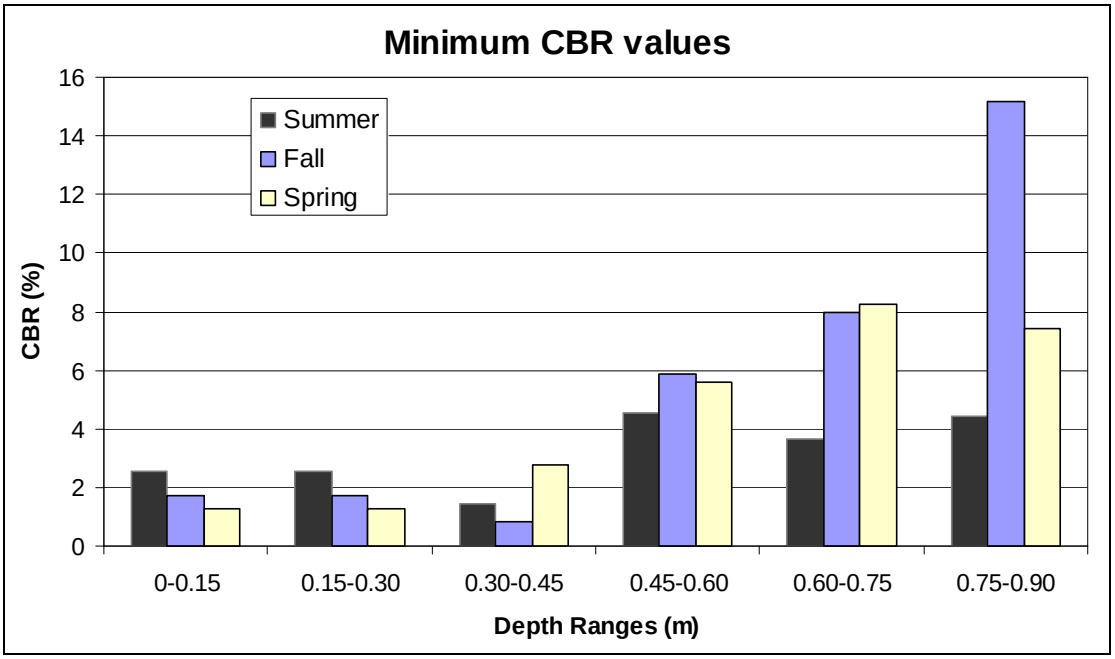
Figure 45. Selected CBR profiles showing layers with weak soil strength taken during IOP #3 at the Fort Bliss RAS.

Table 13 summarizes the CBR values for the DCP profiles and 0.5-kg Clegg measurements for all IOPs. The CBR for 0- to 0.15-m (0- to 6-in.) depths was excluded in the analysis because of the lack of confinement at the top of the surface layer that affects the DCP measurements and assumed that the CBR for the surface is equal to the CBR at 0.15- to 0.3-m depth. To evaluate the loading capacity of the RAS, the analysis was based on the DCP profiles of minimum (Fig. 46a) and 15th percentile of minimum CBR values (Fig. 46b) for 0.15-m (6-in.) incremental layers. For design, it is common practice to take the representative CBR profile by obtaining the 15th percentile of the minimum CBR values from all the DCP data collected

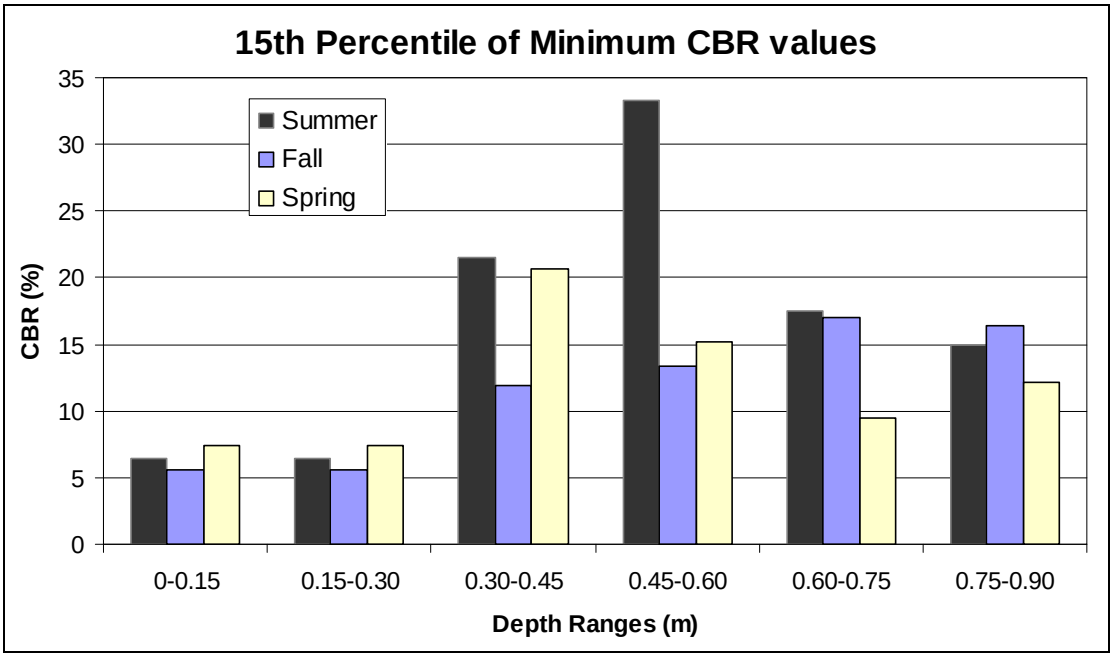
in the test area. The 15th percentile of the minimum CBR profiles at the RAS shows low CBR at 0.15- to 0.3-m depth, then the CBR values slightly increased down to 0.45 m. and stayed uniform at deeper depths (Fig. 46b). There are localized areas (about 2 to 3% of the DCP data) with CBR values less than 2 at 0.15- to 0.45-m depths (Fig. 46c). The percent with CBR values less than 5 during the fall (IOP #2) from the surface down to 0.45 m is higher than summer (IOP #1) and spring (IOP #3) as shown is Figure 46d. However, CBR values significantly increased for soil at deeper depths during all IOPs.

Applying the PCASE program (version 2.08) using the evaluation module for unsurfaced runway on subgrade soils, the results are summarized in Table 15. This analysis was based on CBR profiles for 0.15-m (6-in.) incremental layers using profiles of minimum and 15th percentile of minimum CBR values from the DCP data, as shown in Figures 46a and 46b. The C-130 is able to land on the RAS up to 19 passes with 58 tons (127 kips) of allowable gross load during summer and fall, and up to 48 passes with 64 tons (142 kips) of gross load during spring using the 15th percentile of minimum CBR values profile. The C-17, however, can land on the RAS for only one pass with varying allowable loads using both minimum and 15th percentile of minimum CBR values for all IOPs.

The evaluation using the charts established in ETL 2002-19 (AFCESA 2002a) calculated different loading capacity, and number of passes for C-17 and C-130 compare to the PCASE results. This analysis was based on 0.15-m (6-in.) thickness for the lowest CBR value using profiles of minimum and 15th percentile of minimum CBR values. Because the loading capacity using the minimum CBR is outside the range of the charts for C-130 and C-17, no values are reported (Table 15).

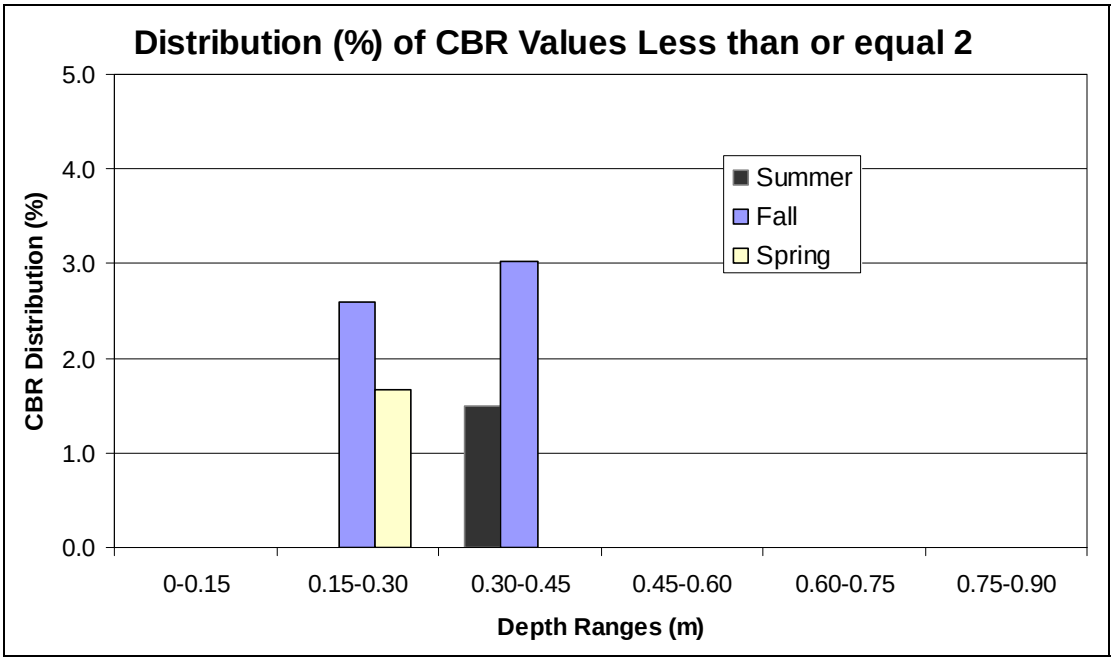


a. Minimum CBR profiles.

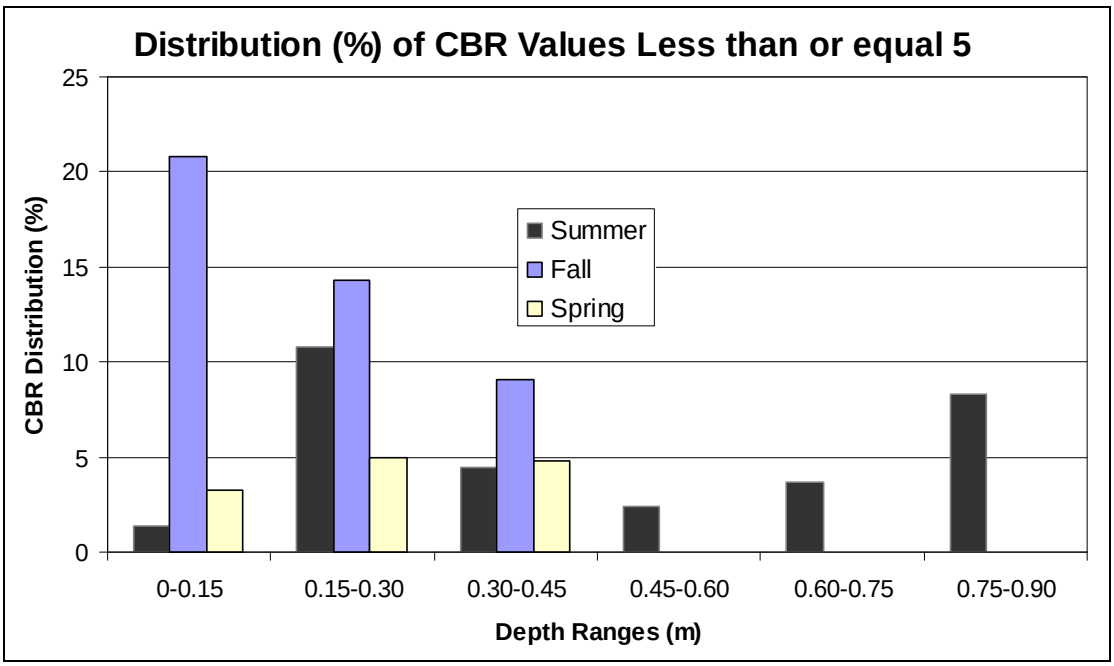


b. 15th percentile of the minimum CBR profiles.

Figure 46. CBR values at each depth range at RAS.



c. Number of DCP measurements with CBR value of 2 or less.



d. Number of DCP measurements with CBR values equal to or less than 5.

Figure 46 (cont'd).

Table 15. PCASE loading capacity results for three seasons based on *estimated* DCP CBR.

	Aircraft	Summer		Fall		Spring	
	Estimated CBR values/profile	Minimum	15th percentile of minimum	Minimum	15th percentile of minimum	Minimum	15th percentile of minimum
Analysis Using Charts (ETL 2002-19)	C-130 AGL, metric ton (kips) Number of passes		70 (155) 60		70 (155) 60		79 (175) 70
	C-17 AGL, metric ton (kips) Number of passes		159 (350) 10		159 (350) 10		208 (460) 10
Analysis Using PCASE	C-130 AGL, metric ton (kips) Number of passes	0.2 (0.4) 1	58 (127) 19	17.2 1	58 (127) 19	0.2 (0.4) 1	64 (142) 48
	C-17 AGL, metric ton (kips) Number of passes	13 (29) 1	127 (280) 1	29.5 1	127 (280) 1	0 0	120 (265) 1
C17 .....Minimum weight = 126.6 metric ton (279,000 lb), maximum weight = 265 metric ton (585,000 lb) C130 ....Minimum weight = 31 metric ton (69,000 lb), maximum weight = 79 metric ton (175,000 lb)							

The RAS condition can be summarized to be capable of supporting landing with several passes for C-130 and limited number of passes for C-17 operations at various loading capacity. The Fort Bliss RAS is rated as unacceptable for the C-17 and marginal for C-130 based on *estimated* CBR analysis.

6 Conditions at Precision Corrected Imagery Runway Assessment Site (PCI-RAS)

Shift on RAS location was found at Fort Bliss as a result of georeferencing level of imagery. The runway location, as presented in Figure 47, appears to be visually shifted on the earth's surface. However, the UTM coordinates have identical values when examined with GIS tools. Because of the variation in levels of geoprocessing between the Landsat imagery (systematic or basic level) and the Orthophoto (precision corrected imagery—high level), there are differences in the placement of runway locations. The coordinates of the several distinct features were obtained from the Landsat7 Systematic, and the coordinates of the corresponding feature also were obtained from the Orthophoto. An average for the offset values representative of this area was computed based on the individual feature's values. The Precision Corrected Imagery Runway Assessment Site (PCI-RAS), white outlined in Figure 47. has easting and northing coordinates of 432787m, 3583792m and 431647m, 3583792m for east and west OLS end points, respectively. Coordinates are UTM Zone 13N projection, WGS 1984 datum. The RAS using precision-corrected imagery (PCI-RAS) is shifted 233 m to the west and 97 m to the north. A verification survey was conducted at the PCI-RAS location. The portion of the actual location is partly covered by the clusters of OLSs in the area (dashed magenta line).

6.1 Surface Condition at Precision Corrected Imagery Imagery RAS (PCI-RAS)

Photographs taken during the IOPs of the landscape (west, north, northwest, and northeast) along the SI-RAS are compiled in Figure 48 to show the similarities or consistency between the SI-RAS and PCI-RAS locations. Because the offset between two locations is relatively small, we can reasonably estimate terrain and soil characteristics in the PCI-RAS location from the SI-RAS conditions. The PCI-RAS should be sloping to the east and southeast with longitudinal and lateral gradient (slope) most likely similar to the SI-RAS location. The undulation or surface roughness of the area is likely to be typical of that of SI-RAS location. The type and distribution of vegetation in the general are expected be the same (see Section 5), including the size and height of the vegetation. Because animal burrows

were observed to be widespread in the area, animal holes are bound to be present on the PCI-RAS location.

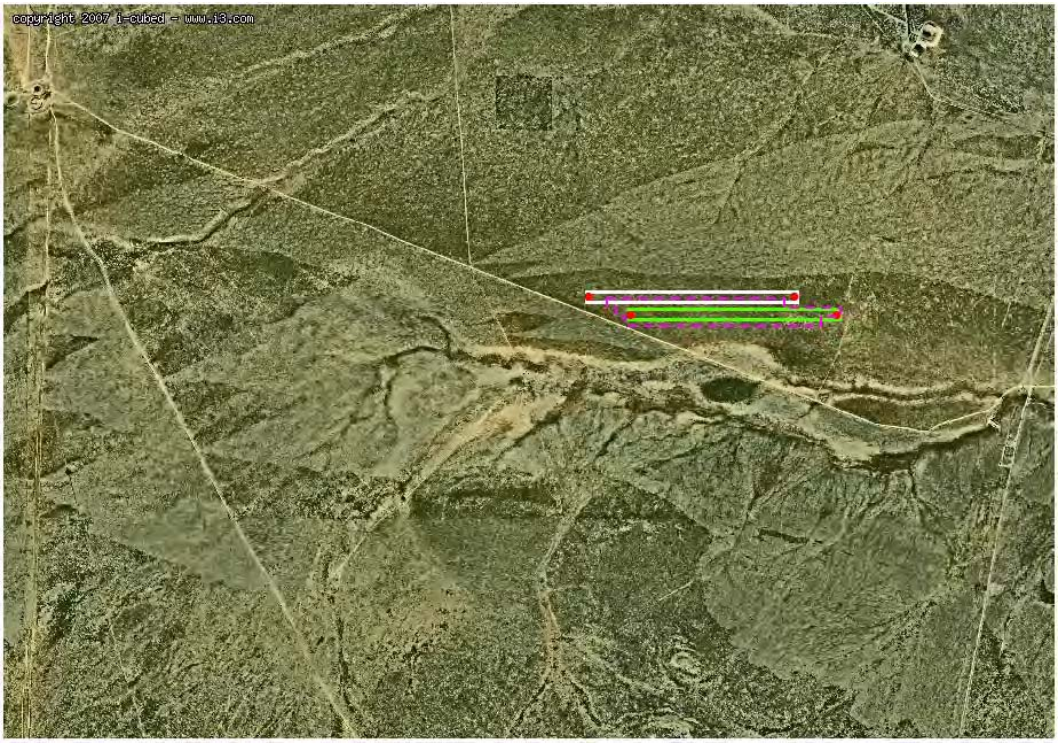
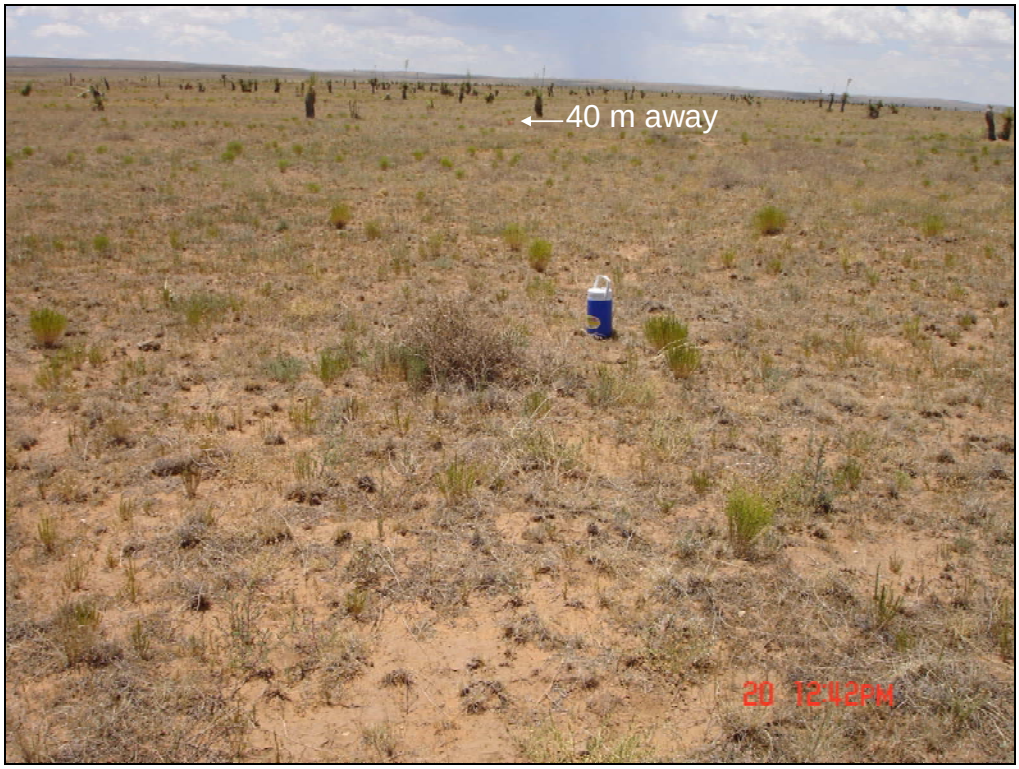


Figure 47. Shift on RAS location due to georectification level of imagery. Fort Bliss RAS Precision Corrected Imagery (PCI-RAS) in white and Systematic georeferenced (SI-RAS) in green. Field work was conducted at the SI-RAS. The magenta broken line shows the boundary of the clusters on OLSs in the area.

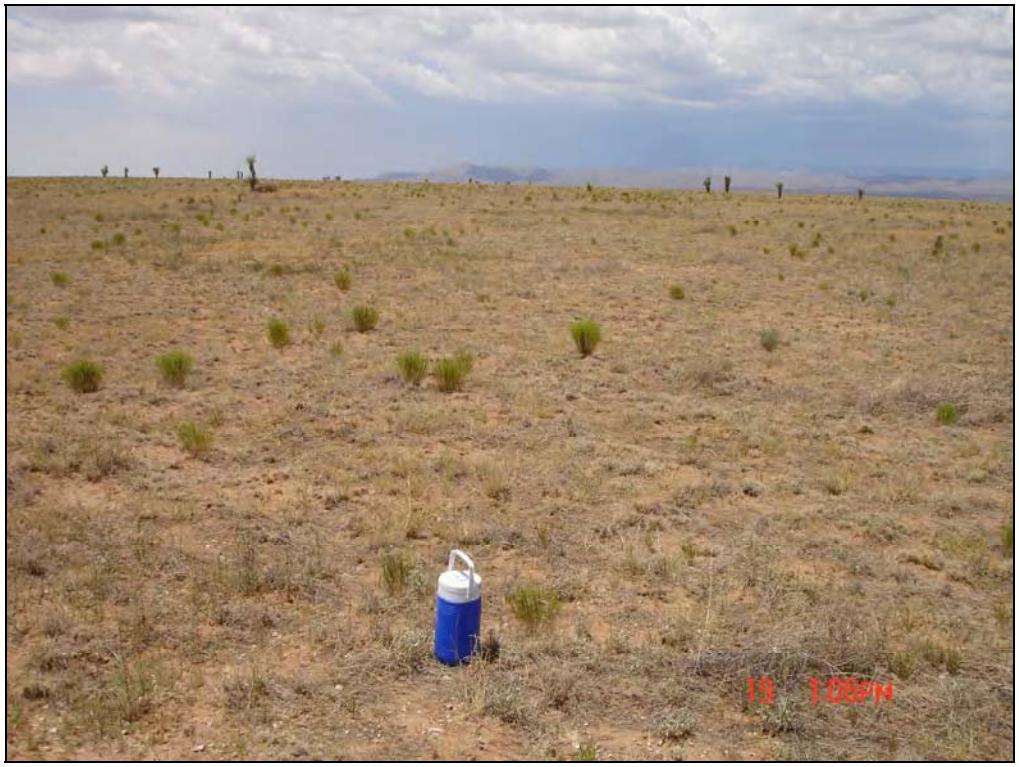


a. At 0+40 CL looking west. Photo taken during IOP #1.



b. At 0+40 CL looking north. Photo taken during IOP #2.

Figure 48. Area west, north, northwest, and northeast of the SI-RAS location.



c. At 1+70 CL looking north. Photo taken during IOP #1.

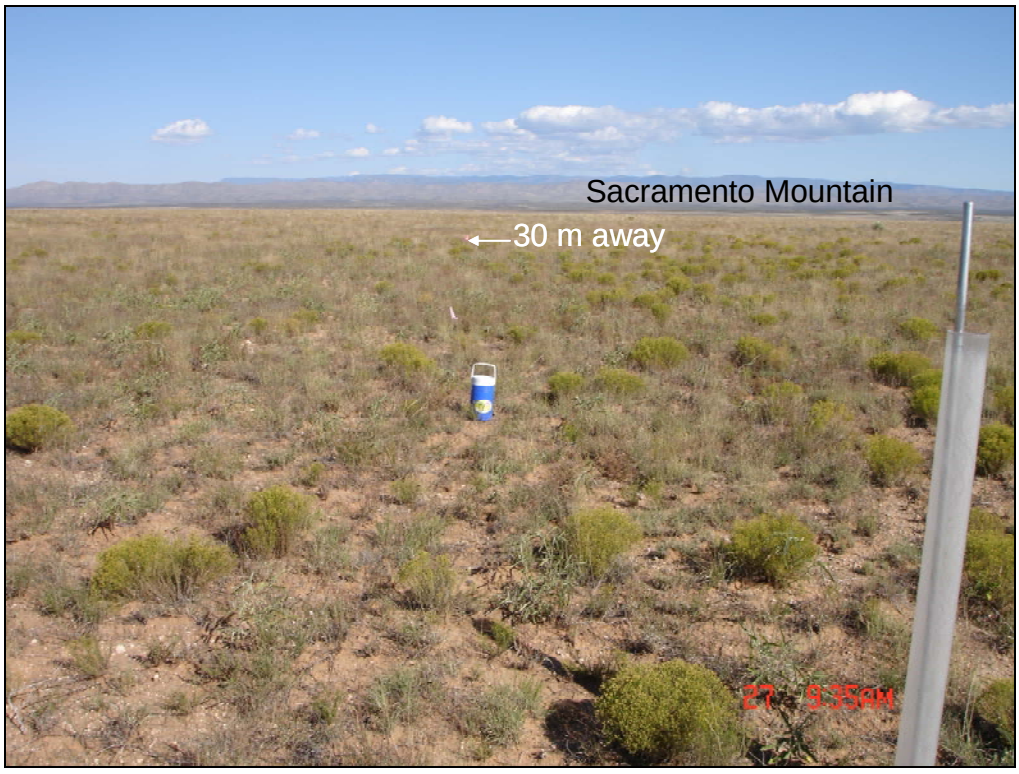


d. At 1+70 CL looking northwest. Photo taken during IOP #1.

Figure 48 (cont'd). Area west, north, northwest, and northeast of the SI-RAS location.



e. At 5+50 CL, looking northwest. Water jug is approximately 6 m away. Photo taken during IOP #2.

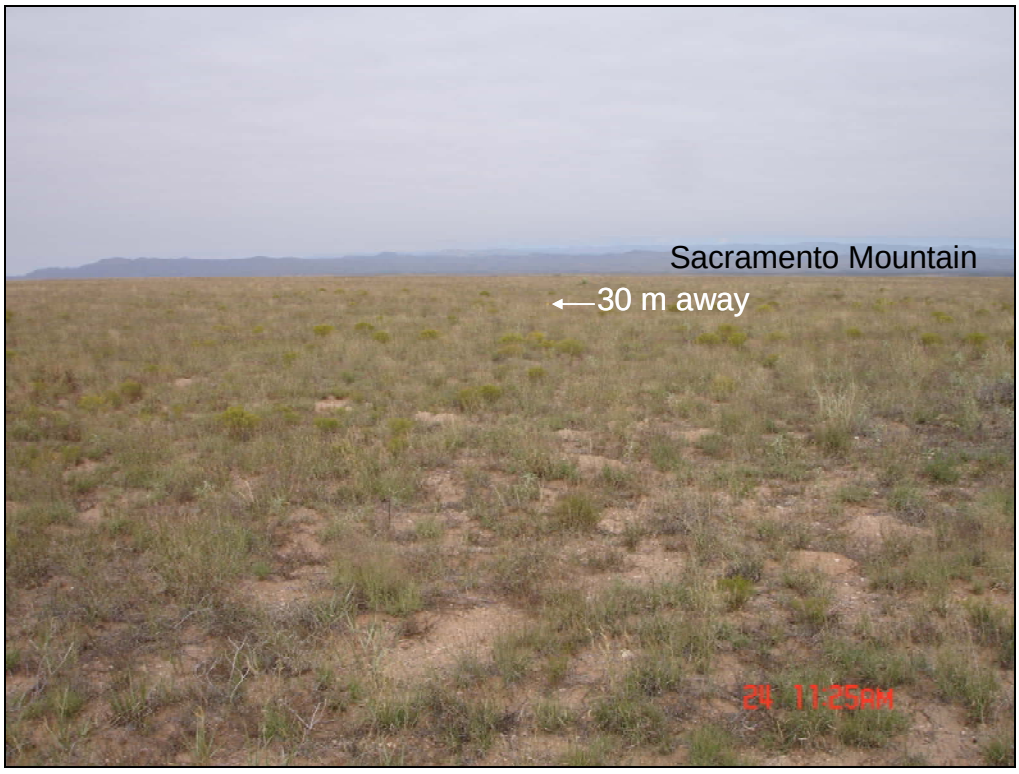


f. At 5+50 CL looking north. Pink flag in the far distance is 30 m away. Photo taken during IOP #2.

Figure 48 (cont'd).



g. At 5+50 CL looking northeast. Water jug is approximately 6 m away. Photo taken during IOP #2.



h. At 10+10 CL looking north. Photo taken during IOP #2.

Figure 48 (cont'd). Area west, north, northwest, and northeast of the SI-RAS location.



i. At 10+10 CL looking northwest. Water jug is approximately 6 m away. Photo taken during IOP #2.

Figure 48 (cont'd).

6.2 Soil Condition at Precision Corrected Imagery Imagery RAS (PCI-RAS)

The soil type was found to be consistent throughout the entire SI-RAS (Table 7), so likelihood for the PCI-RAS to have a soil type of silty sand (SM) can be reasonably expected with varying depths of caliche layer. Soil moisture for each IOP should be the same or at least close. Soil density may vary, but it is safe to assume numbers equivalent to the measured values. Varying soil strength layers were observed on the entire SI-RAS and low strength was found to correspond with the soft soil layers or void in the soil due to animal holes. Low strength similar to what was measured is very likely. The seasonal and spatial variations in soil strength for the entire PCI-RAS can be expected to be similar to SI-RAS.

7 OLS Software Seasonal Analysis

A goal of the OLS program was to determine the ability of the software to locate smooth, flat, and obstruction-free landing sites seasonally. There are two components of the seasonal concept. One involves identifying a season in each climate when the most OLSs are available and using that information to create a strategic OLS inventory. The second concept involves assessing the seasonal capability of the OLS software to accept or reject OLS areas as acceptable.

The first concept involves using a Landsat image taken at a location during one season to locate OLSs, and then to determine whether the OLSs found during that season are valid for all seasons. In this manner, except for land use changes, it would not be necessary to use current Landsat images to inventory potential OLSs for an area of interest. However, such an inventory concept may not be useful where OLS quality, and thus numbers, change dramatically within a region with season, such as in agricultural areas. The concept requires assessing the time of year when the most OLSs would appear in various geographical areas, assuming that OLS availability is a function of a seasonal component, such as greenness or soil moisture. The OLS inventory created from such a search may be of strategic value, but the usefulness of such a list is dependent on the consistency of OLS locations season to season. Tactically, the validity of such a list is also dependent upon weather changes affecting soil moisture, and therefore soil strength.

The second seasonal concept involves evaluating the ability of the software to locate successful OLSs on images each season. That is, the capability of the software may be seasonally dependent and may be more sensitive to some factors affecting OLS quality in some seasons.

These seasonal concepts were evaluated using only the OLS software written to locate smooth, flat, and obstruction-free locations. Soil moisture and soil strength algorithms had not yet been integrated into the software. Soil strength alone could cause an OLS that is acceptable one season to be rejected during another, even if other factors did not change.

7.1 OLS Software Seasonal Consistency

Strategic utility of the OLS software is dependent on its ability to consistently select high-quality OLSs. This is a function of the software's accuracy each season. Developing a strategic inventory of OLSs in regions that do not change seasonally may be useful, and knowing which regions have significant seasonal effects is also useful.

One measure of seasonal OLS consistency is the number of OLSs that are mapped within a Landsat image each season. A consistent number of OLSs located by the software each season suggests that the software is locating the same OLSs each season. However, this may not be true. Though the number of OLSs each season may be similar, the locations of OLSs within that image may be different. Therefore, 2000 OLSs located within an image during the spring may not be in the same locations as 2000 OLSs located in a Landsat image of the same area during summer. It would be useful to know the proportion of OLS that are consistently located at the same place each season.

After techniques demonstrated by Haren (2005, personal communication, WPAFB) while assessing the seasonal accuracy of the OLS software at each RAS, ERDC also tabulated the number of OLSs located per season in each Landsat image in which the RAS was embedded. Figure 49 shows the number of OLSs located in Landsat images at Fort Bliss in path 33, row 37, during the months of May, July, and October 2005, and April 2006 (Table 16). Two versions of the Boeing OLS software were assessed, Version 7 released 28 March 2005, and Version 10 released 12 March 2007 (Almassy and Blake 2005, 2007). Version 7 of the software was used to initially locate the RAS field sites, and Version 10 of the software is the last official software release in FY07.

Figure 49 and Table 16 show that many more OLS are located by both versions of the software during the colder, and possibly drier, months of the year than during the warmer months of the year. Though the numbers of OLSs located at Fort Bliss are represented at only four points in time, they do show general seasonal trends. We did not obtain greenness indices for each of the images. However, images analyzed by Haren (2005, personal communication, WPAFB) in a preliminary analysis showed that the number of OLSs decreases as the greenness index threshold in the software is raised. That is, higher software-specified greenness index thresholds cause areas that are too green to be omitted as candidate OLS locations. In ef-

fect, the same process is occurring seasonally. When the software is executed each season at the same greenness index, areas that display a larger greenness index, especially during more moist months in arid regions—October in this case—will tend to be omitted as candidate OLS locations.

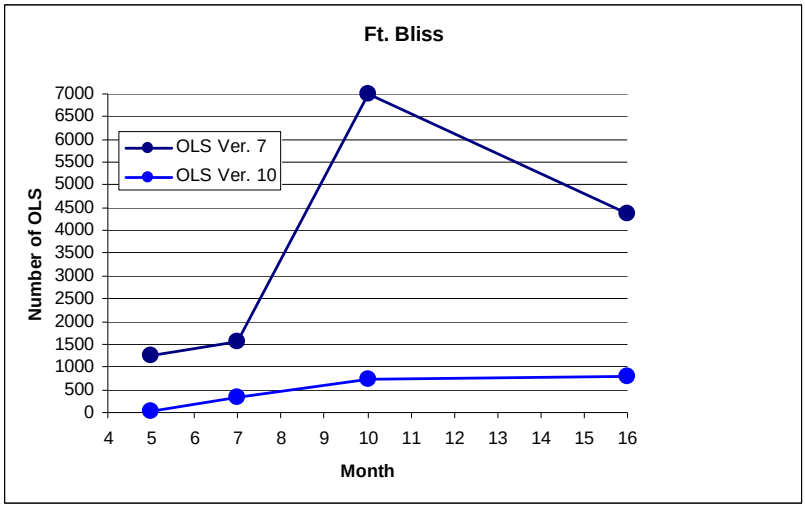


Figure 49. Number of OLSs located seasonally, by software version. June, July, and August are typically the warmest months at Fort Bliss, and July through October typically have the most precipitation.

Table 16. Number of OLSs located seasonally by software.

Image	Date	V7	V10	Notes*
Row 37 Path 33	18 May 2003	1744	64	Few OLSs in cloud
Row 37 Path 33	2 July 2005	1571	347	No cloud
Row 37 Path 33	22 October 2005	6996	731	No cloud
Row 37 Path 33	16 April 2006	4382	800	No cloud

* Comparisons were made only with Landsat images where no or few OLSs were within clouds. OLSs can be plotted in clouds in OLS software V7; software V10 excludes cloudy areas for locating OLSs.

The variation in number of OLSs by season, ranging from 1571 to 6996 for software Version 7, and 64 to 800 for software Version 10, is an expression of seasonal variation in factors that affect OLS quality (Table 16). As in comparisons at the other OLS field sites, El Centro NAF and Indiana (Affleck et al. in prep, Barna et al. 2007), Version 10 of the OLS software located fewer OLSs than the less conservative Version 7 of the software at Fort Bliss. However, unlike the other sites, the season with the maximum number of OLSs located is different for the two software versions at Fort Bliss, October 2005 for software Version 7 and April 2006 for software

Version 10. However, the difference in number of OLSs for Version 10 between October and April is only about 10% (Table 16).

At Fort Bliss it is not clear why these seasonal changes occur. In an arid environment where moisture availability may drive greenness as much or more than thermal and solar flux, the reasons for larger numbers of OLSs in November or April are not clear.

We also assessed the frequency of OLSs plotted in the same location from season to season. The OLS software provides coordinates for the center point, and the orientation, of each OLS. Using those coordinates and orientations, OLS locations for each season were compared. Table 16 shows the number of OLSs compared each season.

The analysis found no occurrences of matching OLS coordinates between any seasons. However, this may not be a true indicator that OLSs are not located at the same location each season. Each Landsat image is unique with regard to its georegistration to the Earth's coordinate system. As a result, it is possible that any two pixels in similar relative positions in Landsat images taken in different seasons would have different Earth-referenced coordinates. Even the same image georegistered to the Earth by two different processes or analysts may produce different Earth coordinates for any single pixel that are within 30–60 meters (one to two Landsat pixels) of one another. Therefore, there is still a possibility that OLSs may be located in nearly the same location for more than one season. Definitive demonstration of this would require overlaying of seasonal, georeferenced images within a geographic information system or conducting a proximity analysis assessing whether the center of OLSs in any season fall within 100 m, for example, of the center of OLSs during any other season.

7.2 OLS Software Seasonal Accuracy

Field work at the Fort Bliss RAS was scheduled to assess the quality of OLSs with season. Field work was conducted in July 2005 (summer), October 2005 (fall), and April 2006 (spring). No winter field work was conducted at this location because of budget constraints. The field team assessed the quality of the selected OLS, or RAS, according to criteria listed in Table 4. Those criteria are scored as pass/fail according to measurements made in the field each season.

Table 12 shows that the Fort Bliss RAS generally passes most evaluation criteria, especially those criteria that do not vary significantly with season. Even being an arid region where vegetation greenness typically varies with moisture content more than it does with seasonal temperature changes, OLSs were still found more frequently in the cooler months than in other seasons, the wet season typically being July through September at Fort Bliss.

We also used Versions 7 and 10 of the OLS software to plot the seasonal location of OLSs in the same vicinity as the location of the OLS that was used for the field work. Repeated locations of OLSs at the same or similar locations each season would support the hypothesis that conditions affecting OLS quality, as assessed by the software, remain fairly consistent season to season. The initial field sites were located using Version 7 of the software with an 18 May 2003 Landsat image. Figure 50 shows the location of the RAS where field work was conducted, in green. The 18 May 2003 Landsat image used to initially locate the field site was georeferenced to the earth's surface using the Landsat satellite's ephemeris—called "Systematic" georeferencing by the USGS—the least accurate georeferencing method. The OLS outlined in white in Figure 50 is a location for the RAS deemed to be more correct because its position was calculated using Landsat images that were "Precision" georeferenced to the Earth's surface. The white and green RASs are offset about 97 m north-south and 233 m east-west.

The 18 May 2003 Landsat scene used to locate the Fort Bliss RAS shows the location of the field site in yellow outline, and locations of approximately 20 OLSs in the vicinity using OLS Version 7 software (Fig. 51). This suggests that conditions in the general area of the RAS field site are favorable to OLSs.

The 2 July 2005 scene shows three OLSs located in the vicinity of the field site with no OLS relocated over the RAS field site (Fig. 52). However, of the three OLSs in the vicinity, the east-west oriented OLS appears, by eye, to be in nearly the same location as an east-west OLS in the 18 April 2003 image. This supports our hypothesis that OLSs may be plotted in nearly the same location season to season, but not at exactly the same pixel coordinates. It also suggests that some OLS locations may be of sufficiently high quality that they are identified during multiple seasons (and a seasonal analysis could be used to locate these high-quality OLSs).

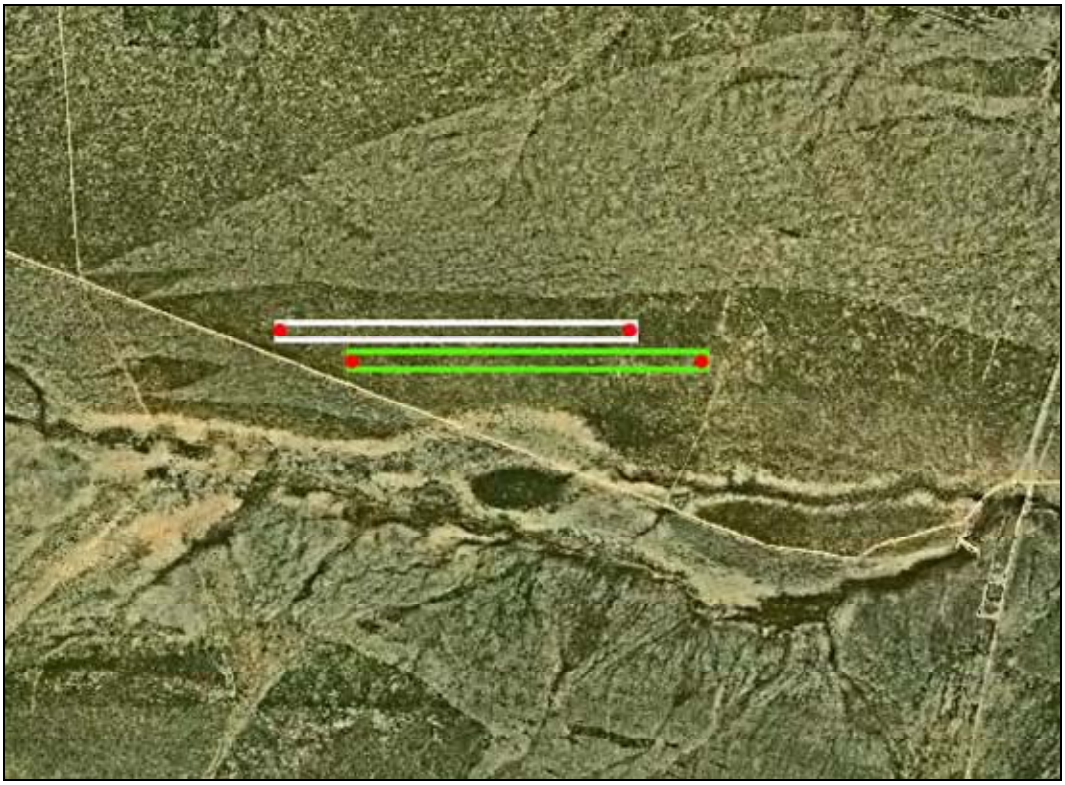


Figure 50. Fort Bliss RAS Precision georeferenced in white outline, and Systematic georeferenced in green outline. Field work was conducted at the green outlined site.



Figure 51. 18 May 2003 Landsat USGS Systematic georeferenced image with Version 7 of the OLS software. All OLSs shown are in Systematic georeferenced positions. The yellow outline OLS is the field site. Over 20 other OLSs are in the immediate vicinity of the field site.



Figure 52. 2 July 2005 Landsat USGS Precision georeferenced image with Version 7 OLS software. Blue OLSs are in Precision georeferenced positions, and the unfilled yellow outline OLS is the field site from the Systematic geoereferenced 18 May 2003 image (Fig. 50).

The 22 October image shows at least three OLSs to the east-northeast of the field site (Fig. 53). These overlap season to season, though not at the exact location or orientation.

The April 2006 image shows more OLSs in the vicinity of the RAS field site than any other image, with more than 20 OLSs (Fig. 54). Though it is difficult to determine whether these OLSs are at the same locations as previous OLSs without creating overlays using a Geographic Information System, the April 2006 OLSs overlap the locations of OLSs on the previous three images. Again, though no OLS is located at the same location and orientation as the field site, one southeast-to-northwest-oriented OLS does enter the field site area.

Version 10 of the OLS software is more conservative than Version 7. Figure 55 shows at least two OLSs were located on the 18 May 2003 Landsat image that was used to locate the RAS field site. Figure 55 also shows that one of these OLSs overlaps much of the field site.



Figure 53. 22 October 2005 Landsat USGS Precision georeferenced image with Version 7 OLS software. Blue OLSs are in Precision georeferenced positions, and the unfilled yellow outline OLS is the field site from the Systematic geoereferenced 18 May 2003 image (Fig. 50).



Figure 54. 16 April 2006 Landsat USGS Precision georeferenced image with Version 7 OLS software. Blue OLSs are in Precision georeferenced positions, and the unfilled yellow outline OLS is the field site from the Systematic geoereferenced 18 May 2003 (Fig. 50).

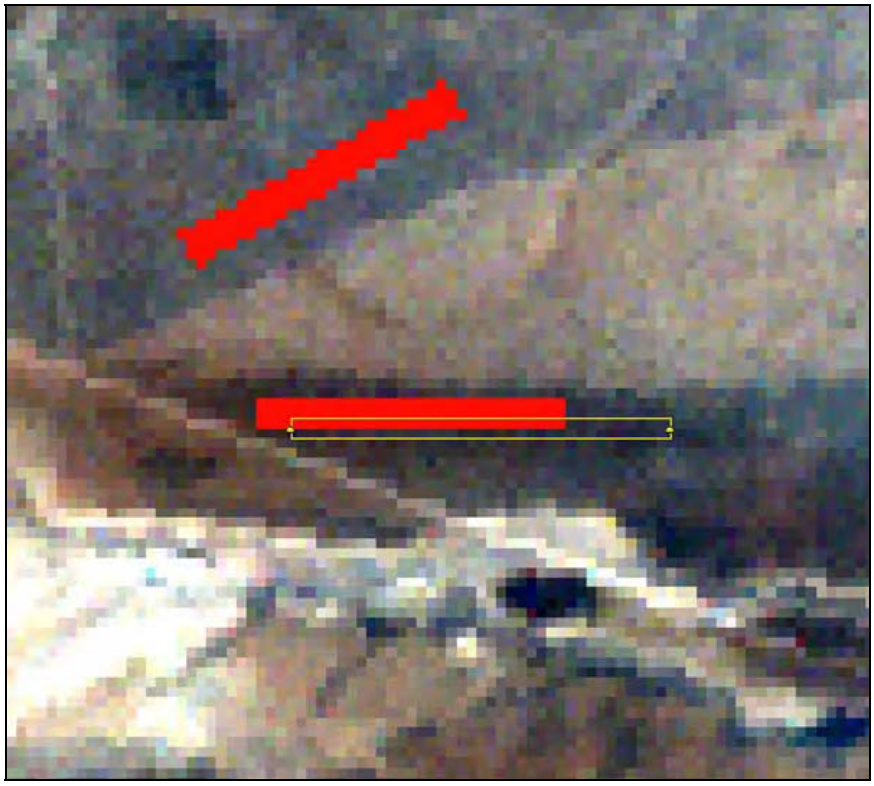


Figure 55. 18 May 2003 Landsat USGS Systematic georeferenced image with Version 10 of the OLS software. The unfilled yellow outline OLS is the field site from the systematic georeferenced 18 May 2003 image using Version 7 of the OLS software. Filled red OLSs were located with Precision georeferencing in Version 10 of the software.

The only other image that showed OLSs in the vicinity of the field site location with Version 10 of the software was the 16 April 2006 image. Here, about 10 OLSs were plotted in the vicinity of the field site (Fig. 56).

The large number of OLSs plotted in several seasons in a broad area around the field site suggests that a large area around the field site is suitable for OLSs. Seasonal changes in position, orientation, and number may be due to changes in greenness, but also to changes in pixel position and minor changes in pixel reflectance due to the seasonal changes, and also perhaps due to the georeferencing process. This analysis indicates that if software Version 10 had been available in April 2005, the RAS where field work was conducted would have been at a slightly displaced location from the site actually used (Fig. 55).

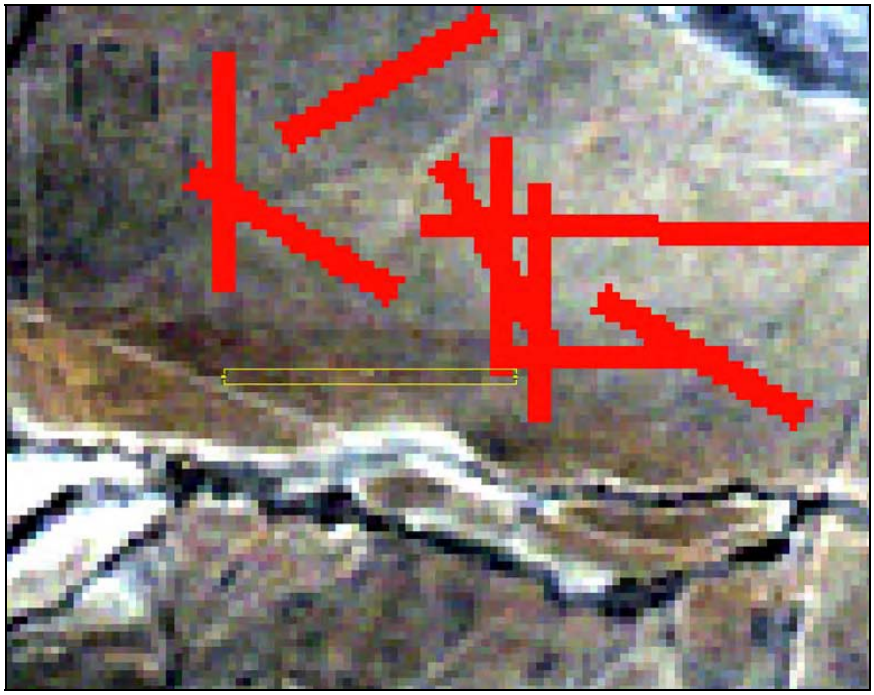


Figure 56. 16 April 2006 Landsat USGS Precision georeferenced image with Version 10 of the OLS software locating the red OLSs. The unfilled yellow outline OLS is the field site from the Systematic geoereferenced 18 May 2003 image (Fig. 50).

8 Overall OLS Rating

The field work at Fort Bliss was conducted to determine whether the OLS software identified suitable landing sites that met both the geometric and strength requirements to land an aircraft. Comprehensive ground truth data collection was conducted on the Fort Bliss RAS during three IOPs to assess adequacy of the OLS. Criteria revised from AFCESA semi-prepared airfield criteria (AFCESA 2002a, 2002b, UFC 3-260-02) were used to assess the OLSs as defined in Section 3, which identified and summarized the Fort Bliss RAS with the following:

a) The terrain topography of the RAS was measured along the longitudinal and the transverse directions of the runway. The overall longitudinal and transverse slopes of the RAS met the design runway criteria (< 3% grade). Undulation or roughness of the ground also was evaluated. At this RAS there is some natural ground roughness over the entire area (1.13 RMS along the longitudinal direction). If an aircraft is to land on this RAS, it would encounter some vibration as a result of surface roughness.

b) The soil physical characteristics and properties evaluated included soil type, density, color, and organic content. The soil type found on the RAS is a non-plastic, Silty Sand (SM) soil. The soil density showed no specific trend with depth and was non-uniform, which is not uncommon with natural soils. Soil density indirectly influences soil strength, therefore variable density will result with inconsistent soil strength. Organic content was found to be insignificant.

c) A caliche layer is found at varying depths. Having a thick caliche layer on the OLS can be advantageous in some cases. The caliche layer is non-uniform, however, and in some areas, broken caliche pieces have sharp edges that can damage aircraft tires and increase FOD. One of the disadvantages of the caliche layer is that it can perch above the water table—especially during rainy season—thus causing higher soil moisture and thereby weakening the soil structure.

d) The soil strength from the 0.5-kg Clegg impact hammer is relevant only for the top portion of the soil (less than 0.15 m or 6 in.). The CBR value from the Clegg hammer must be coupled with CBR values from the DCP profiles in order to asses the entire soil strength capacity for landing a C-130 and C-17 on the OLS.

e) A localized weak soil layer was identified from the DCP profiles on the OLS during all three IOPs. The bearing capacity of the OLS is summarized as capable of supporting a C-130 operation for several passes at various pay loads. The C-130 is allowed to land with varying allowable loads with several passes except using the minimum CBR profile in the fall. On the other hand, the C-17 can land for only one pass with varying allowable loads for all IOPs. If any of these aircraft are to land on this RAS, it is likely that localized soil failure, such as rutting, compaction, and deformation, may occur in areas with animal burrows. It may be necessary to conduct visual survey after a landing (i.e., C-130) to inspect the conditions of the OLS.

f) Vegetation on the RAS would not hinder landing an aircraft and bushes can be pushed away by the force and momentum of a vehicle. Most of the vegetation is low and would not affect the aircraft.

g) Large granular materials are commonly found on this RAS, principally from loose pieces of caliche lying on the surface. The AFCESA criteria required that these loose materials must be removed before an aircraft operation. The amount and size of loose granular materials exposed on the surface of the OLS are a potential hazard for aircraft operation on the OLS. Rocks larger than 0.1 m (4 in.) must be removed from the operational surface (ETL 97-09). Loose aggregate is considered to be a potential cause of FOD that can damage aircraft components. The OLS is rated as “Amber,” designating a loose aggregate cover between 1/10 and 1/2 of the RAS.

h) The soil is very dry most of the year. Dust is common and visibility can be an issue. Also, dust may be drawn into the engine and other parts of the aircraft.

i) Conditions at the Precision Corrected Imagery Runway Assessment Site (PCI-RAS) are most likely to be very similar to the Systematic Imagery Runway Assessment Site (SI-RAS). The PCI-RAS is rated

as “Excellent” for both its geometry properties and surface characteristics. The soil strength capacity is probably comparable to the strength measured at the SI-RAS.

j) The seasonal analysis shows that OLSs can reappear at similar locations in multiple seasons. This occurred at Fort Bliss because a large area around the RAS site is favorable for OLSs. However, demonstrated by Version 10 of the software, OLSs may not appear in every season, even in apparently favorable locations.

The overall rating including surface and subsurface characteristics for Fort Bliss OLS based on the criteria defined in Section 3 is summarized in Table 17 (shown on following page). The rating quantifies and defines the suitability of the OLS. The OLS is capable of landing a C-130 for more than one pass with varying loading capacity during three seasons (summer, fall, and spring). On the other hand, the OLS cannot support the C-17 even at a very low loading capacity primarily because sections of the RAS contained low strength layers with less than the minimum CBR requirement.

The overall rating of the entire OLS is shown in Table 18.

Table 17. Seasonal overall rating for Fort Bliss OLS.

Surface conditions	Summer	Fall	Spring	Comments
Potholes	Pass with caution (Green to Amber)			Bowl-shaped depressions caused by existing and abandoned animal burrows.
Loose aggregate	Pass with caution (Amber)			Existing caliche pieces on the surface that can puncture aircraft tires andbe ingested into an aircraft's engine.
Ruts	Pass (Green)			No ruts—vehicles are not allowed on the OLS.
Rolling resistance material	Pass with caution (Amber)			Loose materials such as caliche pieces along the wheel path of the OLS can increase rolling resistance on the aircraft's tire.
Dust	Pass with caution (Amber)			Dry soil is common in semi-arid areas; dust partially obstructs visibility beyond approximately 400 m.
Animal burrows	Fail (Amber to Red)			Voids and holes created by the animals were commonly found on the OLS. Locations with animal burrows are sign of weak areas. The size of the holes and area are also critical.
Mounds	Pass (Green)			No mounds were observed on the OLS.
Vegetation	Pass (Green)			Mostly grassy-type vegetation with a few yucca trees; most likely would not obstruct on aircraft operation.
Standing water	Pass (Green)			No water ponds were observed on the OLS.
Surface drainage paths	Pass (Green)			No drainage paths.
Surface debris and organics materials	Pass (Green)			Organic materials are insignificant.
Snow depth	Pass (Green)			No snow cover.
Geometry				
Longitudinal grade	Pass (Green)			Grade along the entire OLS is within the criteria.
Transverse grade	Pass (Green)			Lateral grade is within the criteria.
Aircraft				
C-130	Marginal	Marginal	Marginal	Loading capacity (# pass, pay load) based on minimum CBR or the 15th percentile of the minimum CBR value.
C-17	Unacceptable	Unacceptable	Unacceptable	

Table 18. The overall rating of the entire OLS.

Categories	Rating
Surface characteristics	Excellent or Pass
Geometric properties	Excellent or Pass
Aircraft loading capacity C-130 C-17	 Marginal Unacceptable

9 Conclusion and Recommendations

The OLS software is designed to select locations that are smooth, flat, level, and free of obstruction or woody vegetation that would harm the aircraft. It is not yet designed to consider all of the criteria desired by the Air Force. However, the main objective of the RAS field work is to assess the quality of the OLS selected by the Boeing software and to examine the terrain characteristics and soil strength with respect to aircraft operations. Seasonal effects and changes in the RAS, including the soil properties and the capabilities of the software to select OLSs in any season, were evaluated.

From the assessment, the software was able to predict an OLS regarding a piece of land that is smooth, flat, level and relatively free of obstruction at Fort Bliss. The OLS is acceptable in terms of its lateral and longitudinal gradients because slope measurements are below the required AFCESA design criteria. With respect to the bearing capacity, the OLS is adequate for landing a C-130 and is not capable for a C-17 landing. This is true for all three field assessments at Fort Bliss OLS. Soil failure may form in terms of rutting, depression, and irregular compaction in areas with soft soil layers. These soil failures can be substantial for aircraft landing and takeoff, causing significant tire sinkage and soil resistance. It may be necessary to conduct a visual survey after landing (i.e., C-130) to inspect the conditions of the OLS. There also are other features, such as loose materials on the ground on the OLS, that could hinder the aircraft operation.

We conducted a thorough field assessment to characterize the OLS and examine the seasonal changes of the RAS. Acquiring these measurements was time-consuming and labor-intensive. For example, the most accurate way to assess the soil properties (soil type and density) was digging large pits. The nuclear gage was cumbersome to use on the OLS, but it is one of the few reliable instruments for measuring soil density to date for various soil conditions. We also encountered equipment accuracy or precision issues and found that some of the instruments did not work well enough to use in certain soil conditions. For example, soil moisture measurements were made with multiple technologies at the same sampling locations to determine how well they agreed. There often was disagreement among the

instruments; in some cases, instruments would provide values not consistent with physical possibility (i.e., ML2 and PR2). However, the difference in soil moisture between ML2 (HH2) measurements and oven-dry measurements was small. Oven-dried gravimetric measurements are the most direct method of measuring soil moisture and, other than sampling error, which affects all methods, has the least opportunity for error if careful laboratory methods are followed. The DCP is the standard tool for measuring soil strength (in terms of soil shear strength) for airfield design and evaluation and is portable, although it does not measure the surface layer strength. The 0.5-kg Clegg hammer provides a CBR value for the surface layer of the soil based on hammer dynamic impact onto the soil surface (soil stiffness) and can be used with the DCP data to assess the entire soil strength profile. Because of significant variations at the same sampling locations in CBR value between the DCP and the 0.5-kg Clegg hammer, further assessment and correlations are needed between the instruments.

The approach that we used was modified from AFCESA guidelines to be applicable for OLS assessments. Because the guidelines used for assessing the OLS were revised from the AFCESA criteria, there is a need to quantify the ratings given for the other features present on austere and natural terrain and environment. A specific interest for OLS is the need to better quantify the surface roughness (mounds, undulations, swales) or perhaps use another measure of roughness index and adapt an acceptable roughness value for OLS. Also, soil resistance on aircraft landing and takeoff due to surface and loose materials needs to be investigated for OLS application. We especially need to develop an accepted set of guidelines and criteria for evaluating an OLS.

Soil strength was found to vary on the Fort Bliss OLS. We need to examine the spatial and temporal variability of CBR within soil layers with the same soil type. We can enhance the OLS software by relating the measured CBR to the Landsat imagery. Also, there is need to embed a soil strength calculating capability into the OLS system that will use physical properties of the soil to compute soil strength rather than relying upon the software to locate areas that are simply associated with firm soil. Though Version 7 of the OLS software is certainly capable of finding locations that are promising as OLSs, the Fort Bliss example indicates that software changes, or flatness and vegetation indices within the software instruction set, will need some modification before safe OLSs can be consistently selected for transport aircraft operations.

References

Abele, G., 1990, Snow Roads and Runways. US Army Cold Regions Research and Engineering Laboratory, Hanover, New Hampshire, CRREL Monograph 90-3.

AFCESA, 2002a, Airfield Pavement Evaluation, Standards and Procedures. Air Force Civil Engineer Support Agency, Tyndall AFB, Engineering Technical Letter 02-19.

AFCESA, 2002b, Criteria and Guidance for C-17 Contingency and Training Operations on Semi-Prepared Airfields. Air Force Civil Engineer Support Agency, Tyndall AFB, Engineering Technical Letter 97-09.

AFCESA, 2004, C-130 and C-17 Landing Zone (LZ) Dimensional, Marking, and Lighting Criteria. Air Force Civil Engineer Support Agency, Tyndall AFB, Engineering Technical Letter 04-7.

Affleck, R.T., C. Ryerson, L. Barna, K. Claffey, 2008, Suitability Measurement and Analysis for El Centro Naval Air Facility OLS. US Army Engineer Research and Development Center, Cold Regions Research and Engineering Laboratory, Hanover, New Hampshire, ERDC-CRREL Technical Report TR-08-18.

Almassy, R., and P. Blake, 2005, Opportune Landing Site Multispectral (OLS-MS) Software Operation Description, Version 7.0. Boeing Company.

Almassy, R., and P. Blake, 2007, Opportune Landing Site Multispectral (OLS-MS) Software Operation Description, Version 10.0. Boeing Company.

ASTM, 2003, American Society for Testing Materials, West Conshohocken, Pennsylvania.

Barna, L.A., C.C. Ryerson, and R.T. Affleck, 2008, Opportune Landing Site Southeastern Indiana Field Data Collection and Assessment. US Army Engineer Research and Development Center, Cold Regions Research and Engineering Laboratory, Hanover, New Hampshire, ERDC-CRREL Technical Report TR-08-22.

Brown, B., Evaluation Product Manager, Lafayette Instrument Company, PO Box 5729, 3700 Sagamore Parkway North, Lafayette IN 47903, Telephone 765-423-1505, ext. 202, Fax: 765-423-4111, e-mail: bbrown@lafayetteinstrument.com, Web site www.lafayetteinstrument.com.

Clegg, B. (1980). An Impact Soil Test as Alternative to California Bearing Ratio. In *Proceedings, 3rd Australian-New Zealand (ANZ) Geomechanics Conference*, Wellington, New Zealand, 1 225-230.

Crandell, J., Managing Director of Dr Baden Clegg Pty Ltd, Unit 2, 23 Bishop Street, Jolimont, Western Australia 6014, email: J.drclegg@iinet.net.au, website: www.clegg.com.au

Danyluk, L.S., S.A. Shoop, R.T. Affleck, and W.L Wieder. 2007, Opportune Landing Site CBR and Low-Density Laboratory Database. US Army Cold Regions Research and Engineering Laboratory, Hanover, New Hampshire, ERDC-CRREL Technical Report TR-08-9.

EM 1110-2-1906, 1970, Engineering Manual, Engineering and Design, Laboratory Soils Testing, Headquarters, Department of the Army Office of the Chief of Engineers.

Godwin, R., N. Warner, and D. Smith, 1991, The development of a dynamic drop-cone evice for the assessment of soil strength and the effects of machinery traffic. *Journal of Agricultural Engineering Research*, v 48, p. 123–131.

Herrick, J., and R. Jones, 2002, A dynamics cone penetrometer for measuring soil penetration resistance, *Soil Science Society of America Journal*, 66:1320–1324.

Manley, D., 2001, Identifying Unprepared Landing Sites for Advanced Theater Transport Aircraft (and Terrain Trafficability for Military Vehicles). The Boeing Company, Phantom Works, Long Beach, California, 3 p.

Millar, L.R. (1977). An Application of the Soil Impact Tester to Road Pavement Construction, Master's Thesis, University of Western Australia.

Munsell Soil Color Charts, 2000, Revised washable edition, GretagMacbeth, 617 Little Britain Road, New Windsor, NY 12553

Rollings, M., and R. Rollings, 1996, *Geotechnical Materials in Construction*. New York: McGraw-Hill.

Ryerson, C., and J. McDowell, 2007, Anywhere-Anytime: Enhancing Battlespace Vertical Mobility. AIAA 2007-1103, American Institute of Aeronautics and Astronautics 45th Aerospace Sciences Meeting and Exhibit, 8–11 January, Reno, Nevada, 9 p.

Soil Survey of Otero Area, New Mexico, 1981, Parts of Otero, Eddy and Chaves Counties, United States Department of Agriculture Soil Conservation Service and Forest Service in cooperation with the New Mexico State University Agricultural Experiment Station.

Stolf, R., R. Klaus, and C. Vaz, 2005, Response to "Comments on 'Simultaneous Measurement of Soil Penetration Resistance and Water Content with a Combined Penetrometer–TDR Moisture Probe' and 'A Dynamic Cone Penetrometer for Measuring Soil Penetration Resistance.'" Soil Science Society of America Journal, 69:927–929.

User Manual for the Profile Probe type PR2, ftp://ftp.dynamax.com/Manuals/PR2.pdf, Copyright 1999 Delta-T Devices Ltd., 128 Low Road, Burwell, Cambridge, CB5 0EJ, England.

ThetaProbe Soil Moisture SensorTYPE ML2x, User Manual, ftp://ftp.dynamax.com/Manuals/ml2x.pdf, Copyright 1999 Delta-T Devices Ltd., 128 Low Road, Burwell, Cambridge, CB5 0EJ, England.

Vaz, C., and J. Hopmans, 2001, Simultaneous measurement of soil penetration resistance and water content with a combined penetrometer-TDR moisture probe. *Soil Science Society of America Journal*, 65:4–12.

Vincent, R. (unpublished) Continental United States Simulacrums to Four Areas of Interest Overseas.

Vincent, R.K., and D.L. Jennings, 2004, A four-state evaluation of the Boeing Landing Suitability Index (BLSI) for automatically mapping candidate aircraft operating sites in natural terrain from LANDSAT TM Data. *Journal of Terramechanics*, Vol. 41, pp. 151–162.

Webster, S.L., R.H. Grau, and T.P. Williams. 1992. Description and Application of Dual Mass Dynamic Cone Penetrometer, Instruction Report GL-92-3, USAE Waterways Experiment Station, Vickburg, Mississippi.

Webster, S.L., R.H. Grau, and T.P. Williams. 1994. Force Projection Site Evaluation Using the Electric Cone Penetrometer and the Dynamic Cone Penetrometer (DCP). US Army Waterways Experiment Station, Vicksburg, Mississippi, Technical Report GL-94-17.

Appendix A1: CEERD-RS Trip Report, 17 March 2005

FOR: James McDowell, OLS PM, AFRL/VA

CC: Pam Blake, Boeing; Richard Almassy, Boeing; Ray Heron, AFRL/SN; Lieutenant Offner, AFRL/SN; Robert Vincent, BGSU; George Koenig, ERDC/CRREL; Sally Shoop, ERDC/CRREL; Robert Davis, ERDC/CRREL

FROM: Charles Ryerson, Rosa Affleck, and Elke Ochs, ERDC/CRREL

SUBJECT: Trip Report: Fort Bliss OLS Logistics Meeting Potential Field Site Inspection, 8–11 March 2005

1. Objectives

Arrange logistics for OLS field work to be performed at Fort Bliss. Inspect potential field sites selected by software using June 2001 LANDSAT 7 imagery.

2. Participants

David Dodge, Fort Bliss Department of Environment (DOE), David.Dodge@emh10.bliss.army.mil, 915-568-7979; Irene Reed, Chief, Business Management Office, rredi@bliss.army.mil, 915-568-6608; CPT Judith Mendez USACAS S-3, Judith.mendez@emh.bliss.army.mil, 915-569-9505/9353 915-726-6089 (cell); John R. Paul, USACAS S-3, John.paul@bliss.army.mil, 915-569-9214; Bob McDonald, USASAS Range Scheduling, Mcdonaldrc@bliss.army.mil, 915-569-9280; Shane P. Offutt, DOE Range Liaison, offutts@bliss.army.mil, 915-569-9444; Charles D. Carrig, Archaeologist, carrigc@bliss.army.mil, 915-568-2681; Dallas Bush, DOE GIS, bushd@bliss.army.mil, 915-568-3018; Rosa T. Affleck, ERDC/CRREL, Civil Engineer, rosa.t.affleck@erdc.usace.army.mil, 603-646-4662; Charles C. Ryerson, ERDC OLS PM, charles.c.ryerson@erdc.usace.army.mil, 603-646-4487.

3. Subjects Discussed

Ryerson and Affleck briefed participants listed above at 0900 9 March regarding OLS program and intended Fort Bliss field work and goals for visit.

Dodge, Reed, and Ryerson discussed terms of MOA required between ERDC and Fort Bliss to include reimbursement, health and safety plan, project goals, and points of contact. MOA must be in place prior to field work start.

Affleck and Ryerson spent about 1.5 days in field with DOE liaison Shane Offutt and Archaeologist Charles Carrig. Offutt and Carrig are very knowledgeable of Fort Bliss training lands. We visited OLS locations mapped on Fort Bliss by the Boeing software current as of 8 March 2005, using LANDSAT 7 LANDSAT frame 033_038 for 13 June 01. The software was run with a flatness index of 0.02, and a vegetation index of 1.5.

Following are discussions of OLSs located by Boeing software and located at Fort Bliss using a GPS with the Wide Area Augmentation System. The Fort Bliss range liaisons also helped locate OLSs. Figure A1-1 shows 14 areas of OLS groupings mapped by Elke Ochs. Runways are overlaid on 1-m resolution orthophoto imagery from January/February 1996. OLSs are referred to by their area number and the OLS number in the following descriptions. Green arrows denote approximate viewing positions. No OLS was inspected in its entirety to allow time to visit more sites.

OLS 1165 in Area 14 UR (Fig. A1-2) was inspected, along with cursory inspections of the many OLSs around it. OLS 1165 was inspected from its north end, which terminated at a roadway paralleling a pipeline right of way. OLS 1165 runs N–S. The north end was located with the GPS, and direction was determined using a compass corrected for magnetic declination. Figures A1-3 and A1-4 look south from the north end of the OLS. Mesquite dunes stand about 1.5 m high and about 5–10 m across, and are spaced about 5 m apart. An aircraft could not be safely landed in the area. Note large number of OLSs in same environment in Figure A1-2.

OLSs 2189 and 2187 in Area 12LR (Fig. A1-5) are parallel and oriented 30–210 degrees. They cross a dirt road at their southern ends. Terrain (Fig. A1-6) consists of mesquite dunes about 1 m high and 3–4 m wide. Yucca mounds are farther apart. Though fairly flat, the OLS is not adequate for

landing due to roughness. A wash about 1 m deep runs across the OLS (Fig. A1-7, behind mesquite dune). Note large number of OLSs in same environment in Figure A1-5.

OLS 5215 in Area 13 (Fig. A1-8) was inspected near the middle of its length where it crossed a dirt road. The OLS area observed was dominated by 1.5- to 2-m tall mesquite dunes that were about 10 m across (Fig. A1-9 and A1-10). Soils were similar to those found in other mesquite-dominated areas, a silty sandy.

OLSs 1933 and 1936 are located in Area 1 (Fig. A1-11). All four OLSs in the image cross roads and electrical powerlines (Fig. A1-12–A1-14). However, the paved road that now exists, running north–south, was a dirt road when the LANDSAT image was taken in 2001. The power lines have been in place for decades. Overall, the entire location would make ideal runways except for the roads and powerlines. Terrain is flat with some mesquite. The mesquite is not mounded as dunes, and bushes are about 2 m across and stand about 1 m high and, in a few cases, 2 m high. Sand around mesquite roots is only about 6–12 inches high. Relief in 30 m is less than about 0.7 m, and in most cases less than 0.3 m. Vegetation is sparse, covering the ground about 30%.

OLS 2720 is along a pole line in Area 1 (Fig. A1-11). The pole line has been in place for decades, and the maintenance road along pole line is incised about 0.3–0.7 m (Fig. A1-15–A1-16). The road is about 3 m wide.

OLS 3225 in Area 1 has essentially the same conditions as OLSs 1933, 1936, and 2720—all potentially good runways except for power line and road crossings (Fig. A1-17). There are some mesquite mounds about 0.3 m high and a few meters across. Mesquite is about 0.5–2 m high.

OLS 2731, located in Area 3 (Fig. A1-18), consists of a high concentration of large mesquite dunes 2 m tall by 5–10 m across. Blowouts between mesquite dunes were about 10–20 m across (Fig. A1-19–A1-20). Landings would be impossible, and were similar to other OLSs located in mesquite dune areas. Soils are sandy with about 5% silt and no clay or organics. Overall, none of the runways in Area 3 are acceptable because of the prevalence of large mesquite dunes.

OLS 1095 in Area 2 was inspected from its southeast corner. Looking north, large mesquite dunes 5–10 m across and 2 m tall dominated with blowouts about 10 m across (Fig. A1-21–A1-23). Vegetation cover is about 50%.

The following photos illustrate other areas on the fort where the range liaisons and Ryerson and Affleck judged the potential good for safe OLSs. None of these areas were selected by the OLS software. Though there was modest relief of nearly 0.3–0.7 m in 30 m in some areas, there were no mesquite dunes, and vegetation cover varied from about 50% to nearly 80–90% (Fig. A1-24–A1-30).

4. Assessment

The ERDC field team visited areas at Fort Bliss representing about 25–30% of the approximately 400 OLSs mapped on the fort. None of the OLSs visited were suitable as safe landing sites. The primary problem was relief created by mesquite dunes. Some landing sites in Area 1 were good, but they crossed roads and power lines. We hypothesize that OLSs may be improperly selected as a result of interactions between pixel size and mesquite dune size and spacing, giving an illusion of smoothness. The Fort Bliss range liaisons showed us at least five areas that had much higher probabilities of having safe OLSs. The OLS software must be field-checked in several environments at a high level, and corrected if necessary, prior to detailed field assessment.

5. Action Items

Complete MOA with Fort Bliss.

Assist Boeing and AFRL with identification of reasons for incorrect software selection of OLSs.

6. Figures

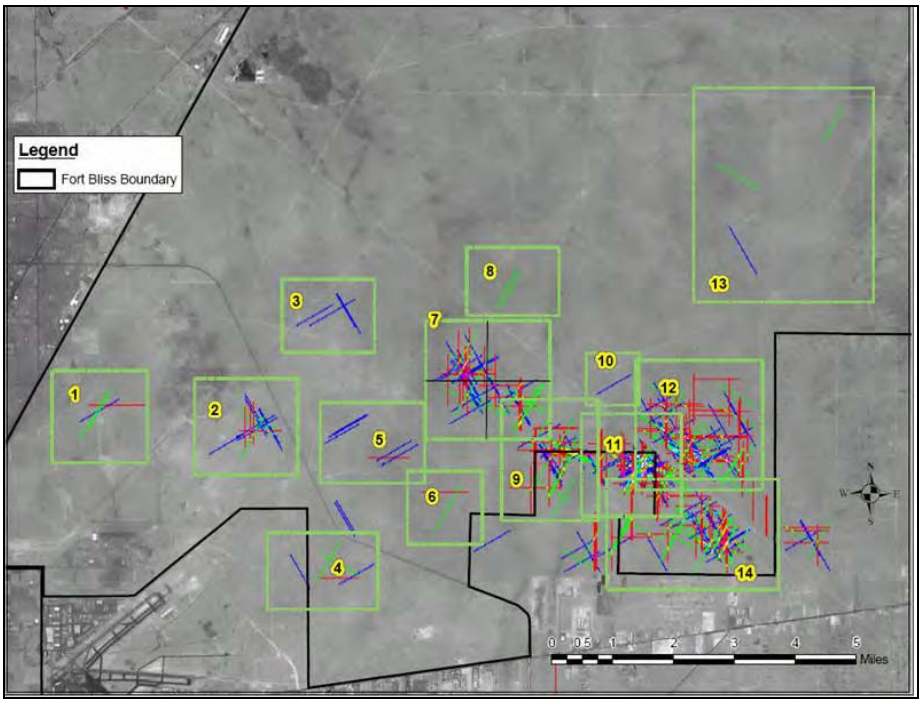


Figure A1-1.

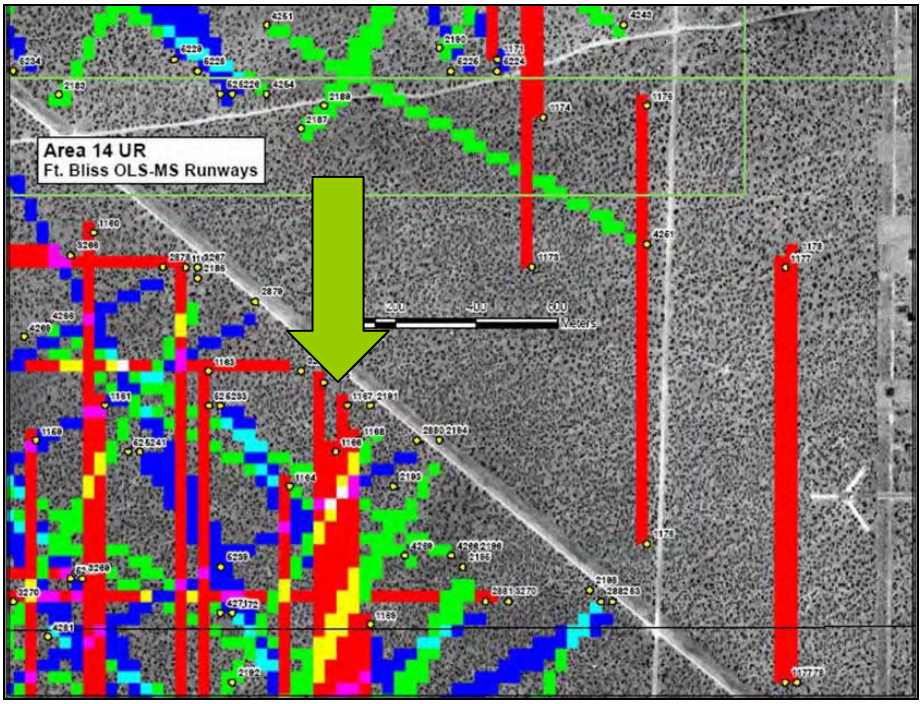


Figure A1-2.



Figure A1-3.



Figure A1-4.

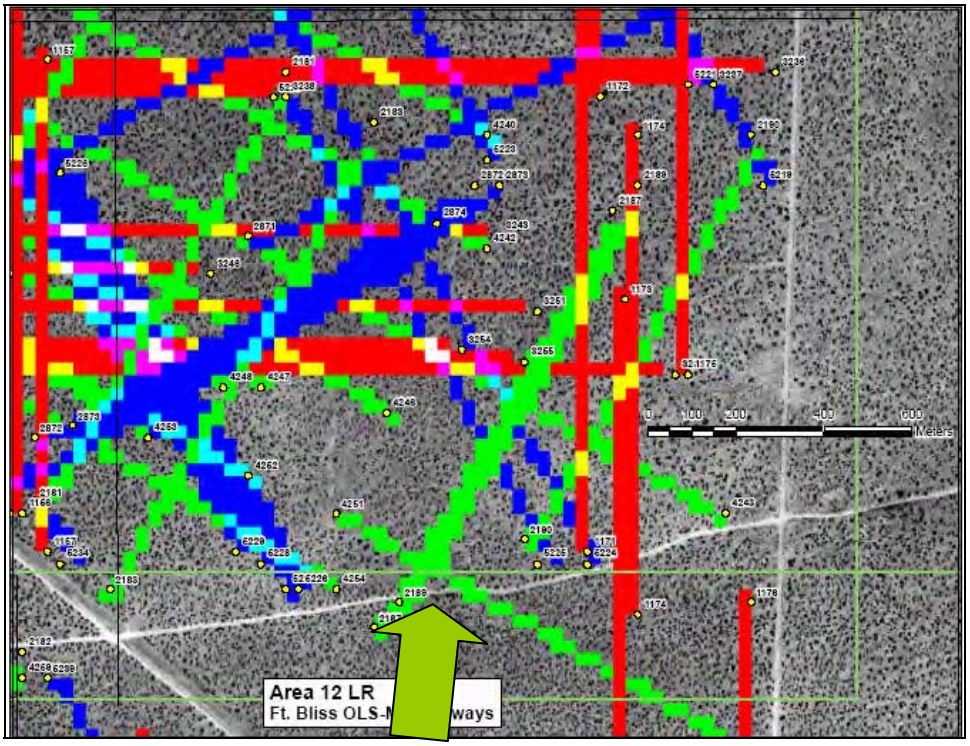


Figure A1-5.



Figure A1-6.



Figure A1-7.

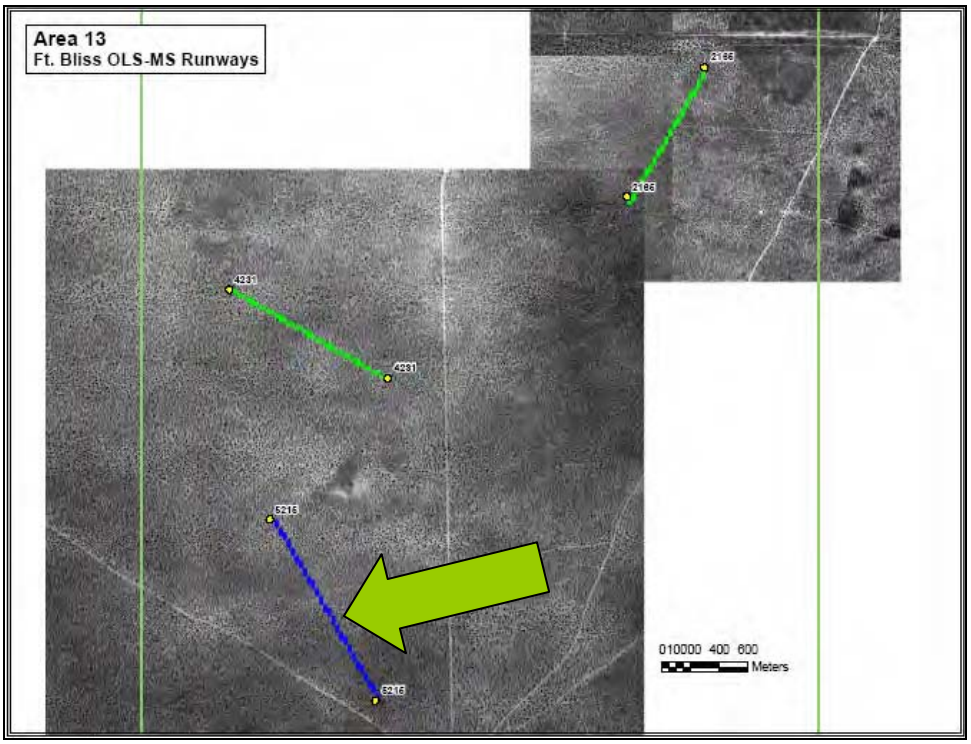


Figure A1-8.



Figure A1-9.



Figure A1-10.

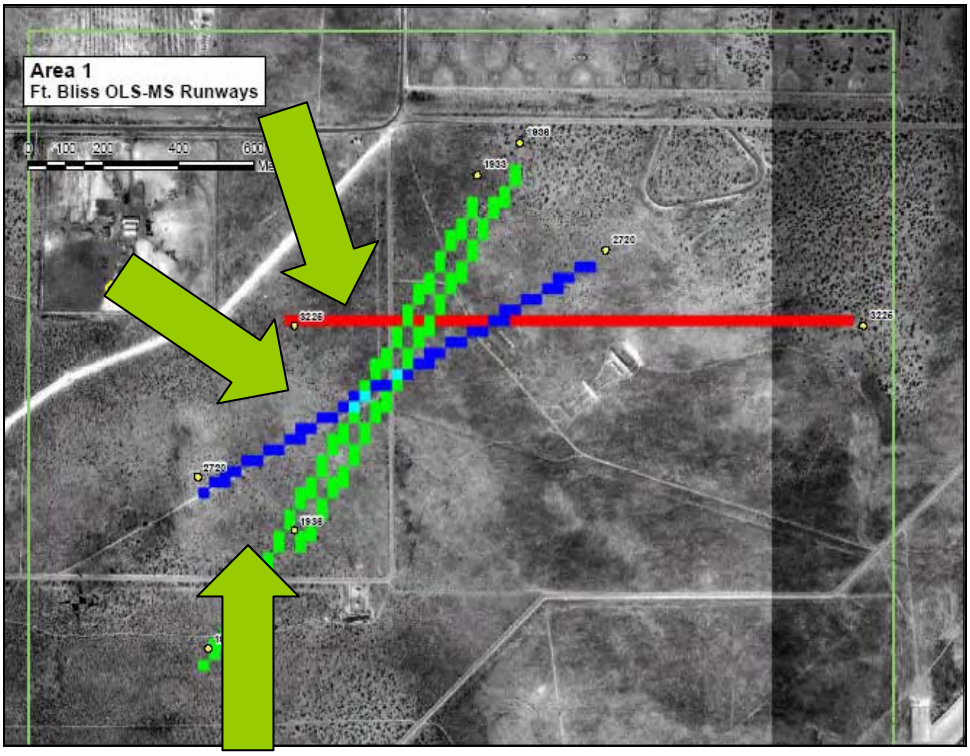


Figure A1-11.



Figure A1-12.



Figure A1-13.



Figure A1-14.



Figure A1-15.



Figure A1-16.



Figure A1-17.

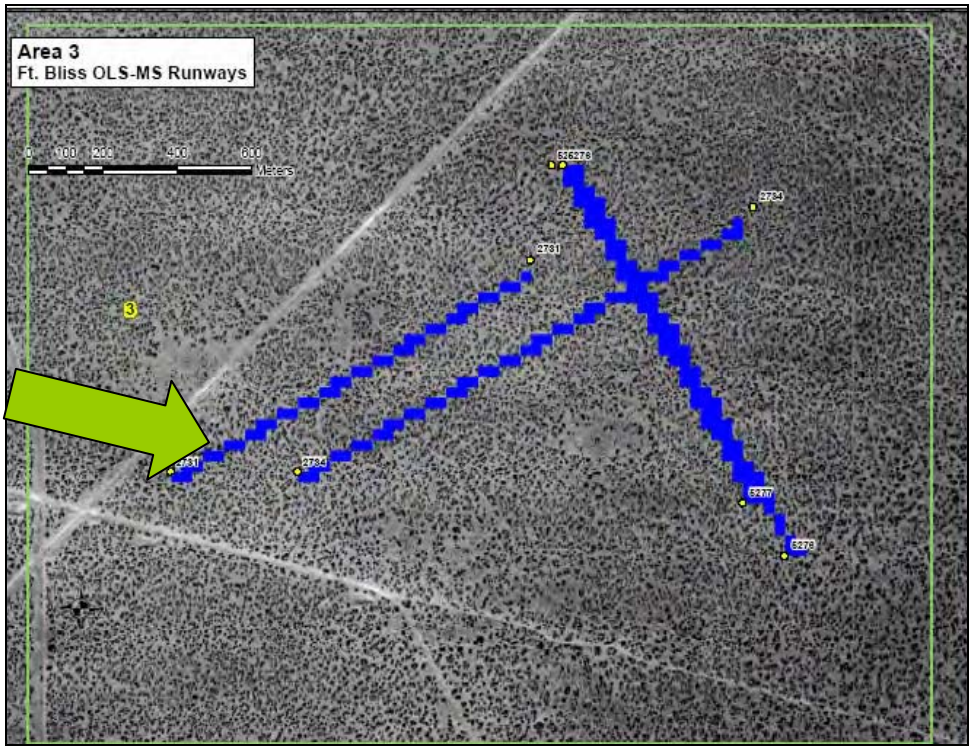


Figure A1-18.



Figure A1-19.



Figure A1-20.

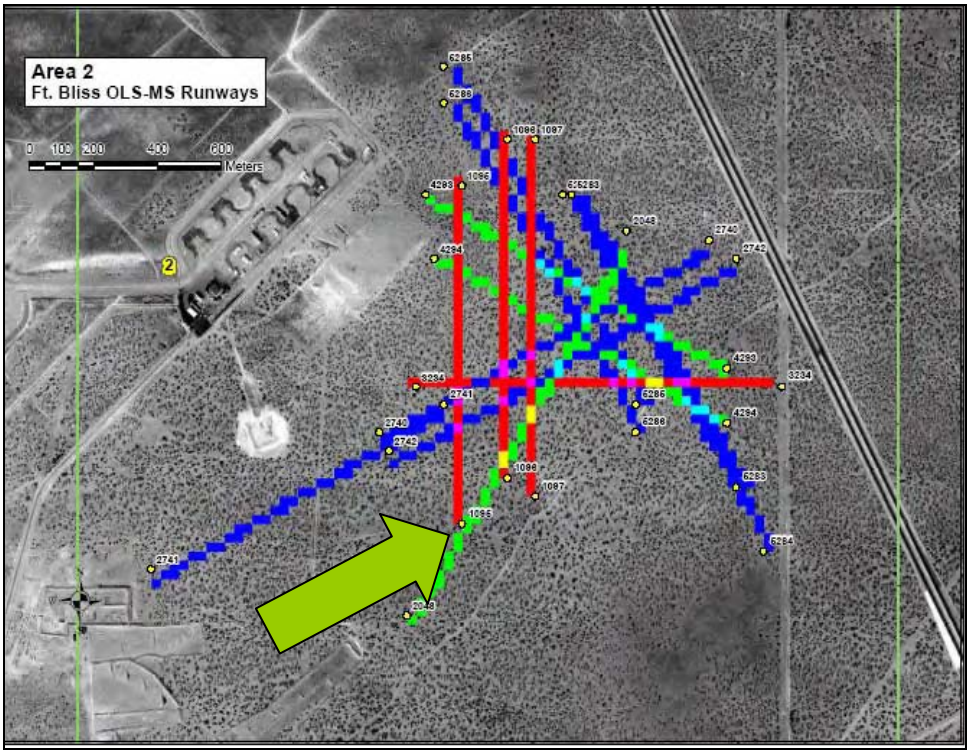


Figure A1-21.



Figure A1-22.



Figure A1-23.



Figure A1-24.



Figure A1-25.



Figure A1-26.



Figure A1-27.



Figure A1-28.



Figure A1-29.



Figure A1-30.

Appendix A2: CEERD Trip Report, Rosa Affleck and Lynette Barna, 6 June 2005

FOR: James McDowell, OLS PM, AFRL/VA

CC: Pam Blake, Boeing; Richard Almassy, Boeing; Ray Heron, AFRL/SN; Lieutenant Offner, AFRL/SN; Robert Vincent, BGSU; George Koenig, ERDC/CRREL; Sally Shoop, ERDC/CRREL; Robert Davis, ERDC/CRREL

FROM: Rosa Affleck, Lynette Barna, Charles Ryerson, and Elke Ochs, ERDC/CRREL

SUBJECT: Trip Report: Selection of OLS site, 6 June 2005

1. Objectives

Select an OLS site.

2. Participants

Charles D. Carrig, Archaeologist, carrigc@bliss.army.mil, 915-568-2681; Rosa T. Affleck, ERDC/CRREL, Civil Engineer, rosa.t.affleck@erdc.usace.army.mil, 603-646-4662; Lynette Barna, ERDC/CRREL, Civil Engineer, lynette.a.barna@erdc.usace.army.mil.

3. Site Surveyed

Affleck and Barna spent most of the day in the northern part of Fort Bliss with DOE Archaeologist Charles "Chuck" Carrig. Carrig accompanied Ryerson and Affleck on the first visit to evaluate OLSs at Fort Bliss in March. On this trip we visited OLS locations mapped on the northern portion of Fort Bliss by the Boeing software that was run using LANDSAT 7, LANDSAT frame 033_037 for 18 May 03. The software was run with a flatness index of 0.02 and a vegetation index of 1.8, using OLS-MS software version 7. The image was run with runway dimensions of 90 ft by 3000 ft, and 270 ft by 4000 ft (Fig. A2-1–A2-2). Both runway dimensions were examined in areas that are accessible, Area 6 in this case.

We headed to Maneuver Area 18 located in Otera Mesa. From El Paso we took Highway 54 North and turned right (east) onto State Highway 506 after the Border Patrol Station. Then we turned right to the entrance to Centennial Bombing Range, which is a gravel access road, passed the Mesa Horse Camp, and continued eastward. This is a free-cattle range area. On occasion we encountered cows near the road. We located OLS 11- and 12-Long located in Area 6 in Otera Mesa (Fig. A2-3). We flagged OLS 11-Long and walked about 1000 ft along the runway. At 230 feet from the start flag there was rebar sticking up vertically out of the ground. This is a demarcation for a Patriot missile setup site (P-site), an area of approximately 1 km^2. There are two of these test areas in this vicinity, both of which are occasionally active, but no firing. At 545 feet down the OLS we noticed a slight undulation of the terrain. The vegetation cover is approximately 60%, composed mostly of desert grass, dry tumbleweed, yucca, and cholla cacti. The terrain is relatively flat. We took photos of the surrounding land surface (Fig. A2-4–A2-13). Overall, the entire location is relatively flat with very slight undulation and is a suitable runway except that it is quite a distance to the road for field logistics.

We also walked toward OLS 17-Long, which is a distance away from the access road. We did not walk all the way to that location, but the general features of the terrain are very similar to OLS 11- and 12-Long.

We then walked south toward an OLS cluster that was 90 by 3,000 feet (Fig. A2-14). This location is an alternate because we are not allowed to drive next to the OLS location during the fieldwork. OLSs 273–277 are also located next to a gravel access road (Fig. A2-15). We flagged OLS 276, which runs to the east, and walked down the throat of the OLS, about 1000 ft along the runway. This area is relatively flat with slight undulations. The vegetation cover is approximately 60%, composed mostly of desert grass and dry tumbleweed. There are a few yucca cactus spaced about 200 ft apart (Fig. A2-16–A2-29). The soil is very dry and crumbly, and is described as silt with few granular materials (Fig. A2-20–A2-21). At approximately 1,000 feet there was some slight undulation of the terrain, widely spaced at about 100 feet apart. There was also a fence post demarcating the perimeter of the P-site. Again, this is not a launching location. However, we did come across some missile debris, such as twisted metal collars and other metal parts. We walked out to a total distance of about 1,130 feet from the start flag. We saw Oryx, which can be aggressive, in the distance.

We drove by OLS 279, which crosses the access road and a chain link fence (Fig. A2-30) on Toy Payne Tank Road. Vegetation off this road varied (Fig. A2-31–A2-32).

Driving along Highway 54 North, we passed Area 3 and attempted to examine the OLSs. This area is on mesquite dunes and has no access (Fig. A2-33, A2-37). We also drove the north side of Area 3, approximately 1.5 miles north of OLS 92 (approximately 4–5 miles north of Wilde Benton Airstrip). We found this location was dominated by 5- to 10-ft-tall mesquite dunes that were about 5–10 ft across and spaced 5–20 ft apart (Fig. A2-34, A2-35). The soil is fine-grained silty sand (Fig. A2-36).

4. Areas That Were Not Surveyed

Areas 1 and 2 are outside of the Fort Bliss boundary.

In Area 4, the OLSs are far from the road; access is the issue.

OLSs in Area 5 are far from the access road. Carrig mentioned that they are located with creosote bushes and several arroyos (dry river beds).

Areas 7 and 8 are in the bombing zone and no access is allowed.

There is no access in Areas 9 and 10.

5. Figures

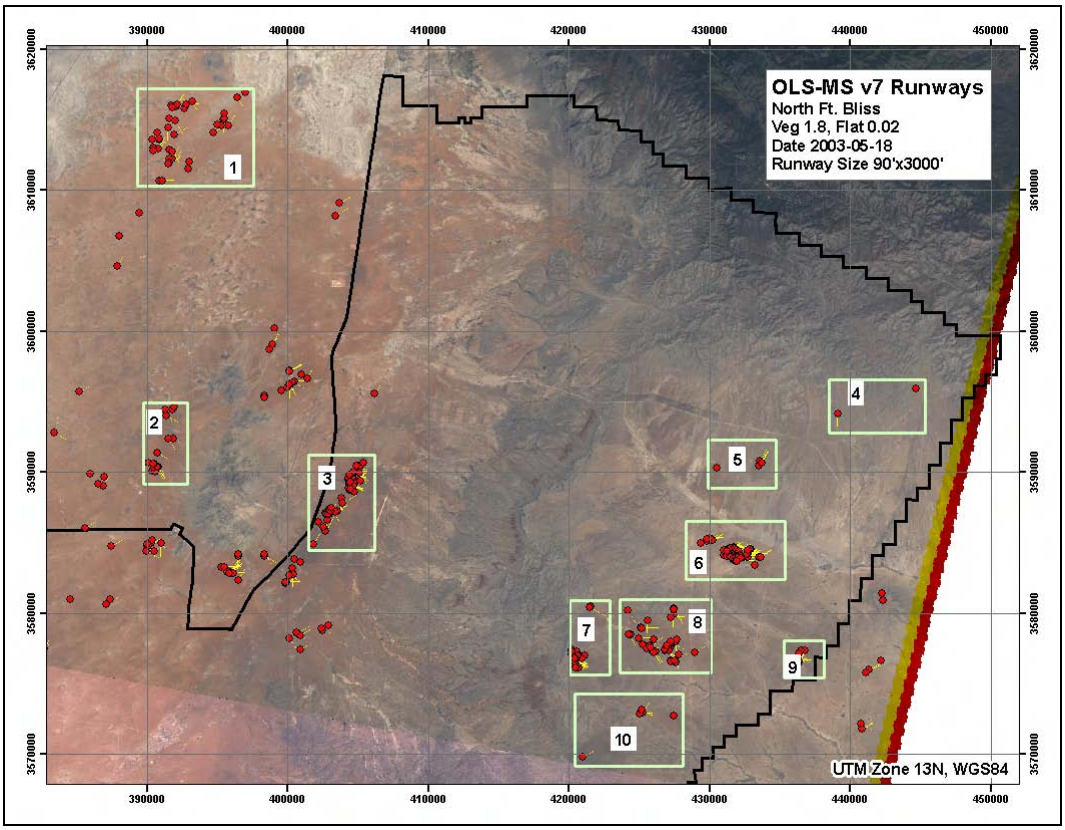


Figure A2-1. 90- × 3000-ft OLSs indicated as OLS Short.

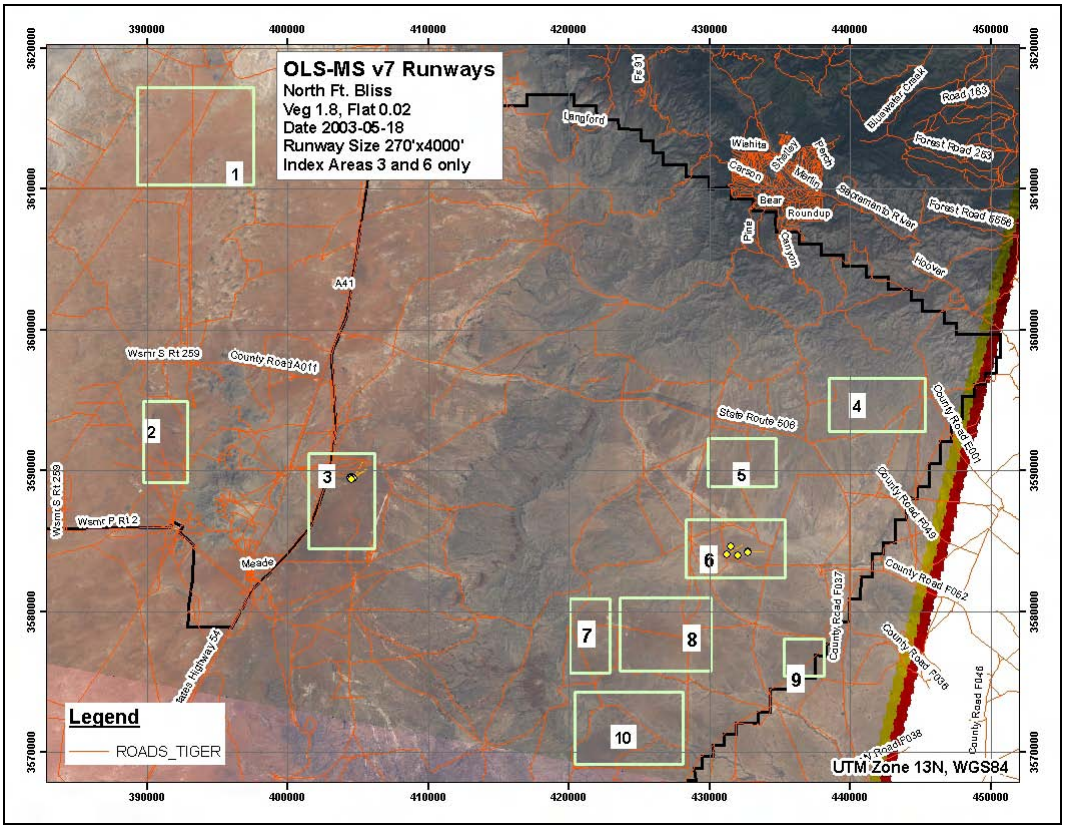


Figure A2-2. 270- × 4000-ft OLSs indicated as OLS Long.

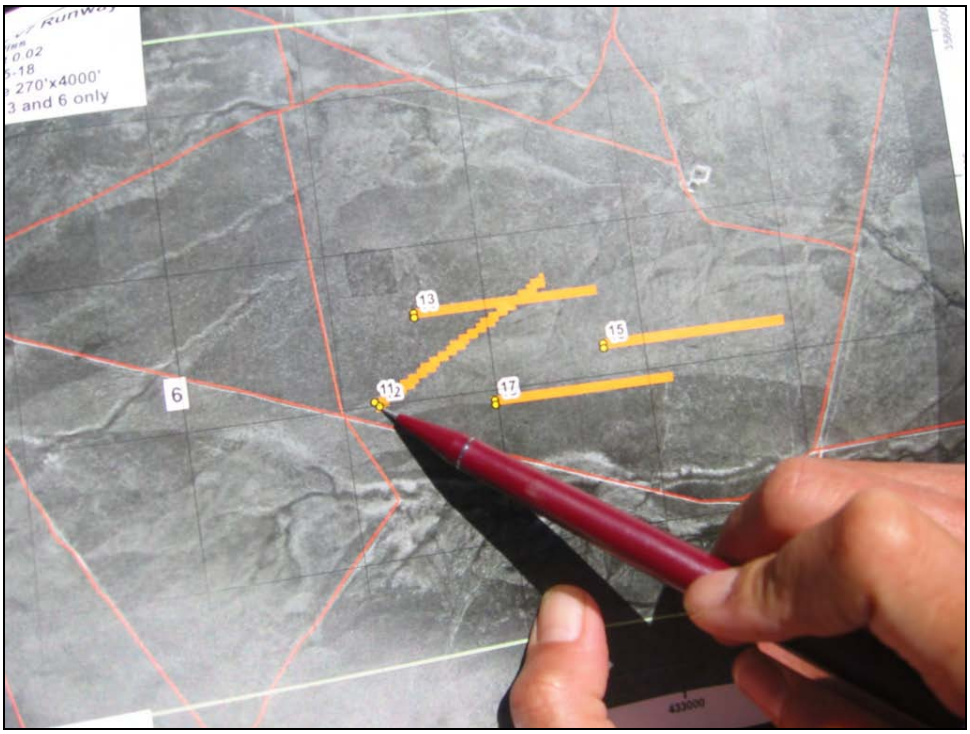


Figure A2-3. Area 6 with 270- × 4000-ft OLS.



Figure A2-4. OLS 11-Long and 12-Long, looking toward the north from flag.



Figure A2-5. OLS 11-Long and 12-Long, looking toward the northwest.



Figure A2-6. OLS 11-Long and 12-Long, looking toward west.



Figure A2-7. OLS 11-Long and 12-Long, looking toward southwest.



Figure A2-8. Due South; yucca trees in the distance are approximately 4–5 feet tall.



Figure A2-9. Looking southeast.



Figure A2-10. Due east.



Figure A2-11. Looking to northeast direction.



Figure A2-12. View down the throat of OLS at 230 feet from the start flag. There was rebar sticking up vertically out of the ground.

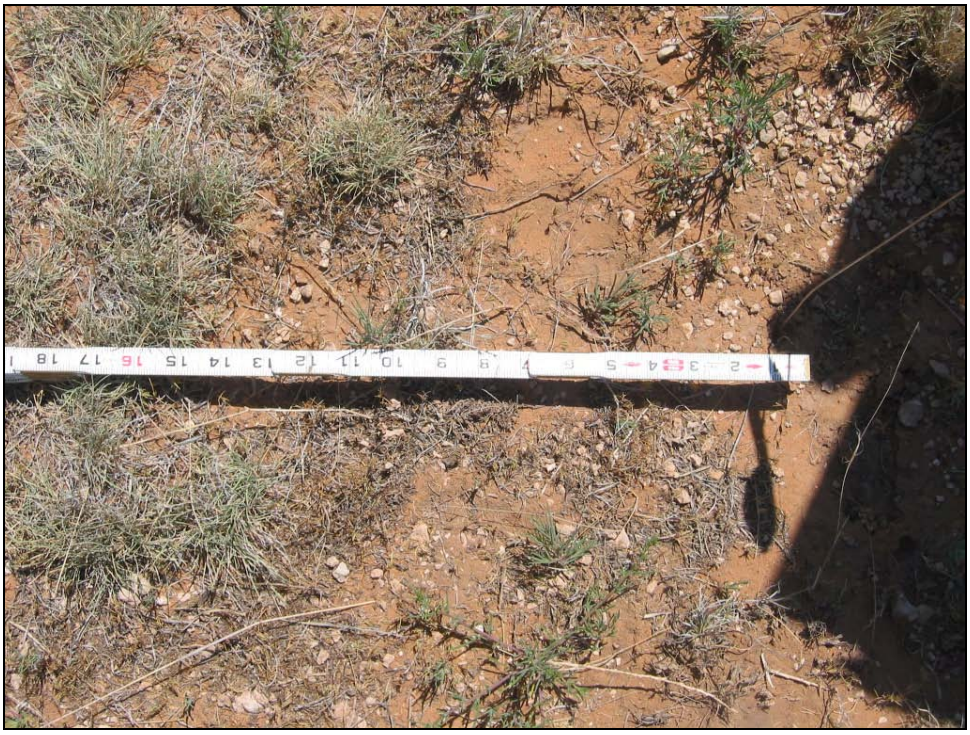


Figure A2-13. Close-up of undisturbed surface conditions within 12 inches north side of flag.

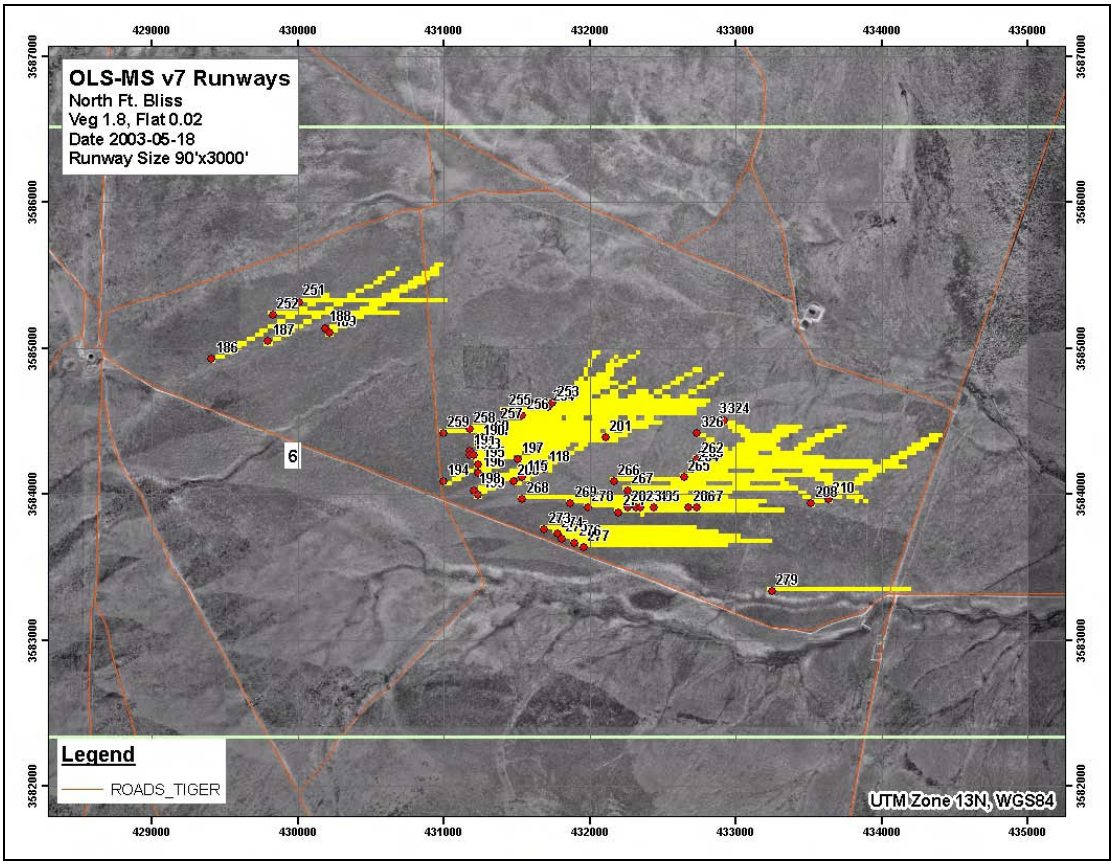


Figure A2-14. Area 6 OLS-Short clusters.

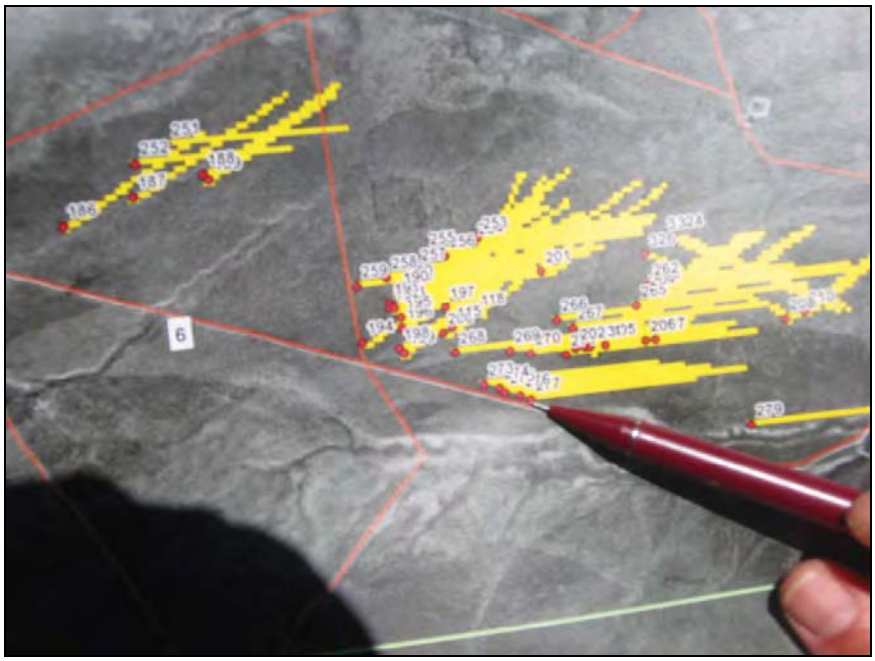


Figure A2-15. This is cluster of OLSs close to the road is a good alternative (90 × 3,000 ft) with easier access.



Figure A2-16. Vegetation in the area. This past spring, this area received a record 30-year precipitation amount, well over the average amount of rainfall. Chuck Carrig said the amount was about 16 inches, whereas they normally get only about 6 inches. The area is quite green with lots of vegetation cover where it would normally be brown.

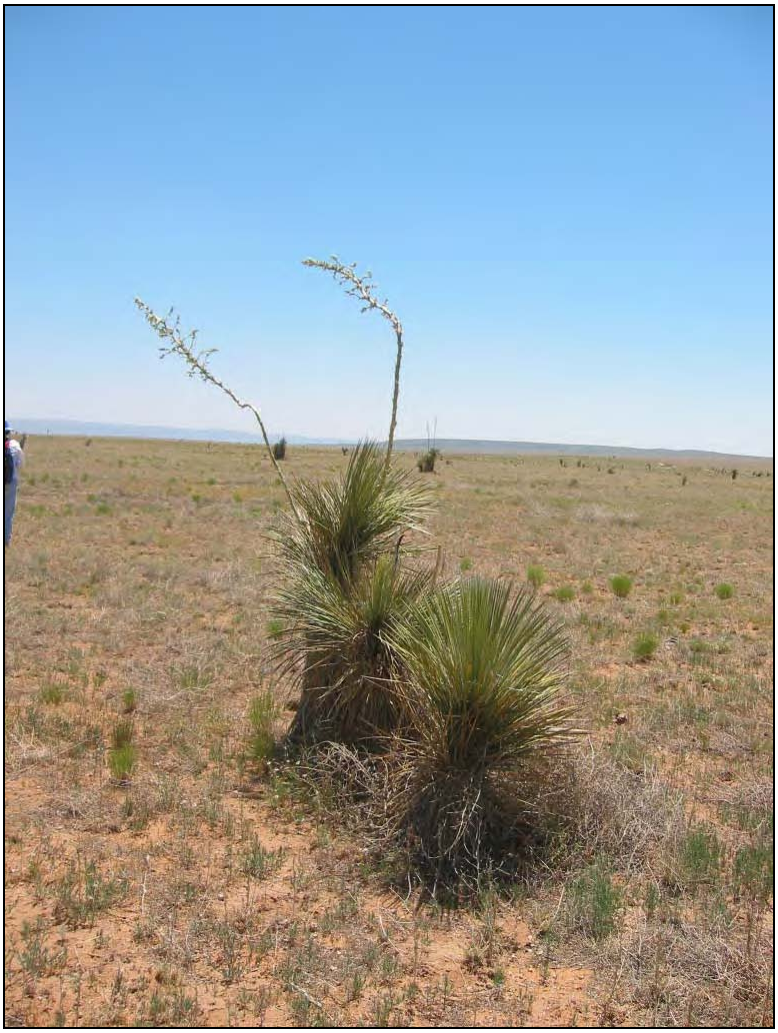


Figure A2-17. Yucca is a fibrous plant with a thick trunk and deep root system. It grows in areas of adequate moisture. The center part of the plant is quite strong and has been used as rope. The plant can reach heights of 5–10 feet, and would be viewed as an obstruction to aircraft operations. It is difficult to push down by human force. In this area the yucca were spaced several hundred feet apart; however, in the area of the OLS cluster they were spaced closer together (see next photo).



Figure A2-18. Along OLS 276-Short looking toward the east. Here, the yucca trees are spaced approximately 20–30 feet apart.



Figure A2-19. Looking slightly more to the northeast. No OLS are located here, but note the yucca trees in an almost straight line on opposite sides of the photo at an estimated distance of 200 feet apart. OLS 276-Short is just to the right of this location.

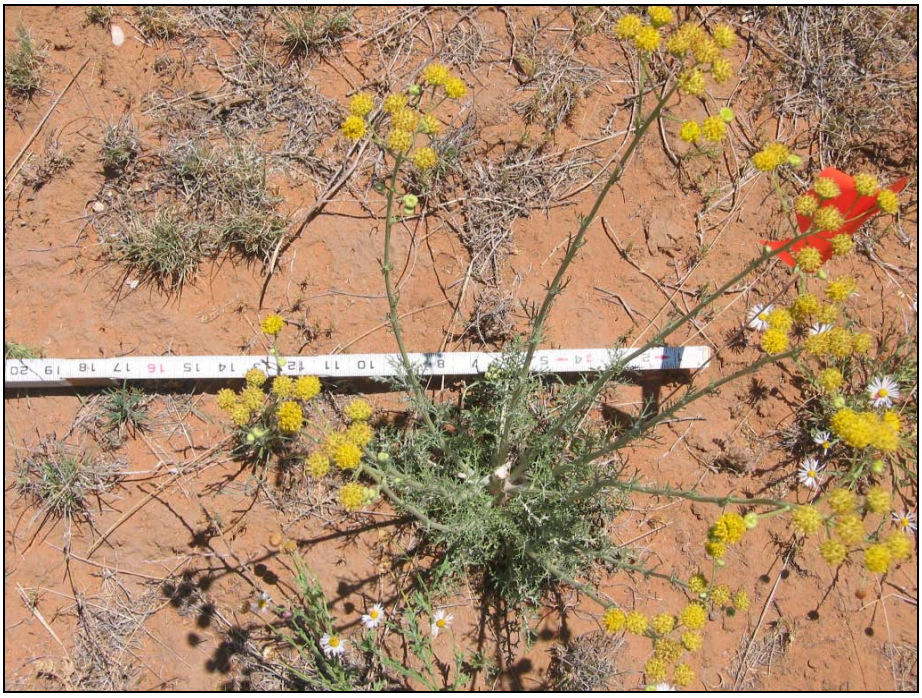


Figure A2-20. OLS 276-Short at start flag and undisturbed soil and vegetation condition on north side of flag. Munsell color chart 10YR 5/4. Field soil is identified as fine-grained soil (silty sand or silt) and a few pieces of gravelly material (caliche pieces). The soil is very dry.



Figure A2-21. Shallow hole was dug approximately 9 inches below surface; soil felt crumbly and powdery. Affleck attempted to push a cone penetrometer and found it difficult to push after 4 inches below the surface.



Figure A2-22. View from start flag looking north.



Figure A2-23. View from start flag looking northwest.



Figure A2-24. View from start flag looking west.



Figure A2-25. View from start flag looking southwest.



Figure A2-26. View from start flag looking south.



Figure A2-27. View from start flag looking southeast.



Figure A2-28. View from start flag looking east.



Figure A2-29. View from start flag looking northeast.



Figure A2-30. OLS 279-Short location where OLS crosses this road and a fence line at a cattle crossing. West end of OLS 279-Short is on left side and the other end is on right side.

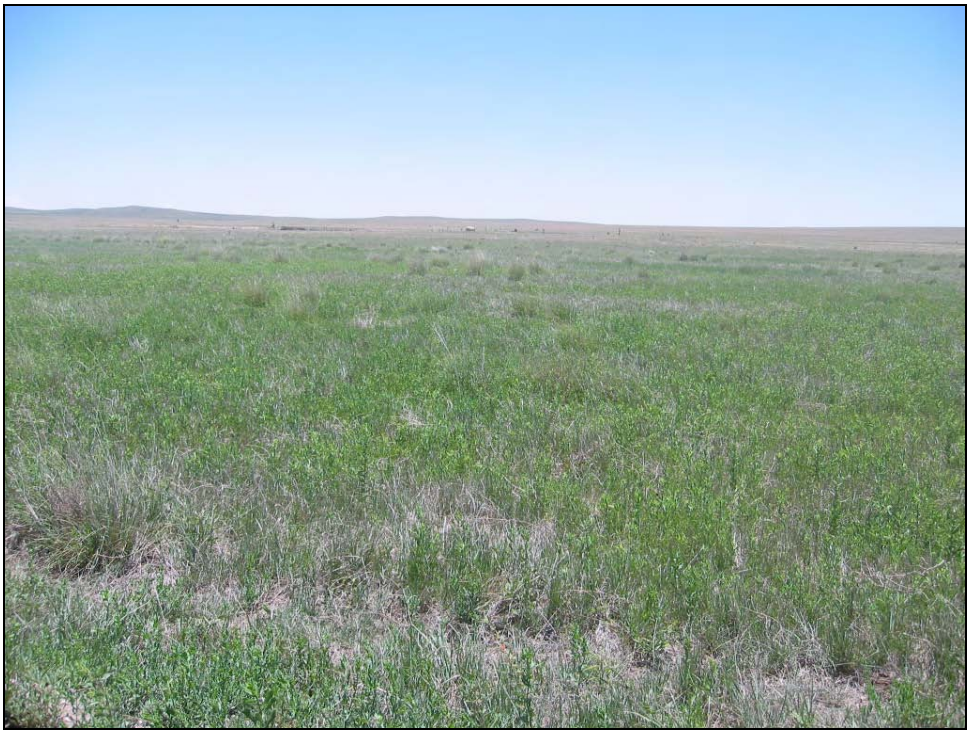


Figure A2-31. Location approximately three miles down the access road from OLS cluster 276-Short. There are no OLSs in this photograph, which illustrates the higher density of vegetation, as this area is slightly lower in elevation and is where water drains. Cattle ranch location ahead in the distance.



Figure A2-32. Another view of area on left side of road. Note the blue norther forming over the Sacramento Mountain range in the distance. Blue northers can bring dangerous weather conditions, including lightning and heavy amounts of rain in a very short duration. Flash flooding is a very severe hazard, particularly in springtime.

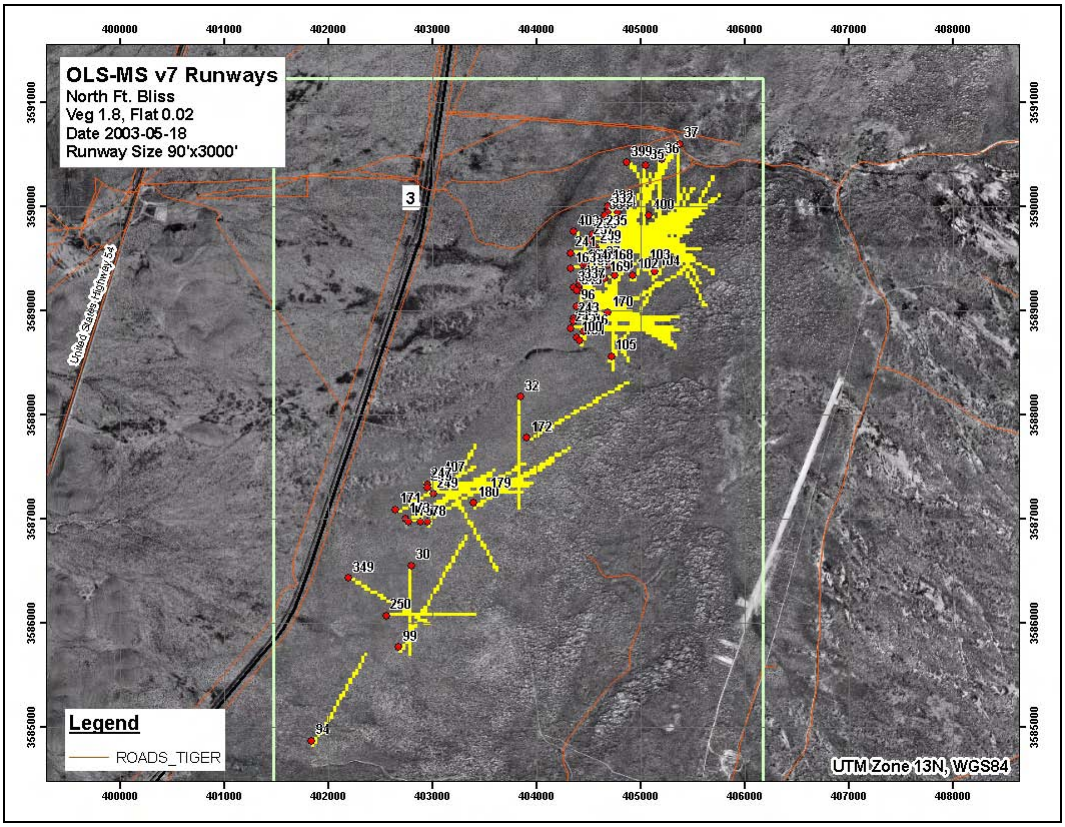


Figure A2-33. OLS in Area 3 where we examined the area on our way back to post.



Figure A2-34. Location about 1.5 miles north of OLS 92-Short. This area is fairly flat over a large distance, but the mesquite bushes with their sharp thorns make this an unsuitable location.



Figure A2-35. Mesquite bushes may range from 2 to 5 feet high and be spaced 10–20 ft apart.

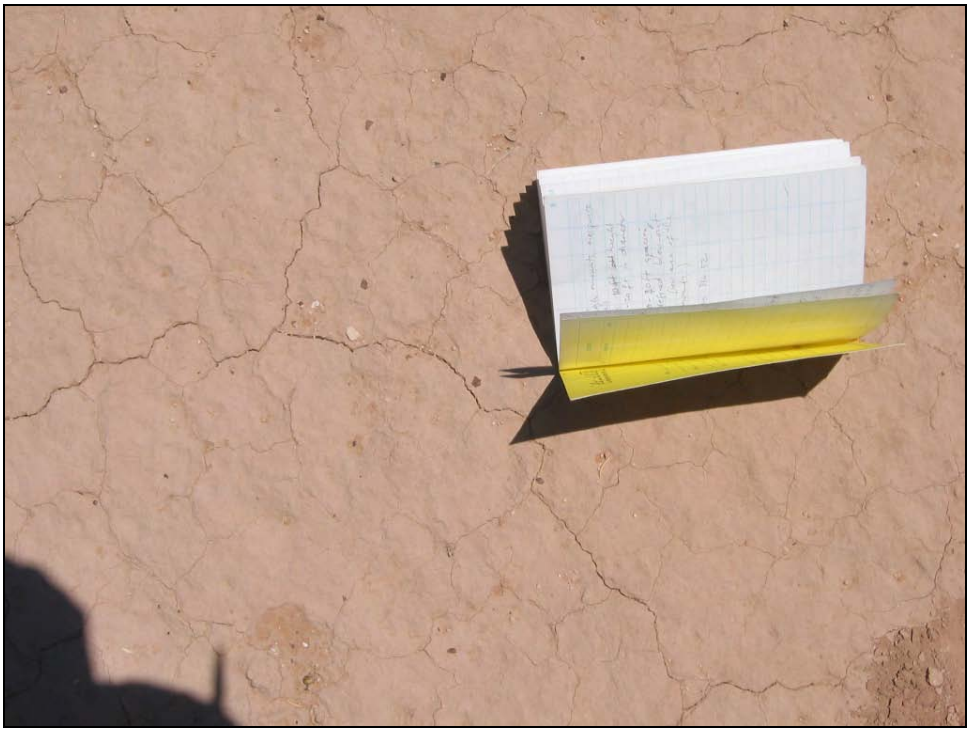


Figure A2-36. Soil surface with cracks; soil is very dry.



Figure A2-37. No access to OLS in Area 3 off Highway 54.

6. OLS Selection

The logistics for field work activities and safety of the field personnel conducting the field work are the primary reason why we selected OLS 276. Because we will be using several pieces of equipment and instruments during the field work, we selected OLS 276 because it is close to the access road. The equipment and instruments are heavy and cumbersome to carry.

Chuck Carrig mentioned that this is a fragile ecosystem and Fort Bliss Department of Environment may not allow us to drive along the runway. If Fort Bliss will allow us to drive along the runway (with permission from the archaeologist and biologist), we need to minimize the impact on the terrain and limit the number of vehicle passes.

7. Directions to OLSs 11-Long and 276

The duration of travel is close to two hours.

From Fort Bliss, take the exit from the post on Fred Wilson Avenue to Interstate 54 East (will change to I-54 North). Go approximately 56 miles on I-54 North and turn right onto Route 506 (unmarked access road) just past the border checkpoint. On Route 506 drive approximately 14 miles

and turn right onto the access road with a sign “US Air Force Centennial Bombing & Gunnery Range” to Mesa Horse Camp (you will see a water tank), then go East on Toy Payne Tank Road. OLS 276 is within a half-mile. The location of our OLS is on Otera Mesa in Maneuver Range #18. The mountains to the north (left side) are the Sacramento Mountains.

8. Issues

a. MOU

We need to finalize the MOU between Fort Bliss and ERDC/CRREL.

b. Logistics

Fort Bliss Form 88;

Time to drive back and forth;

Project partners: Will Boeing and AFRL be there?

c. Testing and Sampling

For soil pits and density measurements, we may not be able to dig 3-ft-deep pits because of caliche.

For soil strength measurements, the standard 4.5-kg Clegg hammer might work. Any implications for DCP?

d. Safety

On our first day before going to the field, Fort Bliss safety personnel will give to everyone going to the field a 45-minute required briefing on range safety.

The weather in July is very hot.

There could be a blue norther, which is a massive storm from the north. If this happens, the field work group has to leave the mesa together.

e. Communication

Cell phones and radios to communicate to Range Control do not work in Otera Mesa. Satellite radio (SATCOM) is our option. Handheld two-way radios may work to communicate within the group during fieldwork.

Before going to the mesa, when turning right onto Route 506, we need to radio Range Control and mention the following: group name, destination, purpose, duration (time of exit), number of people, names, number of vehicles, and vehicle licenses.

Appendix B: Description of Terrain Features at Fort Bliss

Station 0+00 to 0+40

- Both live and dead plants, total vegetation cover is approximately 70–80%;
- Gently sloping to the south;
- Typical ground roughness was taken by a profilometer;
- Mounds with 3- to 4-in.-diameter animal holes on both south side and south edge of the runway;
- Few yucca;
- Reddish brown color, powdery material, silt soil on the surface.



Soil on the surface at Station 0+00 centerline.



Due east along the center of the runway at Station 0+00.



Granular material on the surface adjacent to the animal hole.

Station 0+40 to 0+90

- Gently sloping to the south;
- Vegetation cover is approximately 60–70% with both live and dead plants;
- Some roughness and undulation (waviness along the runway);
- Few yucca;
- Reddish-brown color, powdery material, silt soil with granular (caliche pieces) material 0.5- to 4-in. size on the surface.



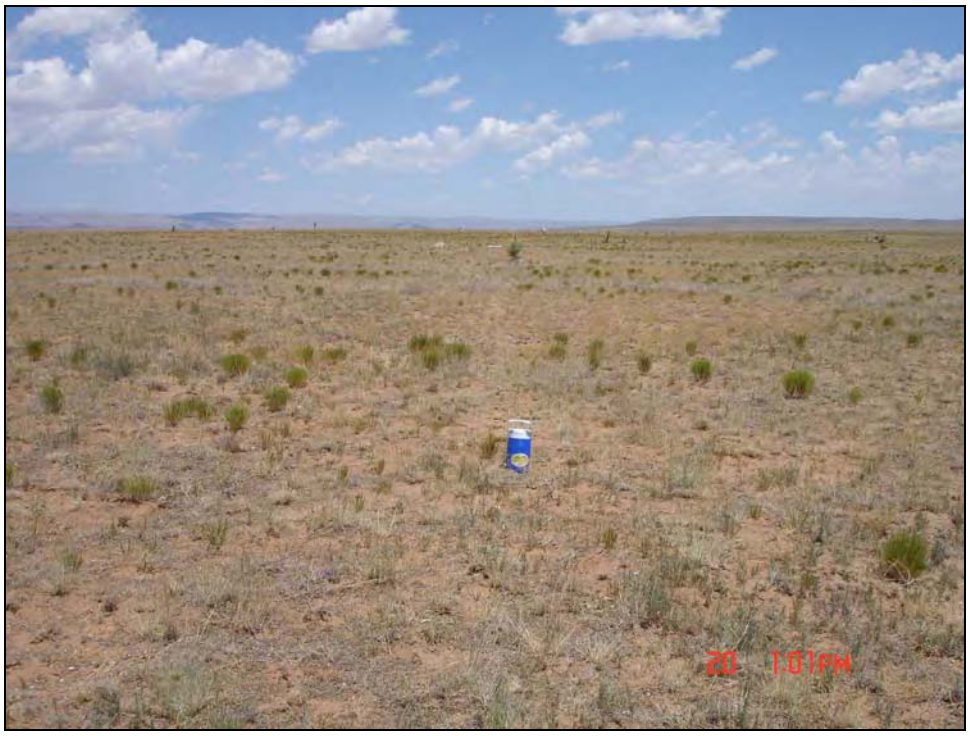
Dead and live vegetation cover and exposed soil at Station 0+40 centerline.



Due east along the center of the runway at Station 0+40.

Station 0+90 to 1+30

- Gently sloping downhill to the south;
- Vegetation cover is approximately 60–70% with both live and dead plants;
- Some roughness and undulation (waviness along the runway);
- Reddish-brown color, powdery material, silt soil with granular (caliche pieces) material 0.5- to 3-in. size on the surface;
- Existing mound with 8-in.-diameter animal holes.



Due east along Station 0+90 centerline.



Along the center of the runway looking west at Station 0+90.

Station 1+30 to 1+70

- Gently sloping to the south;
- Vegetation cover is approximately 60–70% with both live and dead plants;
- Some undulation or waviness of the ground along the runway;
- Few yucca;
- Reddish-brown color, powdery material, silt soil with granular (caliche pieces) materials 0.5- to 3-in. size on the surface;
- Mounds with granular materials on the surface adjacent to the animal holes;
- Granular materials ranging from 0.25- to 3-in. size are noticeable along the wheel paths or the center of the runway.



Along the center of the runway at Station 1+30 due east.



Due west at Station 1+30 centerline.

Station 1+70 to 2+10

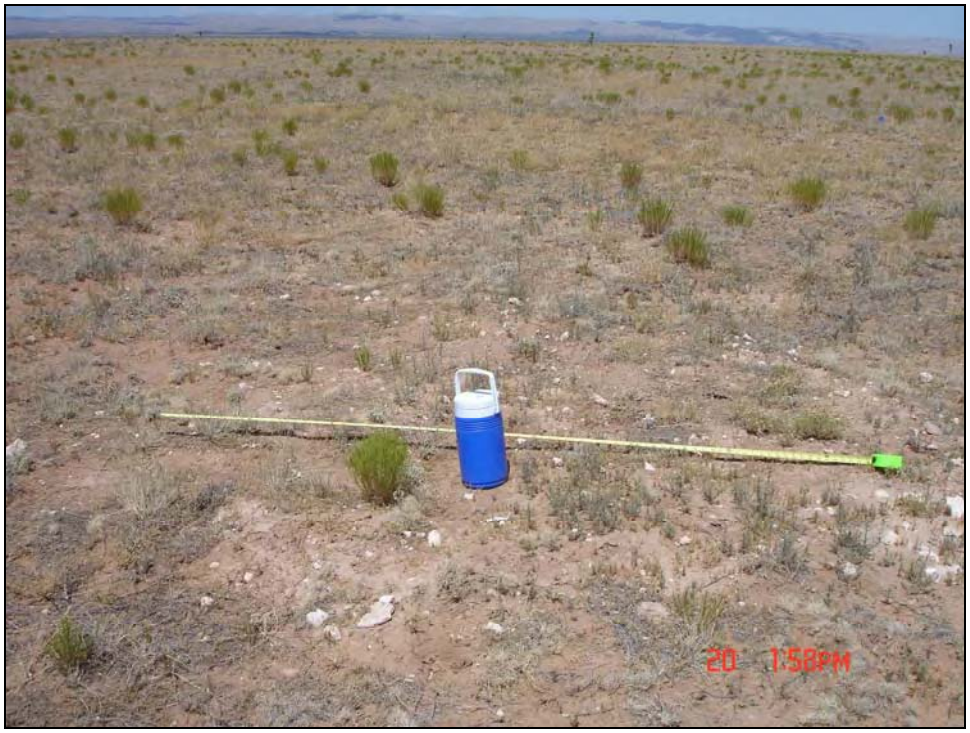
- Gently sloping to the south;
- Vegetation cover is approximately 60–70% with both live and dead plants;
- Some undulation or waviness along the runway;
- Typical surface roughness based on the profilometer;
- A couple of yucca;
- Reddish-brown color, powdery material, silt soil with granular (caliche pieces) material 0.5- to 4-in. size on the surface;
- Mounds with no distinct animal burrows located adjacent to the areas with animal holes;
- A mound with granular material (caliche pieces) ranging from 1- to 5-in. size on the surface.



Ant burrow west of Station 1+70



At Station 1+70 looking west along the center of the runway.



Mound with noticeable gravelly materials on the surface.

Station 2+10 to 2+50

- Vegetation cover is approximately 60–70% with both live and dead plants;
- Some roughness and undulation (waviness) along the runway;
- Few yucca on the south side of the runway;
- Reddish-brown color, powdery material, silt soil with granular (caliche pieces) material 0.5- to 4-in. size on the surface;
- Mounds with animal holes ranging from 3- to 6-in. diameter;
- A patch of area with vegetation clearing and gravelly materials on the surface.



Due east.



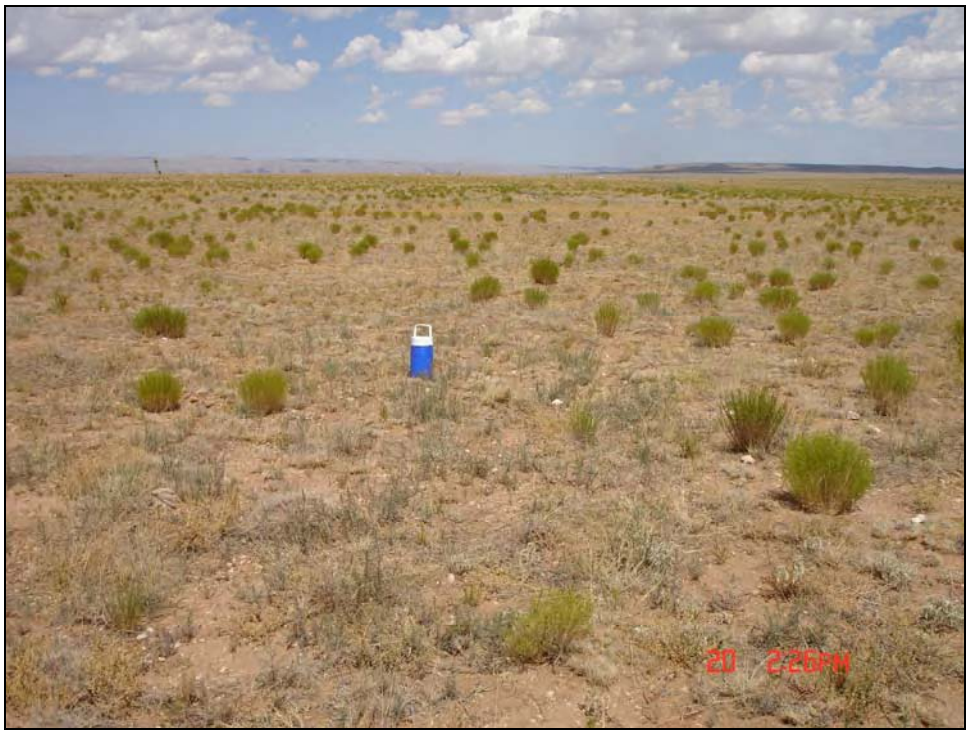
Due west.



Soils and vegetation cover at Station 2+10.

Station 2+50 to 3+30

- Gently sloping to the south;
- Vegetation cover is approximately 60–70% with both live and dead plants;
- Some roughness and undulation (waviness along the runway);
- Few yucca;
- Reddish-brown color, powdery material, silt soil with granular (caliche pieces) material 0.5- to 4-in. size on the surface;
- Areas with 2-in. diameter animal holes.



Due east at Station 2+50 along the center of the runway.



Mound with animal holes near Station 2+80.



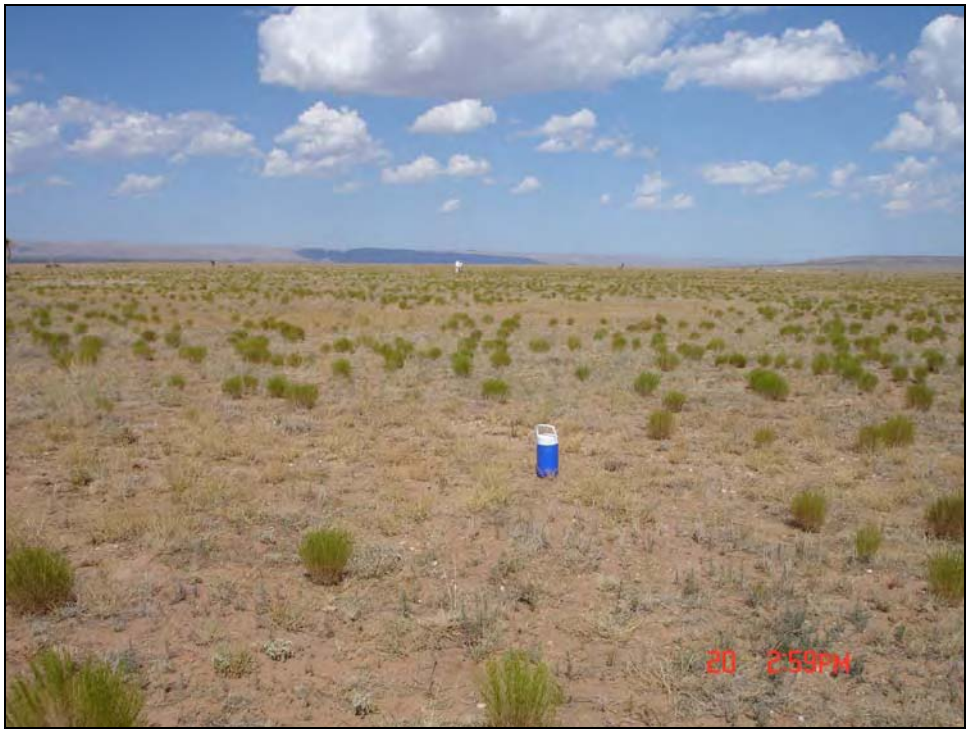
Mound with animal holes and gravelly (caliche pieces) materials on the surface near Station 3+30.

Station 3+30 to 4+70

- Gently sloping to the south;
- Vegetation cover is approximately 60–70% with both live and dead plants;
- Some roughness and undulation (waviness) along the runway;
- Reddish-brown color, powdery material, silt soil with granular (caliche pieces) material 0.5- to 4-in. size on the surface;
- Areas with animal holes ranging in size from 2- to 6-in. diameter;
- Patches of mainly one type of vegetation.



Due west at Station 3+30 along the center of the runway.



Station 3+30 centerline due east.



Station 3+30 centerline, due west.

Station 4+70 to 5+50

- Gently sloping to the south and southeast;
- Vegetation cover is approximately 60–70% with both live and dead plants;
- Some roughness;
- Reddish-brown color, powdery material, silt soil with granular (caliche pieces) material 0.5- to 4-in. size on the surface;
- Mounds with animal holes ranging in size from 2- to 6-in. diameter;
- Areas of mainly one type of vegetation with 4-in. mound.



Areas or patches of mainly one type of vegetation.



At centerline of Station 4+70 looking east.

Station 5+50 to 6+30

- Sloping to the south;
- Vegetation cover is approximately 60–70% with both live and dead plants;
- Slight undulation (waviness) along the runway;
- Reddish-brown color, powdery material, silt soil with granular (caliche pieces) material 0.5- to 2-in. size on the surface;
- Areas with animal holes ranging in size from 2- to 6-in. diameter;
- Patches of mainly one type of vegetation;
- A few yuccas.



Looking west along the center of the runway at Station 5+50.



Due east along the center of the runway at Station 5+50.



Clearing area with an ant hole in the middle.

Station 6+30 to 7+00

- Several yucca trees or bushes ranging from 1 to 6 ft high;
- Sloping to the south;
- Vegetation cover is approximately 60–70% with both live and dead plants;
- Slight undulation (waviness) along the runway;
- Reddish-brown color, powdery material, silt soil with granular (caliche pieces) material 0.5- to 4-in. size on the surface;
- Areas with animal holes ranging in size from 2- to 6-in. diameter;
- Patches of mainly one type of vegetation.



Due west at Station 6+30 along the center of the runway.



Yucca near Station 6+30.

Station 7+00 to 7+70

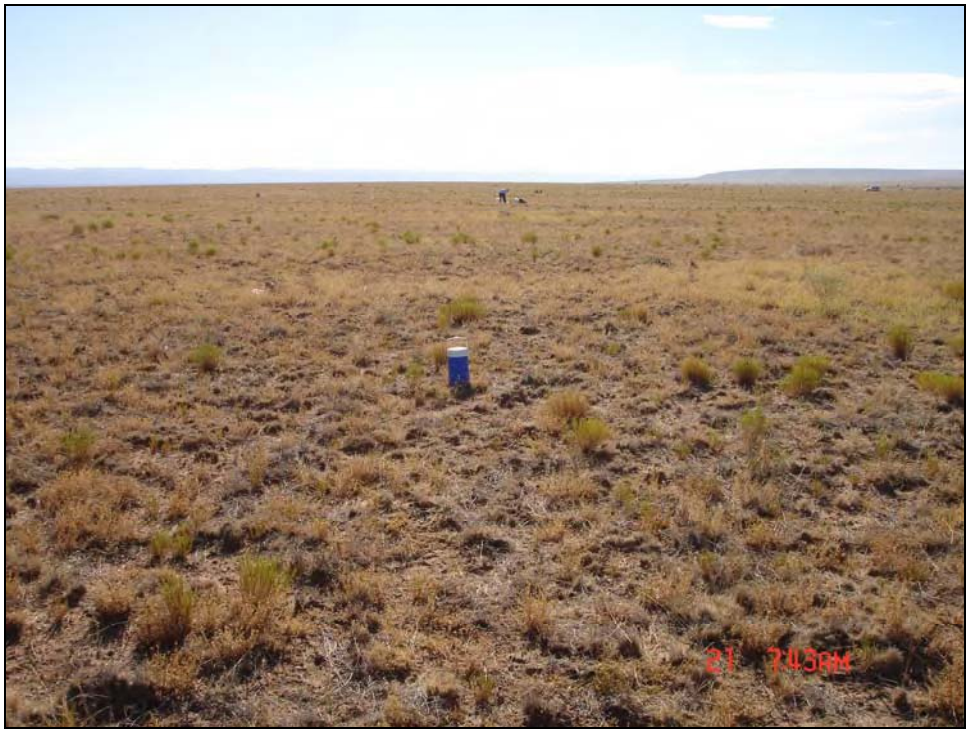
- Sloping to the south;
- Vegetation cover is approximately 60–70% with both live and dead plants;
- Slight undulation (waviness) along the runway;
- Reddish-brown color, powdery material, silt soil with granular (caliche pieces) material 0.5- to3-in. size on the surface;
- Areas with animal holes ranging in size from 2- to 6-in. diameter;
- A couples of spots with animal holes, some of which are 6- to 8-in. diameter;
- Areas with ant holes;
- A few yuccas.



Exposed soil and caliche chunk on the surface.



East Station 7+00 along the center of the runway.



At centerline of Station 7+70 due east (with Lynette in the background at station 8+50).

Station 7+70 to 8+50

- Sloping to the south;
- Vegetation cover is approximately 60–70% with both live and dead plants;
- Slight undulation (waviness) along the runway;
- Reddish-brown color, powdery material, silt soil with granular (caliche pieces) material 0.5- to 3-in. size on the surface;
- Areas with animal holes ranging in size from 2- to 6-in. diameter;
- Spots with light vegetation, some with 2- to 3-in. animal holes;
- Area with caliche pieces on the surface;
- Drainage path of surface scour that runs from north to south.



Due west along the center of the runway at Station 7+70.



Caliche pieces on the surface; photo taken due west at station.



Drainage path east of Station 8+20 that runs from north to south.



Soil at Station 8+20.



Due east at Station 8+20 centerline.

Station 8+50 to 9+30

- Sloping to the south;
- Vegetation cover is approximately 60–70% with both live and dead plants;
- Slight undulation (lateral waviness) to relatively flat;
- Reddish-brown color, powdery material, silt soil with granular (caliche pieces) material 0.5- to 3-in. size on the surface;
- A few yucca bushes;
- Some areas clear of vegetation with ant holes in the middle;
- Depression areas (approximately 3–4 in. deep) with animal holes ranging in size from 2- to 4-in. diameter;
- Spots with light vegetation, some with 2- to 4-in. animal holes;
- Area with caliche pieces on the surface.



Caliche cobbles west of Station 8+50.



Along the center of runway at Station 9+30, due west. (People in the background are at Station 8+50.)

Station 9+30 to 10+10

- Sloping to the south;
- Vegetation cover is approximately 60–70% with both live and dead plants;
- Slight undulation (lateral waviness) to relatively flat;
- Reddish-brown color, powdery material, silt soil with granular (caliche pieces) material 0.5- to 3-in. size on the surface;
- A few yucca bushes;
- Some areas clear of vegetation with ant holes in the middle;
- Depression areas (approximately 3–4 in. deep) with animal holes ranging in size from 2- to 4-in. diameter;
- Spots with light vegetation, some with 2- to 4-in. animal holes;
- Area with caliche pieces on the surface.



At Station 10+10, along center of runway looking west.



At Station 10+10 centerline, due east.



Approximately 50-ft-long scraped path west of Station 10+70.



Looking west at east end of runway centerline.

Appendix C: Calibration of Soil Moisture Measuring Instruments[1]

Introduction

Soil moisture is a key OLS system parameter because of its significance for estimating soil strength. Soil strength measurements were made at the OLS field sites using a dynamic cone penetrometer. Soil moisture measurements typically were made near soil strength measurements, allowing moisture to be used in relationships used to predict soil strength. Although other soil parameters, e.g., texture and density, are important factors in predicting soil strength, soil moisture is the only soil physical variable that has an important impact on soil strength and also can vary over a large range in a short time. Therefore, because soil strength is as important to the success of an OLS as is its flatness, smoothness, and freedom from obstructions, the accuracy of soil moisture measurements has a significant effect upon the prediction of soil strength. In the case of the OLS field measurements at El Centro NAF, Fort Bliss, and in southern Indiana, soil strength prediction methods are validated using the in-situ soil moisture and soil strength measurements.

Measurement of soil moisture during the OLS field validation program required the use of several soil moisture measurement techniques. Electronic instruments were used for most measurements because they provided rapid response, and because they were able to provide soil moisture time series at a few locations. Measurements also were made with a Troxler nuclear gauge because moisture measurements were easily obtained as density measurements were made with this instrument. Finally, soil moisture measurements were made by taking samples either with a drive cylinder, or by taking soil samples with a spoon. These samples were then weighed, oven-dried, and reweighed to determine the percent soil moisture in the samples as a function of weight.

In some cases, soil moisture measurements were made with multiple technologies at the same sampling locations to assess how well the different

[1] Appendix C was written by Charles C. Ryerson, Kevin L. Bjella, Lynette A. Barna, Christopher M. Berini, Forrest R. Scott, Keran J. Claffey, and Gary E. Phetteplace.

measurement methods agreed. In these cases there often was disagreement among the instruments. Also, in some cases instruments would provide values that were not consistent with physical possibility.

The purpose of this appendix is to assess which instruments provided the most accurate soil moisture measurements and to assess how well other instrument measurements compared to the most accurate measurements. It concludes with recommendations of how to use measurements from each of the measurement methods.

OLS Soil Moisture Measurement Methods

Electronic instruments, as indicated above, were used to make most OLS soil moisture measurements. Electronic instruments are fast and allow time series to be made when monitored with a data logger. Dynamax instruments were used at the OLS field sites. The Dynamax ML2 was used for all sample location measurements at the soil surface. It also was used to measure soil moisture at depth either by measuring moisture in the bottom or sides of a soil pit, or by measuring moisture in increments as a hole is augured (Fig. C-1). The ML2 technology is described in the instrument literature (Delta-T Devices 1999). Measurements are made by pushing 60-mm-long tines on the base of the instrument into the soil; the value displayed on the attached HH2 digital readout represents the soil moisture measured within the soil volume encompassed by the tines.



Figure C-1. Using ML2 and HH2 readout to measure soil moisture at depth within auger hole.

Soil moisture time series measurements were made with the Dynamax PR1 and PR2 instruments. The PR1 was used at the North Vernon, Indiana, airport weather station site, and the PR2 was used at the Ford Farm, Fort Bliss, and El Centro NAF OLS weather station sites. The PR1 and PR2 use a technology somewhat different from the ML2; they consist of a 1-m rod that is placed inside a sleeve in the soil, with soil moisture measured at fixed depths when interrogated by a data logger (Delta-T Devices 2001, 2004) (Fig. C-2). Typically, the instruments were located approximately 1 km from the OLSs, at the OLS weather stations. However, some sleeves were placed in the El Centro NAF and Fort Bliss Runway Analysis Sites (RAS), and spot measurements of soil moisture content with depth were made at those locations.



Figure C-2. Dynamax PR1 ThetaProbe inside (left) and outside (right) of access tube (Delta-T Devices 2001). The PR2 is identical in appearance.

The PRI and PR2 instruments are of similar construction, but their electrical response to soil moisture is considerably different, as indicated in the instrument literature (Delta-T Devices 2001, 2004). Responses by the PR1 instrument with moisture contents that were inconsistent with possible soil moisture magnitudes, such as providing moisture volume fractions greater than one, provided the impetus to conduct the work described in this appendix (Fig. C-3).

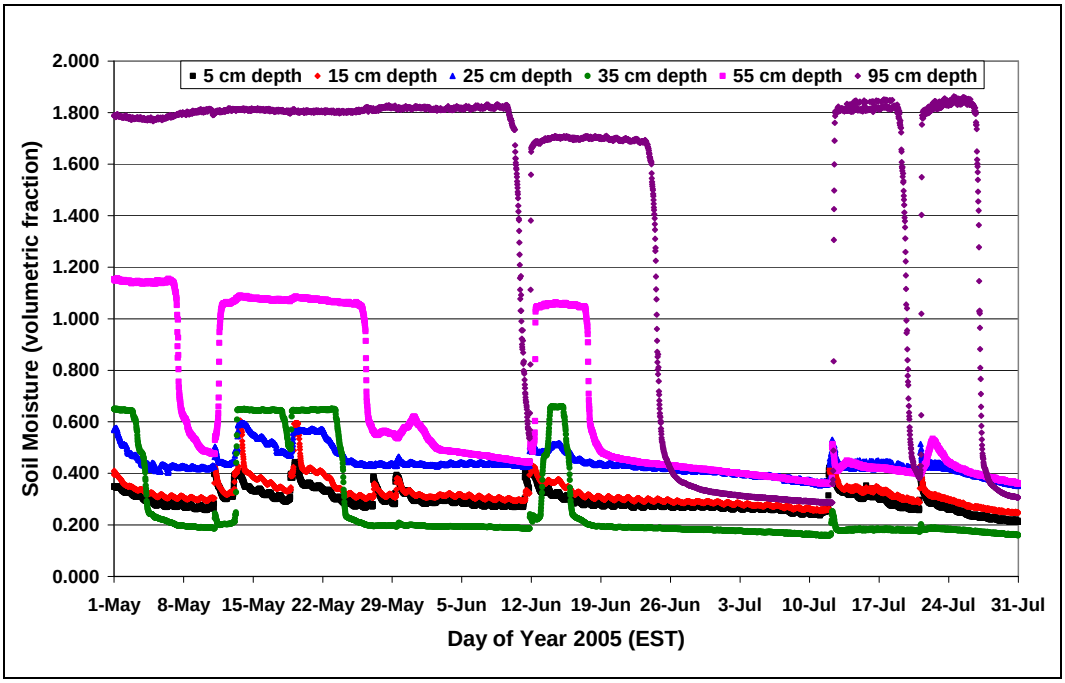


Figure C-3. Soil moisture measured by PR1 probe at North Vernon Airport. Note larger than physically possible volume fractions at depths of 55 cm and 95 cm.

Soil moisture measurements also were made with the Troxler 3440 nuclear gauge. The Troxler was used primarily to make soil density measurements at the RASs. However, because the instrument also measures soil moisture to provide moisture-corrected soil density values, moisture content also was recorded (Fig. C-4). The Troxler 3440 uses an americium beryllium radiation source to emit neutrons from the base of the instrument. The neutrons collide with water hydrogen atoms and slow. The instrument reads the number of backscattered neutrons that have been slowed by collisions with hydrogen. Generally, the instrument measures moisture content in the soil volume down to a depth of about 10 cm immediately below the instrument base. Depth of readings penetrates deeper as soil becomes drier, extending to a depth of about 15 cm (Troxler 2006).

Soil moisture also was measured by oven-drying samples that had been removed from the field. Spoon and drive cylinder samples were obtained from soil pits, the soil surface, and from cuttings as auger holes were drilled.

Measurement Accuracy

The electronic instrument measurements initially were suspect because the PR1 instrument provided soil moisture contents larger than physically

possible—greater than saturation at depths where saturation may have occurred (Fig. C-3). Also, visual comparisons of ML2 and PR2 measurements with one another, and with oven-dry and Troxler measurements, showed considerable scatter (Fig. C-5).



Figure C-4. Troxler nuclear gauge (yellow instrument) in moisture-reading configuration at the base of the soil pit. The Dynamax ML2 is held ready for measurement of soil moisture content, with the four stainless steel measuring rods visible at the right pit wall.

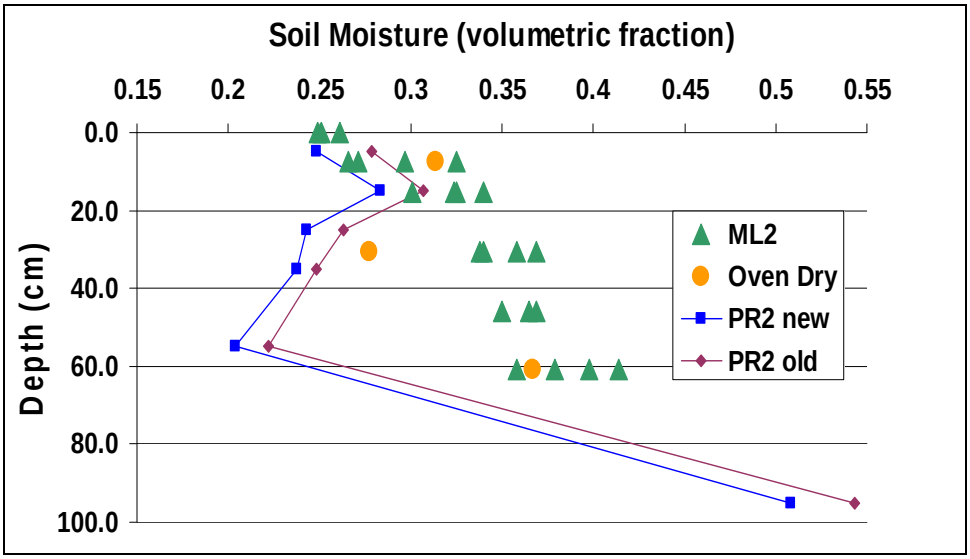


Figure C-5. Scatter of moisture readings at Ford Farm with different technologies. Note that the PR2 observations were made approximately 1 km from the other observations.

The Dynamax instruments all operate by assuming that soil moisture content is approximately proportional to the dielectric properties of the soil (Delta-T Devices 1999, 2001, 2004). The soil moisture is then computed from a polynomial fit between the instrument voltage and the soil moisture for a generic mineral soil. In examples provided by Dynamax, when considering errors caused by "soil heterogeneity, the number of samples taken, the extent to which it is possible to perform an accurate calibration on an 'undisturbed' sample, and inserting the probe without causing air pockets or localized soil compression," possible errors in measurements can be ± 5% for a probe calibrated for a given soil, and ± 6% for measurements where the probe is not calibrated to the specific soil (Delta-T Devices 1999, 2001, 2004).

The Troxler nuclear gauge measures soil moisture, as described above, by measuring the receipt of neutrons that are slowed by hydrogen atoms within soil water. Because neutrons are emitted and reabsorbed at the base of the instrument when it is placed upon the soil surface, an important source of moisture measurement error for the nuclear gauge is air gaps between the base of the instrument and the soil (Rollings, personal communication, 2006) (Rollings and Rollings 1996). In general, Troxler instrument measurements should compare within 2% of oven-dry values (personal communication, R. Myers, Troxler, Inc., 16 November 2006).

The most acceptable method of measuring soil moisture is the oven-dry gravimetric method (R. Rollings, personal communication, 14 November 2006). Though error may be caused by poorly calibrated balances, loss of soil between weighings, and other procedural problems, it is considered the "standard" method of measuring soil moisture. Gravimetric water content may be converted to volumetric water content by multiplying gravimetric moisture content by the dry density of the soil and dividing by the unit weight of water. A major source of error can be the soil dry density measurement, which is most accurate when measured by a Troxler nuclear instrument (Rollings and Rollings 1995; R. Rollings, personal communication, 14 November 2006).

As a result of these sources of instrument error, and because most of the OLS RAS measurements were made with the Dynamax instruments because of their ease of use, a recalibration of the Dynamax instruments was conducted. The recalibration was conducted after obvious instrument malfunctions, such as readout device errors, had been corrected.

Dynamax Instrument Calibrations

Instrument Operation

Soil moisture was measured electronically with three models of Dynamax instruments: the ML2, PR1, and PR2, manufactured by Delta-T Devices Ltd., UK. Measurement is accomplished by inducing a 100-MHz sinusoidal signal into the soil with either a pair of stainless steel bands (PR1 and PR2) (Fig. C-2), or four stainless steel rods (ML2) (Fig. C-4). The impedance of these conductors varies with the impedance of the soil, which consists of two components: the bulk dielectric constant and the ionic conductivity. The 100-MHz signal minimizes the effects of the ionic conductivity. Thus, the moisture measurements rely almost exclusively on the bulk dielectric constant. The dielectric constant of water (~81) is much higher than that of soil (3 to 5) and air (1). Because the dielectric constant of water is significantly larger than that of soil mineral and organic materials or air, the overall dielectric constant of the soil is primarily determined by its water content.

The impedance of the conductor affects the reflection of the 100-MHz signal, and the reflections combine with the applied signal to form a voltage standing wave along the conductor. The output of the instrument is an analogue voltage proportional to the difference in amplitude of this standing wave at two points, and this forms a sensitive measure of the soil water content. The correlation between the square root of the dielectric constant ($\sqrt{\varepsilon}$) and the volumetric moisture content (θ) is nearly linear for many soil types, and is reported as $m^3\ m^{-3}$. In the field, either the measured voltage or θ can be collected utilizing the manufacturer's handheld data collector, or a commercial data logger can be installed.

The ML2 consists of four 60-mm stainless rods attached parallel to each other and mounted in a plastic base. The rods are inserted into the soil and a measurement is taken with the handheld HH2 data readout displaying soil moisture either in voltage or θ. The ML2 also can be buried for prolonged measurements at depth, but this was not done in the OLS program.

The PR1 and PR2 are 1-m-long multi-depth probes with sensors arranged at 100, 200, 300, 400, 600, and 1000 mm from the top of the rod. A thin fiberglass sleeve is installed into the ground by first auguring a hole into the soil, installing, and backfilling, ensuring that no air voids occur along the length of the sleeve (Fig. C-6). The probe is either permanently placed

inside of the sleeve and connected to a data logger, or can be inserted and removed at each site visit. The advantage of the PR1 and PR2 is the ability to take in-situ measurements at determined depths fairly easily.



Figure C-6. Top of PR1 at North Vernon Airport protruding above soil surface when in monitoring position. White plastic sleeve is visible below dark instrument top.

Instrument Calibration

Polynomial equations are provided by the manufacturer, allowing the user to input voltage and determine $\sqrt{\varepsilon}$. The equations are best-fit curves to the square root of the dielectric constant versus measured voltages, and they are significantly different among the three instruments. The equations are listed as follows:

ML2

$$\sqrt{\varepsilon} = 1.07 + 6.4V - 6.4V^2 + 4.7\ V^3; \quad (1)$$

PR1

$$\sqrt{\varepsilon} = 0.88 + 4.24V + 65.6V^2 - 272.7\ V^3 + 402.9V^9; \quad (2)$$

PR2

$$\sqrt{\varepsilon} = 1.125 - 5.53V + 67.17\,V^2 - 234.42V^3 + 413.56\,V^4 - 356.68\,V^5 + 121.53\,V^6. \quad (3)$$

Applying these equations with voltages from known soil moistures allows the determination of two calibration constants, a_0 and a_1, derived from linear regression, where a_0 is the y-intercept and a_1 is the slope of the line. These can then be applied to give θ where

$$\sqrt{\varepsilon} = a_1 \cdot \theta + a_0. \quad (4)$$

For soil moisture determination, Equations 1-3 are rewritten as

ML2

$$\theta = [(1.07 + 6.4V - 6.4V^2 + 4.7\,V^3) - a_0]/a_1; \quad (5)$$

PR1

$$\theta = [(0.88 + 4.24V + 65.6V^2 - 272.7\,V^3 + 402.9V^9) - a_0]/a_1; \quad (6)$$

PR2:

$$\theta = [(1.125 - 5.53V + 67.17\,V^2 - 234.42V^3 + 413.56\,V^4 - 356.68\,V^5 + 121.53\,V^6) - a_0] / a_1. \quad (7)$$

The HH2 handheld readout applies equations 5–7 to display θ if desired. The calibration constants can be specified by the user, and the manufacturer suggests using the values listed in Table C-1 for general cases where a soil-specific calibration has not been performed and the soils are not high in clay content, very stony, desiccate on drying, or are extremely saline.

Table C-1. Manufacturer calibration constants.

Soil type	a_0	a_1
Mineral	1.6	8.4
Organic	1.3	7.7

Dynamax Instrument Comparisons

As described above, the manufacturer states that, for all three instruments, the effective measurement error considering all factors that can affect measurement quality without calibration is ± 0.06 $m^3\ m^{-3}$, and with soil specific calibration is ± 0.05 $m^3\ m^{-3}$. To verify this, a column of soil (USCS SM-ML soil) was assembled in a 20-cm-diameter, meter-long plastic cylinder, which was placed upright and loaded with the soil and a PR1/PR2 sleeve installed in the middle (Fig. C-7). Six 4.5-cm-diameter holes were drilled on the outside of the cylinder at the same depth as the sensor rings for the PR1/PR2 probes to allow for coincident measurement utilizing the ML2. To allow verification at a variety of moisture contents, known volumes of water were added to the column to wet the soil to specific moisture contents, and measurements then were made after time had elapsed to allow moisture in the column to equilibrate. However, it was recognized that soil moisture most probably was not completely uniform from top to bottom of the column due to permeability and capillary action.



Figure C-7. Soil column for testing PR1, PR2, and ML2 probes. The PR1 and PR2 sleeve ran through the center of the column. The black, sealed holes on the side were used to measure moisture with the ML2 at the same depths as the PR1 and PR2 sensor rings.

Utilizing the manufacturer's calibration constants for mineral soil, and estimating the column moisture content at 15%, average values for each instrument were calculated and are listed in Table C-2, columns two and three. The ML2 performed most accurately with a difference of 2.0% from the estimated soil volumetric moisture content. The PR1 performed the poorest, with a 94% difference. These results suggested that a soil-specific calibration for each instrument was necessary, utilizing the four soils from the OLS field work: North Vernon Airport, the Ford Farm, El Centro NAS, and Fort Bliss. A calibration also was conducted on the soil in the column to verify the results.

Table C-2. Comparison of default and calibrated constants for θ of 15% in the column soil.

	θ utilizing manufacturers' constants	Error from estimated moisture content of 15%	θ utilizing calibrated constants	Error from estimated moisture content of 15%
PR1	29.1 %	+ 94 %	17.1 %	+14 %
PR2	19.5 %	+ 30 %	14.2 %	–5.3 %
ML2	14.7 %	–2.0 %	12.2 %	–18.6 %

Dynamax Soil-Specific Calibrations

An apparatus was devised that allowed for pre-wetted soil to be placed around a PR1/PR2 sleeve, and the PR1 and PR2 then were tested by lowering each sensor to the mid-point of the soil section and taking three readings by rotating the probe 120° between each reading (Fig. C-8). Oven-dry measurements of the soil moisture content were not made, thereby limiting the accuracy of the calibrations. Each soil section averaged approximately 23 cm in diameter and 10 cm in thickness. The ML2 was tested by taking five readings at different locations on the surface of the soil section. The four project soils were tested at moisture contents of 0.0%, 10.0%, and near saturation, which varied for each soil from 15.0% to 25.0%. The column soil was tested at 0.0% and 20.0% only. All soil moisture contents were established by adding a known volume of water to the soil samples.

Results were averaged for each depth for the PR1 and PR2 probes, and for the five readings taken with the ML2, and the data plotted to obtain the soil-specific calibration constants (Table C-3). Differences between the calibrated and default constants were found for all soils; however, exceptionally large changes occurred in the a_1 constant in the Fort Bliss and El Centro soils.

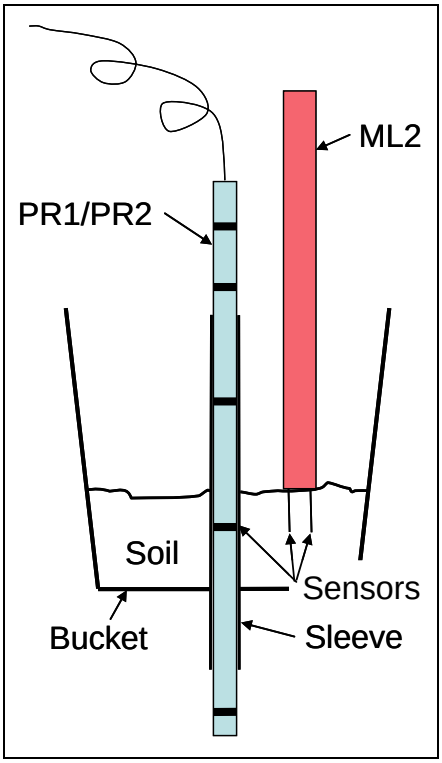


Figure C-8. Cross section of apparatus to measure soil moisture in OLS field soils with the ML2, PR1, and PR2 probes.

Table C-3. Calibration constants for each instrument at each depth, in millimeters.

		Ford Farm		Airport		Ft. Bliss		El Centro		Column Soil		Default	
PR-1	Depth	a0	a1	a0	a1	a0	a1	a0	a1	a0	a1	a0	a1
	100	1.63	10.8	1.62	13.95	1.75	9.8	1.78	9.51	2.00	10.3		
	200	1.61	11.5	1.68	14.88	1.77	12.0	1.83	9.51	1.97	11.3		
	300	1.53	11.5	1.62	15.07	1.73	13.0	1.76	10.2	1.89	11.4		
	400	1.51	11.6	1.57	15.17	1.73	12.3	1.71	9.78	1.87	11.5		
	600	1.89	10.3	1.95	17.59	1.96	8.29	2.07	9.94	2.19	12.6		
	100	2.22	7.65	2.06	12.65	1.95	11.3	2.10	11.4	2.45	12.2		
	Average	**1.57**	**11.3**	**1.62**	**14.8**	**1.74**	**11.8**	**1.77**	**9.76**	**1.93**	**11.1**	**1.60**	**8.40**
PR-2	100	1.43	8.13	1.39	8.79	1.70	5.39	1.66	4.83	1.77	10.0		
	200	1.47	8.20	1.46	8.59	1.70	5.54	1.66	4.82	1.84	10.1		
	300	1.48	8.26	1.46	9.19	1.71	5.69	1.67	4.90	1.83	10.2		
	400	1.42	8.80	1.48	9.07	1.73	6.18	1.68	5.05	1.82	10.0		
	600	1.47	8.32	1.46	9.81	1.73	5.73	1.59	5.47	1.86	10.1		
	1000	1.49	8.07	1.38	7.29	1.61	6.02	1.46	6.04	1.72	9.75		
	Average	**1.46**	**8.30**	**1.44**	**8.79**	**1.70**	**5.76**	**1.62**	**5.19**	**1.81**	**10.0**	**1.60**	**8.40**
ML-2	**Average**	**1.46**	**11.4**	**1.50**	**10.5**	**1.62**	**10.2**	**1.57**	**9.99**	**1.71**	**9.33**	**1.60**	**8.40**

* For PR-1 Data in red are omitted from the average due to possible faulty sensors.

Applying the new constants to the 15% column soil moisture content using Equations 5–7 allowed comparison of the default constants to the new constants. These results, listed in columns four and five of Table C-2, still produce errors larger than ± 0.05%. The error for the PR1 and PR2 probes with the new constants is smaller than the error with the default constants; however, the ML2 error increased.

Statistical Comparisons

Comparisons were made between coincident oven-dried soil moisture measurements and the ML2 to determine whether they were statistically from the same population. If the electronic and oven-dry measurements were found to be statistically from the same population, then it may be argued that the electronic measurements may be used with some confidence.

Only ML2 and oven-dry measurement pairs were compared. Troxler nuclear gauge moisture measurements are considered generally less accurate than oven-dried moisture contents, so comparisons were not made between the Troxler and other moisture measurements. PR1 and PR2 measurements also were not compared to oven-dry moisture contents because paired observations—those made at essentially the same location and time—were not available.

Statistical comparisons were made in the following groupings: North Vernon Airport, Ford Farm, Fort Bliss, and El Centro NAS. North Vernon Airport and Ford Farm also were combined into an Eastern Sites group, and El Centro NAS and Fort Bliss were combined into a Western Sites group.

Non-parametric statistical methods were used for comparison because measurements often were not normally distributed, and sample sizes often were sufficiently small that assumptions were not satisfied for parametric statistics, making non-parametric statistics necessary. The Wilcoxon Difference of Means test was used to determine whether oven-dried and ML2 default calibration moisture magnitudes, and the oven-dried and ML2 soil-specific calibration moisture magnitudes, were from the same population. The Spearman Rank Correlation Coefficient was used to determine whether there was a significant correlation between the pairs of measurements. In all cases, the probabilities were set at $\rho > 0.05$, not significant; $\rho = 0.01$ to 0.05, significant; $\rho = 0.001$ to 0.01, very significant; and $\rho < 0.001$, extremely significant. Software used for non-parametric analyses was GraphPad (1998), and for plots and linear regressions was Microsoft Excel.

North Vernon Airport, Ford Farm, and Eastern Sites

Correlations between oven-dry and ML2 soil moisture percentages were very low (column 4), and not significant (column 5) with the small sample

sizes available in Indiana, 27 at the North Vernon Airport and 22 at Ford Farm (column 10) (Table C-4). All r^2 were less than 0.06. Figures C-9–C-11 show the large scatter in the oven-dry to ML2 relationships.

Only one of the Wilcoxon difference of means tests, for the Ford Farm default ML2 calibration, showed no significant difference between the oven-dry and electronic soil moisture measurements (columns 2 and 3) (Table C-4). At North Vernon Airport and Ford Farm individually, and at the two sites combined, the two-tailed ρ values and the differences between the oven-dry and electronic measurements means show that the default calibration provided by Dynamax compared better to the oven-dry samples than did the soil-specific calibrations. The mean differences (column 9) also were smallest for these cases (Table C-4).

Table C-4. Comparisons between oven-dry and ML2 soil moisture percentages in southern Indiana.

1	2	3	4	5	6	7	8	9	10
	Wilcoxon two-tailed ρ	Sig*	Spearman r	One-tailed ρ	Sig*	Oven-dry mean**	ML2 mean**	Mean difference**	N
Airport default	0.0200	S	0.10	0.3057	NS	33.5	30.8	2.7	27
Airport calibrated	<0.0001	S	0.06	0.3825	NS	33.5	24.5	9.0	27
Ford default	0.0634	NS	–0.24	—	—	33.8	30.3	3.5	22
Ford calibrated	<0.0001	S	–0.25	—	—	33.8	22.9	10.9	22
Eastern default	0.0034	S	–0.05	—	—	33.6	30.6	3.0	49
Eastern calibrated	<0.0001	S	–0.01	—	—	33.6	23.8	9.8	49

* Sig is significance of the relationship. S is significant at a probability of 0.05, and NS is not significant at a probability of 0.05.

** Volumetric soil moisture content in percent.

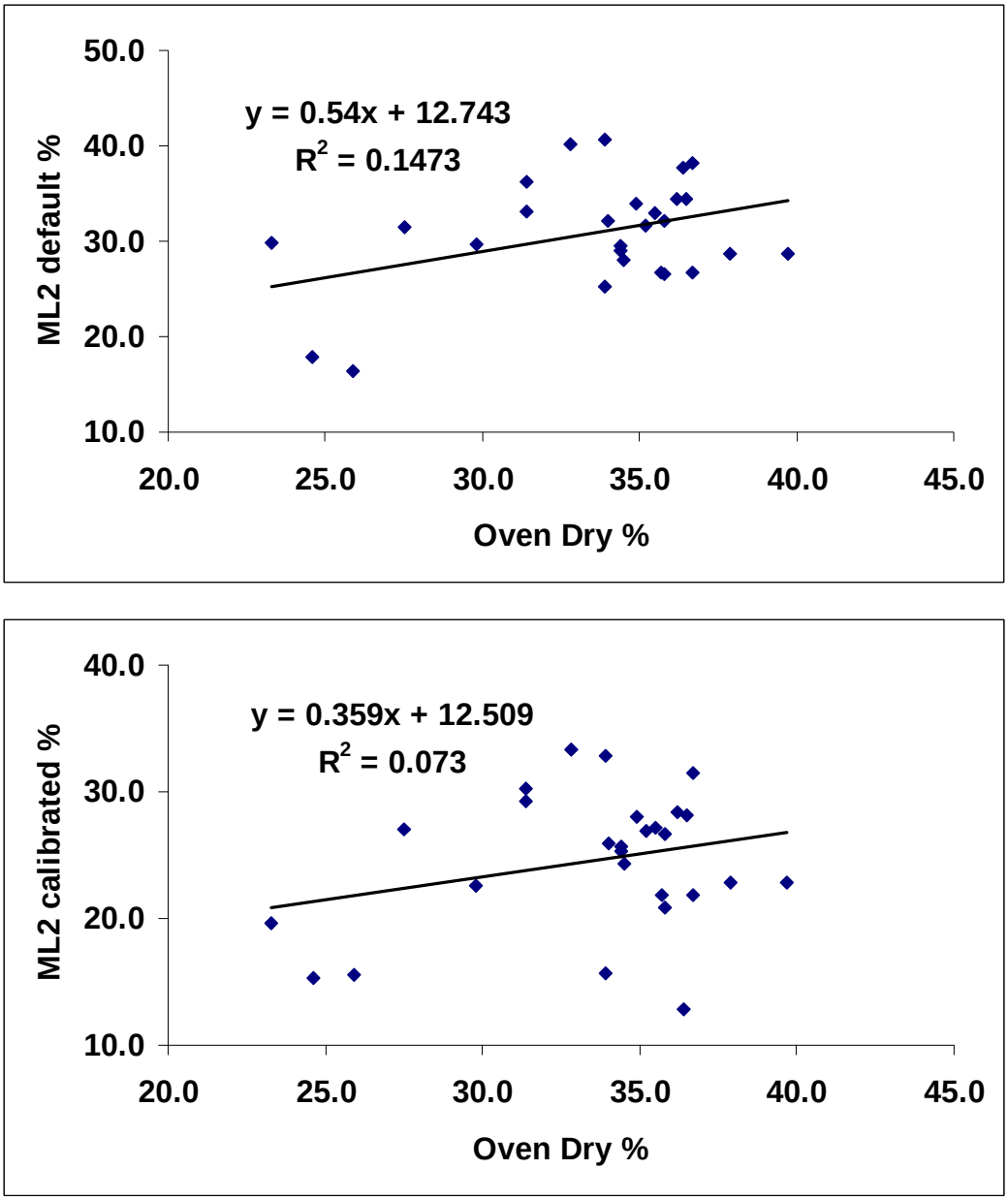


Figure C-9. Scatter plots and Pearson parametric linear regressions for North Vernon Airport moisture contents. Oven-dry versus ML2 default calibration (top) and soil-specific calibration (bottom).

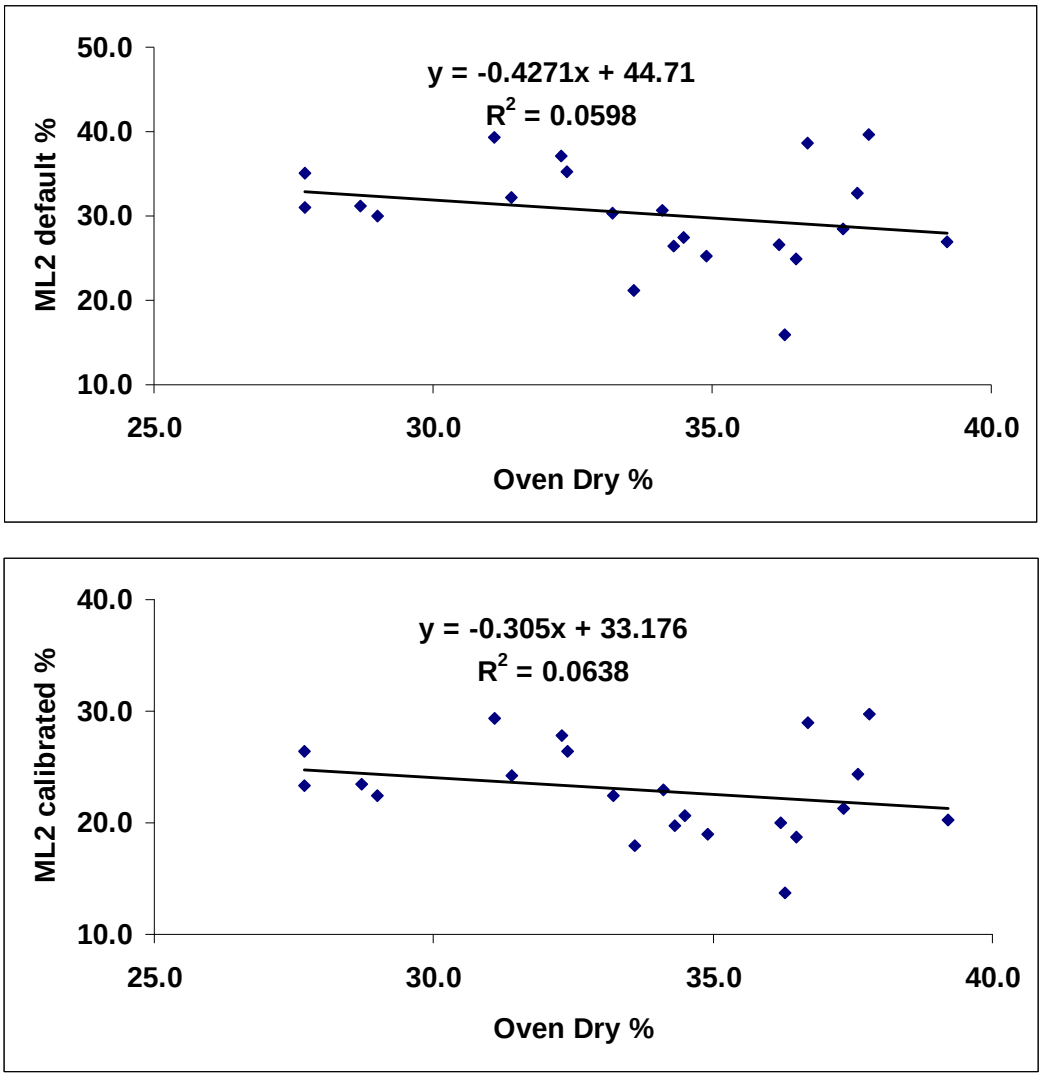


Figure C-10. Scatter plots and Pearson parametric linear regressions for Ford Farm moisture contents. Oven dry versus ML2 default calibration (top) and soil-specific calibration (bottom).

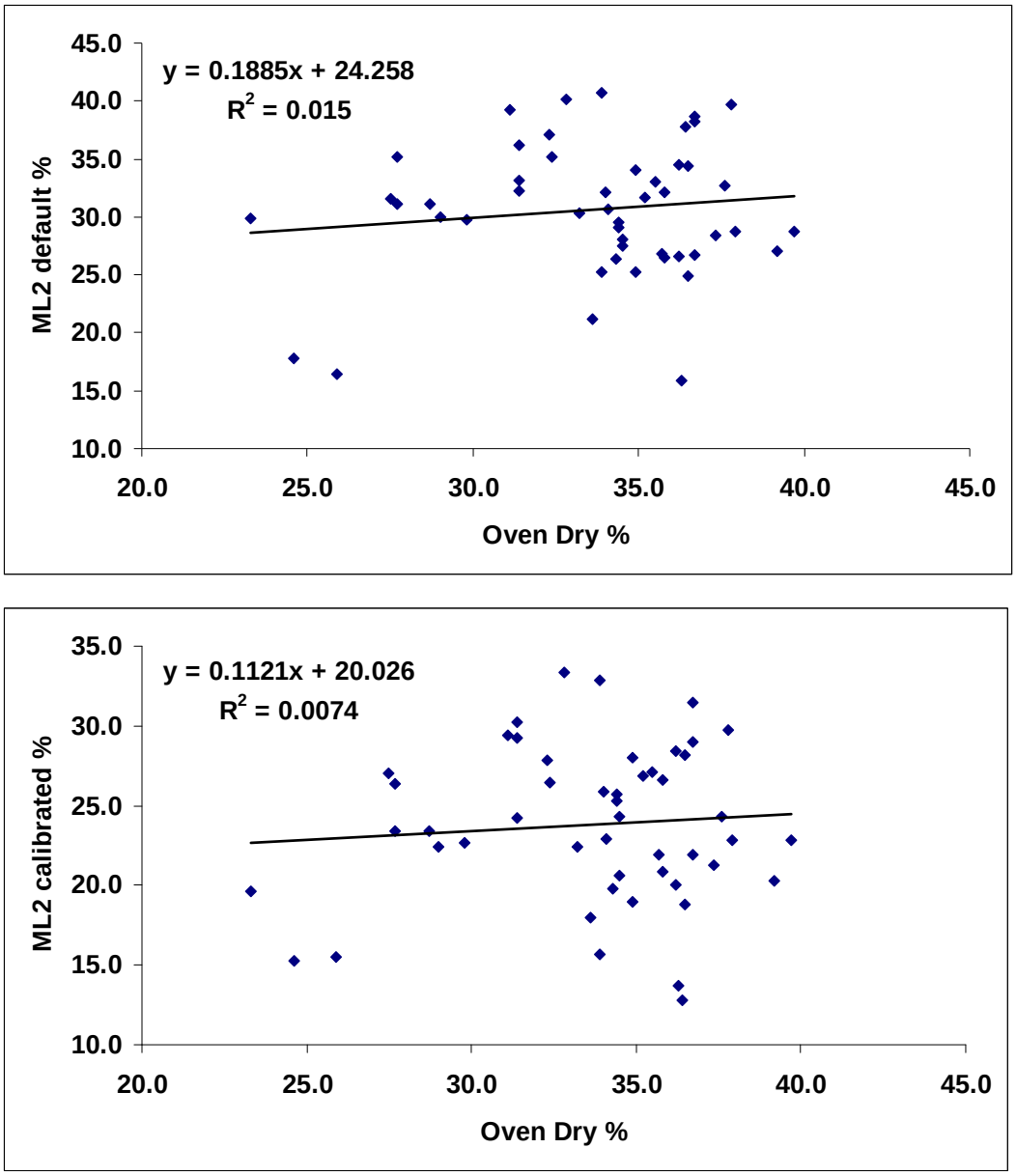


Figure C-11. Scatter plots and Pearson parametric linear regressions for the Eastern Site moisture contents. Oven-dry versus ML2 default calibration (top) and soil-specific calibration (bottom).

Fort Bliss, El Centro NAS, and Western Sites

Correlations between oven-dry moisture contents and the ML2 electronic measurements were higher in the western soils than in the eastern soils, with r^2 values all larger than 0.41 (Table C-5). Though scatter plots of the Fort Bliss, El Centro NAS, and combined sites all show considerable scatter, the correlations are all significant (Fig. C-12–C-14, Table C-5).

The Wilcoxon difference of means test, however, showed large differences between the oven-dry and ML2 default and calibrated soil moisture contents at Fort Bliss and at El Centro NAS (columns 2 and 3) (Table C-5). However, relationships were not significant, meaning that there is no significant difference between the means when the moisture measurements from both western sites were compared (Western Default and Western Calibrated rows, columns 2 and 3) (Table C-5). Therefore, statistical assessment of whether the default ML2 algorithms or the algorithms calibrated with the field soils compare better with the oven-dry soils is difficult to determine from the statistical analyses alone.

Table C-5. Comparisons between oven-dry and ML2 soil moisture percentages in western sites.

1	2	3	4	5	6	7	8	9	10
	Wilcoxon two-tailed ρ	Sig*	Spearman r	One-tailed ρ	Sig*	Oven-dry mean**	ML2 mean**	Mean difference**	N
Fort Bliss default	0.0009	S	0.82	<0.0001	S	10.7	7.8	2.9	15
Fort Bliss calibrated	0.0001	S	0.84	<0.0001	S	10.7	6.5	4.2	15
El Centro default	0.0011	S	0.78	<0.0001	S	7.2	9.5	–2.3	24
El Centro calibrated	0.0075	S	0.78	<0.0001	S	7.2	8.4	–1.3	24
Western default	0.5047	NS	0.71	<0.0001	S	8.5	8.8	–0.3	39
Western calibrated	0.3534	NS	0.69	<0.0001	S	8.5	7.7	0.9	39

* Sig is significance of the relationship. S is significant at a probability of 0.05, and NS is not significant at a probability of 0.05.

** Volumetric soil moisture content in percent.

The Fort Bliss and El Centro default and calibrated ML2 measurements both compare poorly with the oven-dried moisture contents even though correlations are high. However, the mean differences (column 9) may provide additional guidance. The default Fort Bliss and default combined Western site ML2 measurements had smaller mean differences with the oven-dry measurements than the calibrated algorithms. This suggests that the default soil calibration algorithms may be “best.” The exception was that the El Centro calibrated mean difference was somewhat smaller than the default difference. Because all of the mean differences are small for the

default calibrations, the default calibrations would, overall, be the best to use.

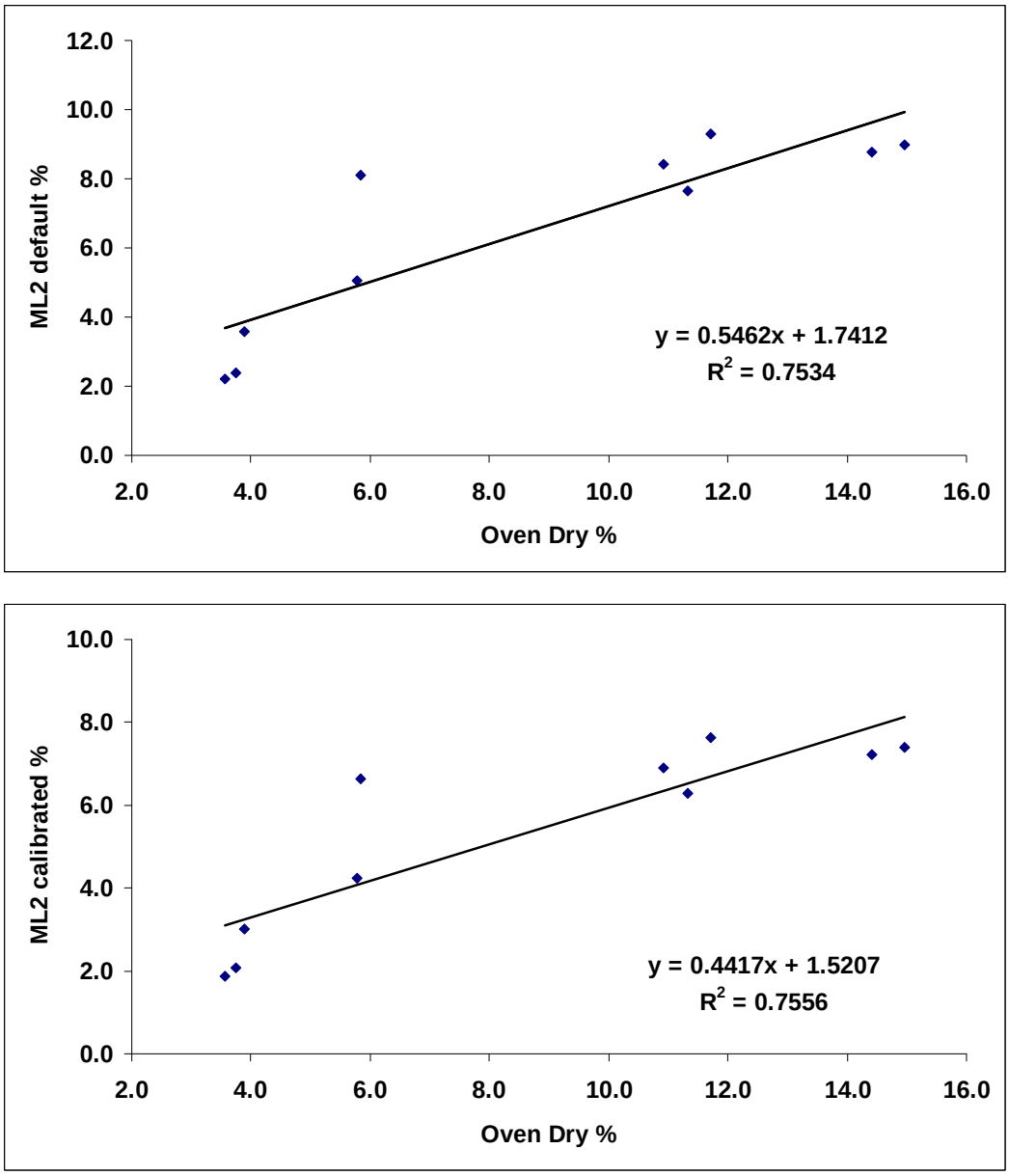


Figure C-12. Scatter plots and Pearson linear regressions for Fort Bliss moisture contents. Oven-dry versus ML2 default calibration (top) and soil-specific calibration (bottom).

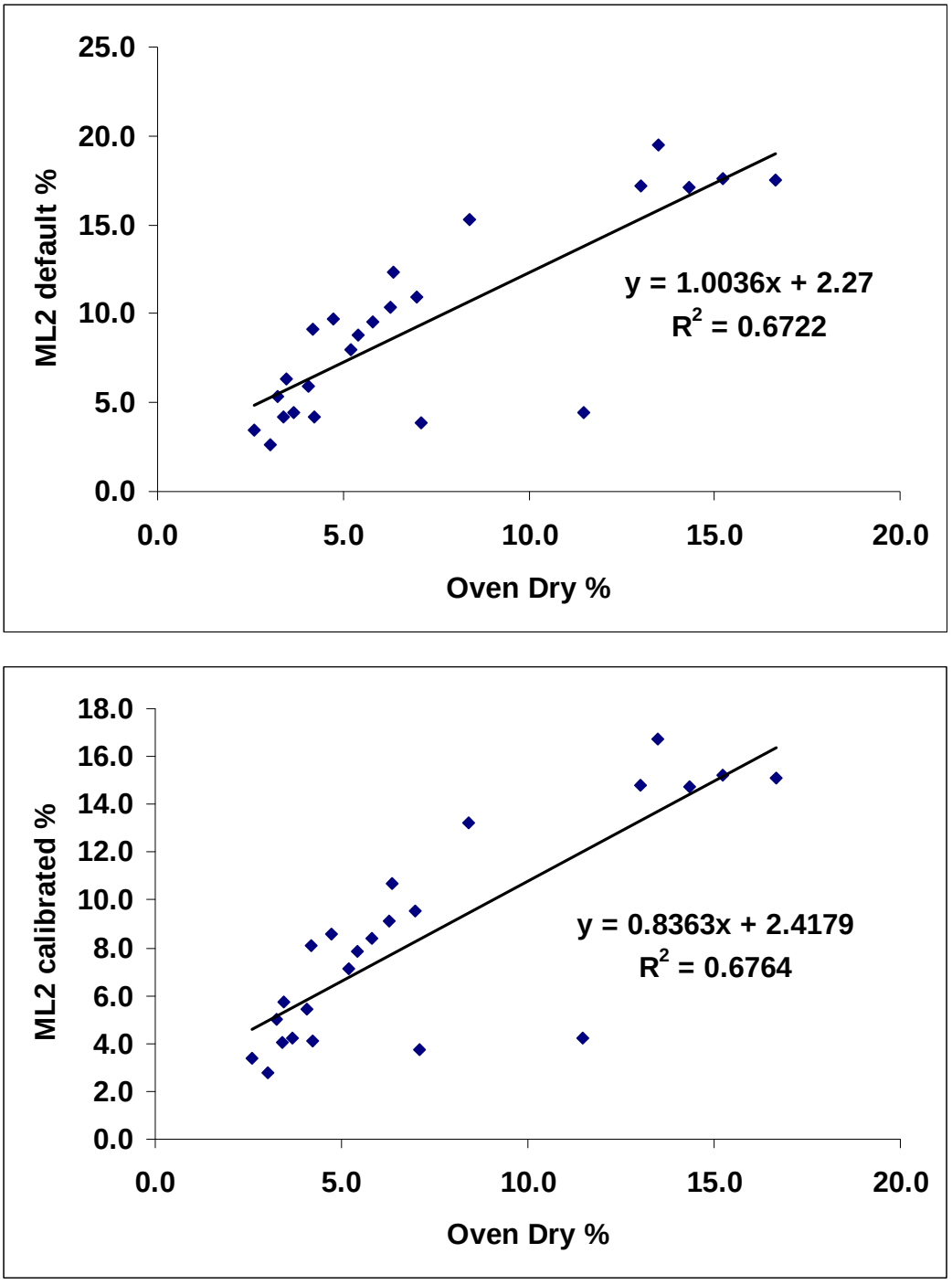


Figure C-13. Scatter plots and Pearson linear regressions for El Centro NAS moisture contents. Oven-dry versus ML2 default calibration (top) and soil-specific calibration (bottom).

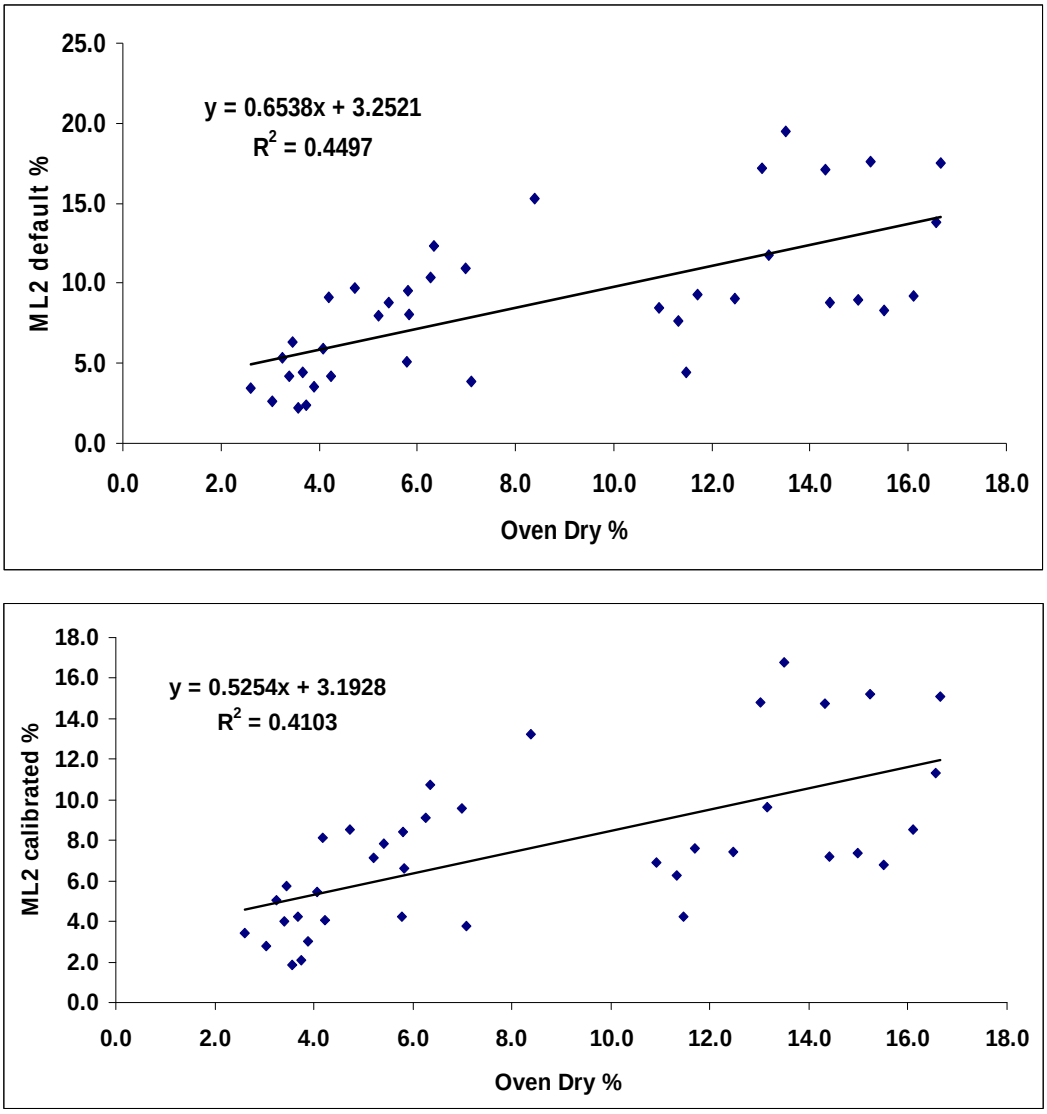


Figure C-14. Scatter plots and Pearson linear regressions for Western Sites moisture contents. Oven-dry versus ML2 default calibration (top) and soil-specific calibration (bottom).

Summary and Recommendations

The purpose of this appendix is to determine which instruments used to measure soil moisture in the OLS field program provide the most accurate measurements for use in soil moisture and soil strength modeling verification work, and for reporting soil moisture to other program partners via field reports and the database archive. This was accomplished by comparing electronic methods used with the potentially more accurate oven-dried moisture contents.

The oven-dry (gravimetric) technique is generally considered the most accurate method for measuring soil moisture content (Rollings and Rollings 1995; R. Rollings, personal communication, 2006). Oven-dried gravimetric measurements are the most direct method of measuring soil moisture and, other than sampling error, which affects all methods, has the least opportunity for error if careful laboratory methods are followed. The field gravimetric readings, therefore, were accepted as the standard to which electronic methods were compared.

The Troxler nuclear gauge is also a source of soil moisture measurements that is considered acceptable, especially if it compares well to oven-dry gravimetric measurements. However, we did not focus on the Troxler in this analysis because relatively few Troxler measurements were made. The most important interest was to assess the accuracy of the Dynamax electronic instruments, especially the ML2, because they were used to make the majority of moisture measurements that define spatial and temporal changes in OLS soil moisture content.

Because capability was provided by Dynamax for calibrating the PR1, PR2, and ML2 probes to specific soils, and because sufficient soil samples were brought to CRREL from the field, each electronic instrument model was calibrated to the four RAS soils. Then, selected cases where physical soil samples were taken in the field for laboratory oven-dry gravimetric analyses, and electronic (always ML2) measurements taken immediately before or after in the same vicinity (within 1 m), were compared statistically.

Unfortunately, the results of the statistical analysis were not defining. Correlations were weak for the Indiana soils. However, oven-dry gravimetric measurements generally, but not typically significantly, compared best to ML2 measurements made with the default Dynamax calibration. Therefore, best practice is to use the ML2 default measurements when working with the Indiana soil moisture measurements.

Correlations at the western sites were much larger than at the eastern sites, and the relationships were positive. However, the Wilcoxon test indicated that differences in the means of the ML2 and oven-dry measurements were still too large at Fort Bliss and El Centro for the samples to have been taken from the same population. However, when the two sites were grouped, both the default and calibrated ML2 values compared well with the oven-dry measurements.

The lack of discrimination in the statistical analysis leaves only one other value to assess, and that is the absolute difference in means between the ML2 and oven-dry gravimetric measurements. Comparisons suggest that, with a few exceptions, the default calibrations for mineral soils provided by Dynamax performed marginally better than the soil-specific calibrations. Mean differences between the gravimetric and default measurements all fall within the ± 5% effective measurement error that Dynamax exemplifies in its literature (Delta-T Devices 1999). Therefore, the default Dynamax ML2 calibrations provide answers, in general, that are closest in magnitude to the oven-dry measurements, and also fall within the effective error range suggested by the manufacturer. Though there is no compelling reason not to use the default Dynamax calibrations for the ML2 instrument at all sites, the values should be used recognizing that comparisons with the oven-dry samples are not typically statistically significant.

With regard to the PR1 and PR2 probes, statistical comparisons with oven-dry measurements were not possible because no oven-dried samples were taken near these probes. However, the soil-specific calibrations did show reduced error for measurements in the column soil at a moisture content of 15%, when compared to the default calibration. This one comparison suggests that PR1 and PR2 performance may be more accurate using the soil-specific calibrations. However, the comparisons are limited in number and moisture content range and were not made in in-situ field soils, and the calibration soil moisture was only estimated and not taken from oven-dried measurements. Therefore, it would be prudent to not use the PR1 and PR2 measurements as absolute values, but to use them only for guidance to assess trends and to identify major wetting or drying events.

References

Delta-T Devices (1999) *Theta Probe Soil Moisture Sensor User Manual Type ML2x*. Delta-T Devices, Cambridge, England.

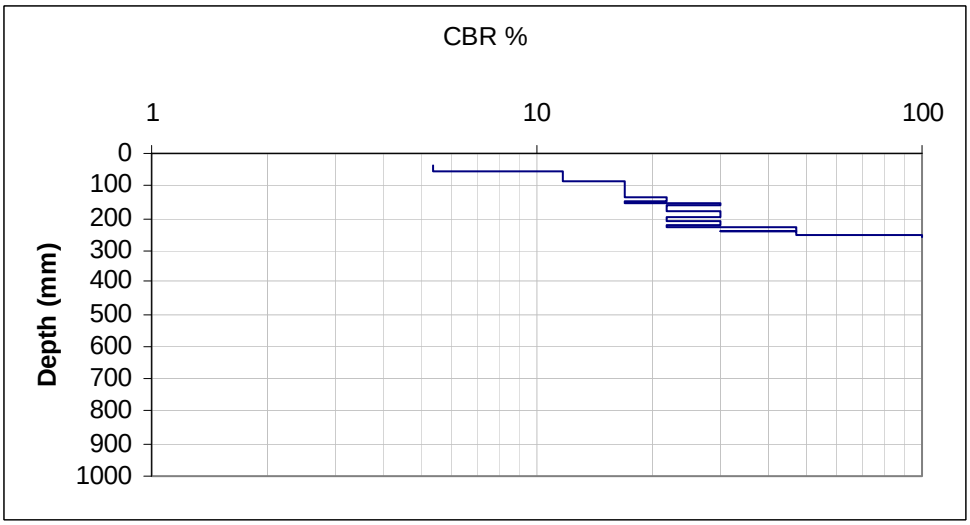
Delta-T Devices (2001) *User Manual for the Profile Probe Type PR1*. Delta-T Devices, Cambridge, England.

Delta-T Devices (2004) *User Manual for the Profile Robe Type PR2*. Delta-T Devices, Cambridge, England.

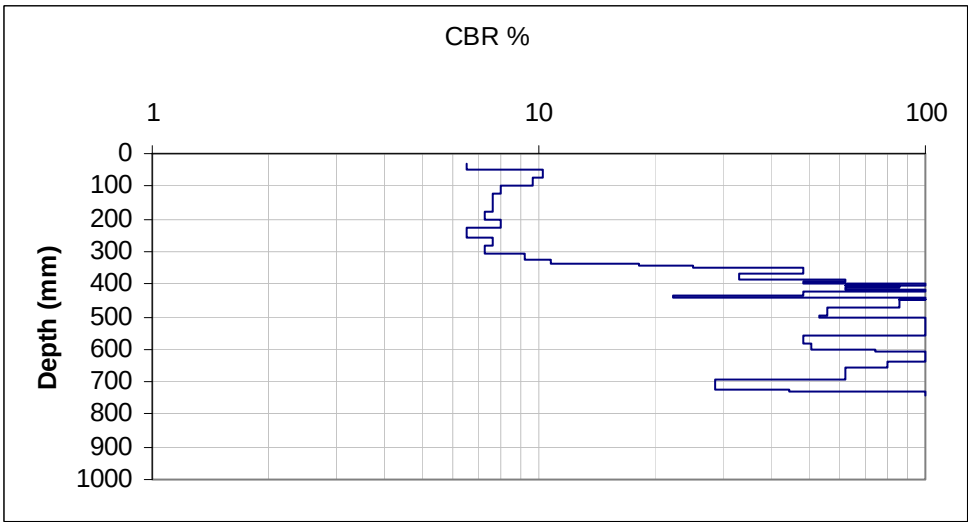
GraphPad (1995) InStat version 3.00 for Windows 95. GraphPad Software, San Diego California USA (www.graphpad.com).

Appendix D: Compilation of DCP Profiles from OLS at Fort Bliss

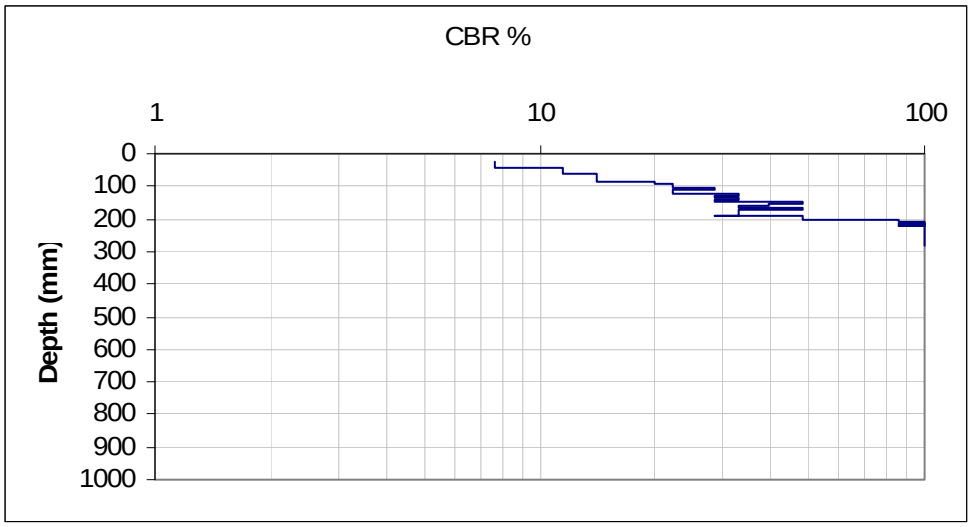
D1. IOP #1, July 11-15, 2005



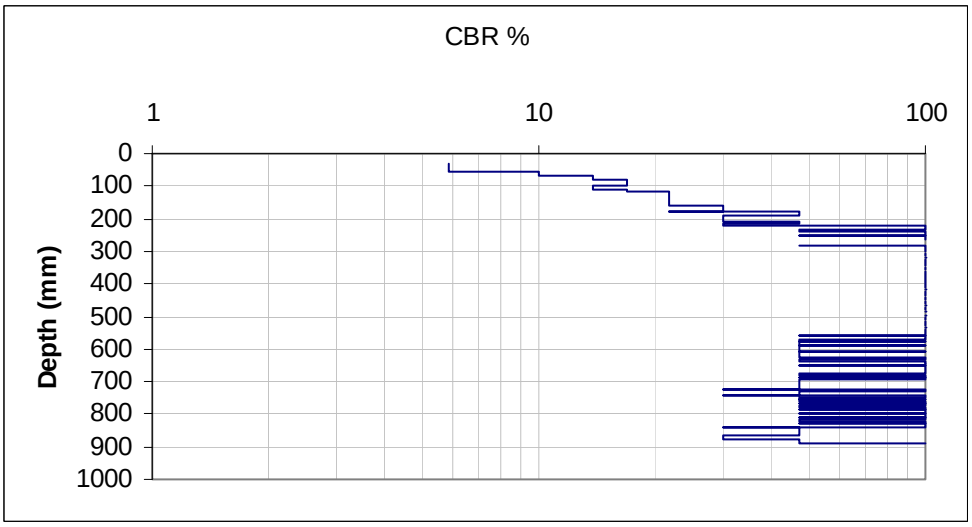
0+40 CL – auto



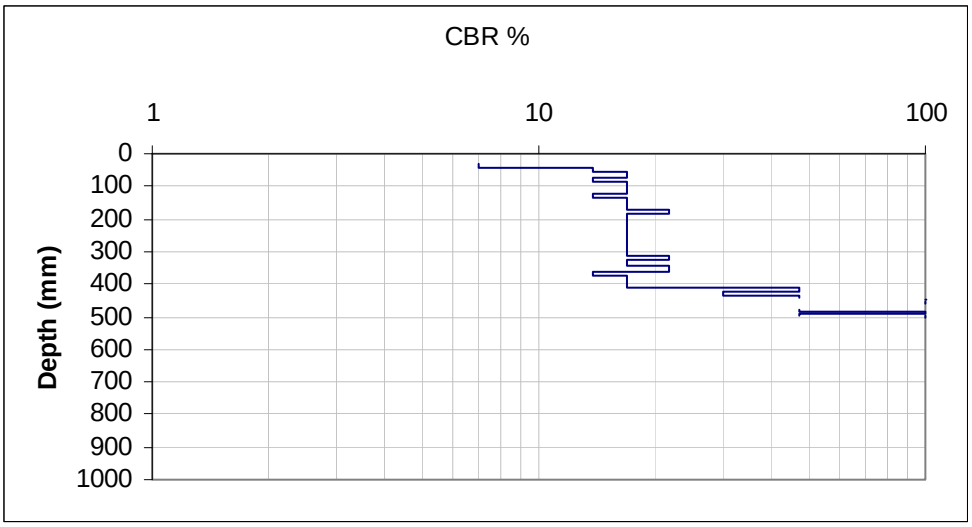
0+40 – 20N – manual



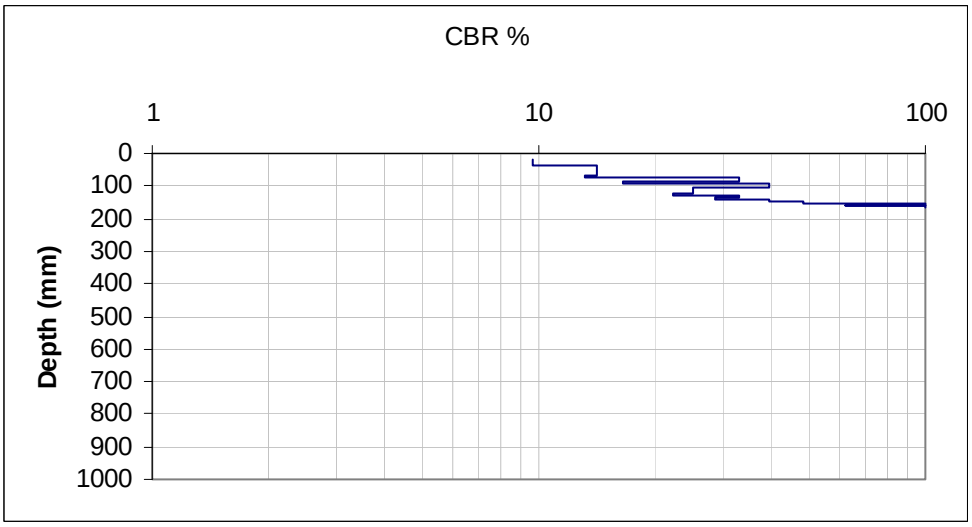
0+40 20S – manual



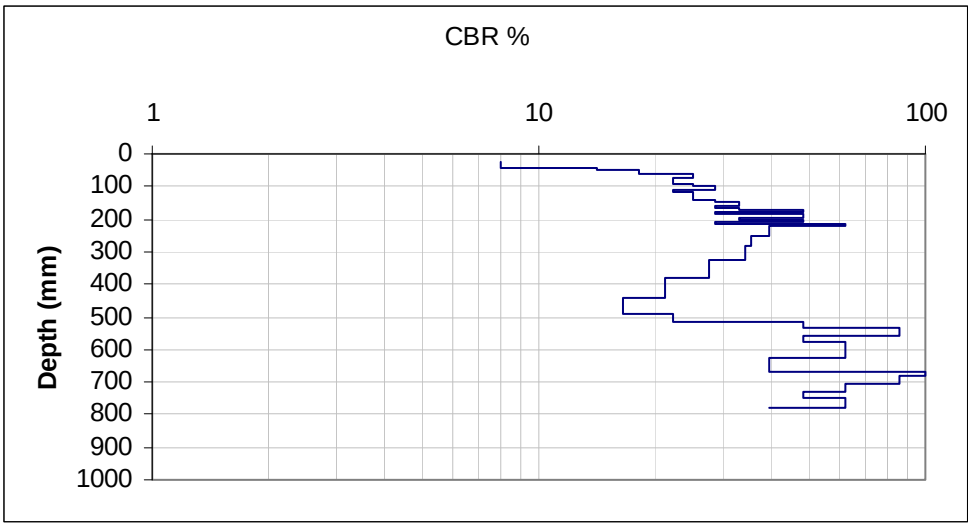
0+90 CL – auto



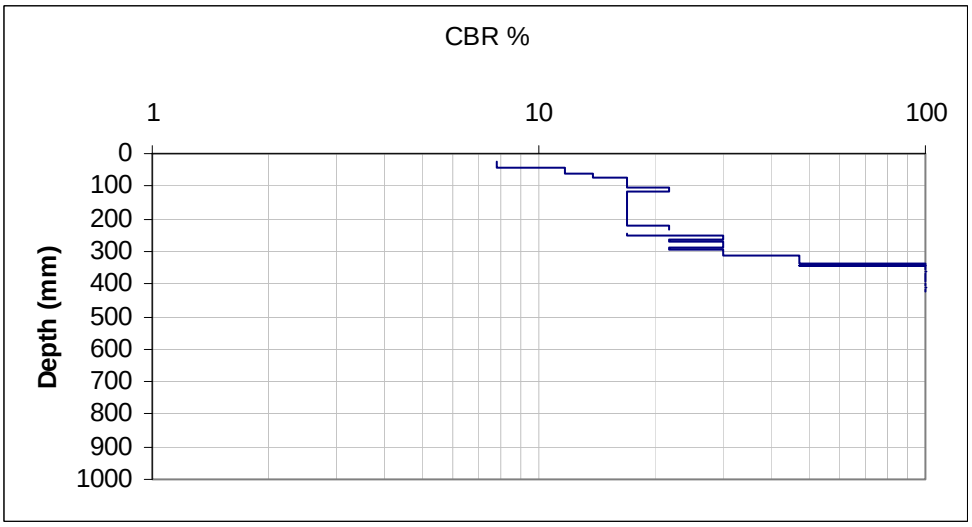
0+90 30S – auto



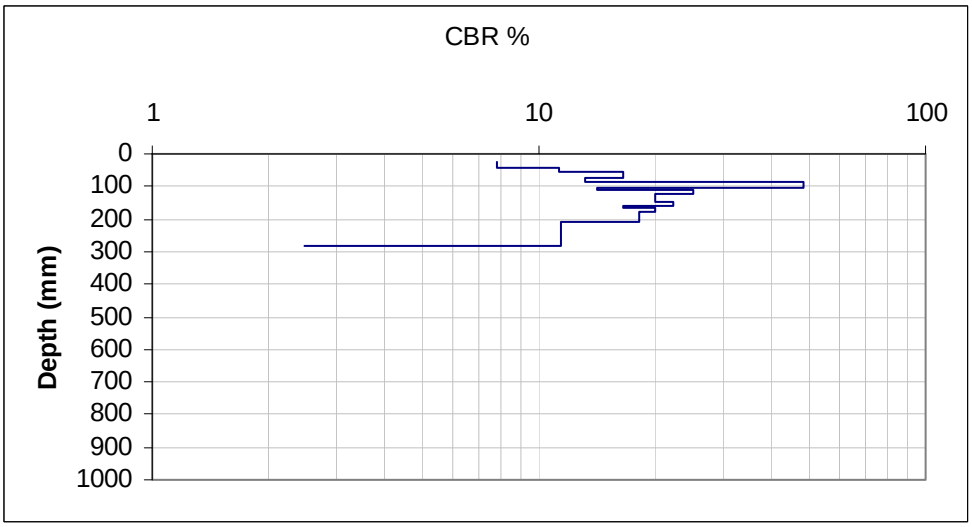
0+90 10S – manual



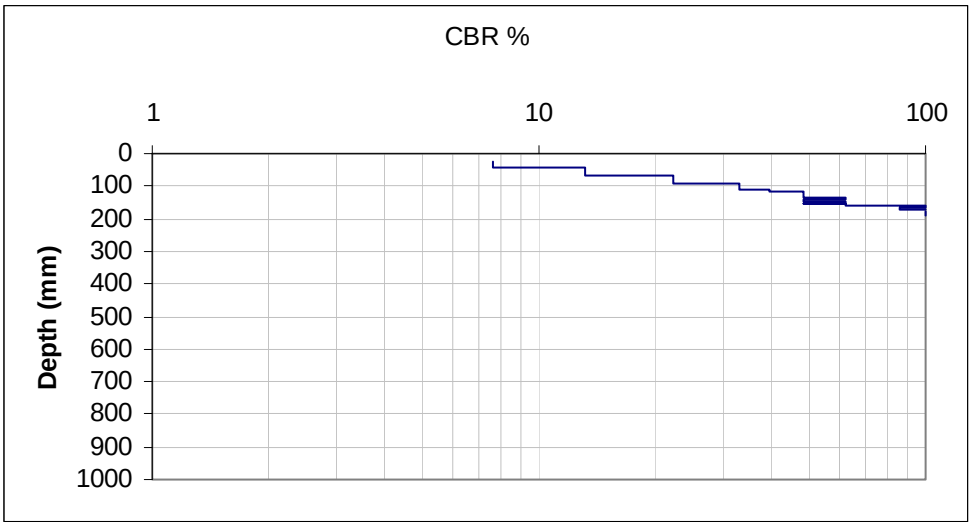
0+90 10N – manual



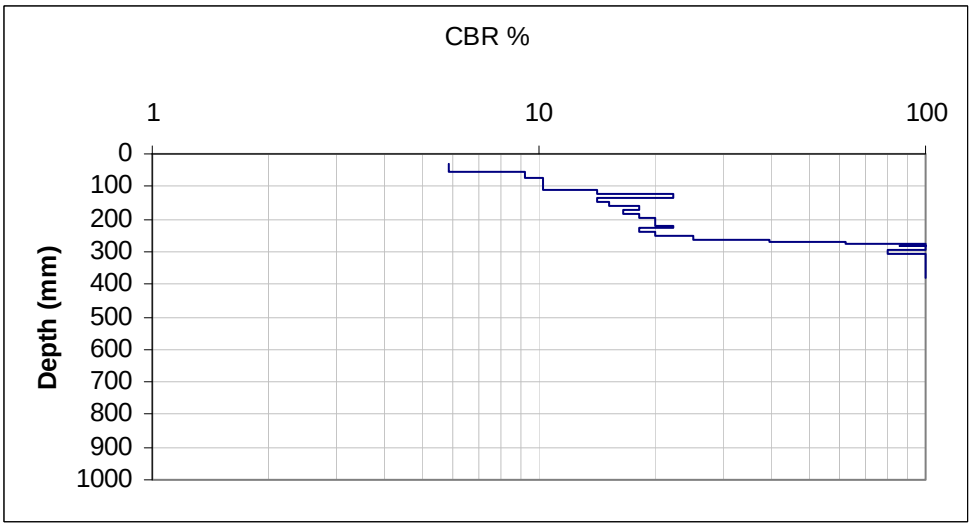
0+90 30N – auto



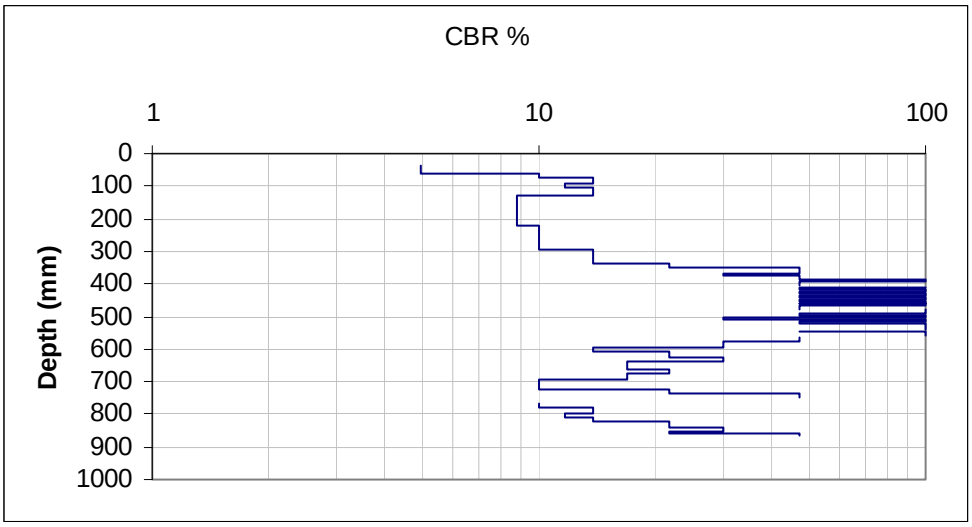
0+90 30N — manual



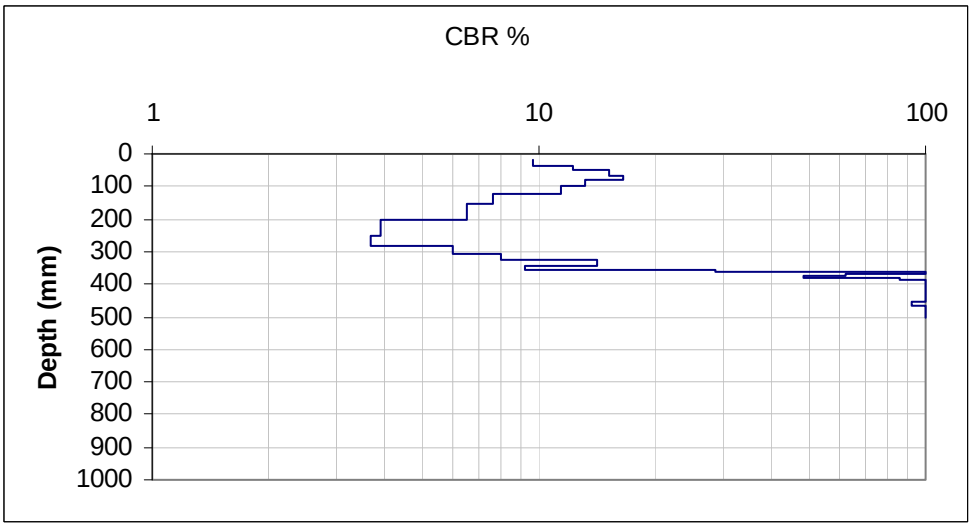
1+30 2N — manual



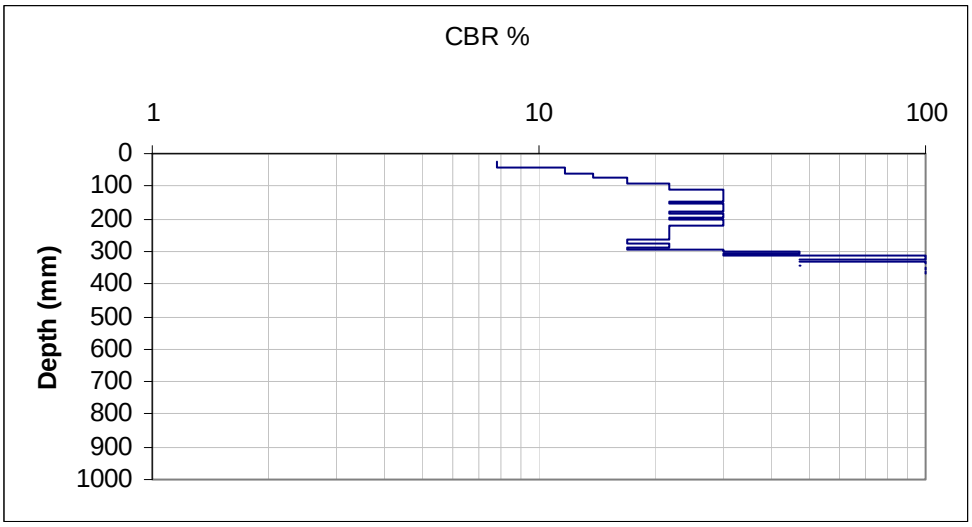
1+30 2S – manual



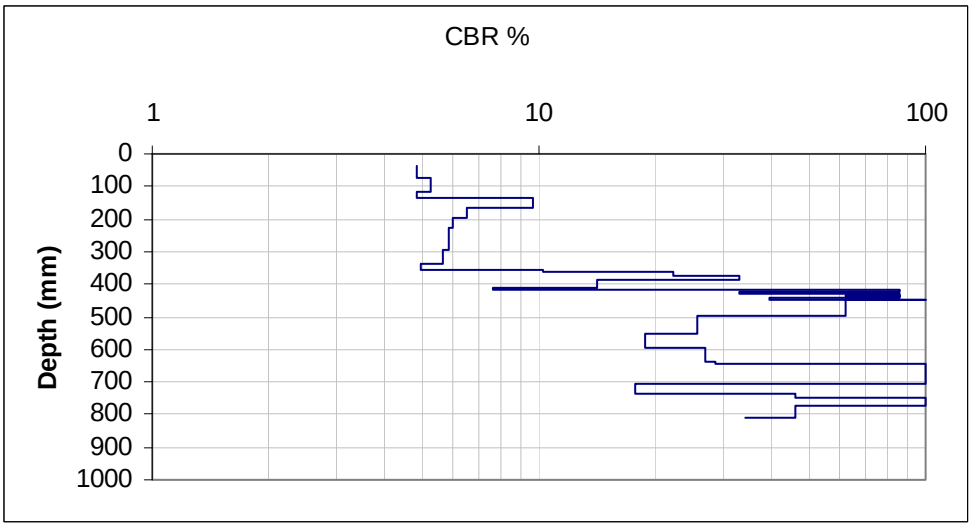
1+70 CL – auto



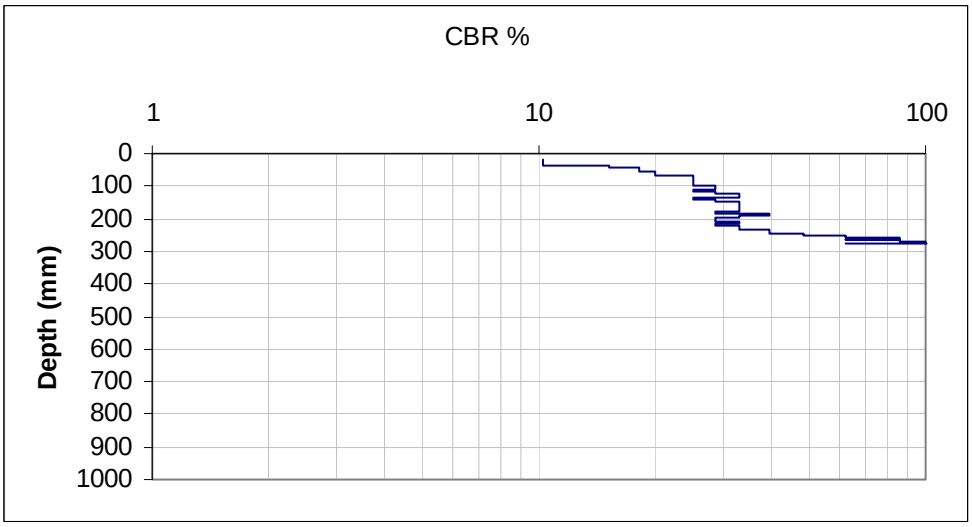
1+70 2N — manual



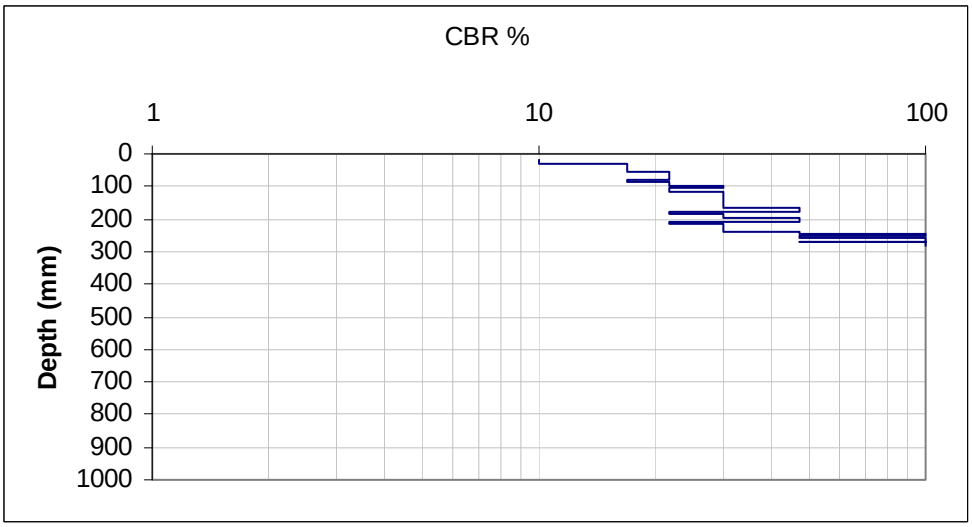
1+70 20S — auto



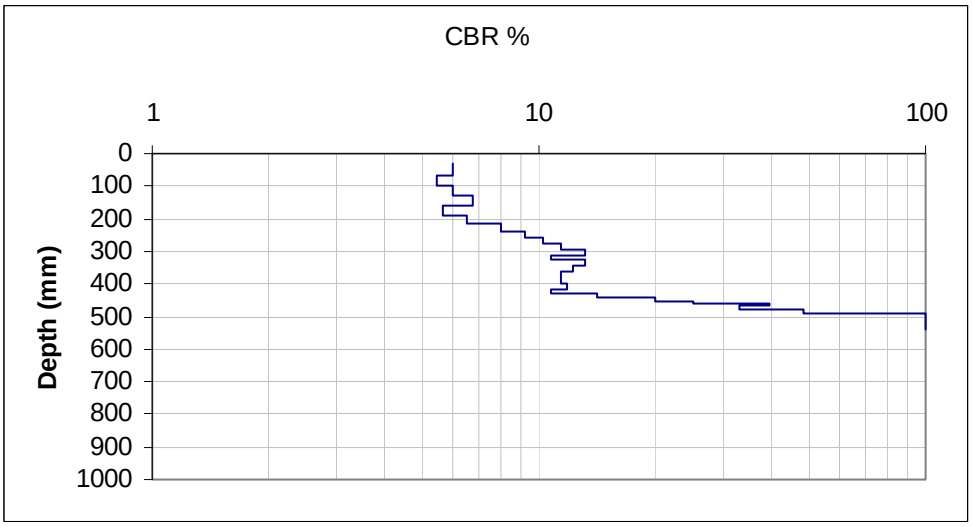
1+70 2S – manual



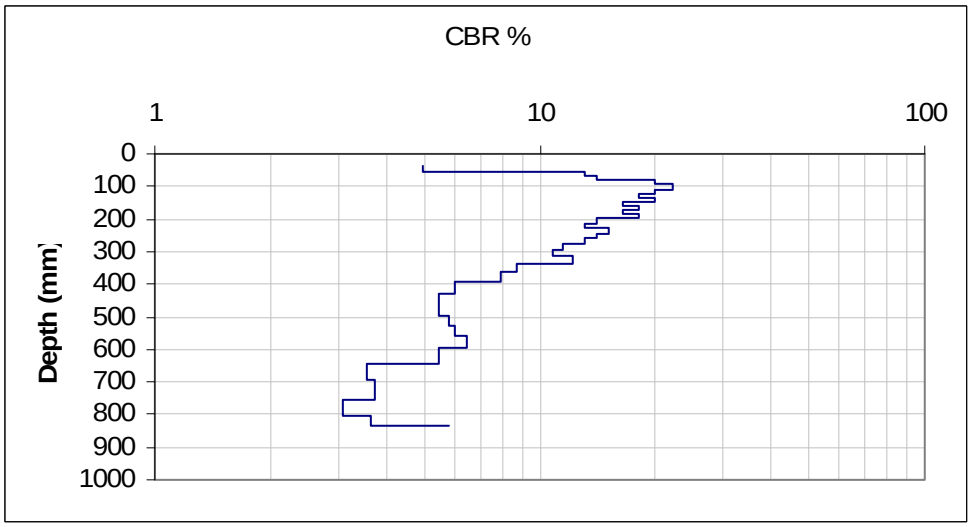
1+70 20N – manual



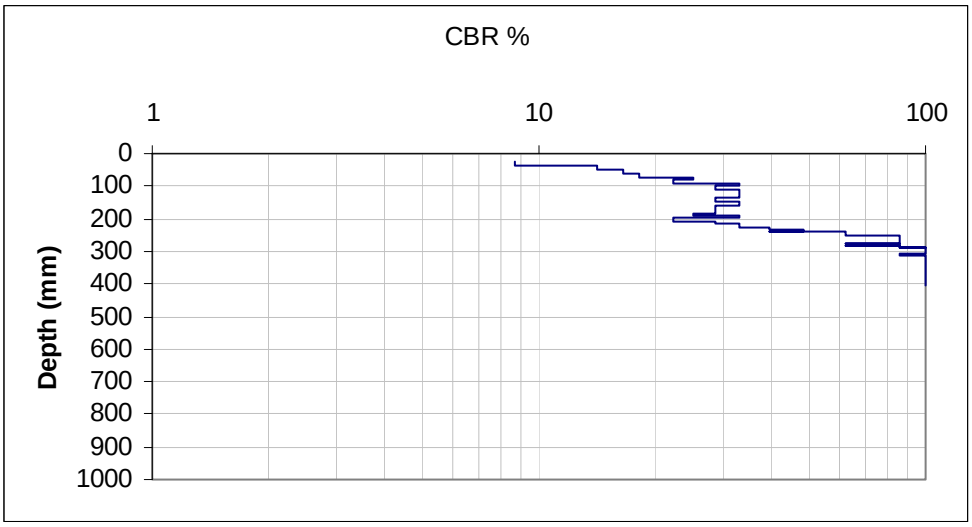
1+70 20N — auto



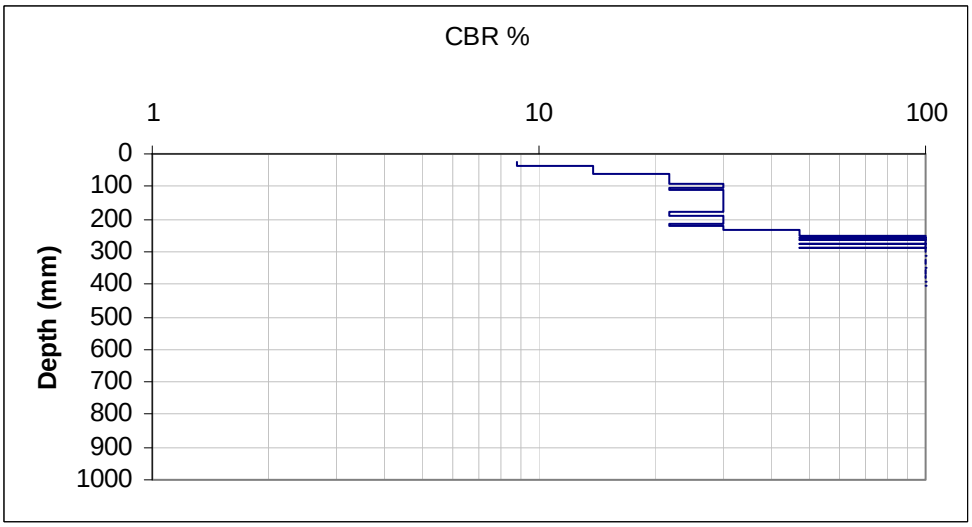
2+10 2S — manual



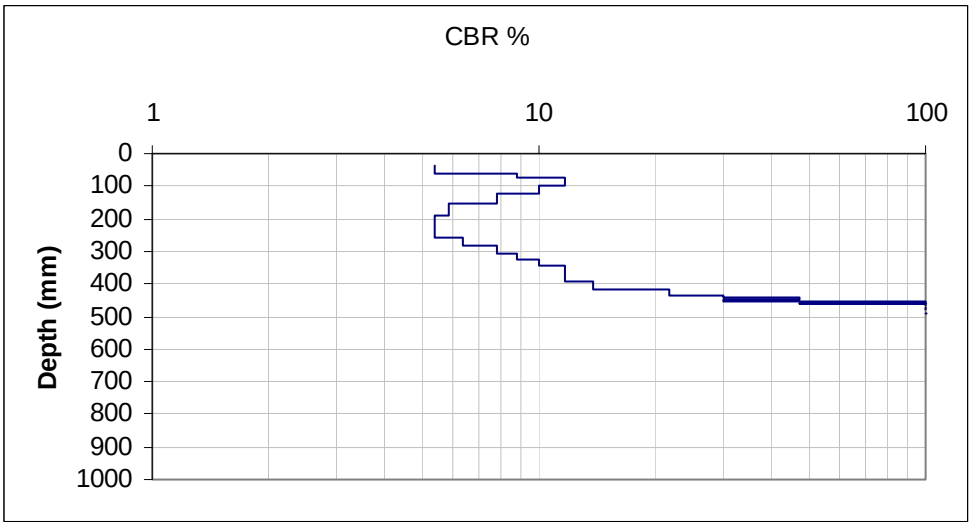
2+10 2N – manual



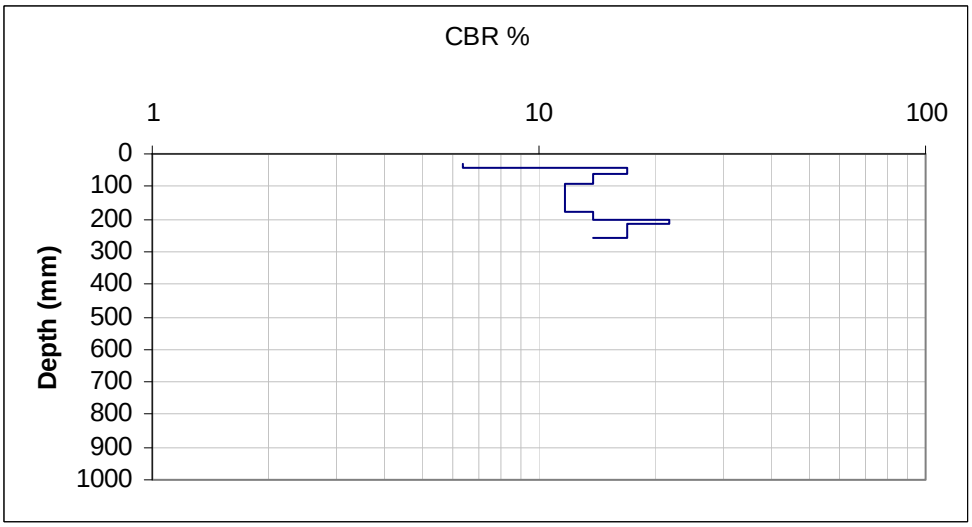
2+50 CL – manual



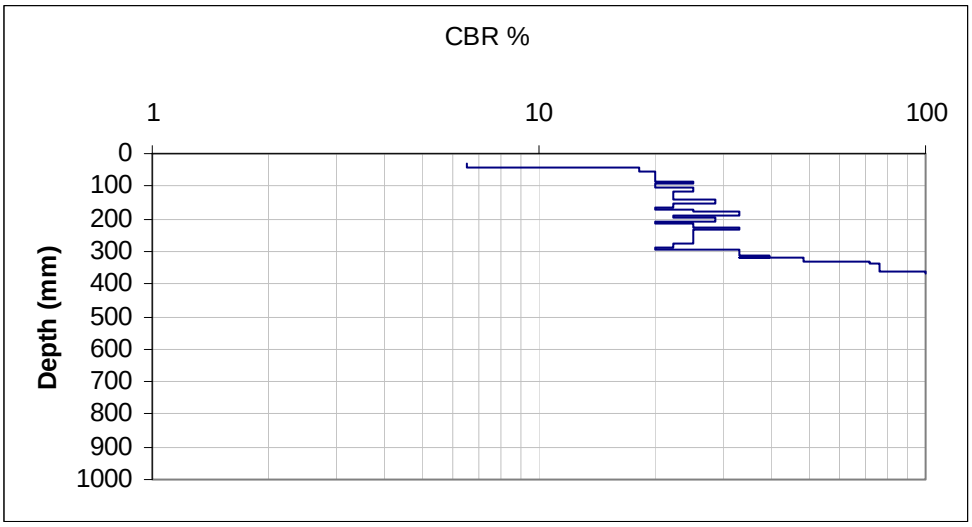
2+50 CL – auto



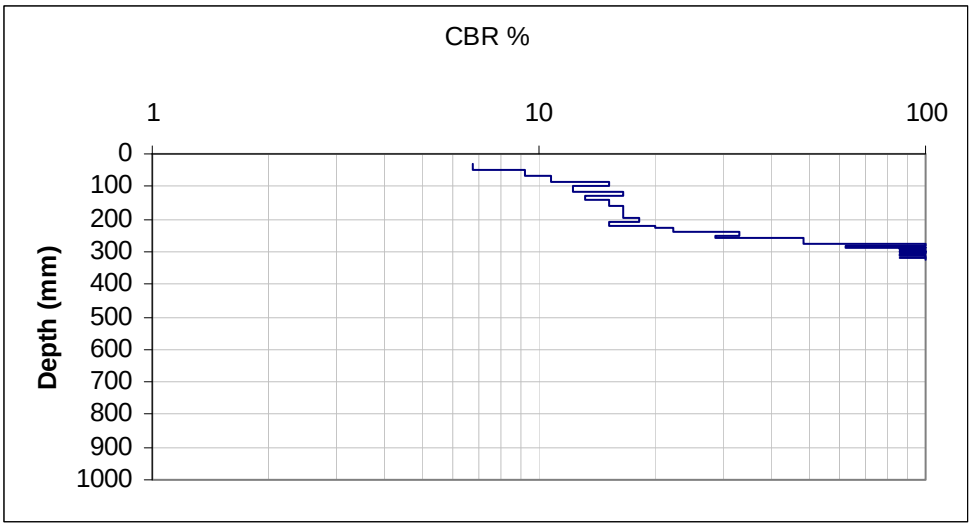
2+50 10S – auto



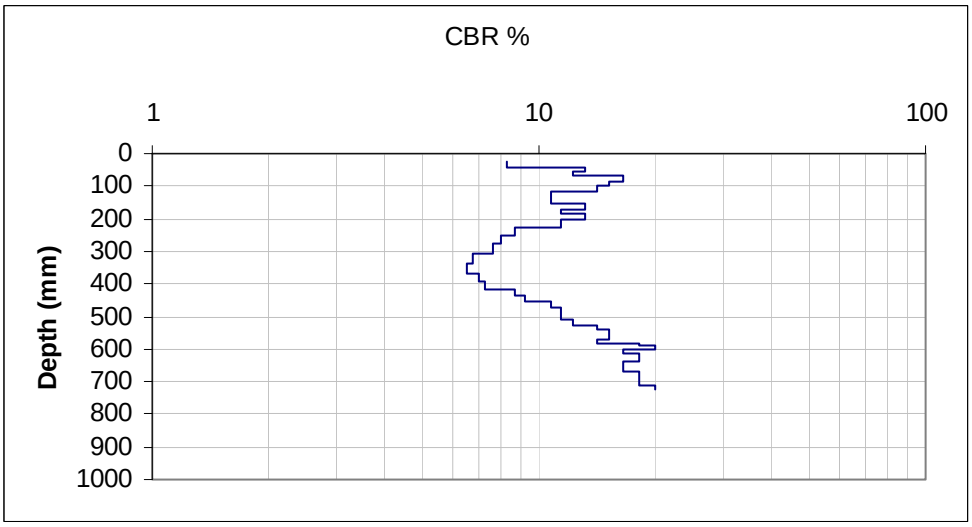
2+50 10N – auto



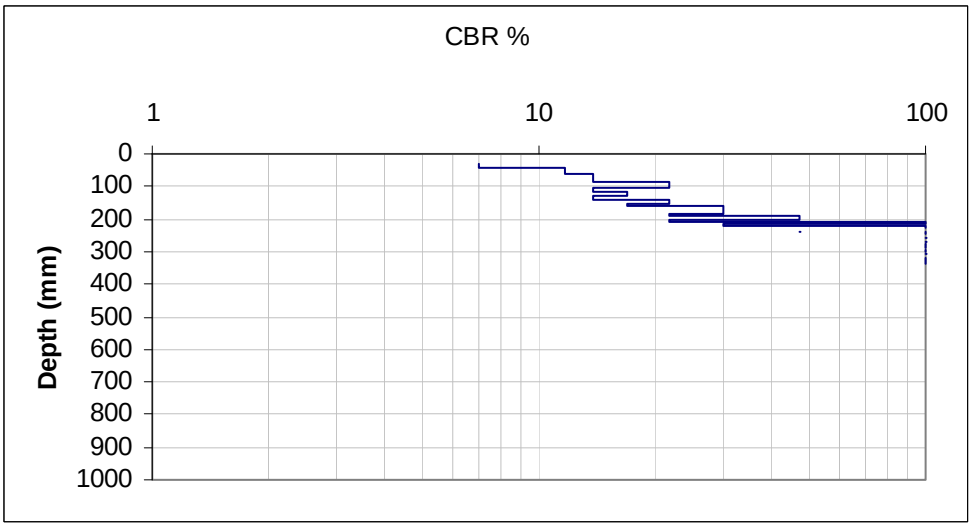
2+50 10N – manual



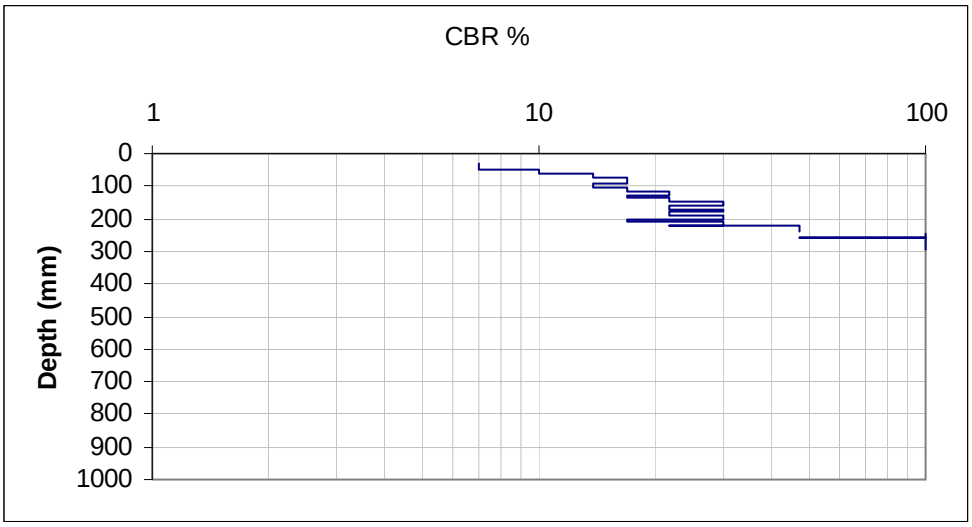
2+80 2S – manual



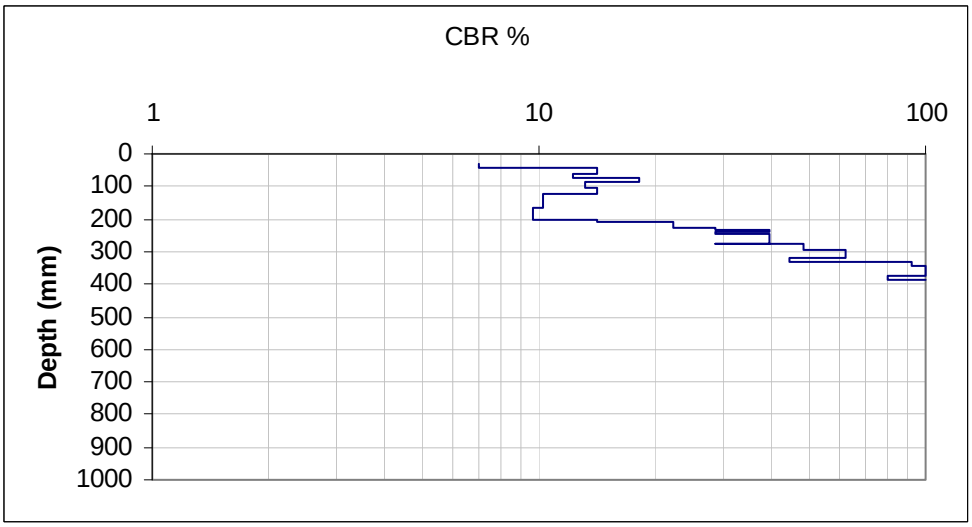
2+80 2N – manual



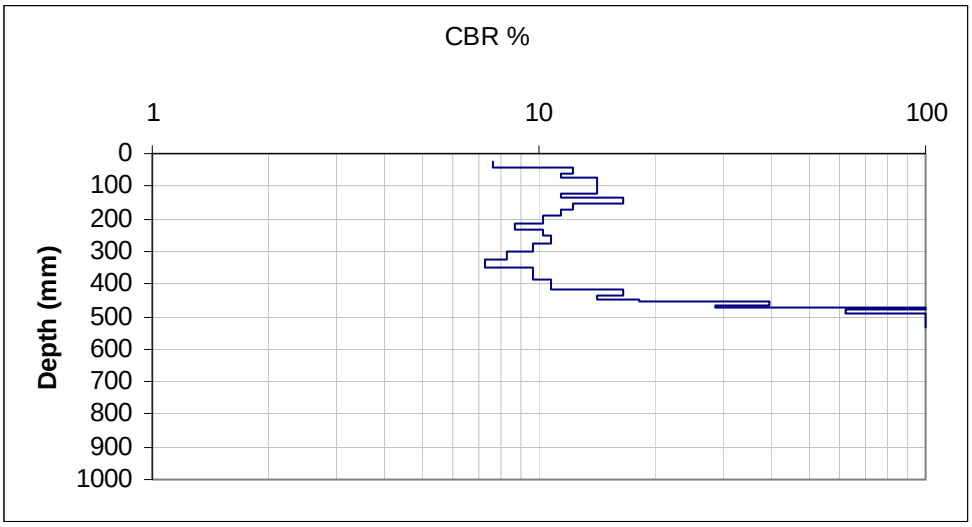
3+30 2N – auto



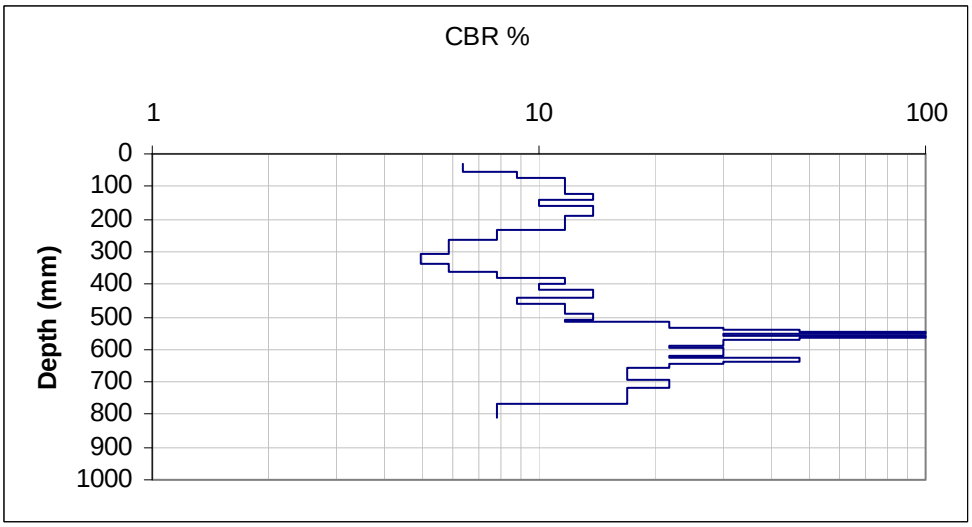
3+30 2S – auto



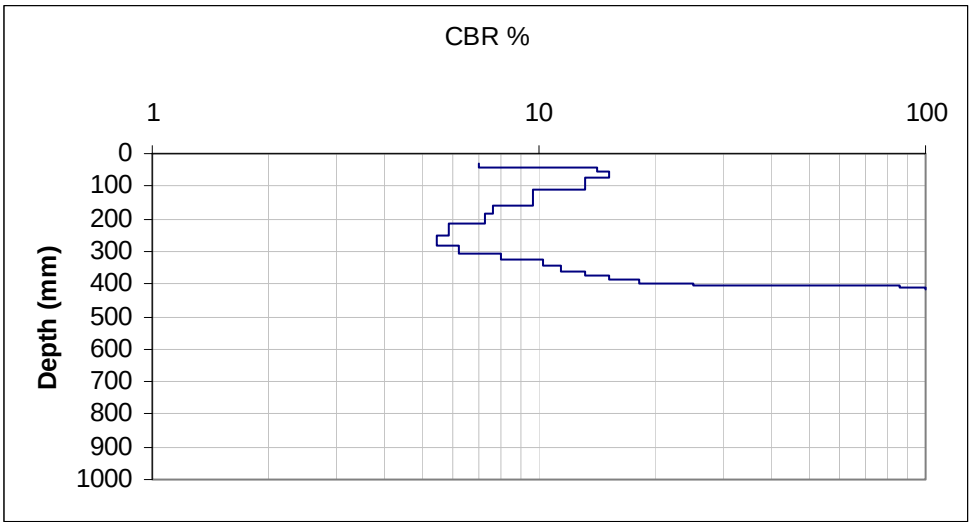
3+30 20N – manual



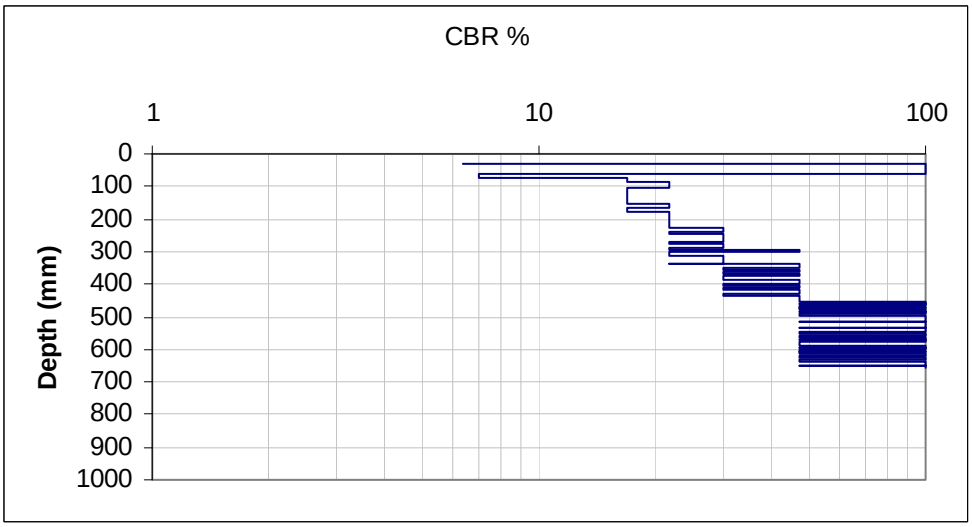
3+30 20S – manual



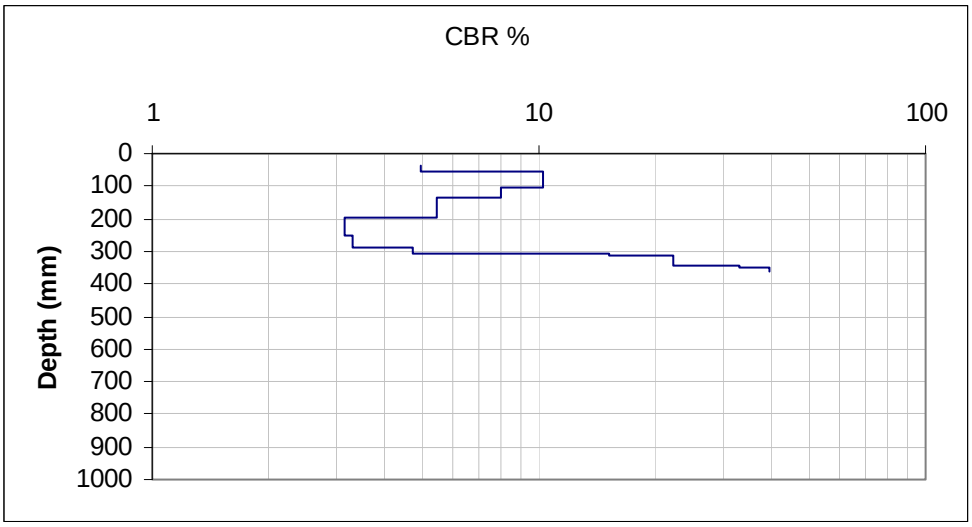
4+00 CL – auto



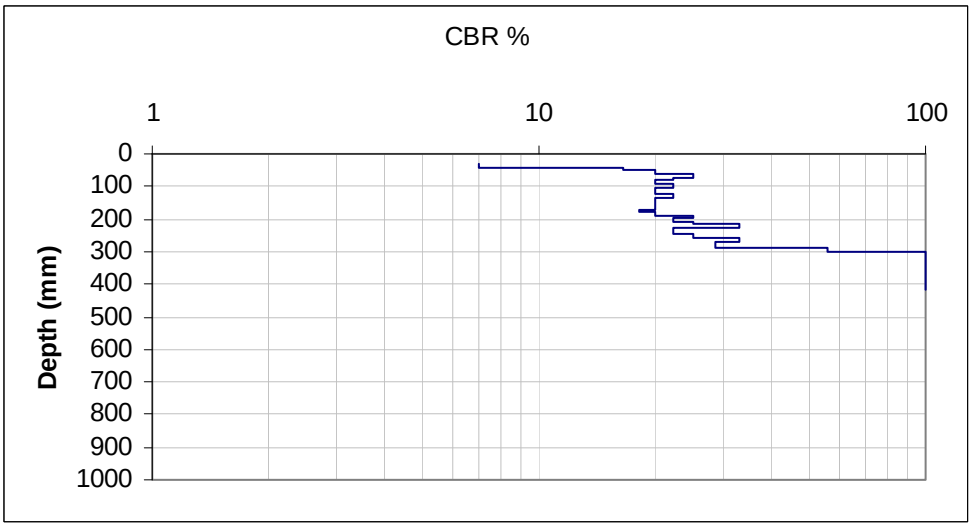
4+00 10S – manual



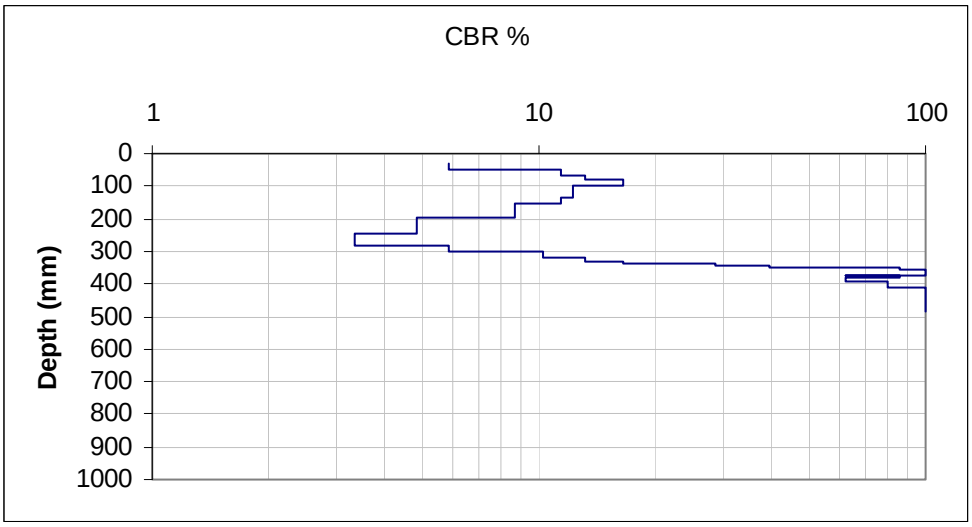
4+00 10N — auto



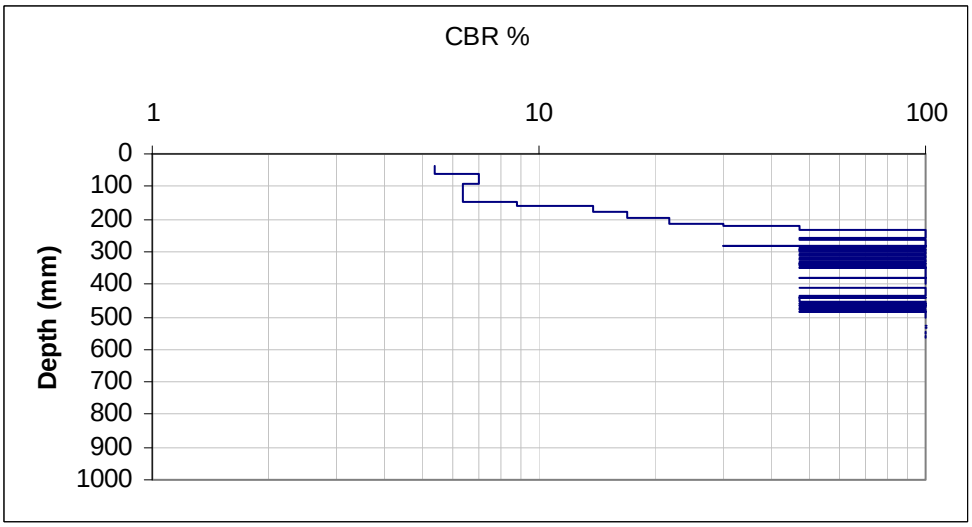
4+70 2N — manual



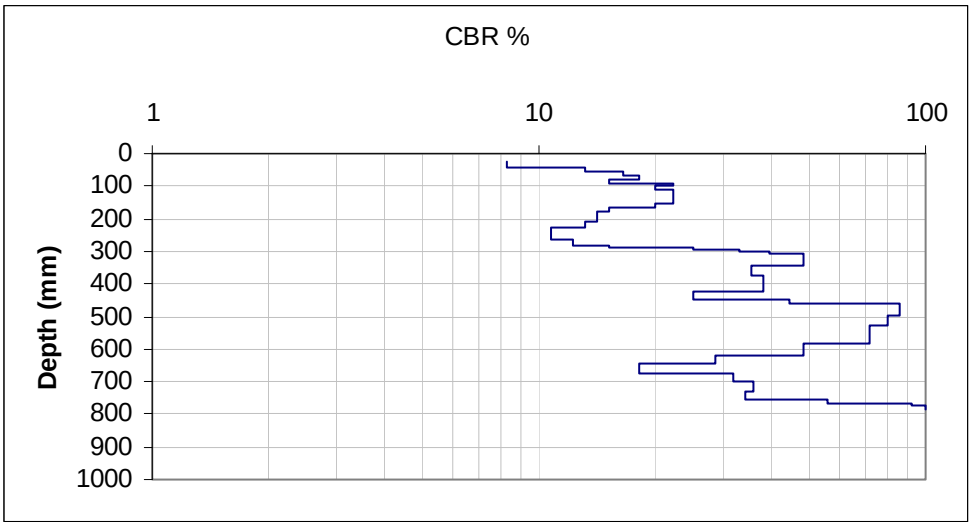
4+70 2S – manual



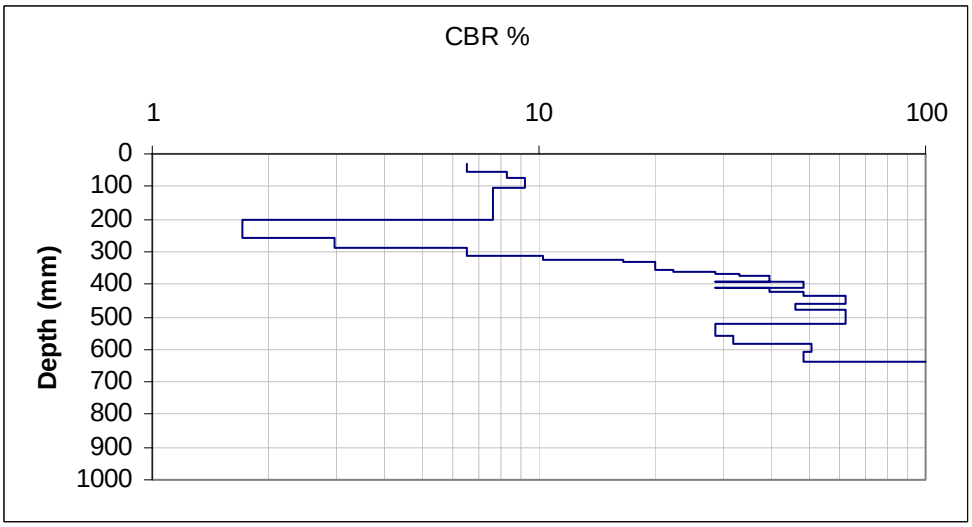
4+70 20S – manual



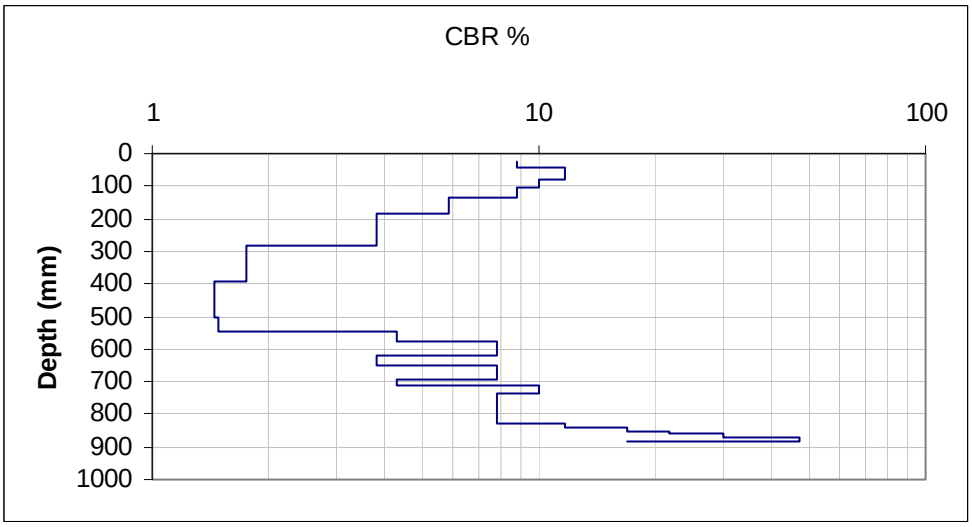
4+70 20N — auto



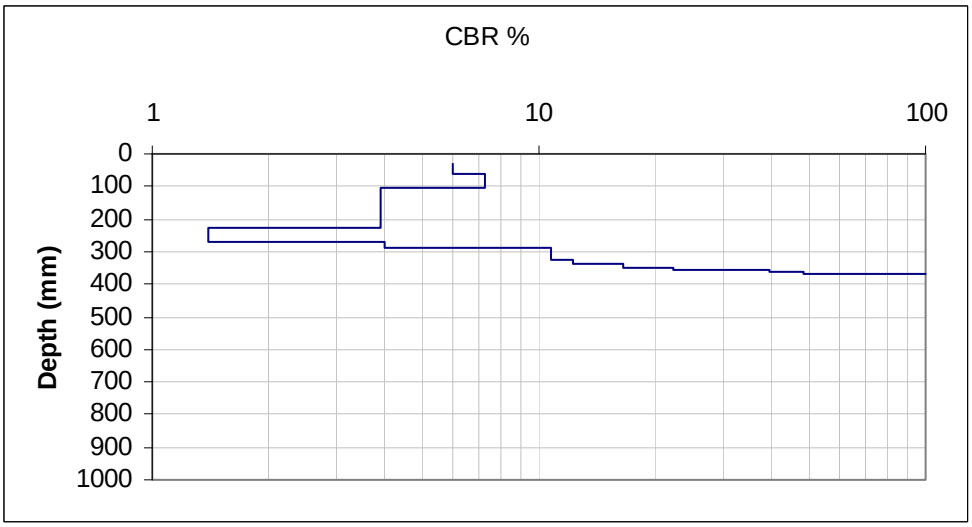
5+20 2S — manual



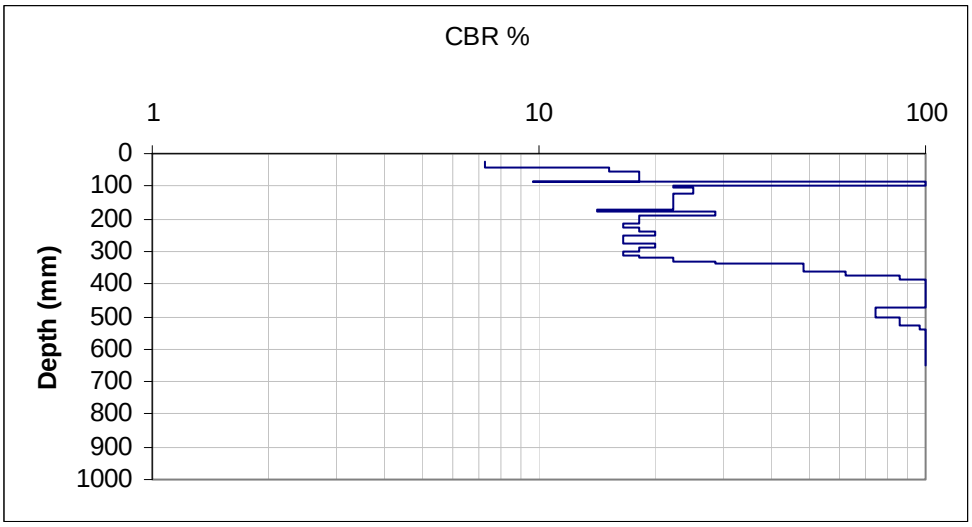
5+20 2N – manual



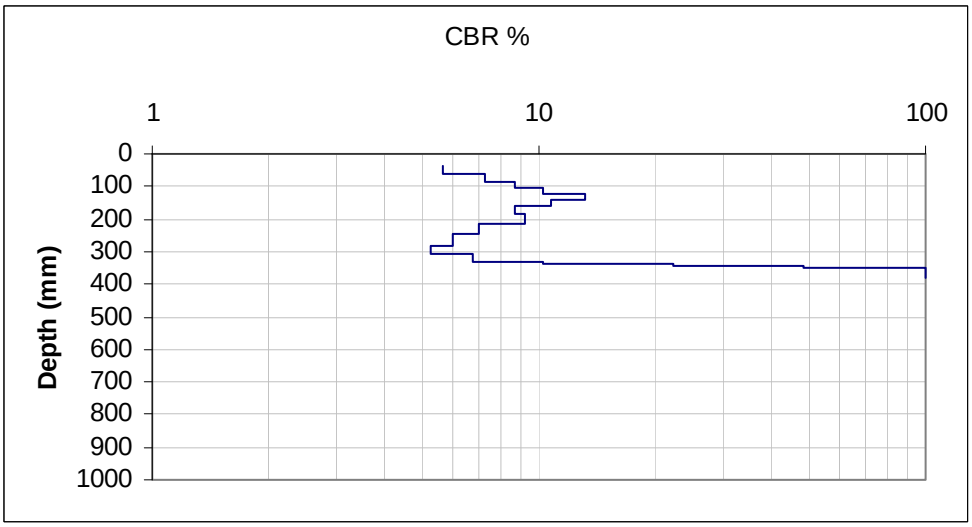
5+50 CL – auto



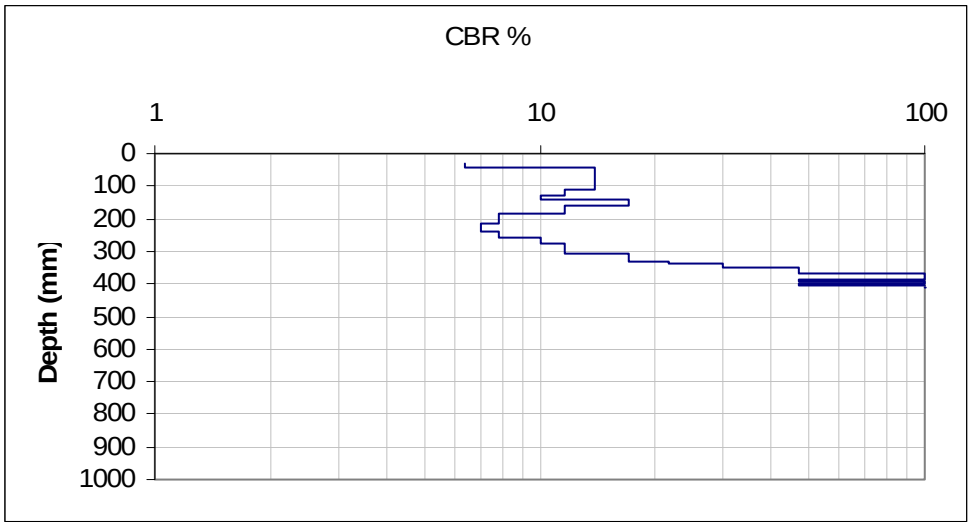
5+50 30S – manual



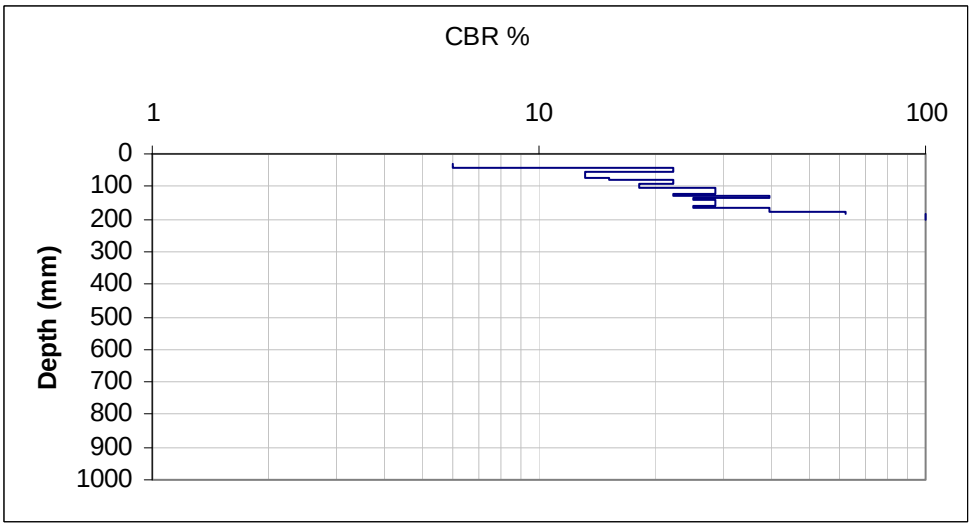
5+50 10S – manual



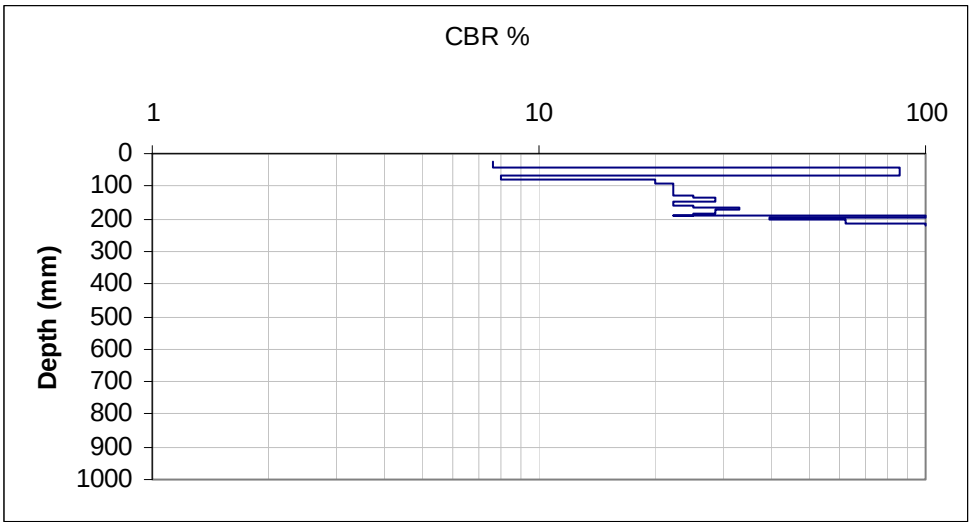
5+50 10N – manual



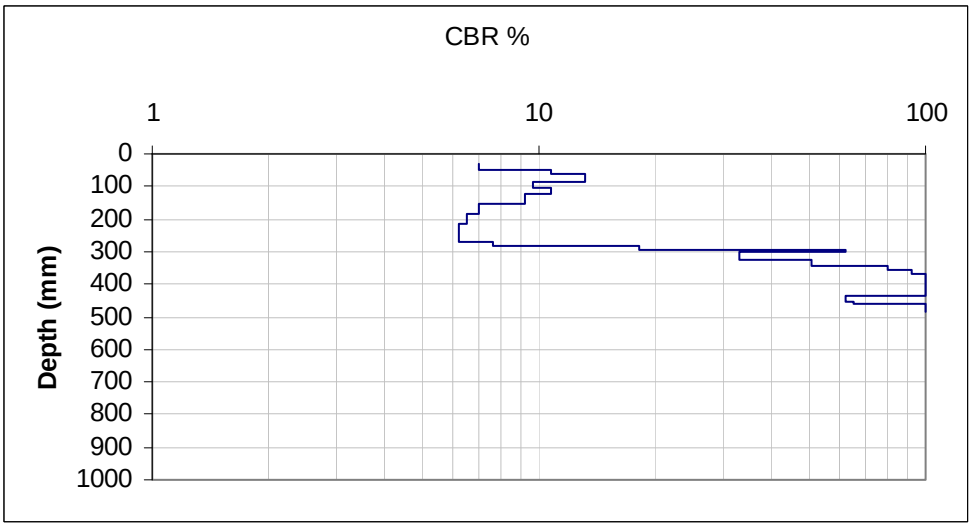
5+50 30N – auto



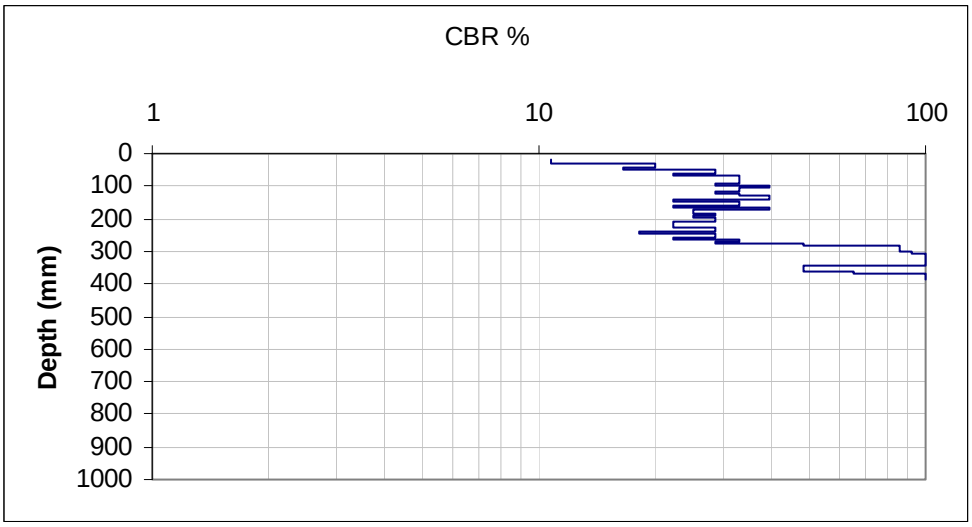
5+80 2S – manual



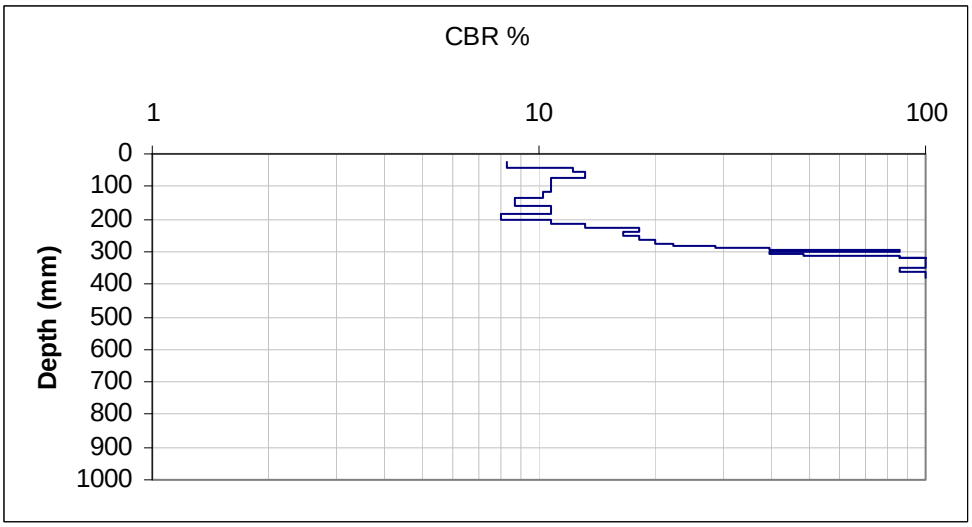
5+80 2N – manual



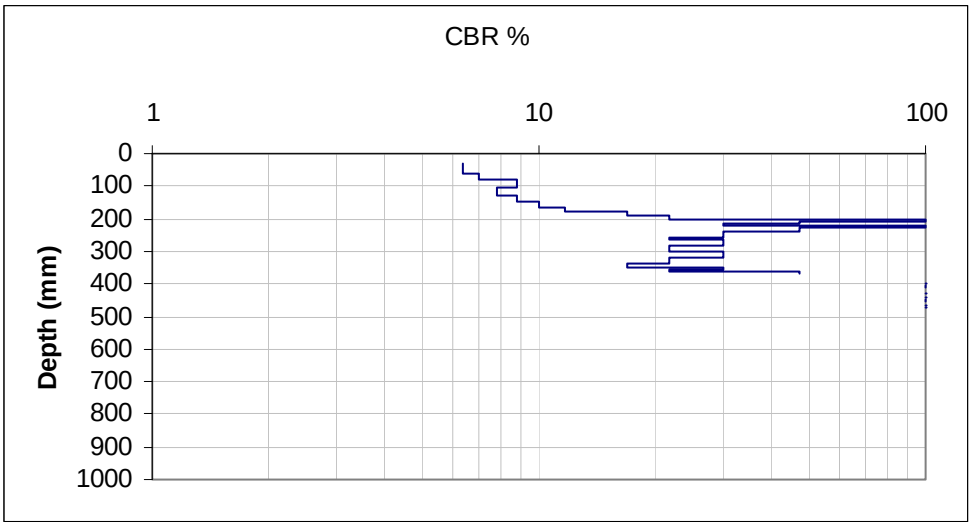
6+30 2S – manual



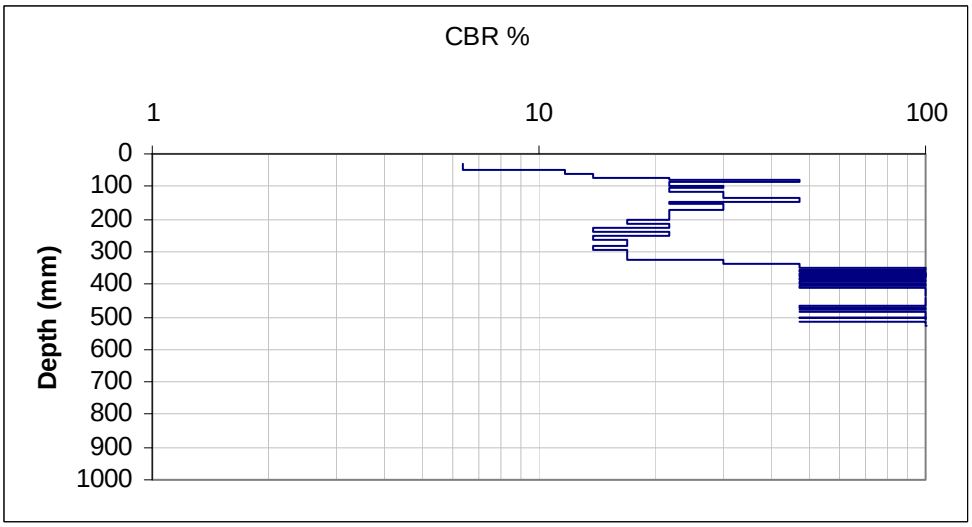
6+30 2N – manual



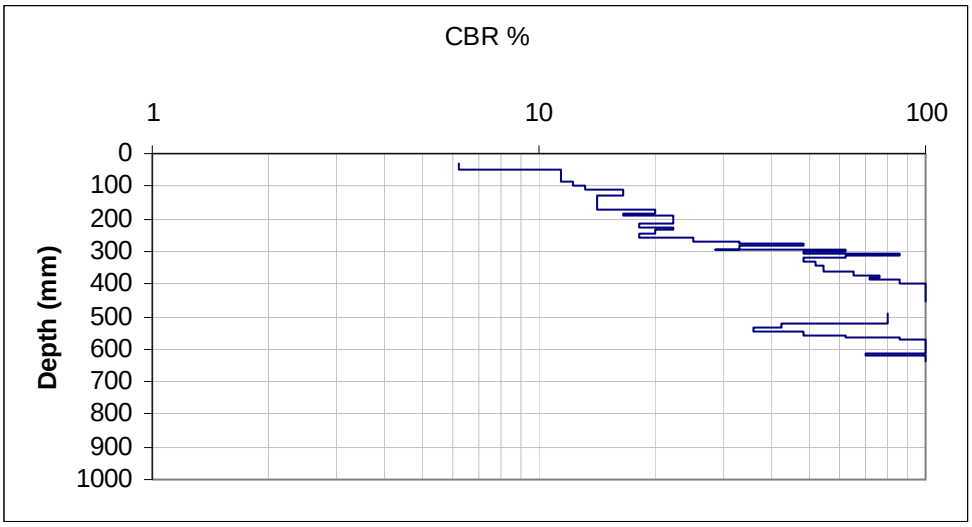
6+30 20S – manual



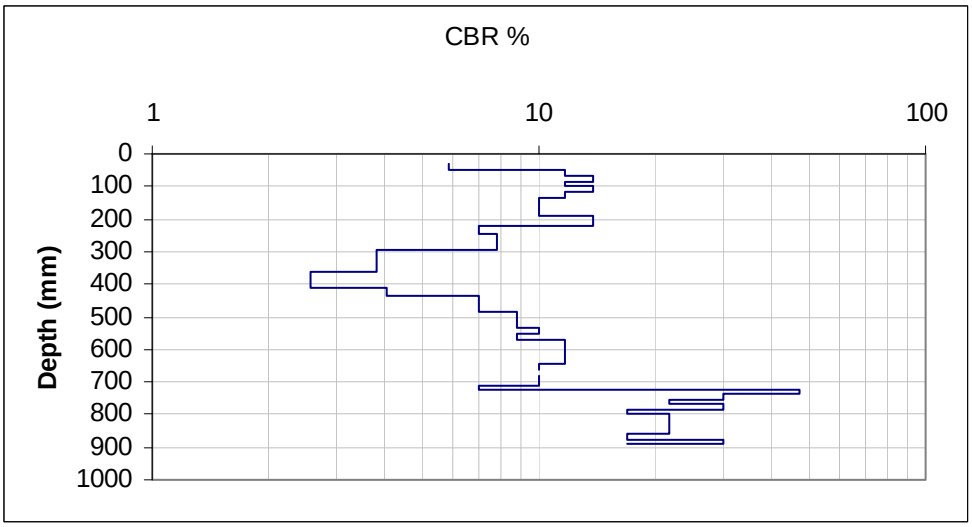
6+30 20N – auto



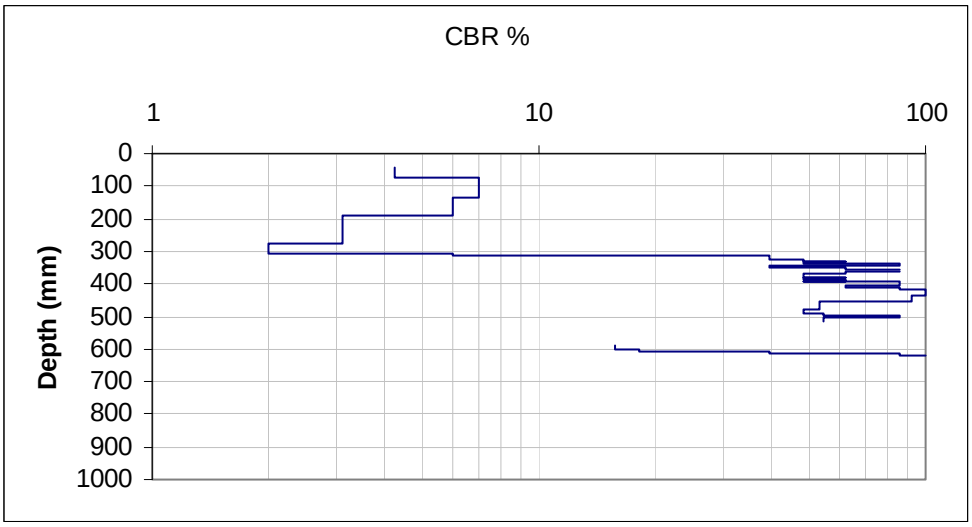
7+00 CL – auto



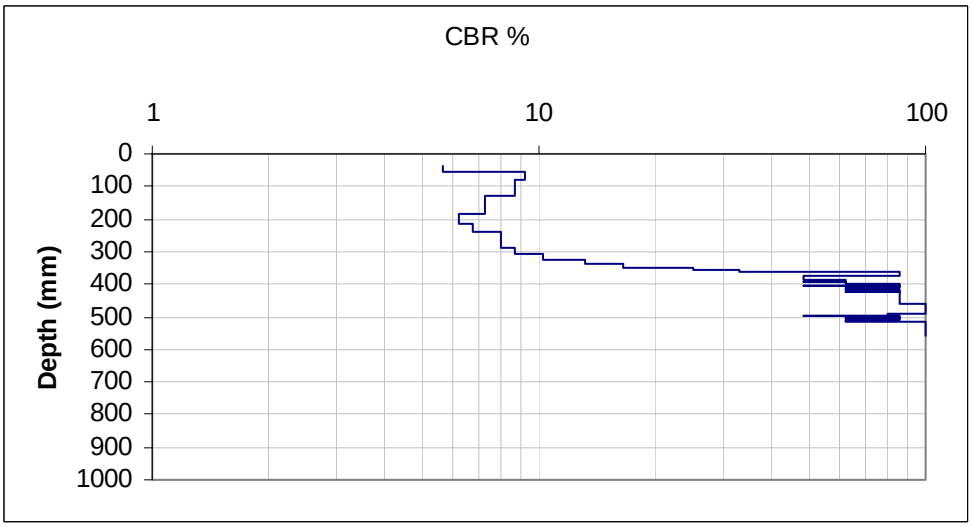
7+00 10S – manual



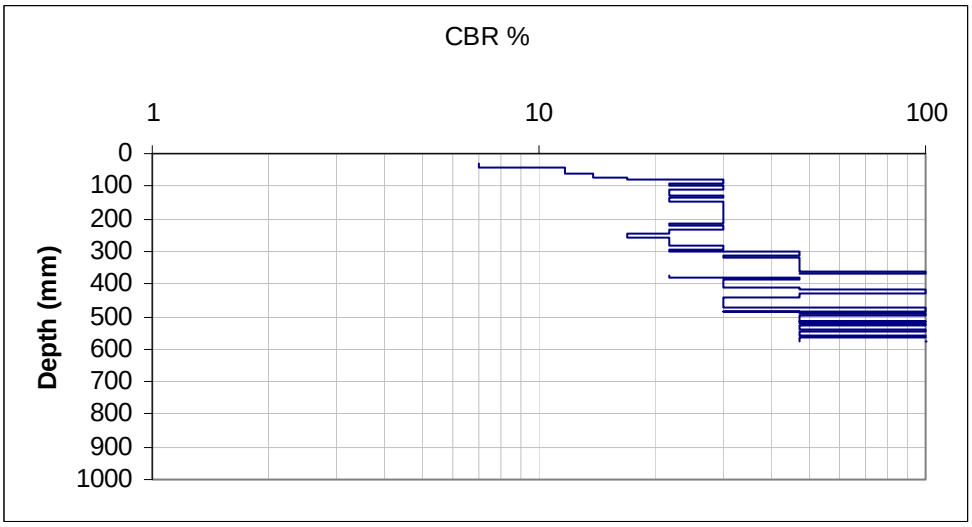
7+00 10N – auto



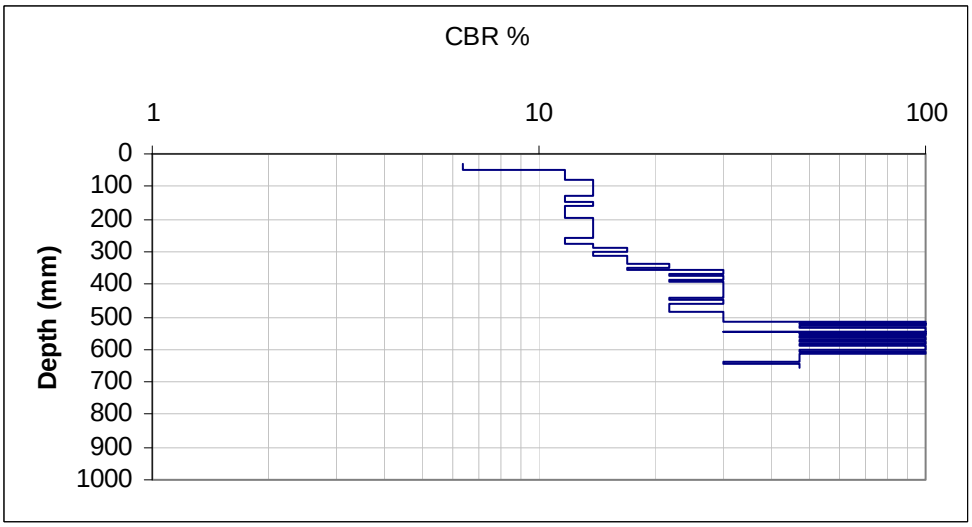
7+00 30N – manual



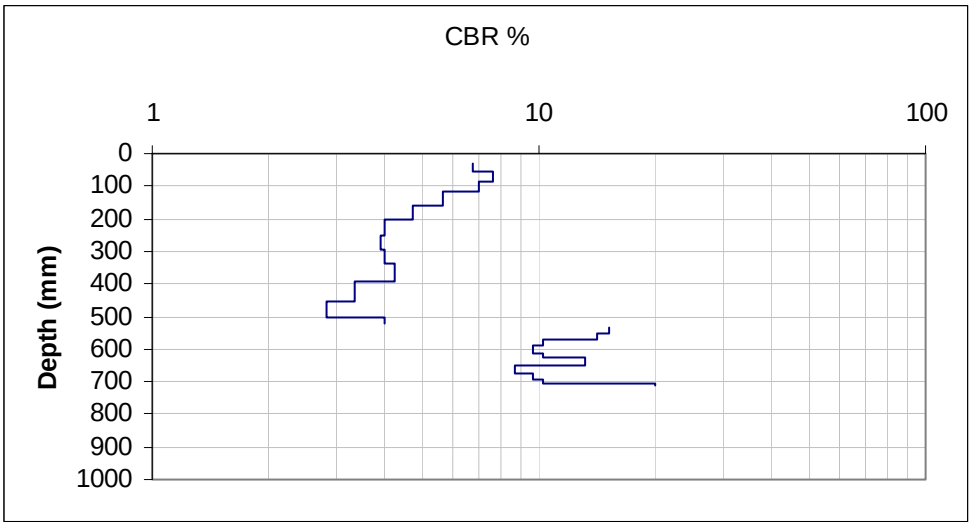
7+00 30S – manual



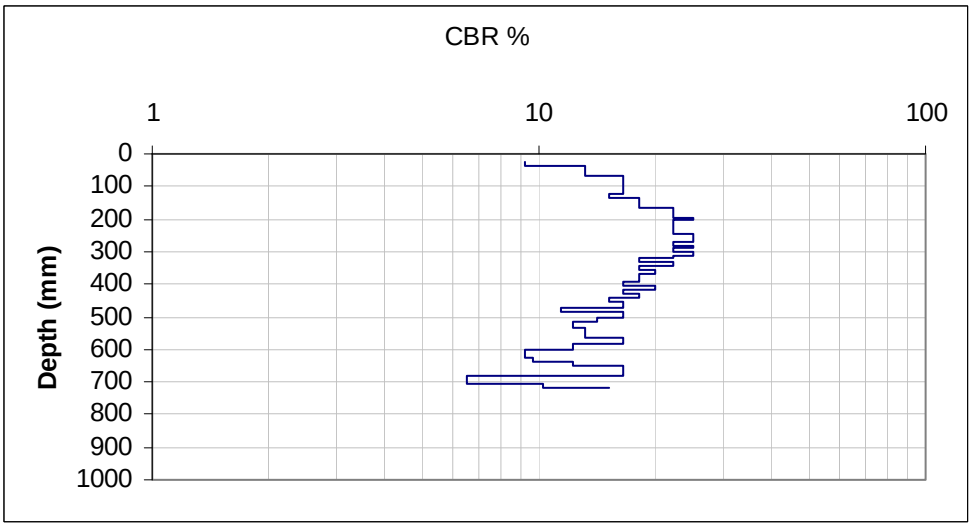
7+70 2S – auto



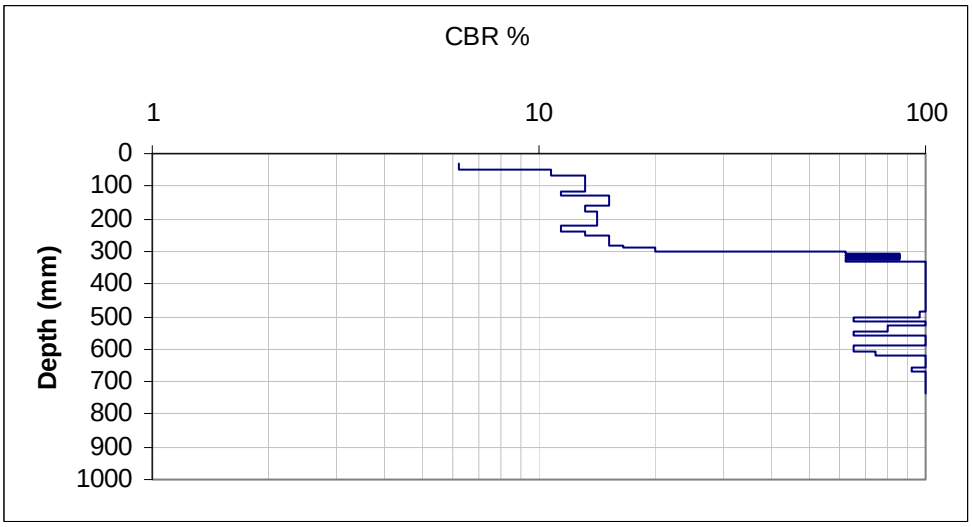
7+70 2N – auto



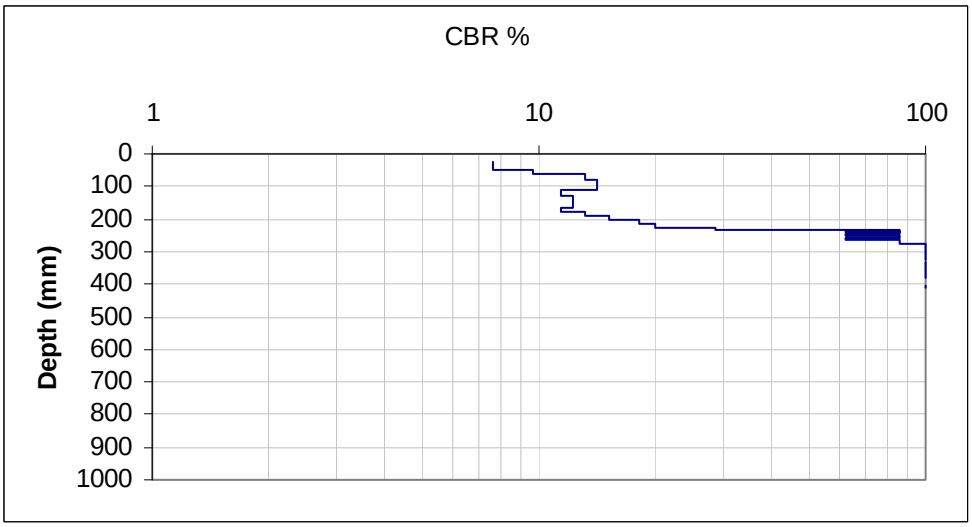
7+70 20S – manual



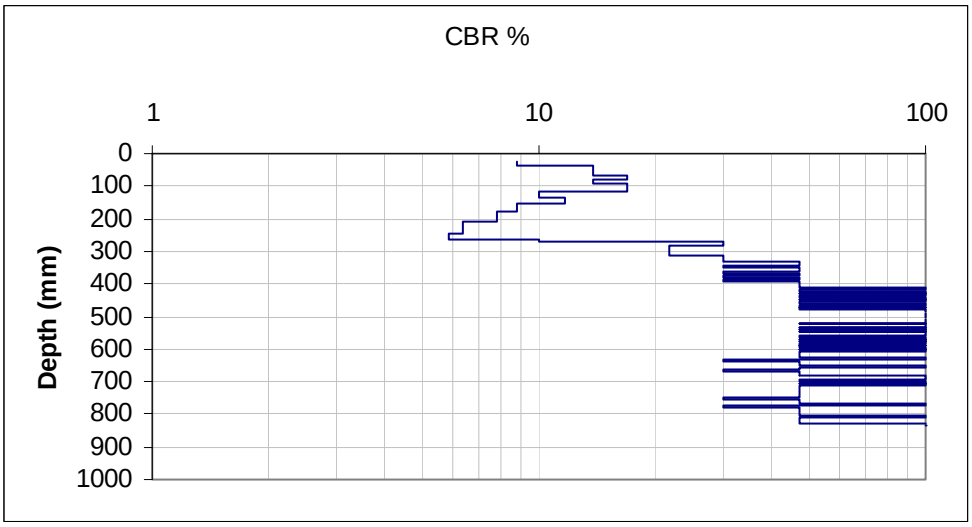
7+70 20N — manual



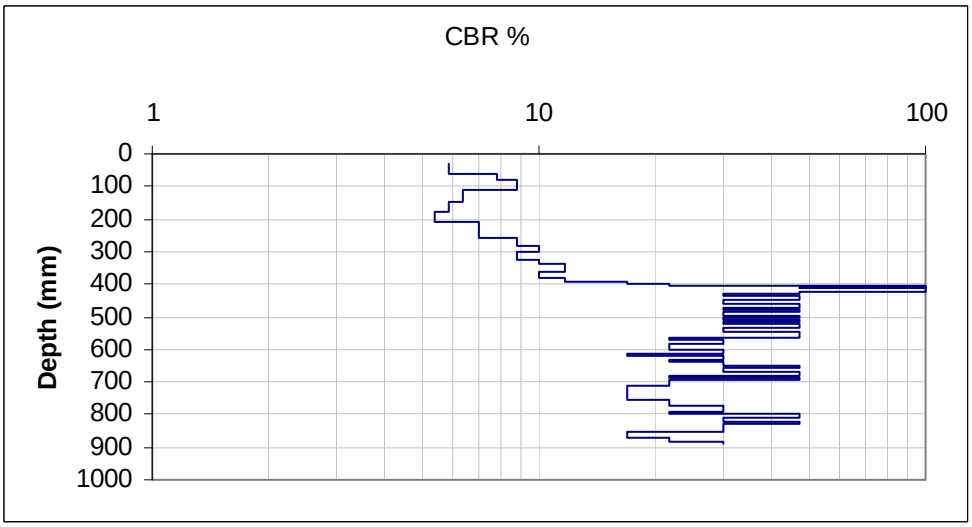
8+20 2S — manual



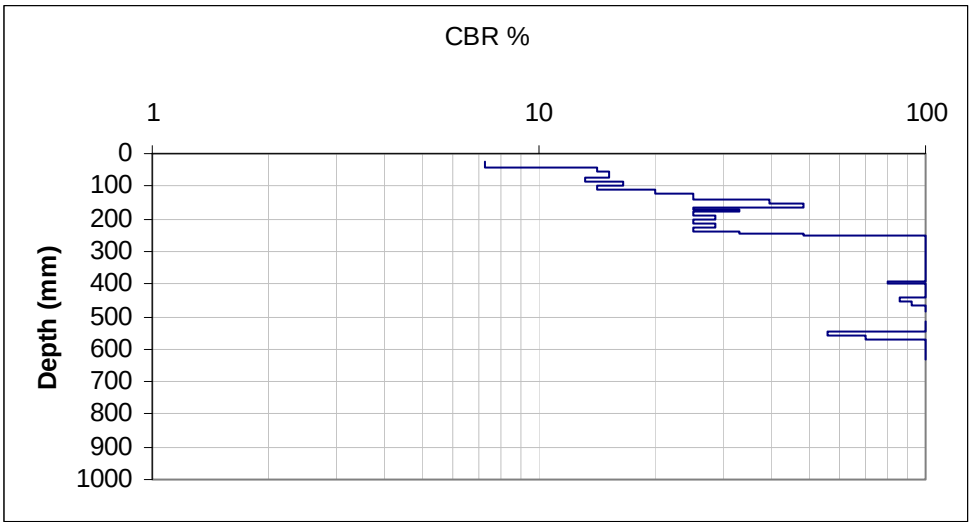
8+20 2N – manual



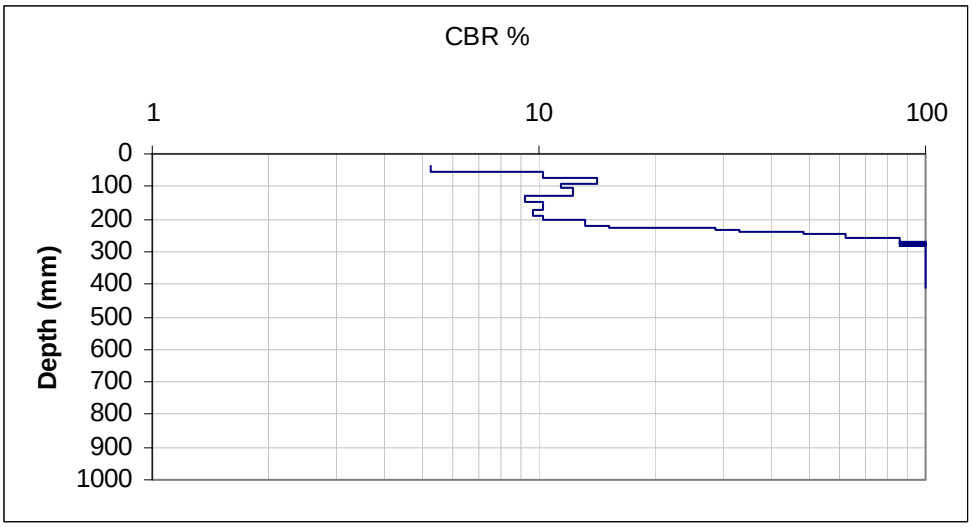
8+50 CL – auto



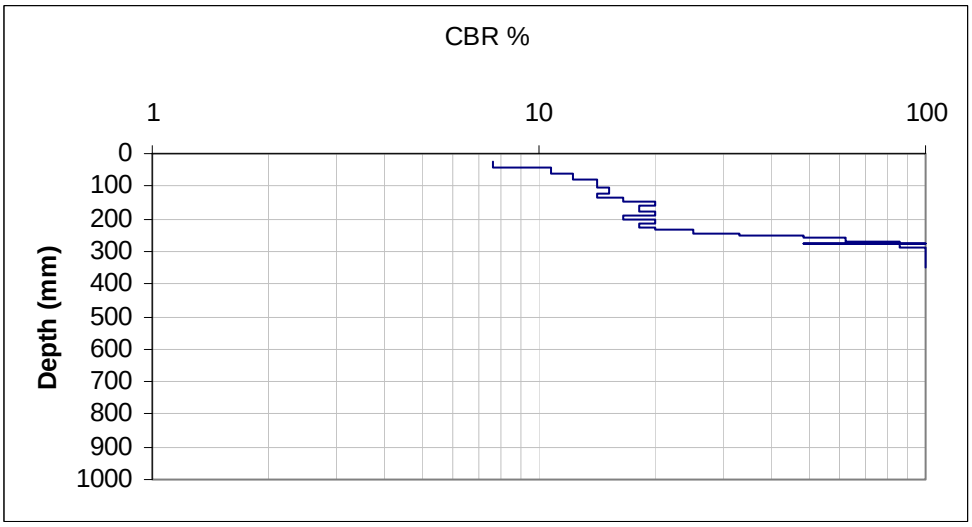
8+50 10S – auto



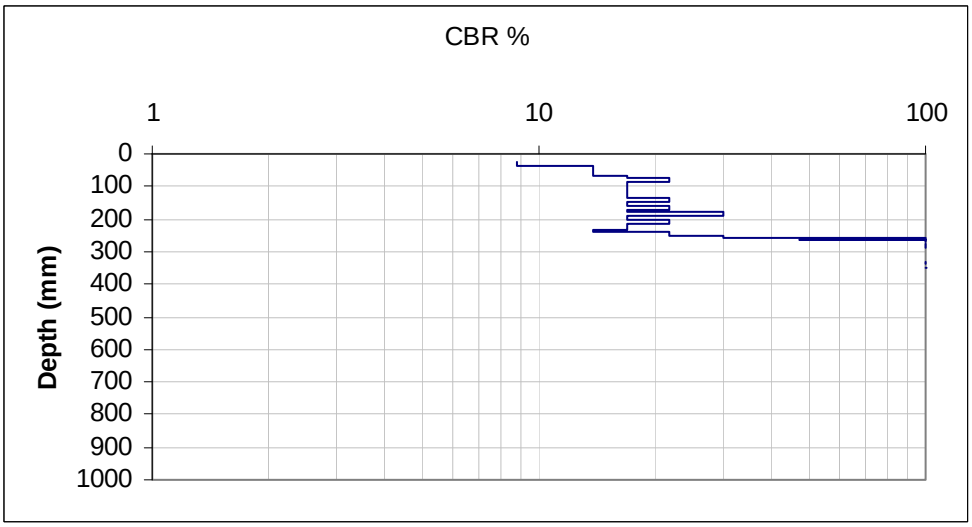
8+50 10N – manual



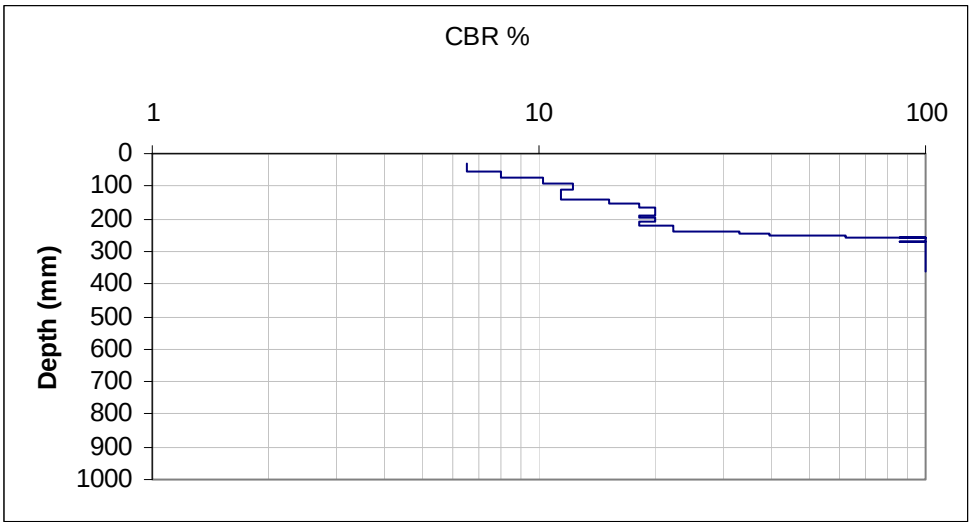
8+90 2S – manual



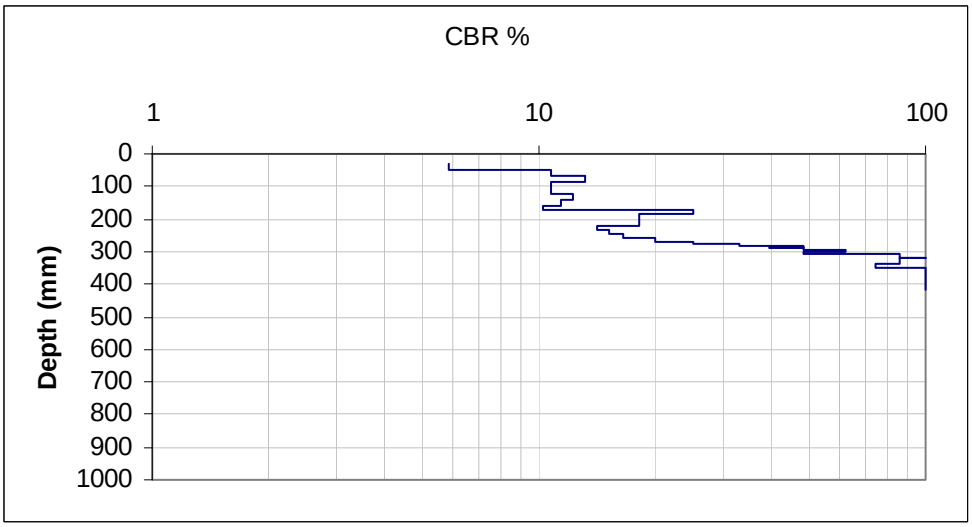
8+90 2N – manual



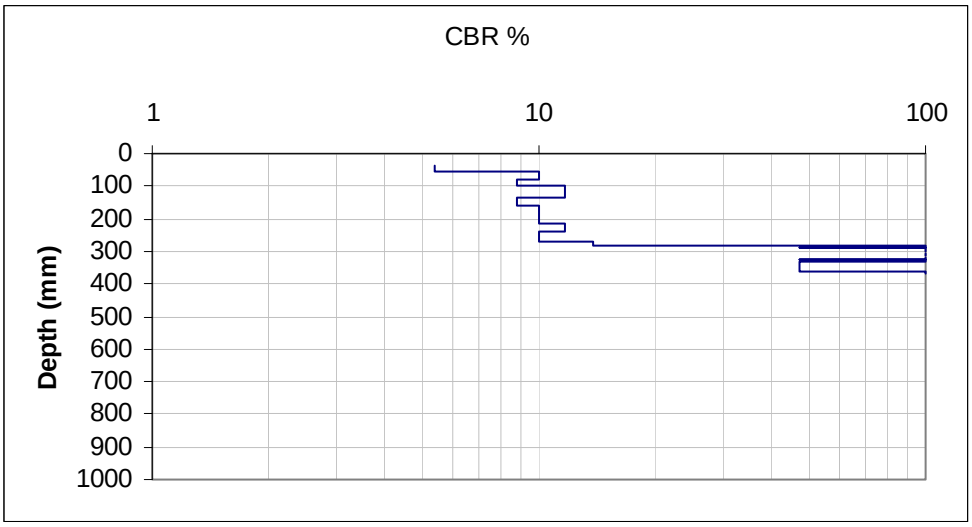
9+30 CL — auto



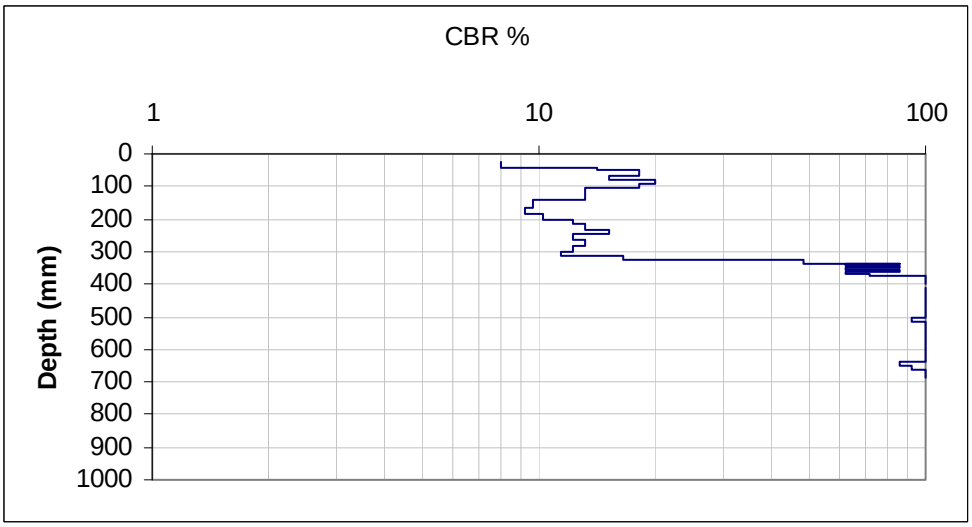
9+30 2N — manual



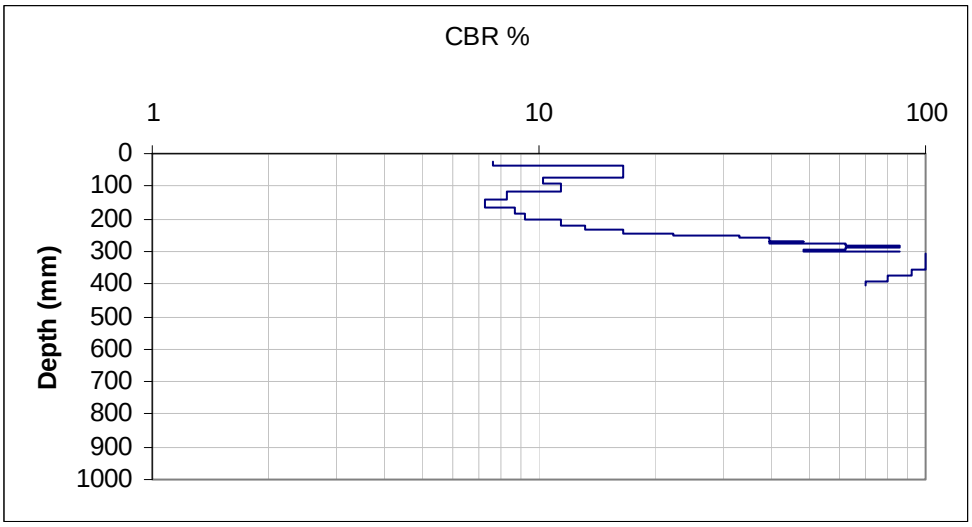
9+30 2S – manual



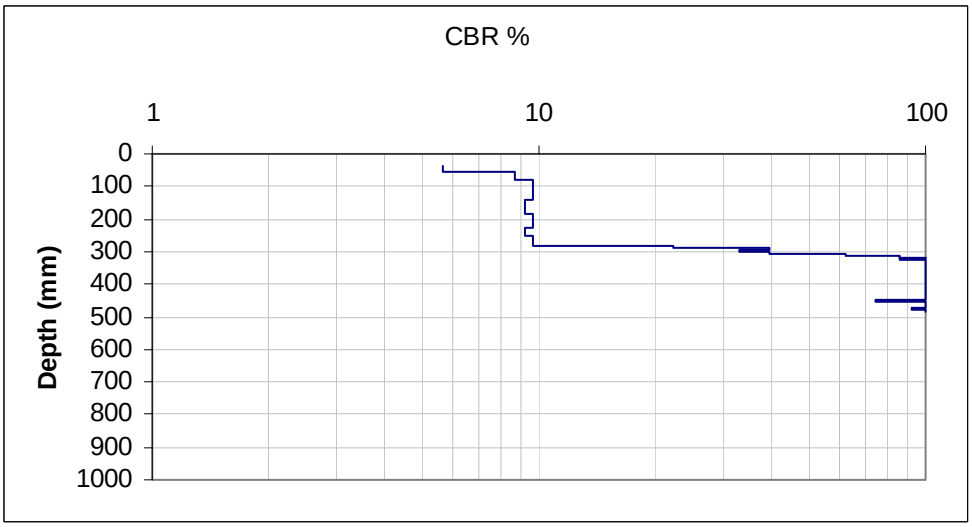
9+30 20S – auto



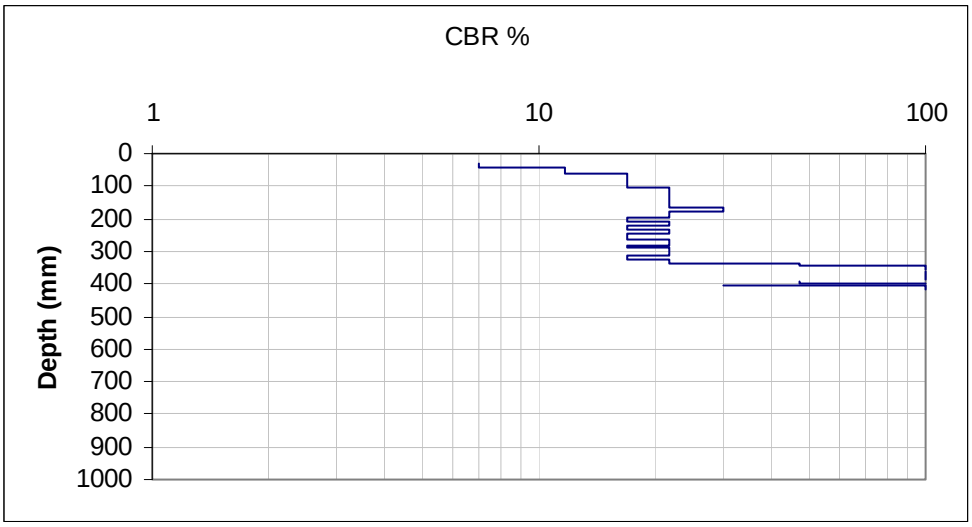
9+30 20N – manual



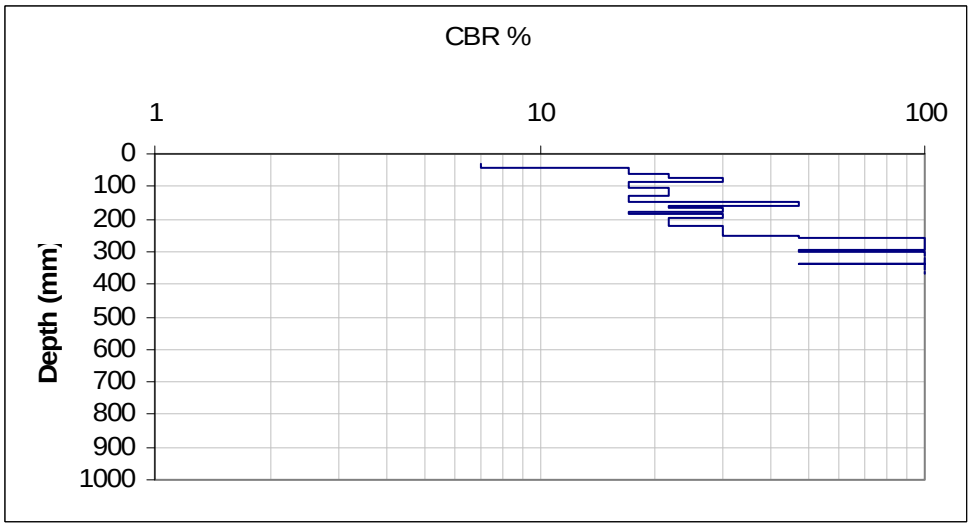
9+70 2S – manual



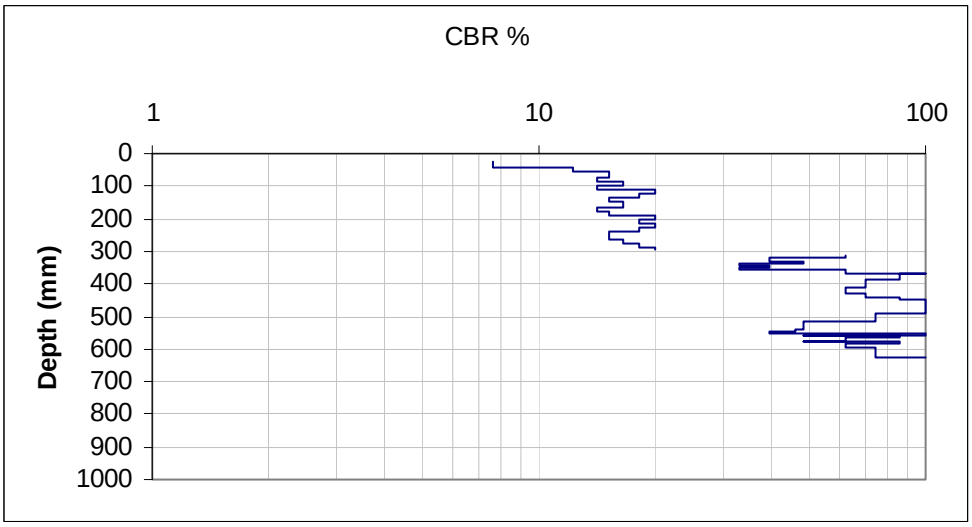
9+70 2N — manual



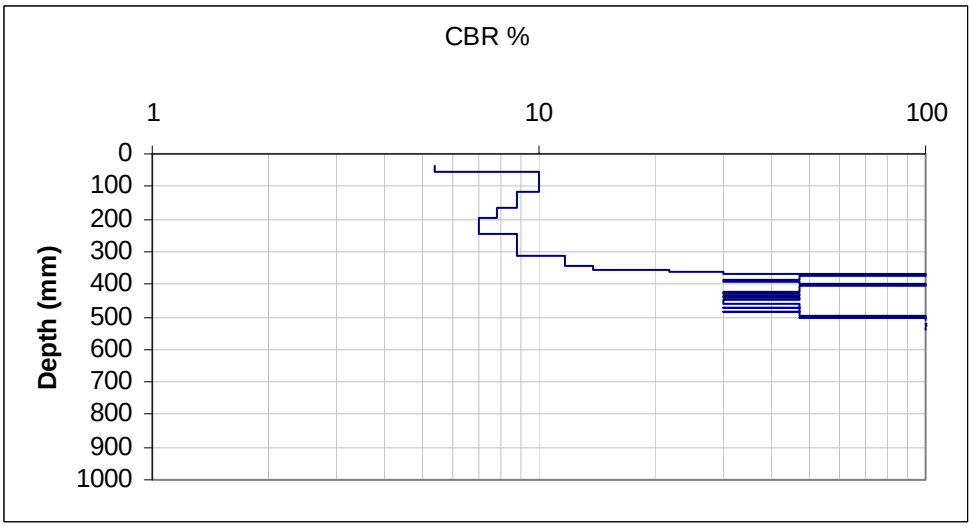
10+10 CL — auto



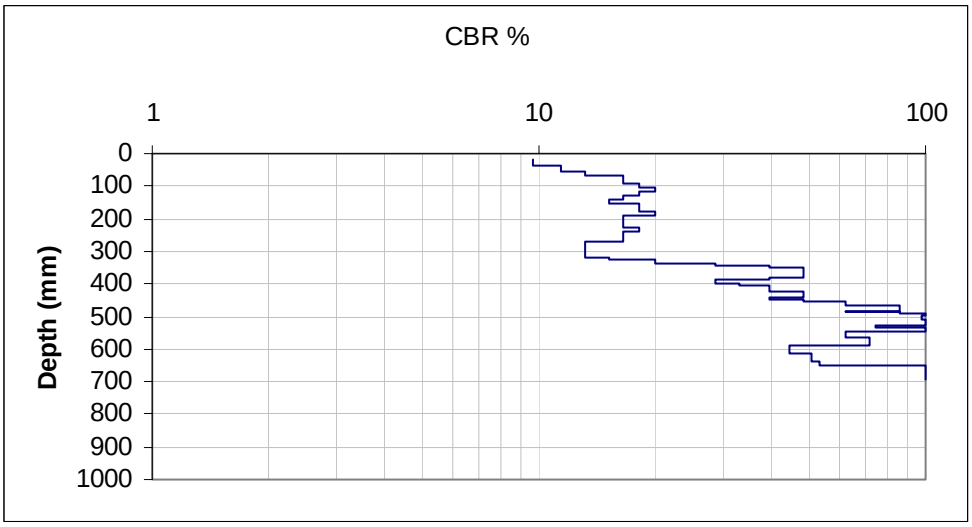
10+10 30S – auto



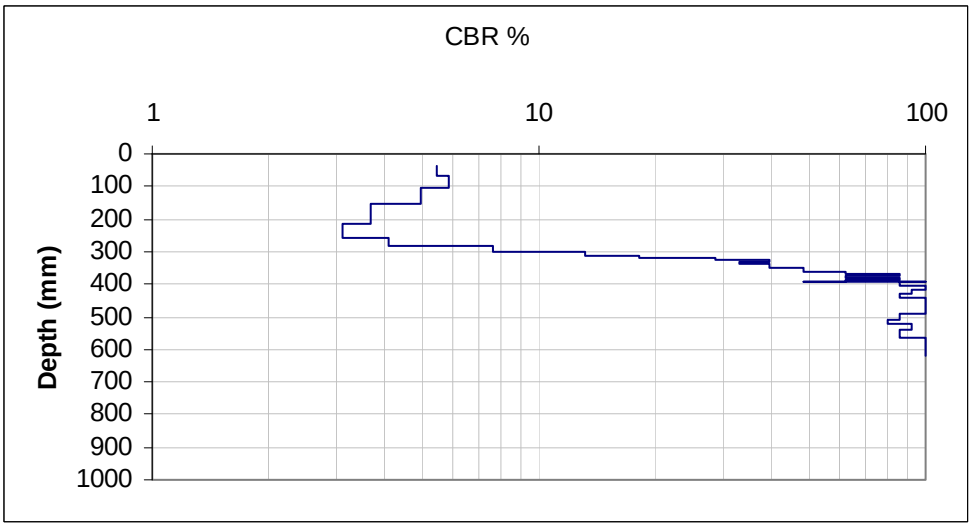
10+10 30N – manual



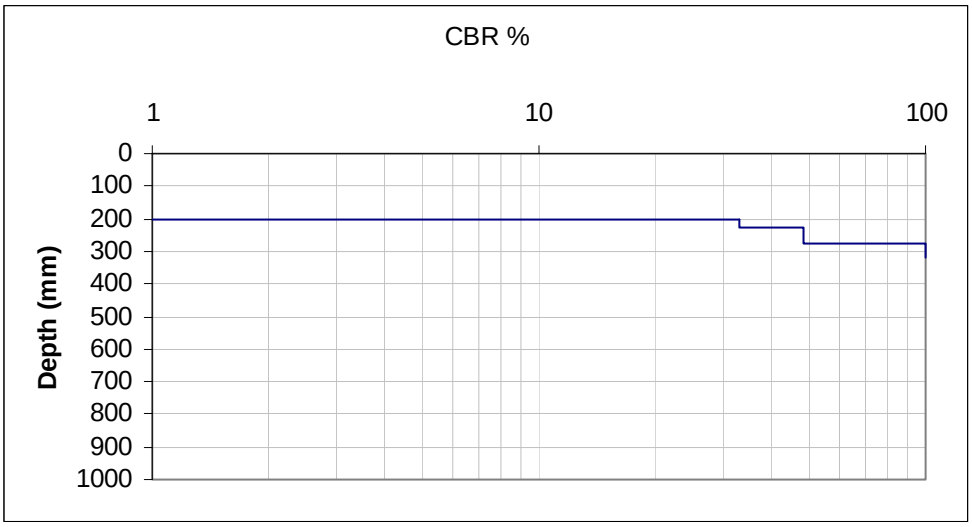
10+70 CL – auto



10+70 10N – manual

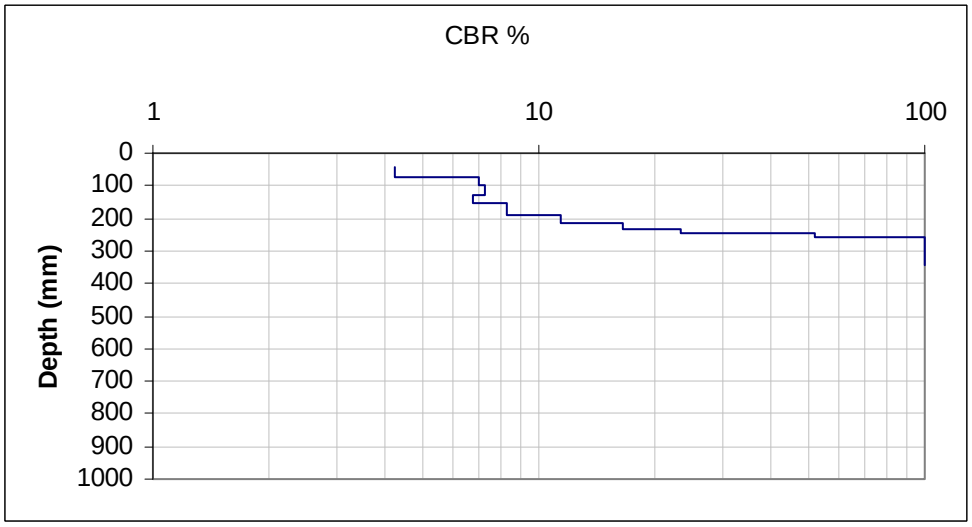


10+70 10S — manual

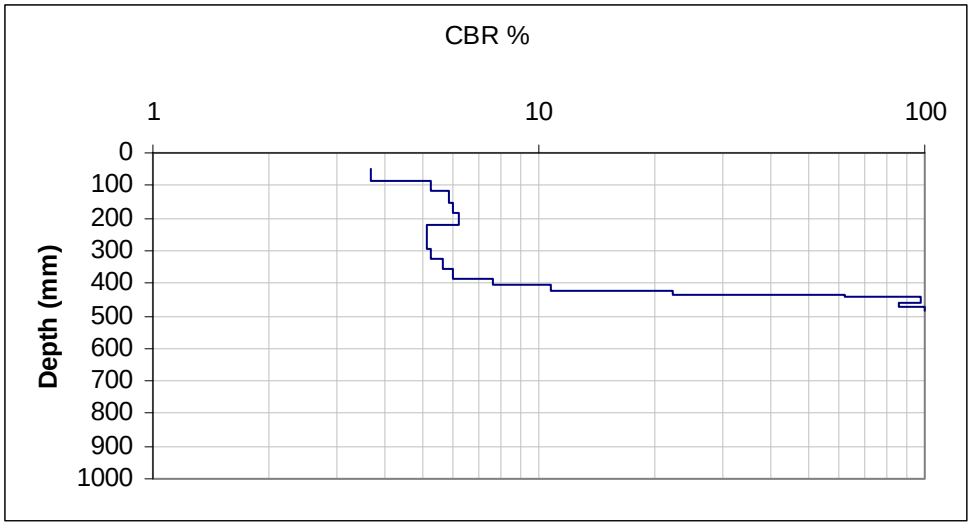


Weather Station — manual

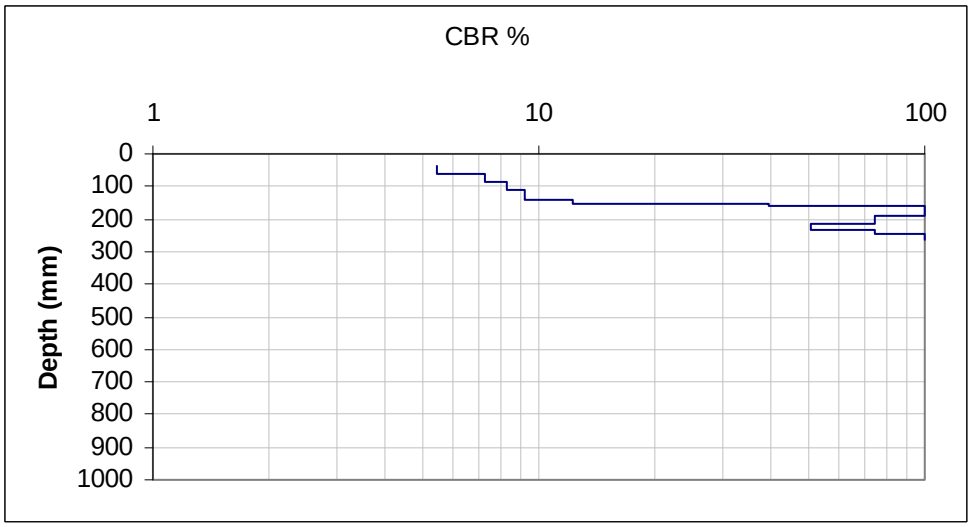
D2. IOP #2, October 24–28, 2005, all manual readings



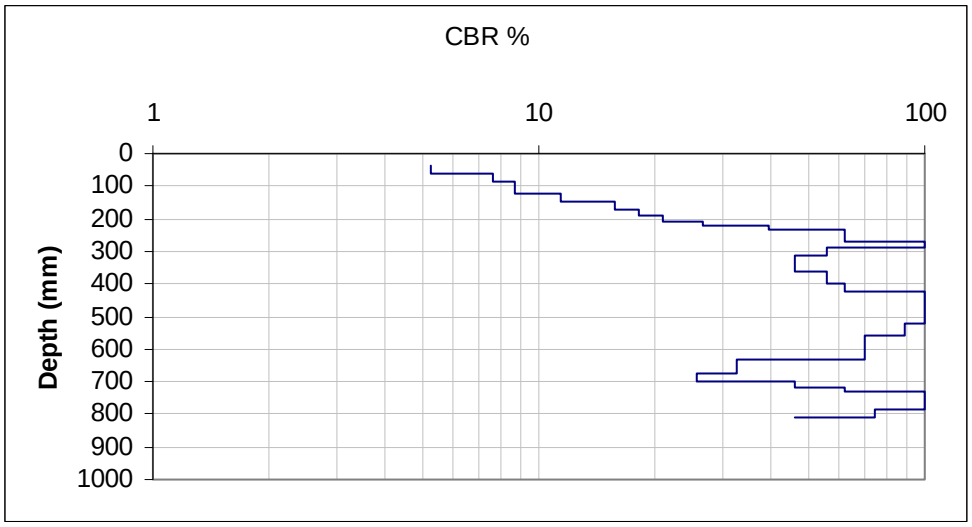
0+40 CL



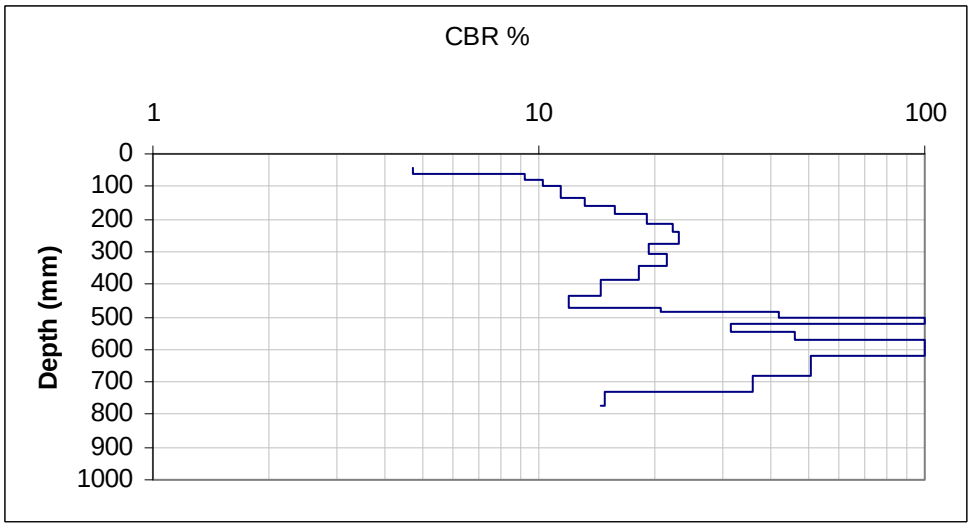
0+40 20N



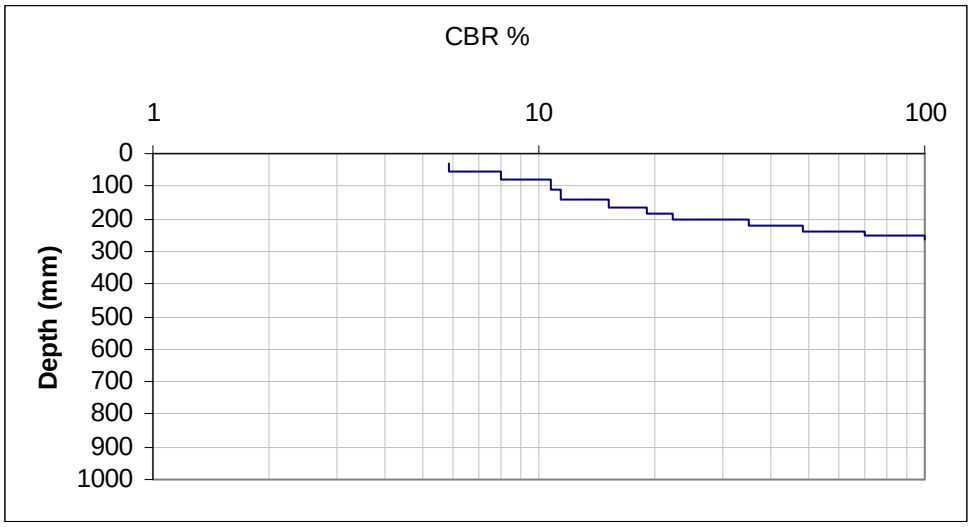
0+40 20S



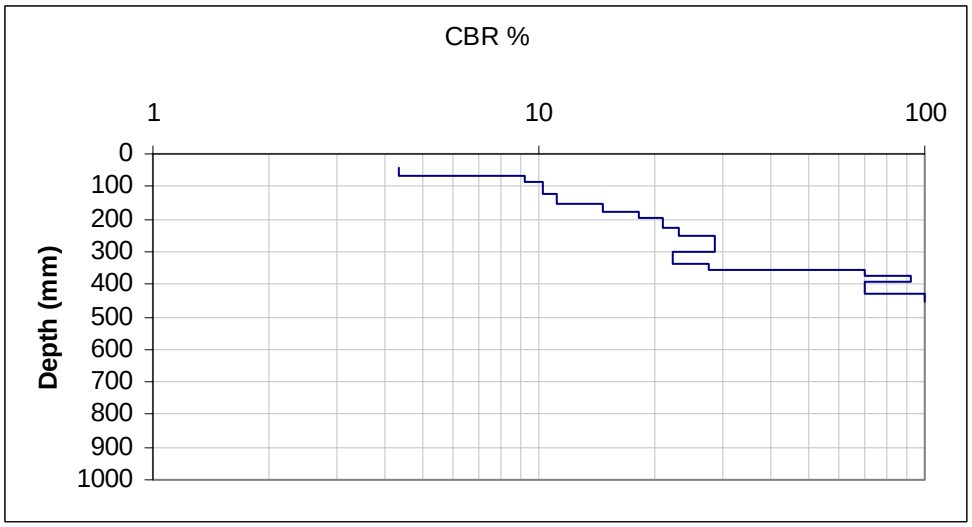
0+90 CL



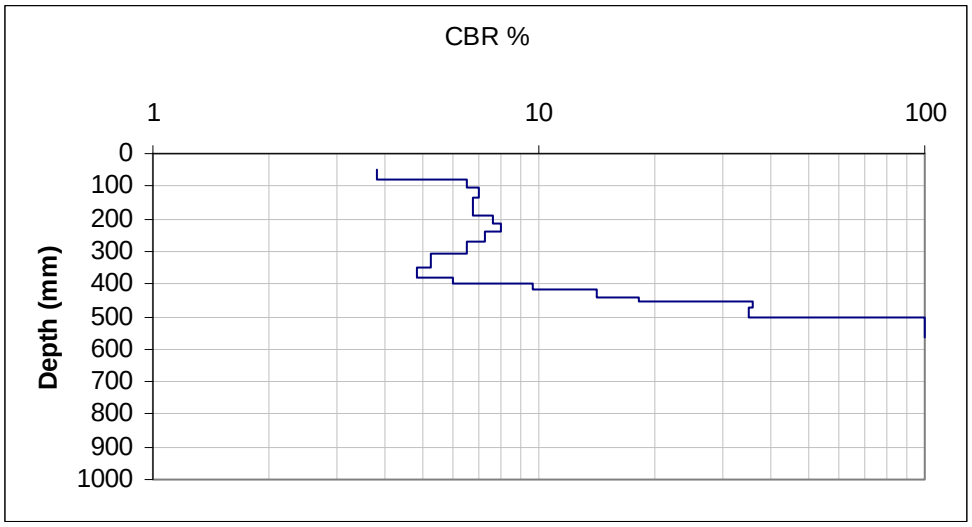
0+90 10N



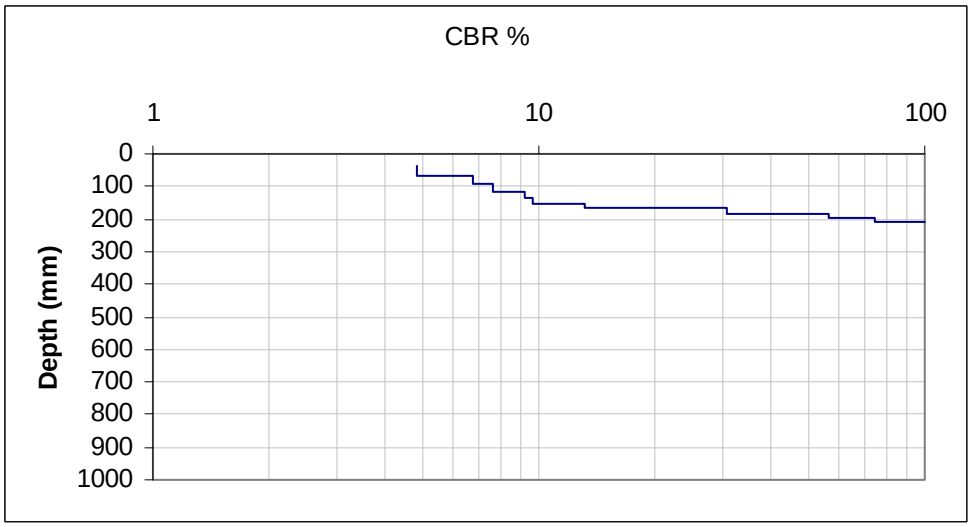
0+90 10S



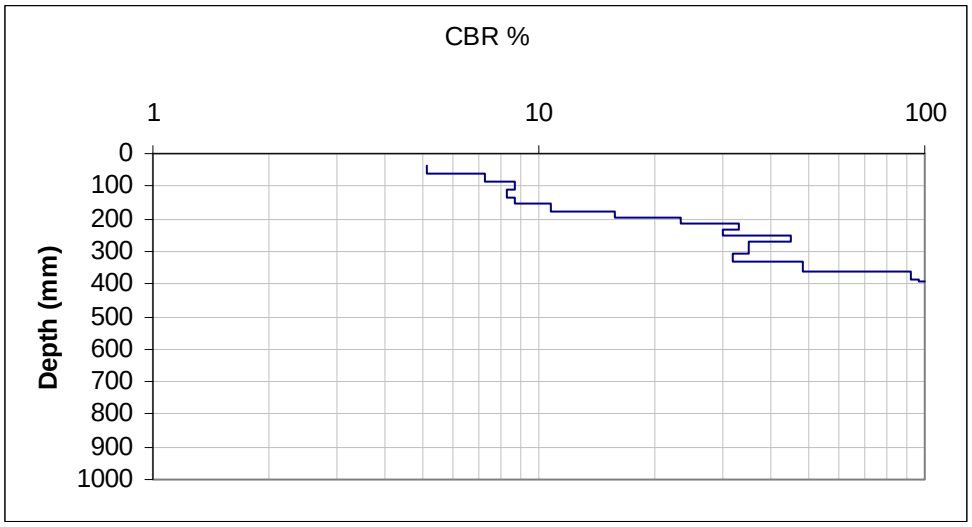
0+90 30N



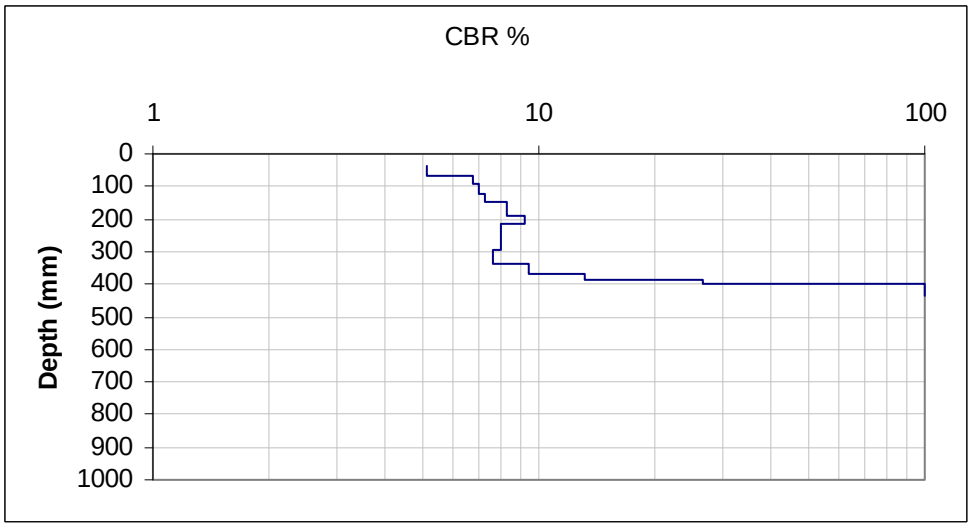
0+90 30S


CBR %
1
10
100
Depth (mm)
0
100
200
300
400
500
600
700
800
900
1000

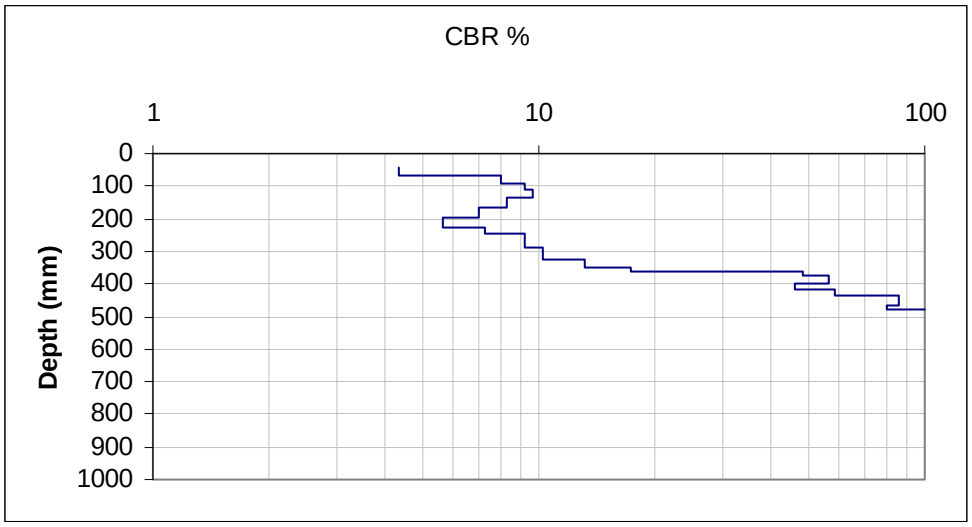
1+30 2N


CBR %
1
10
100
Depth (mm)
0
100
200
300
400
500
600
700
800
900
1000

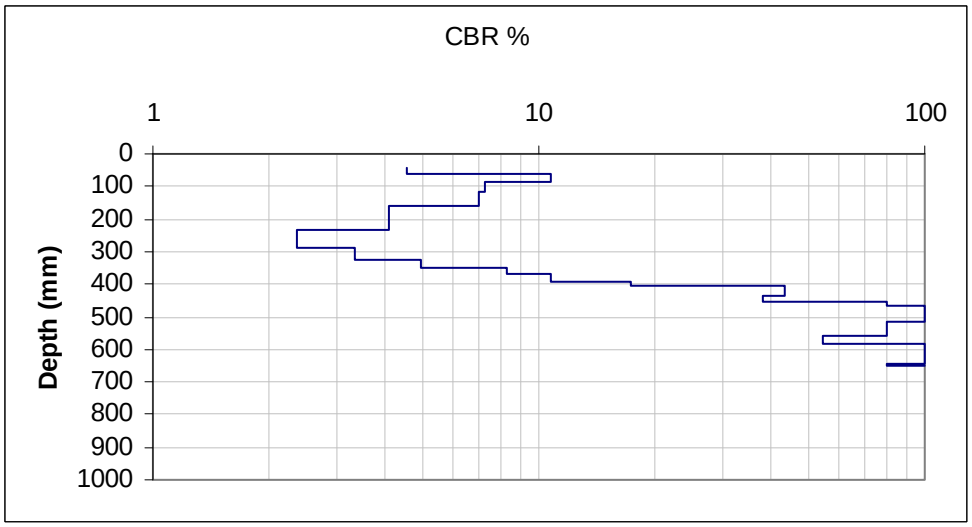
1+30 2S


CBR %
1
10
100
Depth (mm)
0
100
200
300
400
500
600
700
800
900
1000

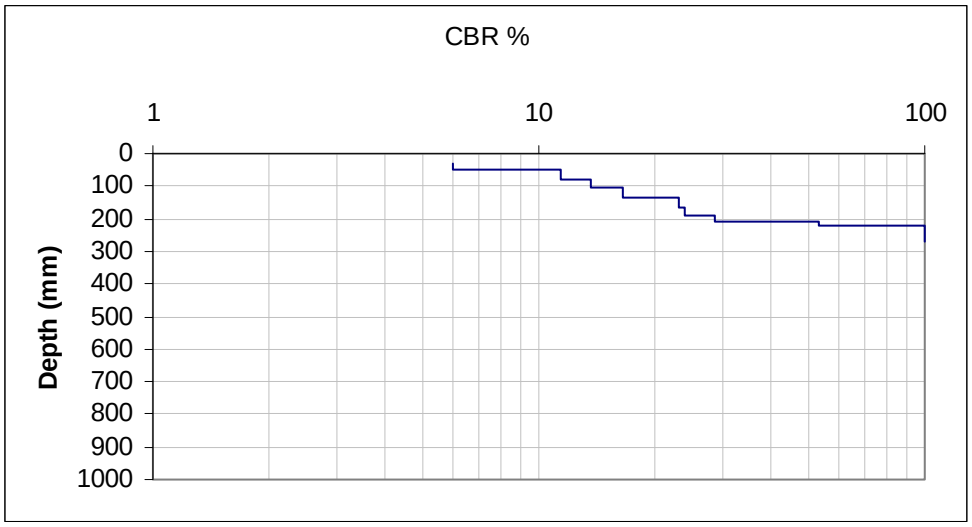
1+70 CL


CBR %
1
10
100
Depth (mm)
0
100
200
300
400
500
600
700
800
900
1000

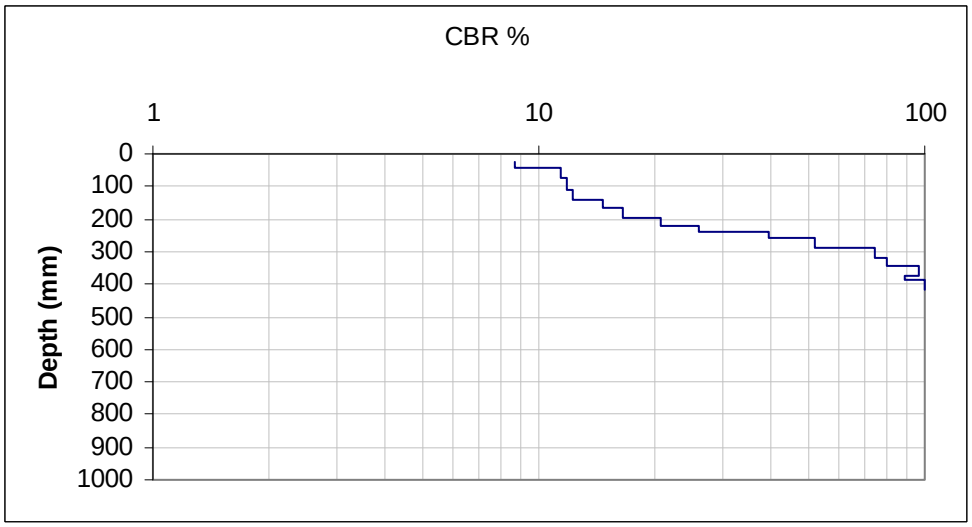
1+70 2N



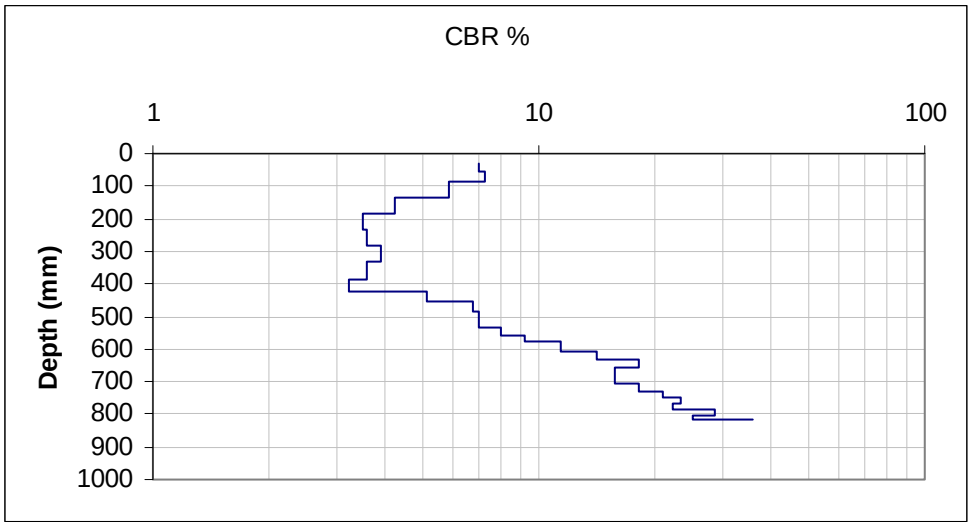
1+70 2S



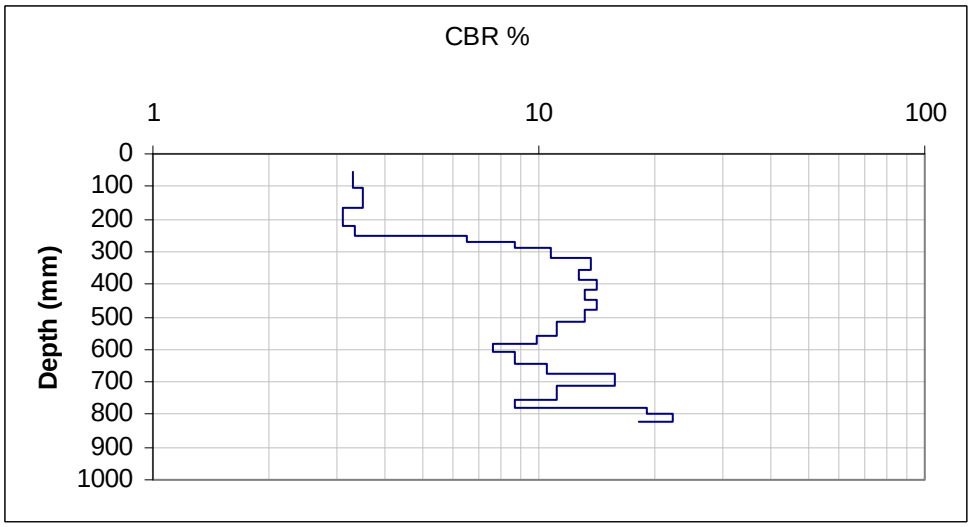
1+70 20N



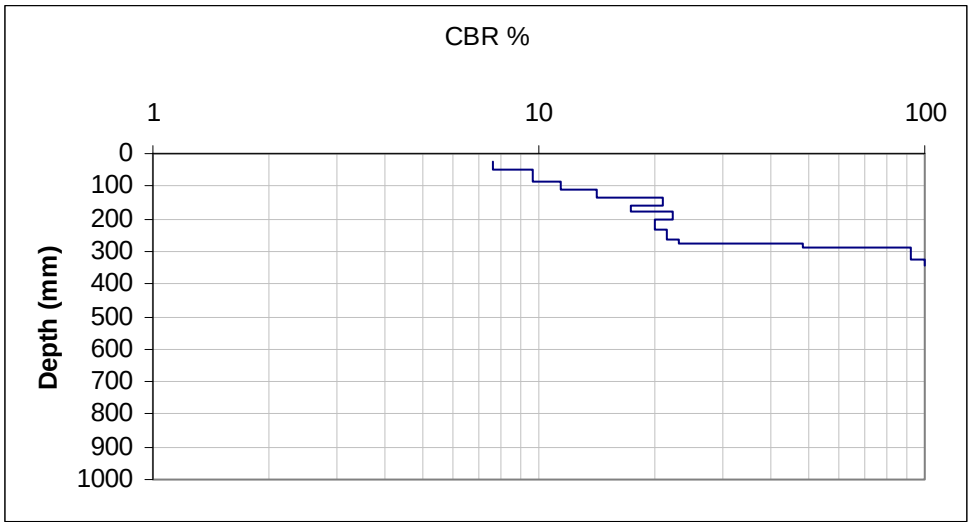
1+70 20S



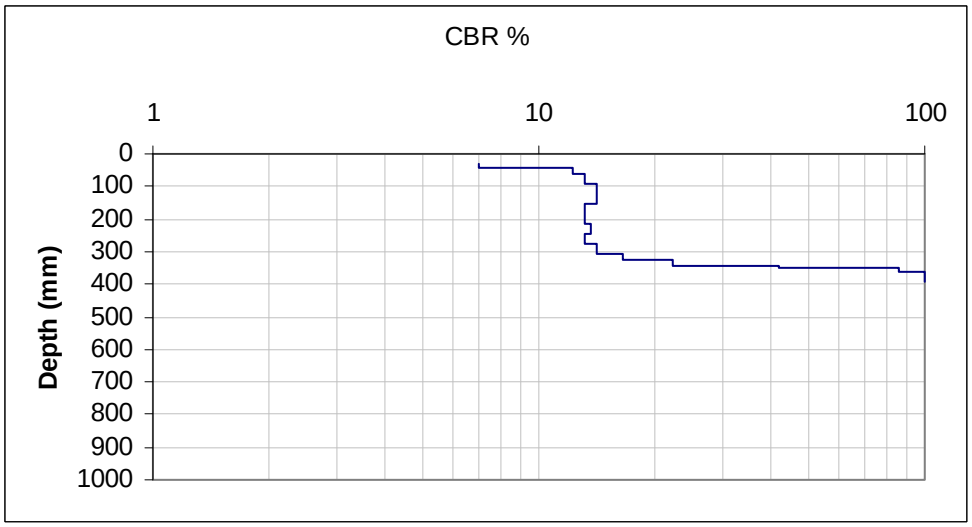
2+10 2N


CBR %
1
10
100
0
100
200
300
400
500
600
700
800
900
1000
Depth (mm)

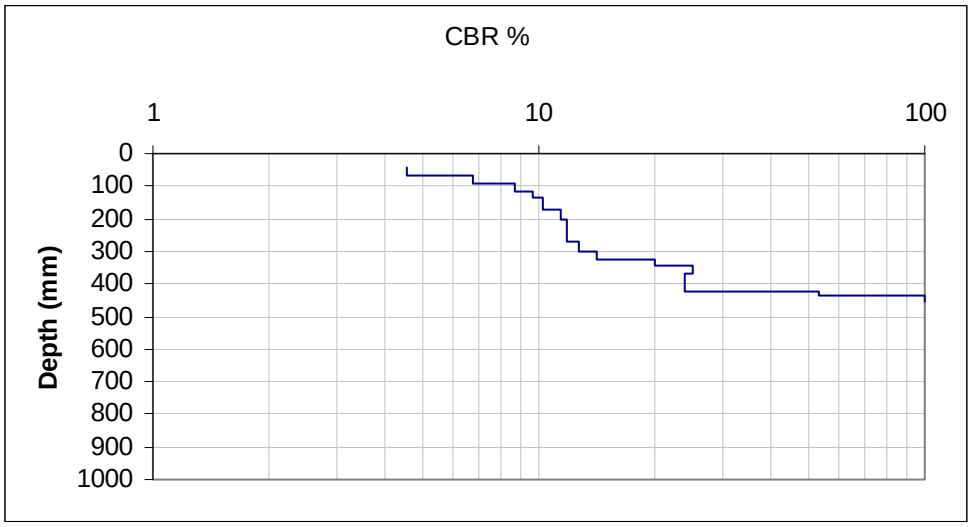
2+10 2S


CBR %
1
10
100
0
100
200
300
400
500
600
700
800
900
1000
Depth (mm)

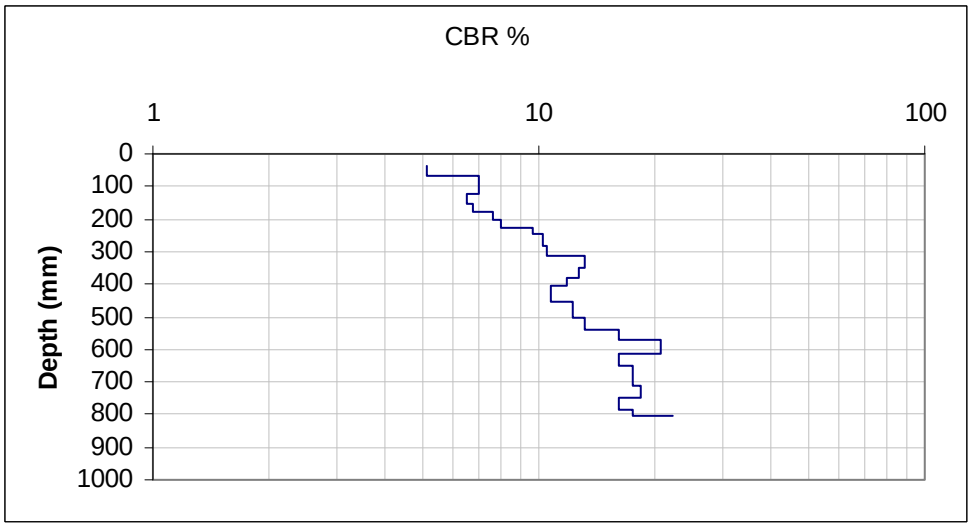
2+50 CL



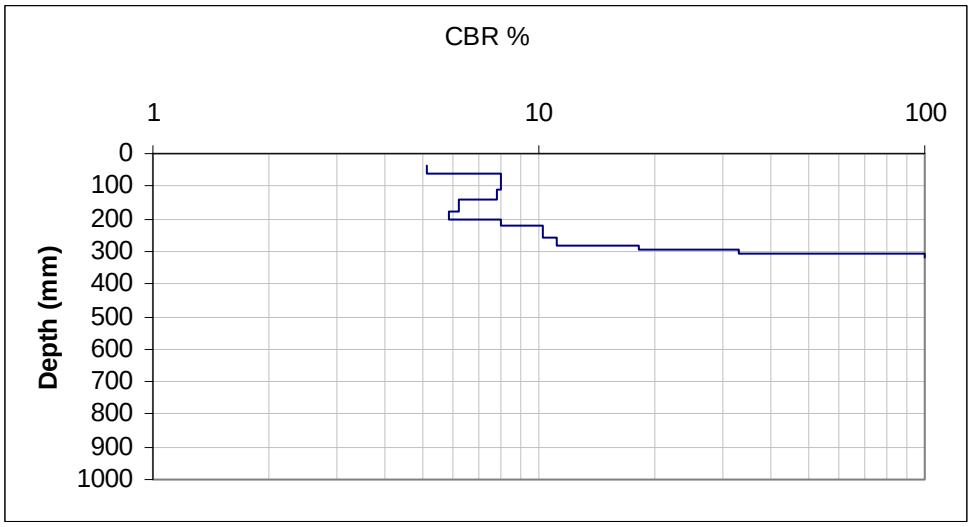
2+50 10N



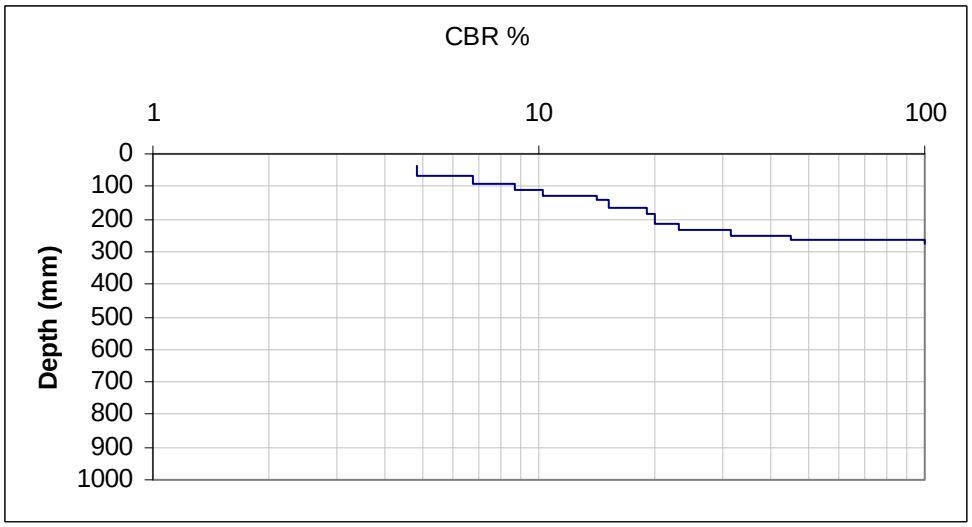
2+50 10S


CBR %
1
10
100
0
100
200
300
400
500
600
700
800
900
1000
Depth (mm)

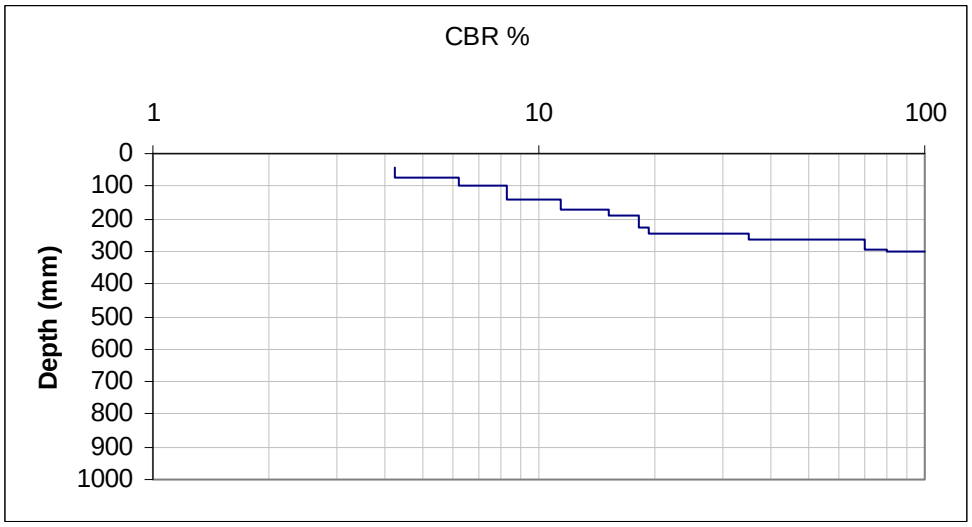
2+80 2N


CBR %
1
10
100
0
100
200
300
400
500
600
700
800
900
1000
Depth (mm)

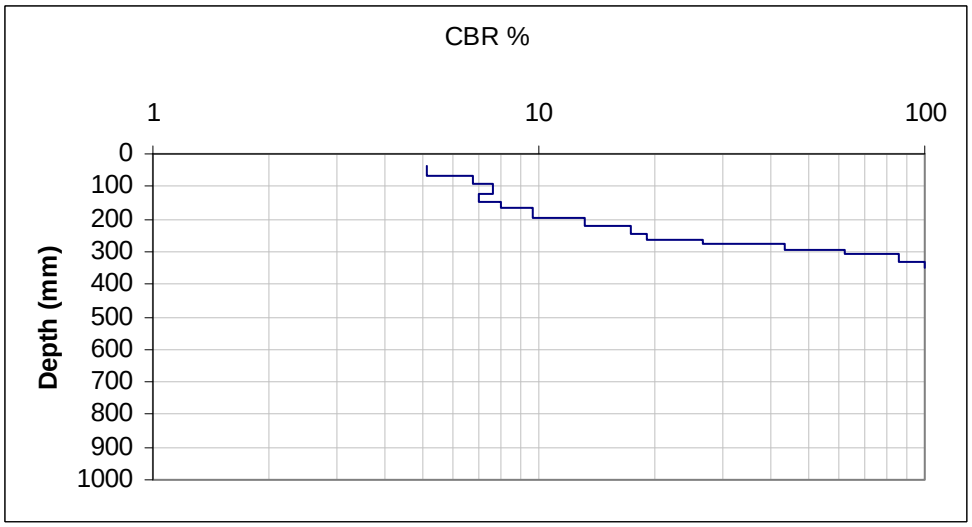
2+80 2S


CBR %
1
10
100
Depth (mm)
0
100
200
300
400
500
600
700
800
900
1000

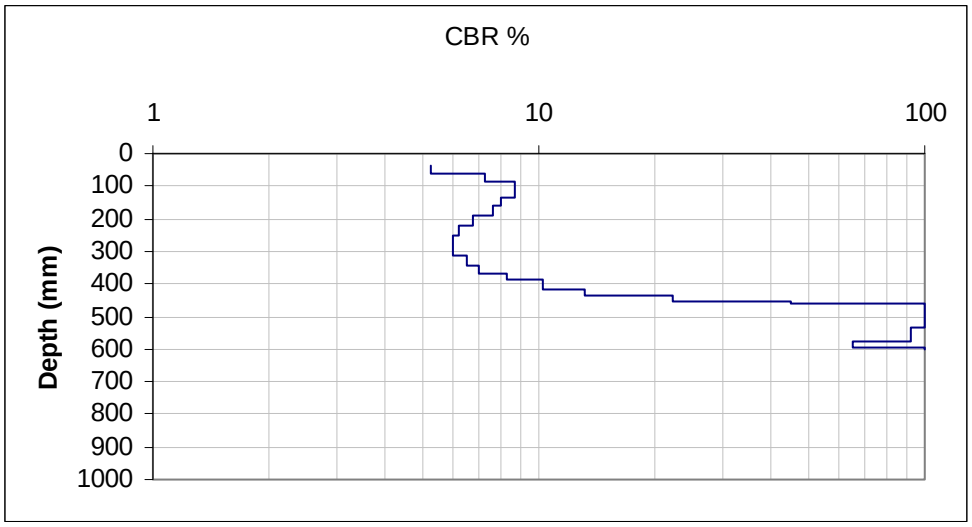
3+30 2N


CBR %
1
10
100
Depth (mm)
0
100
200
300
400
500
600
700
800
900
1000

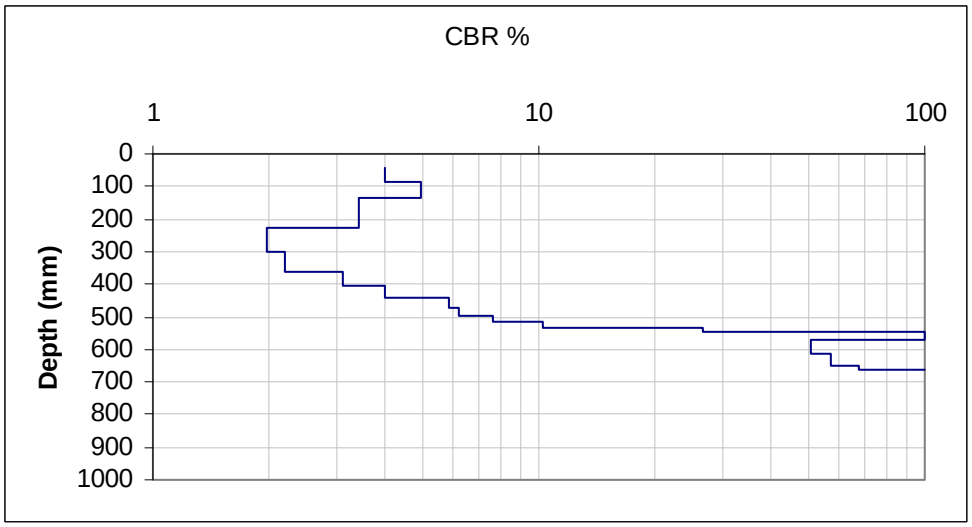
3+30 2S



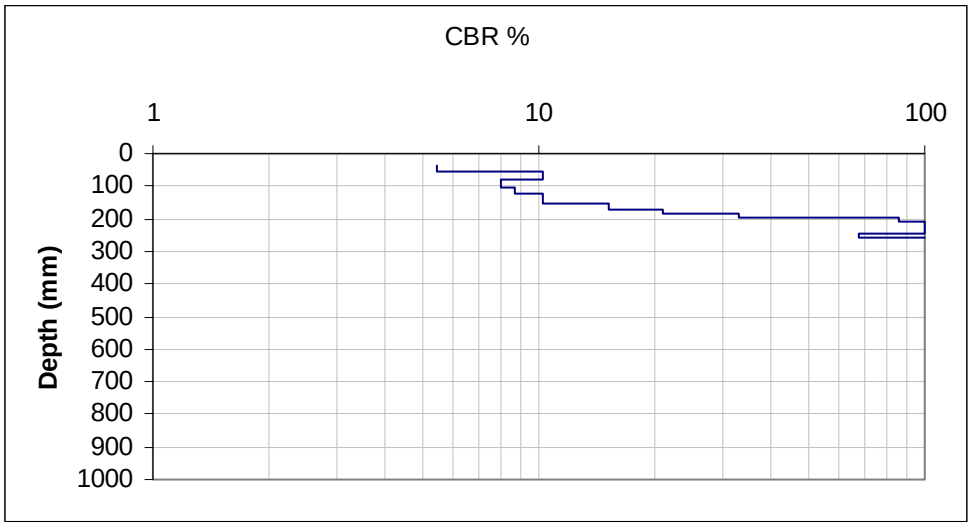
3+30 20N



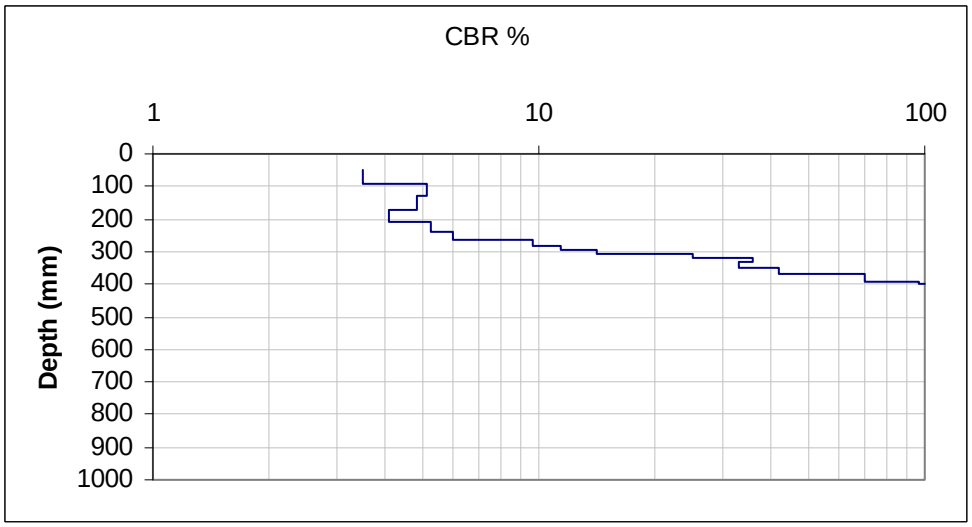
3+30 20S



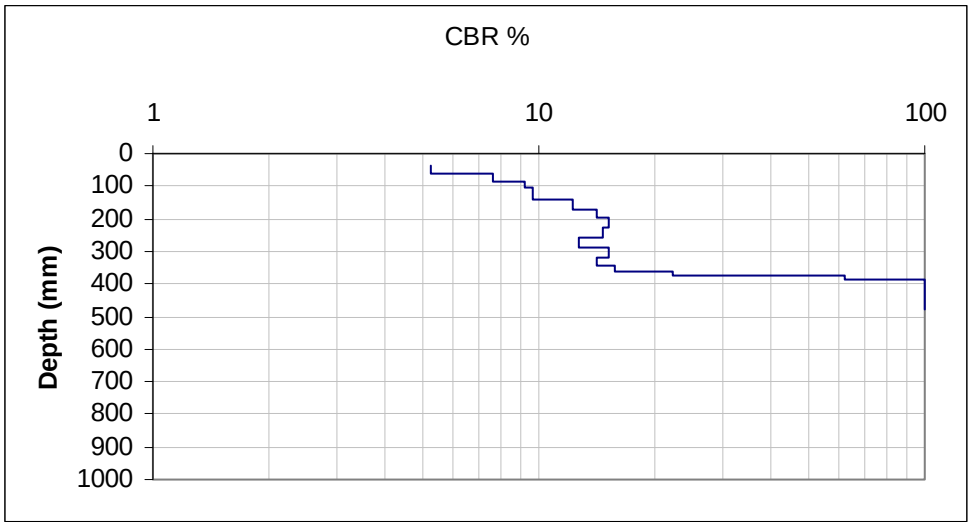
4+00 CL



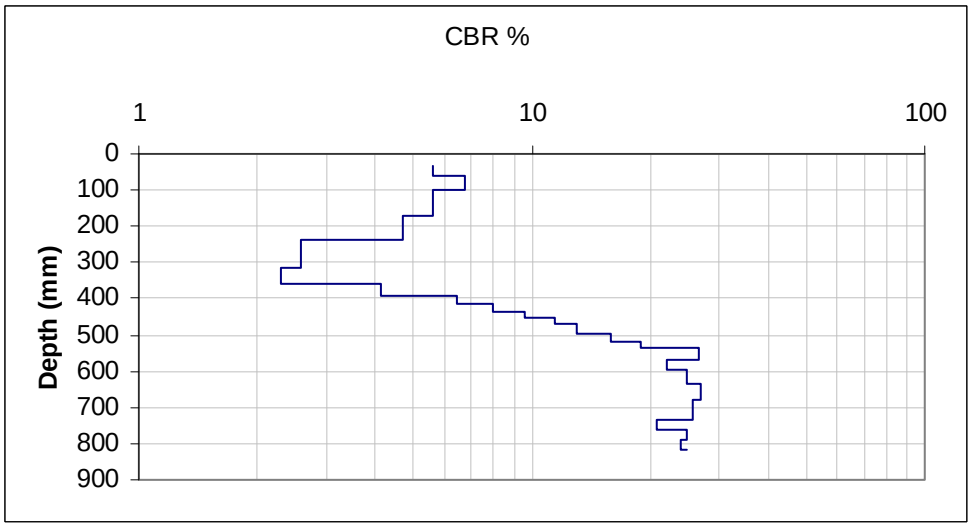
4+00 10N



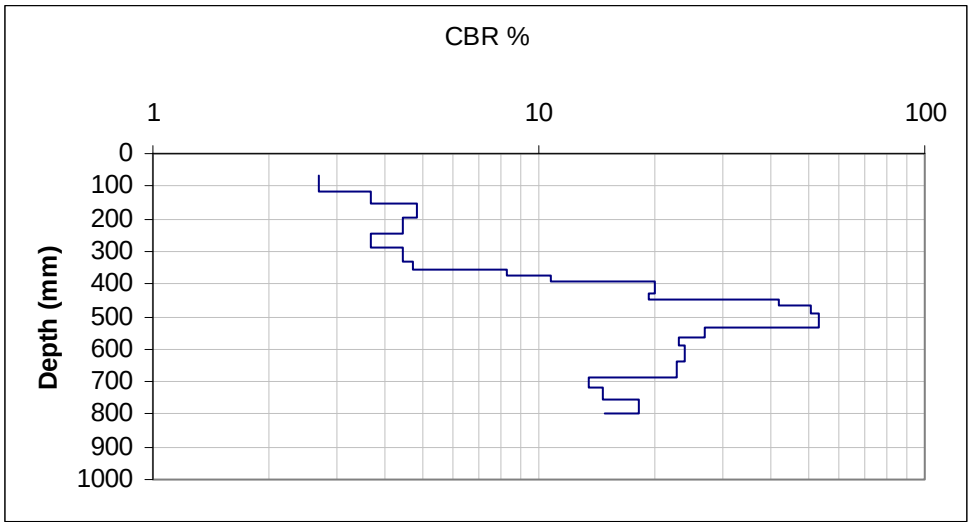
4+00 10S



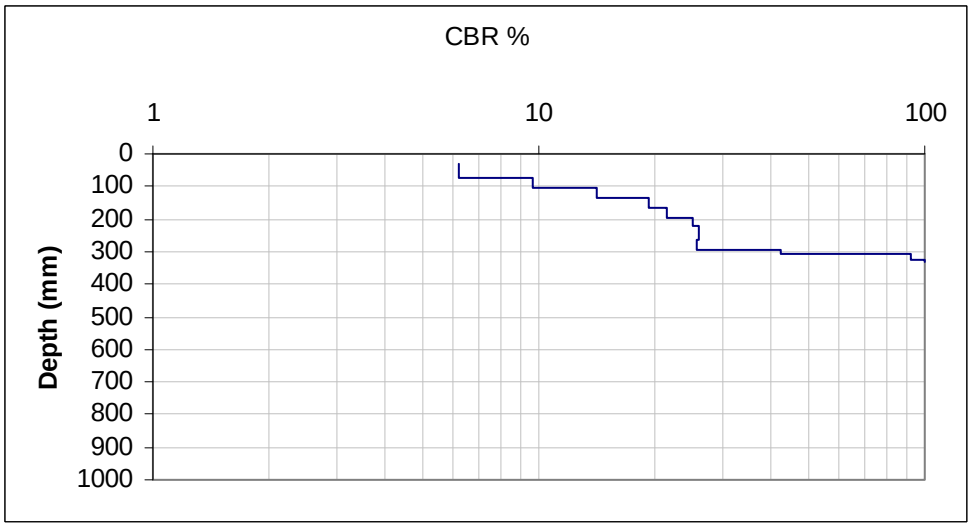
4+00 30N



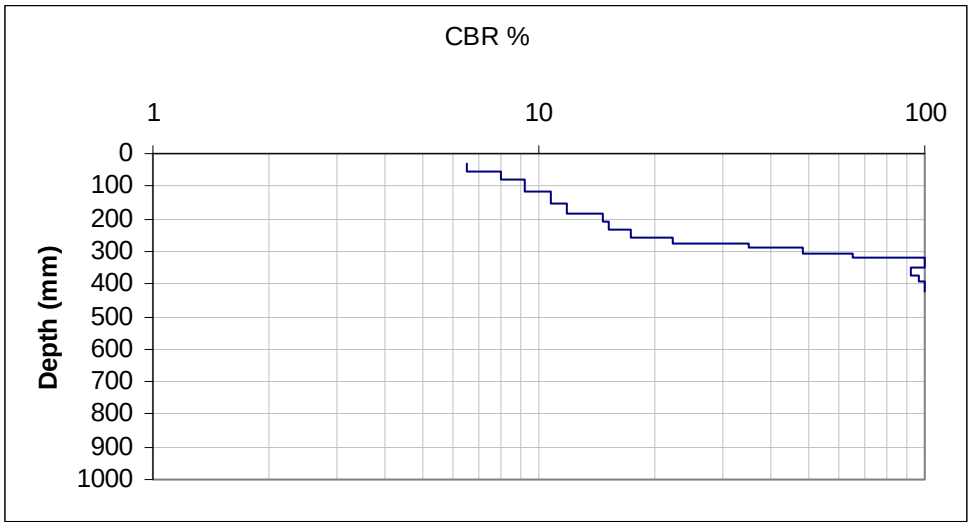
4+00 30S



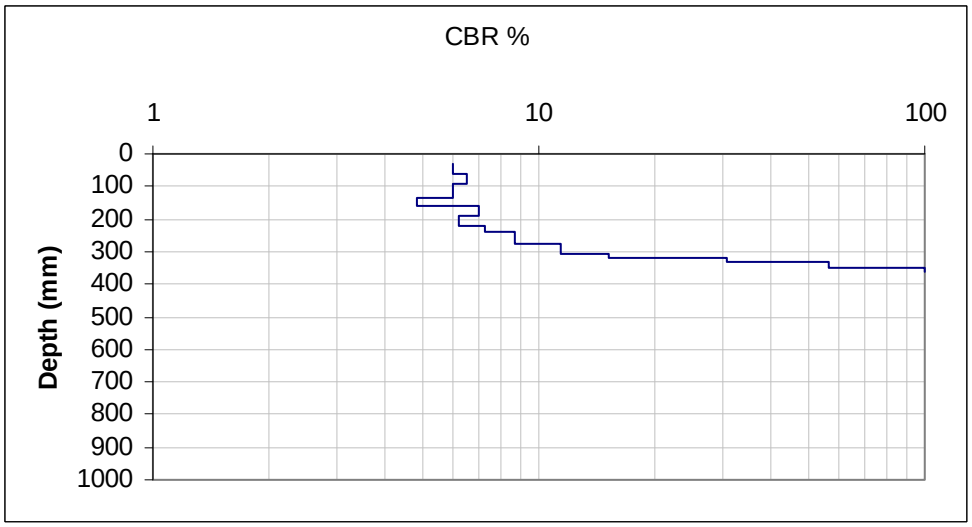
4+70 2N



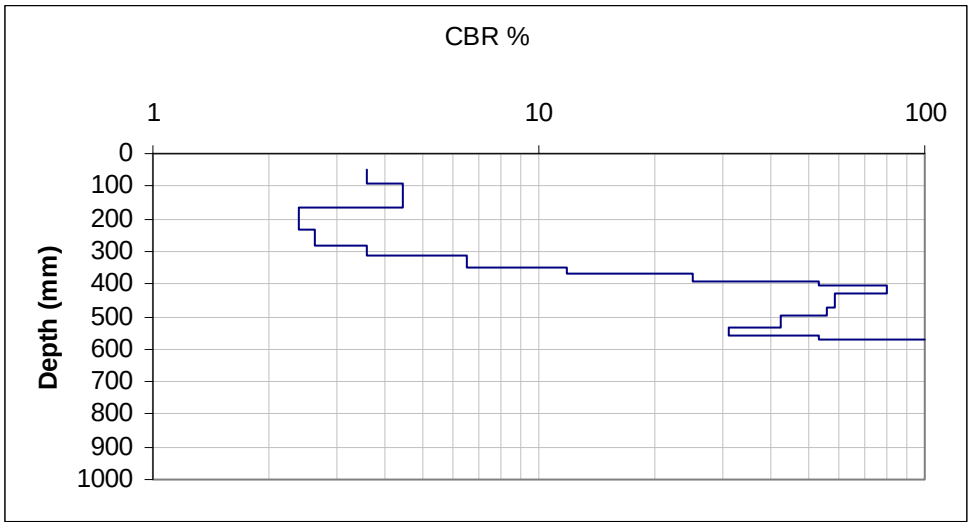
4+70 2S



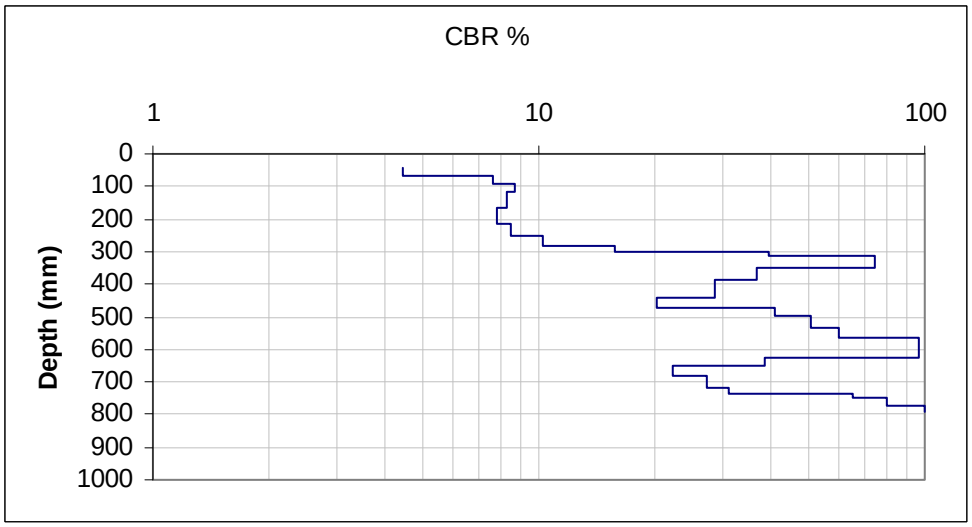
4+70 20N



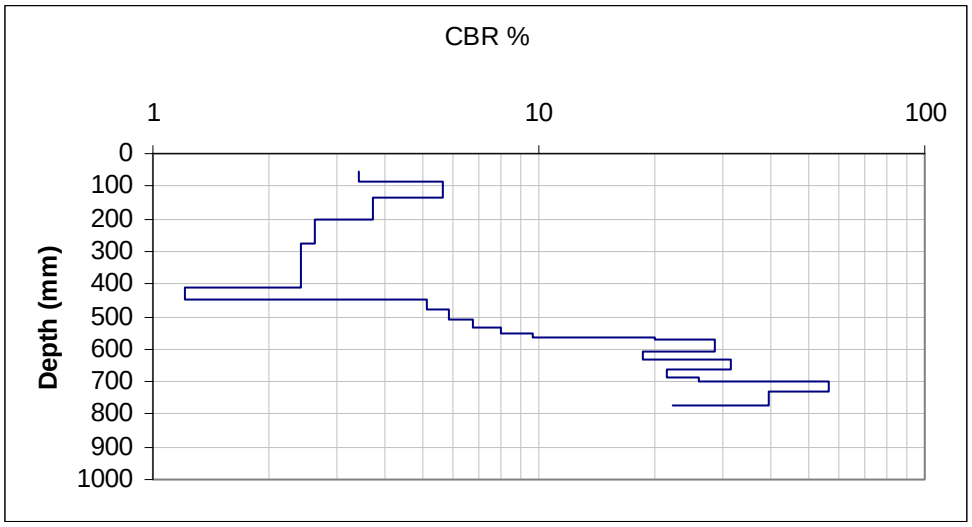
4+70 20S



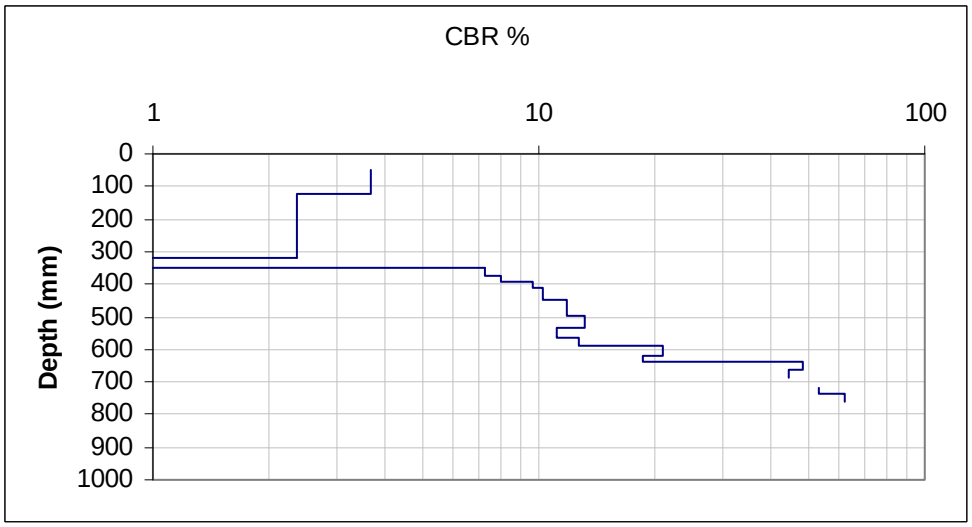
5+20 2N



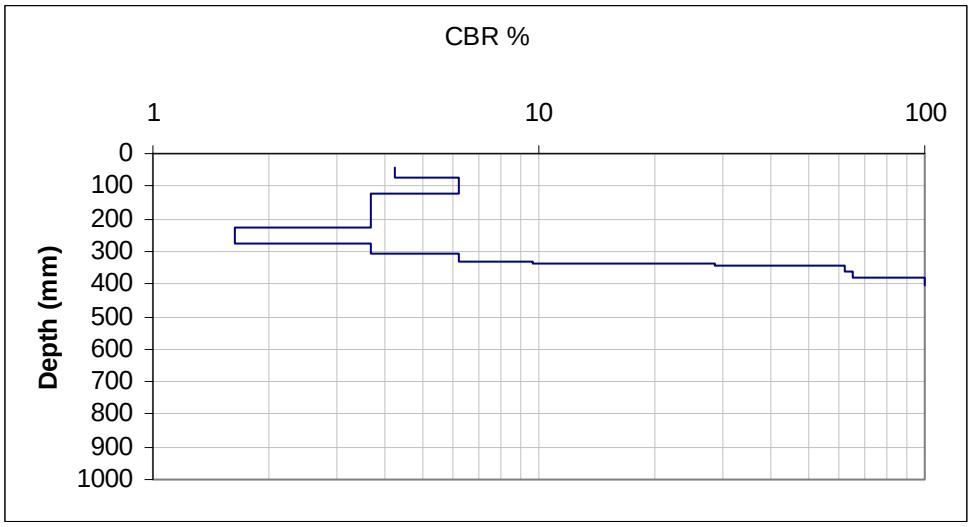
5+20 2S



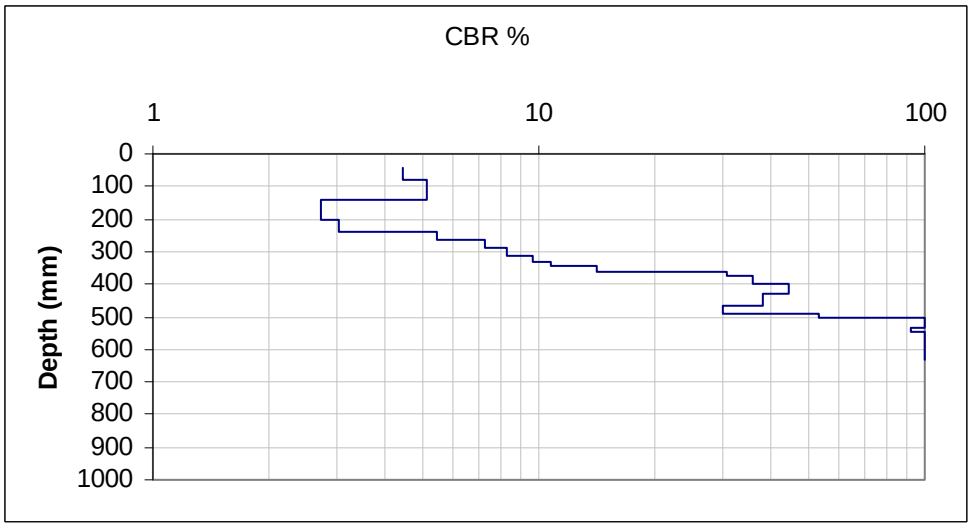
5+50 CL 1 meter south of flagging



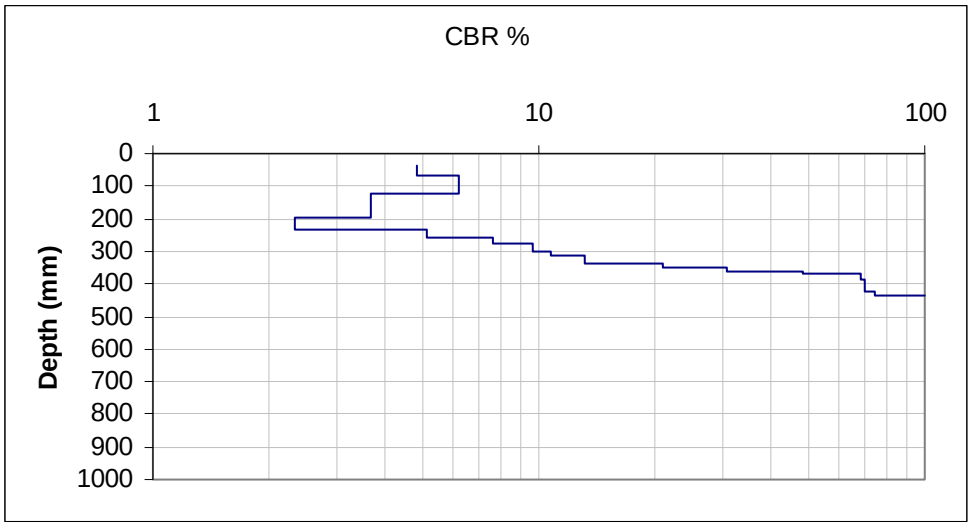
5+50 CL 1 meter north of flagging



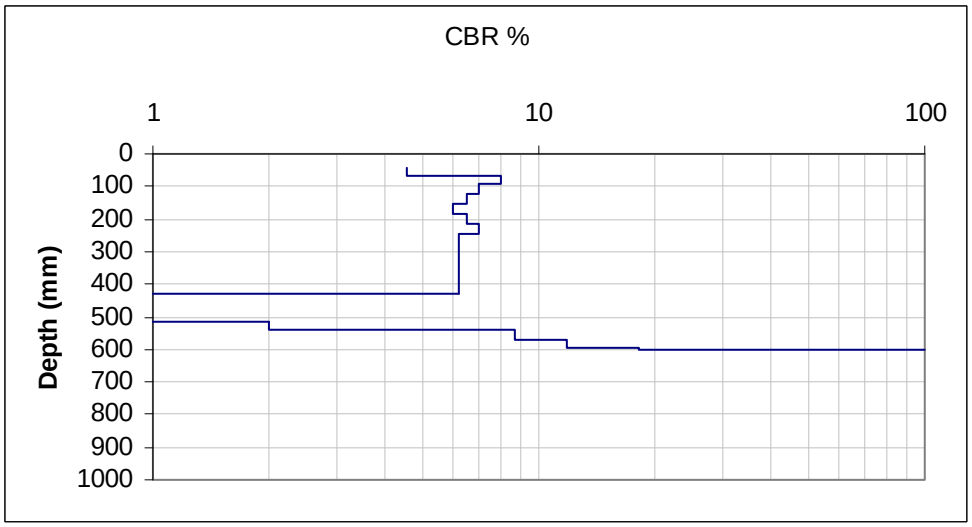
5+50 10N



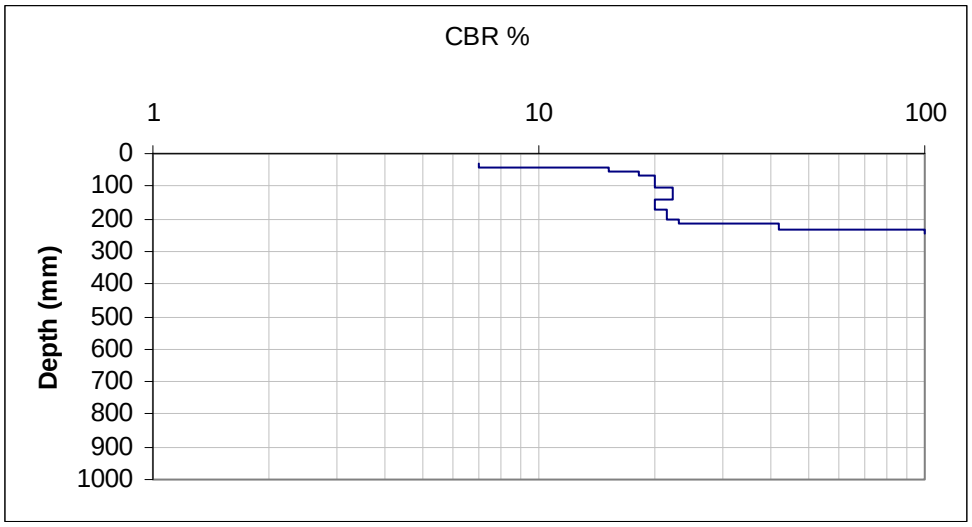
5+50 10S



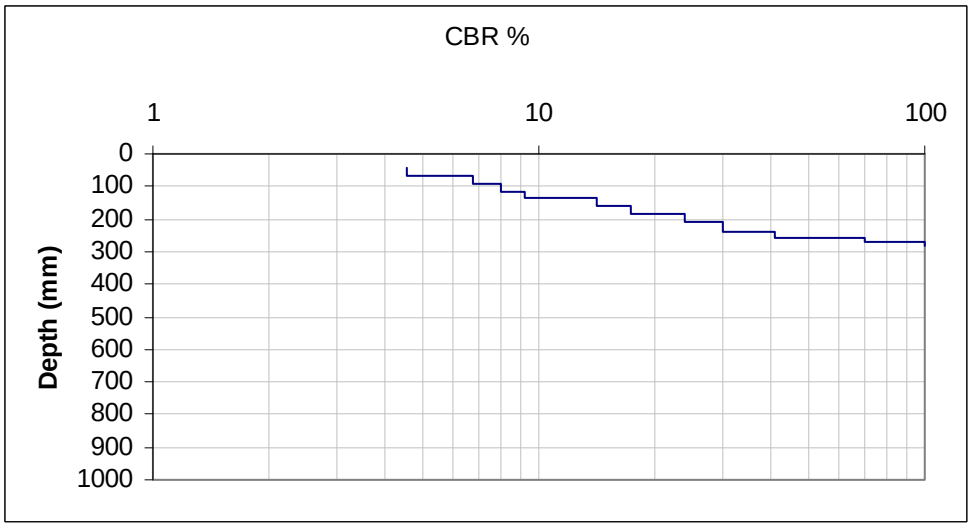
5+50 30N



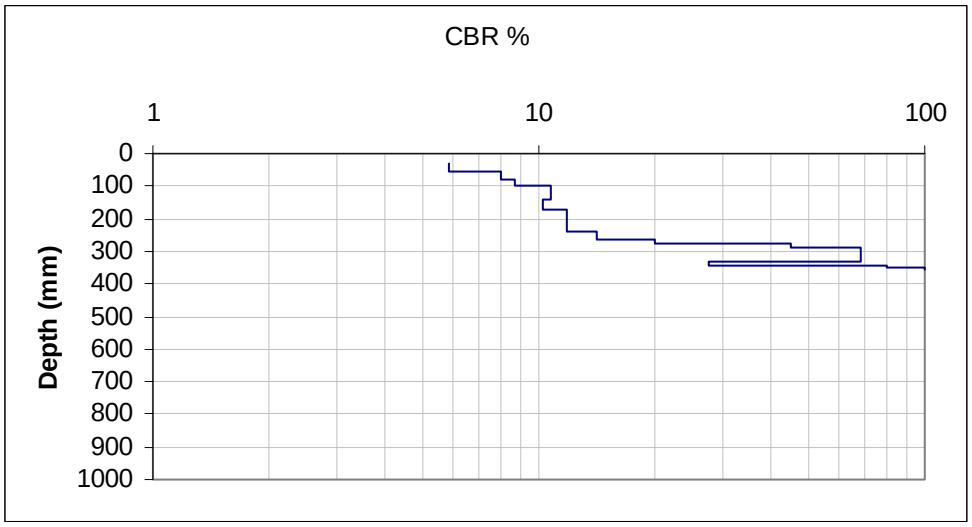
5+50 30S



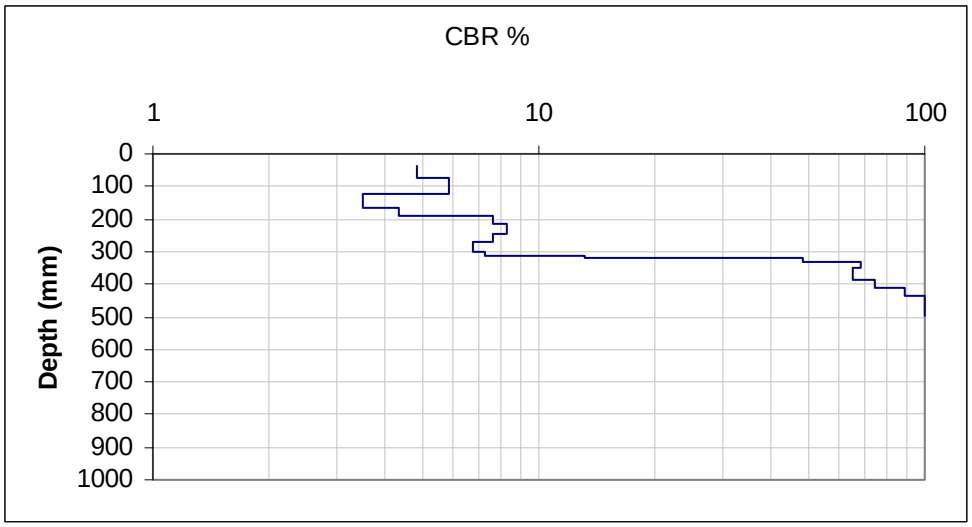
5+80 2N


CBR %
1
10
100
Depth (mm)
0
100
200
300
400
500
600
700
800
900
1000

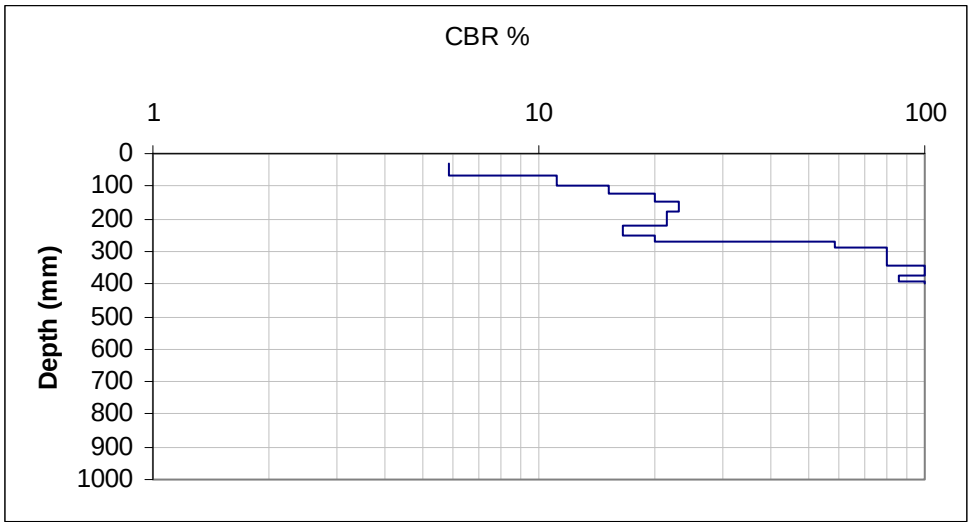
5+80 2S


CBR %
1
10
100
Depth (mm)
0
100
200
300
400
500
600
700
800
900
1000

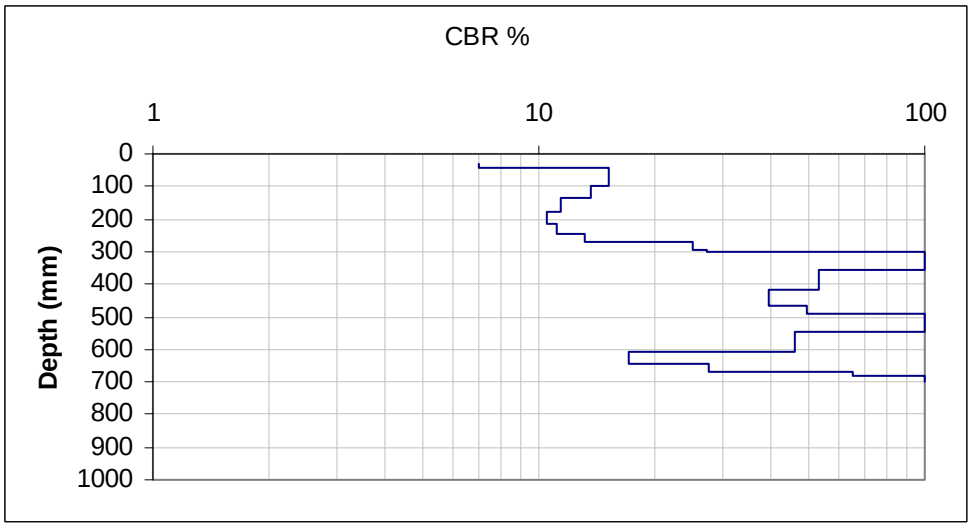
6+30 2N



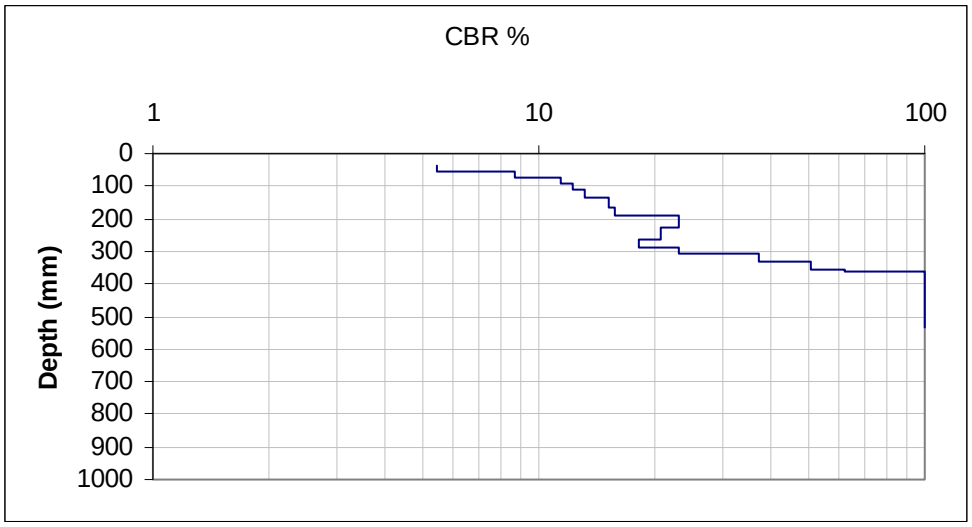
6+30 2S



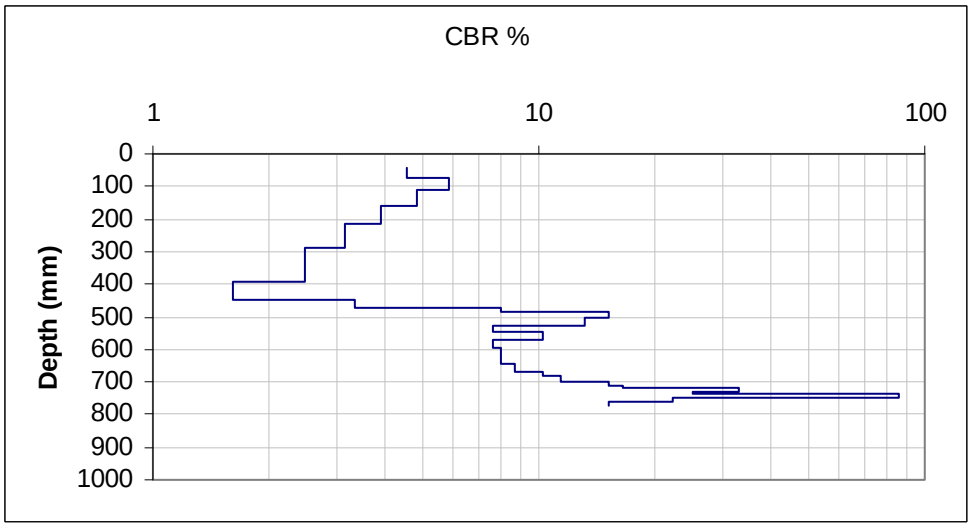
6+30 20N



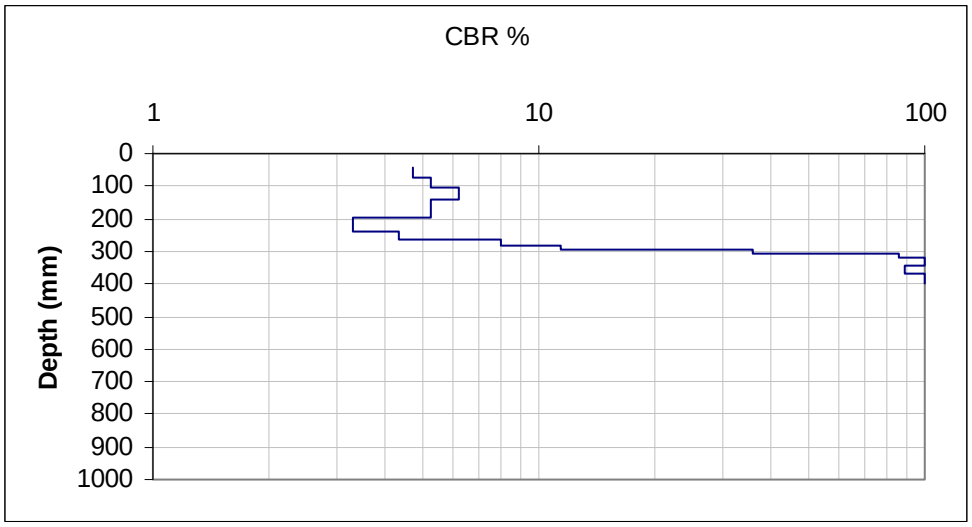
6+30 20S



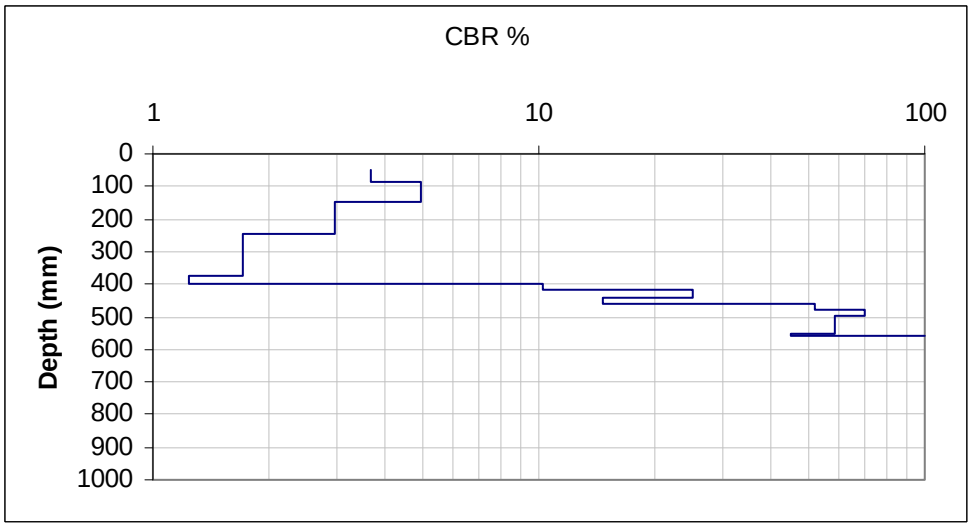
7+00 CL



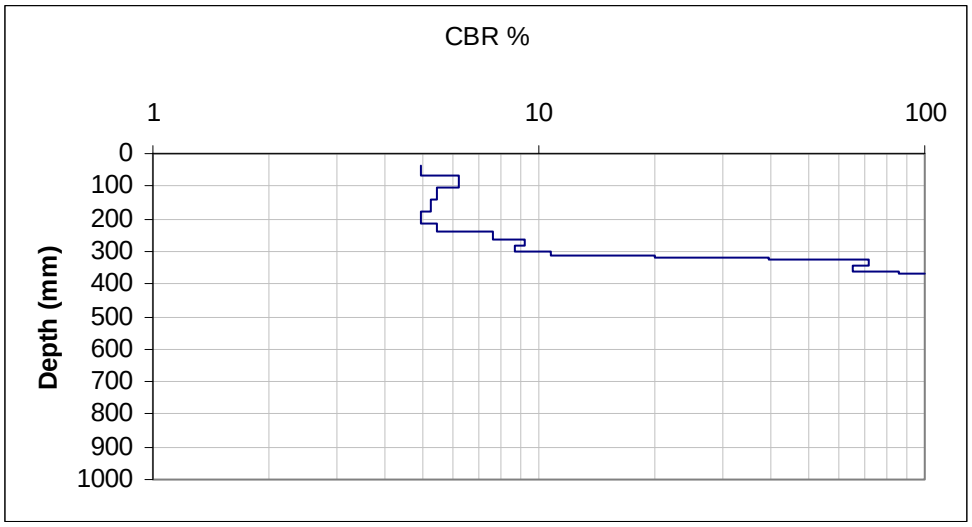
7+00 10N



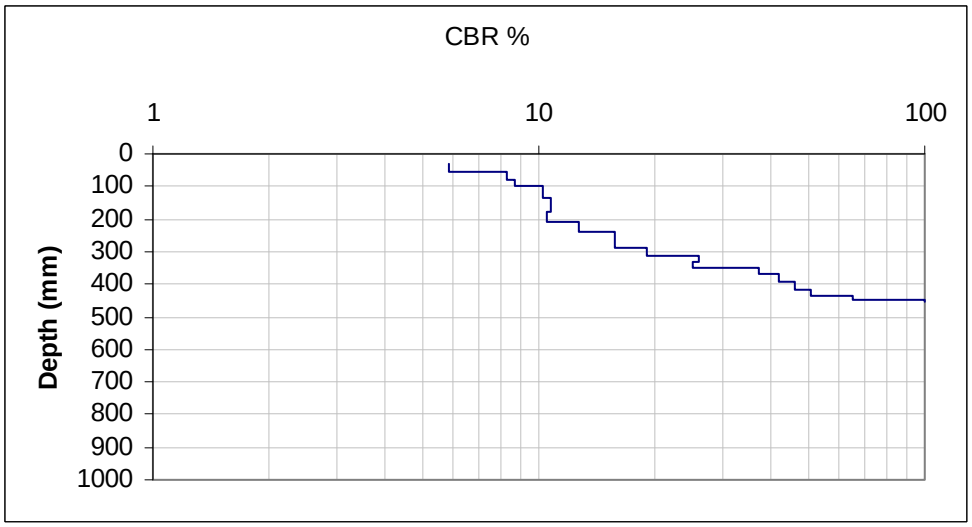
7+00 10S



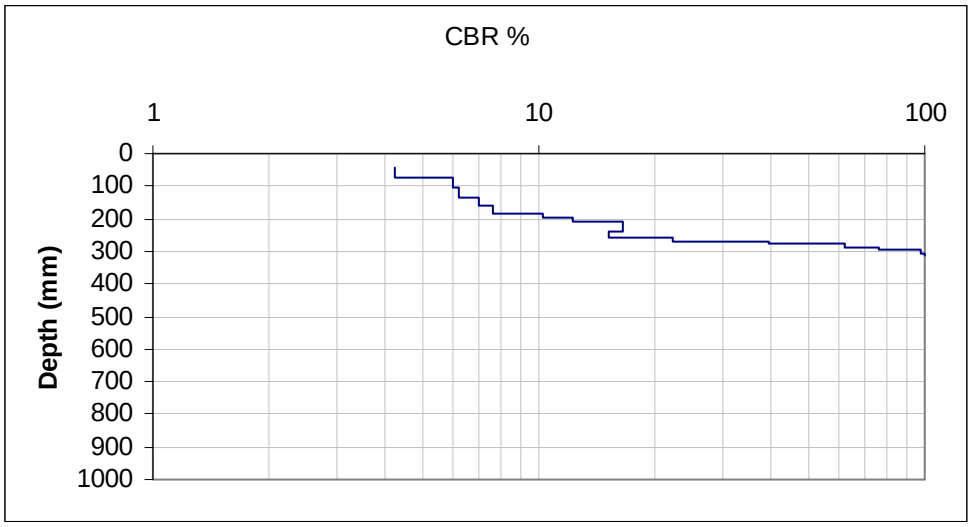
7+00 30N



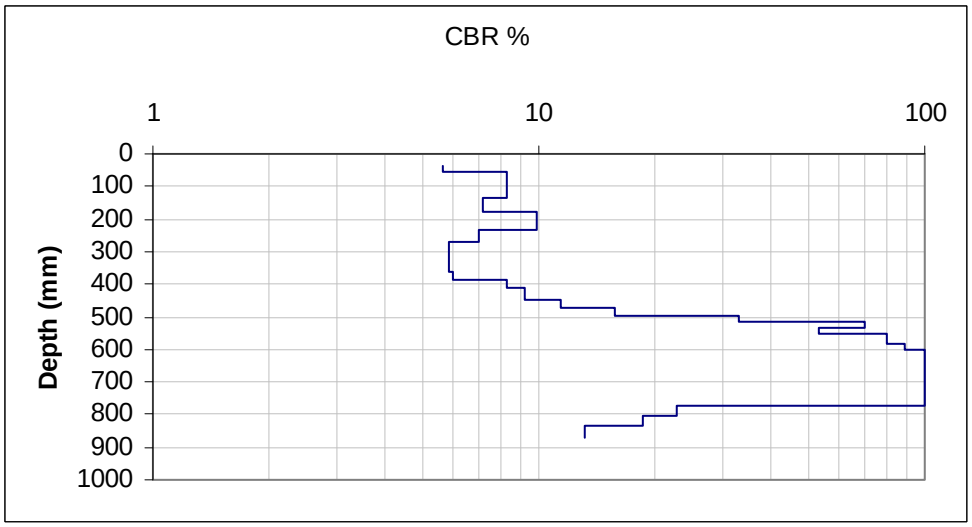
7+00 30S


CBR %
1
10
100
Depth (mm)
0
100
200
300
400
500
600
700
800
900
1000

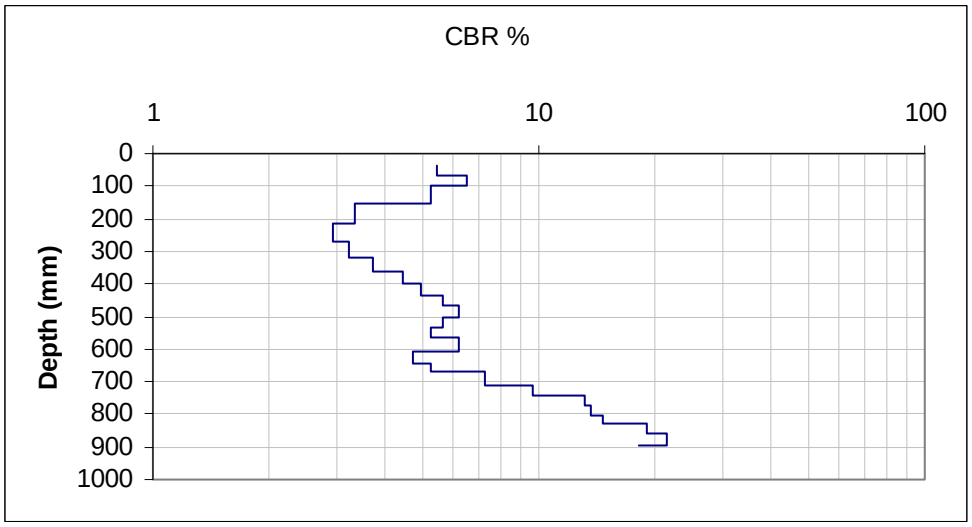
7+70 2N


CBR %
1
10
100
Depth (mm)
0
100
200
300
400
500
600
700
800
900
1000

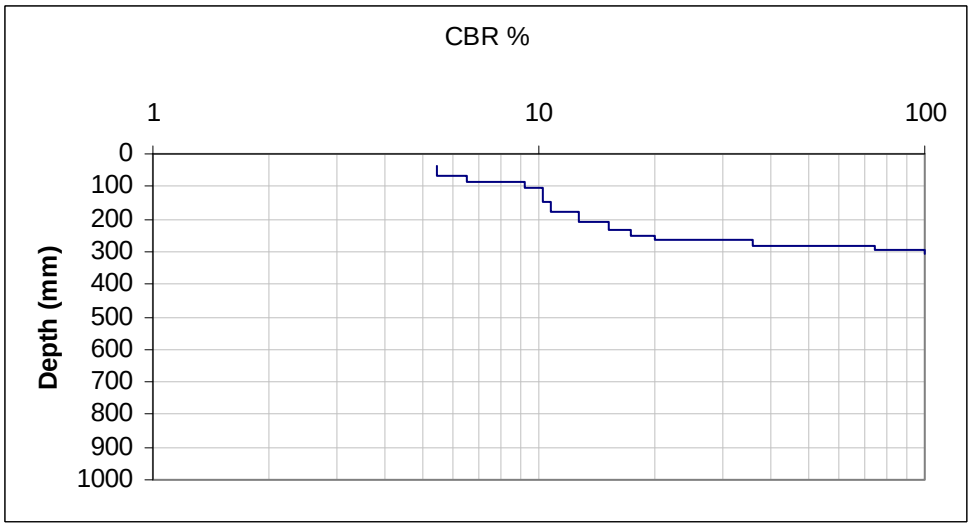
7+70 2S



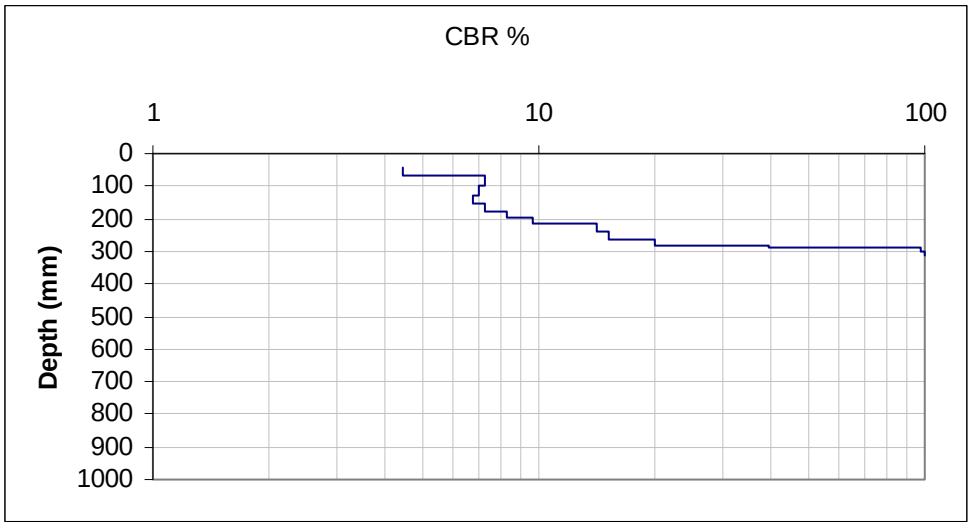
7+70 20N



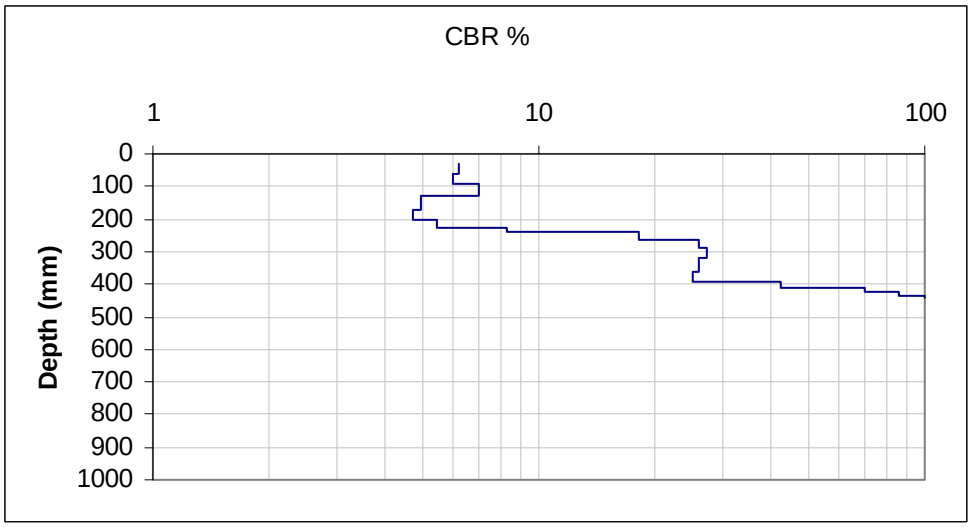
7+70 20S


CBR %
1
10
100
Depth (mm)
0
100
200
300
400
500
600
700
800
900
1000

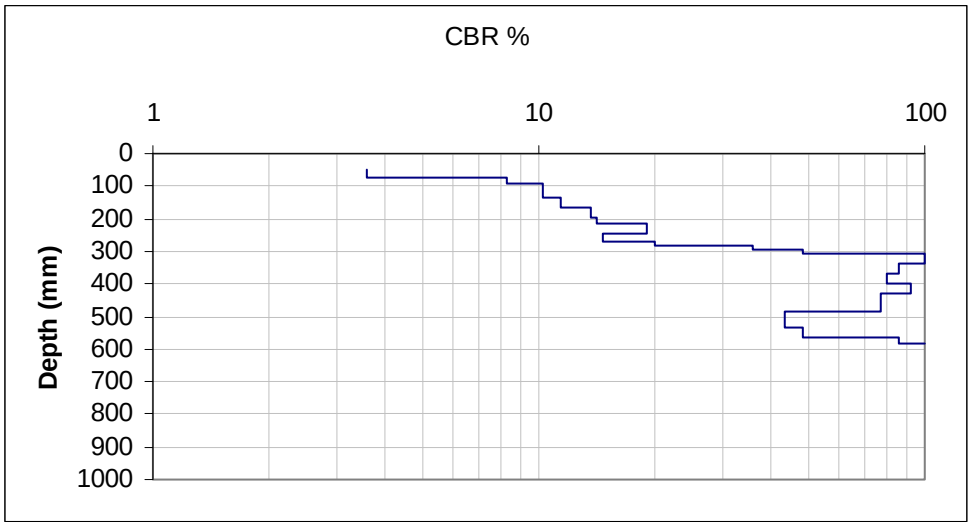
8+20 2N


CBR %
1
10
100
Depth (mm)
0
100
200
300
400
500
600
700
800
900
1000

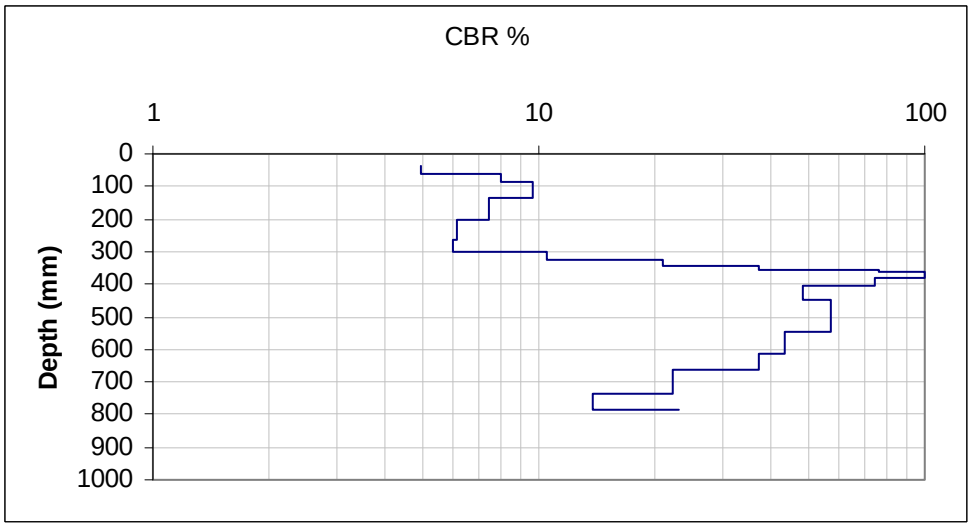
8+20 2S



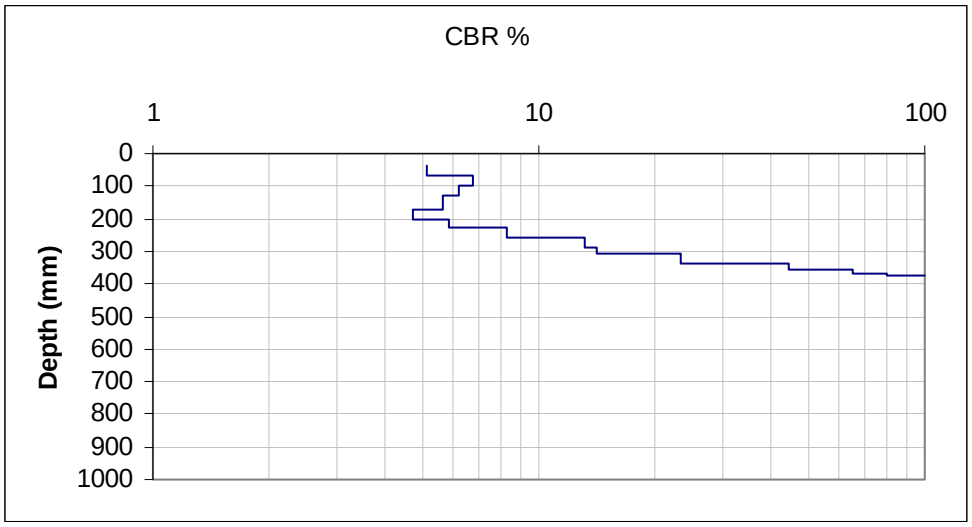
8+50 CL



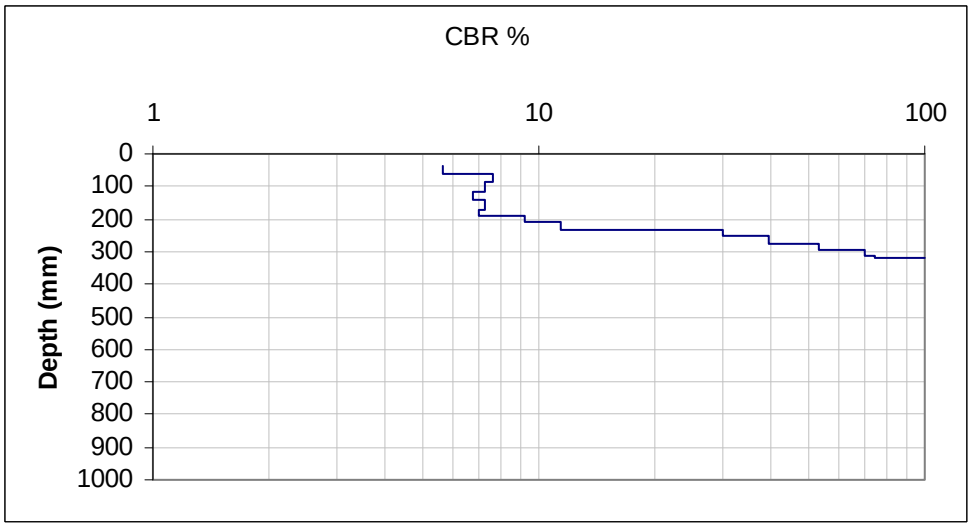
8+50 10N



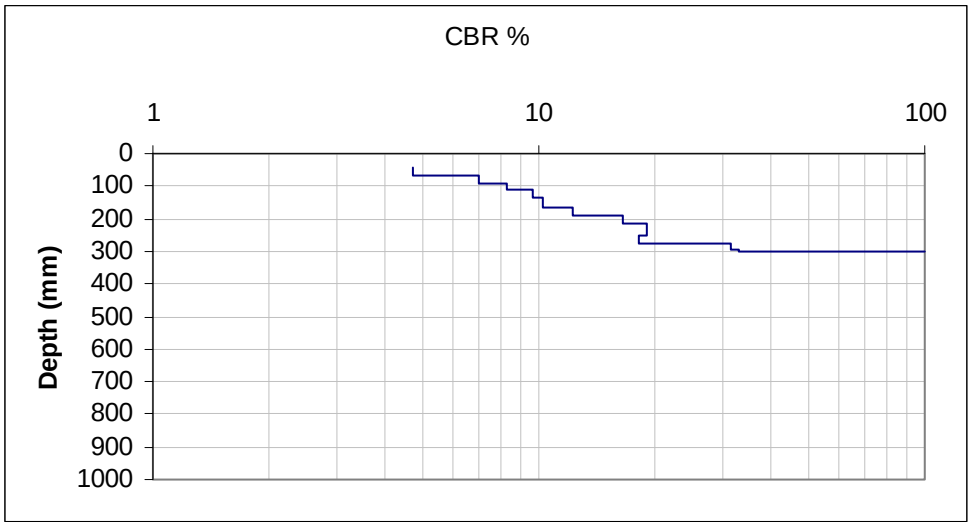
8+50 10S



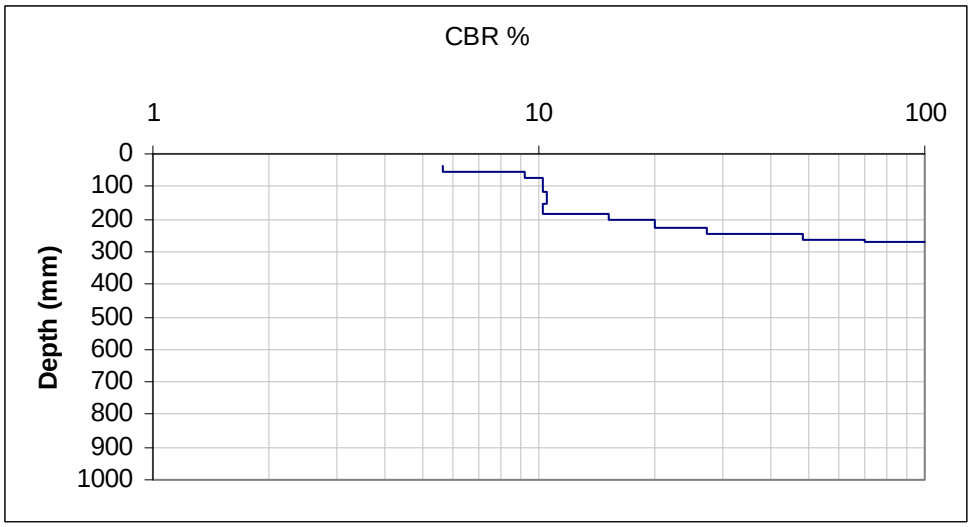
8+90 2N


CBR %
1
10
100
Depth (mm)
0
100
200
300
400
500
600
700
800
900
1000

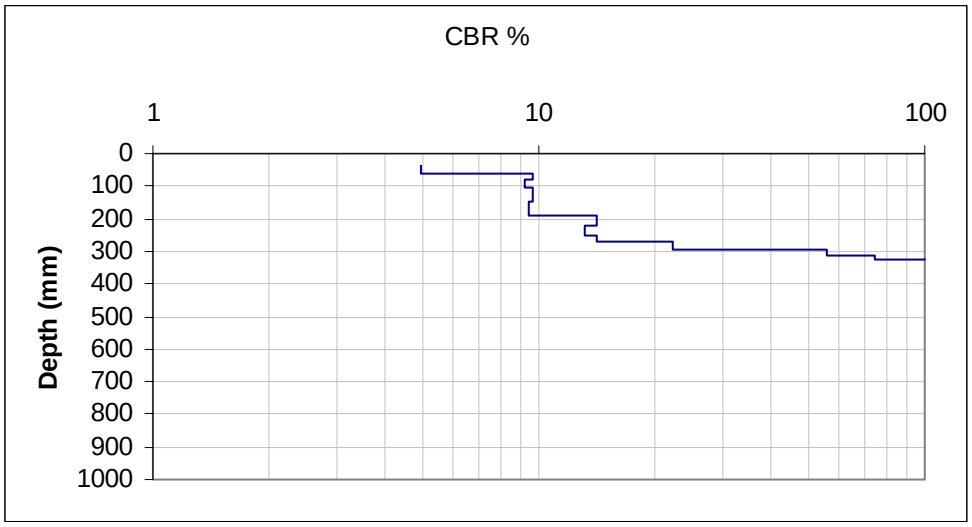
8+90 2S


CBR %
1
10
100
Depth (mm)
0
100
200
300
400
500
600
700
800
900
1000

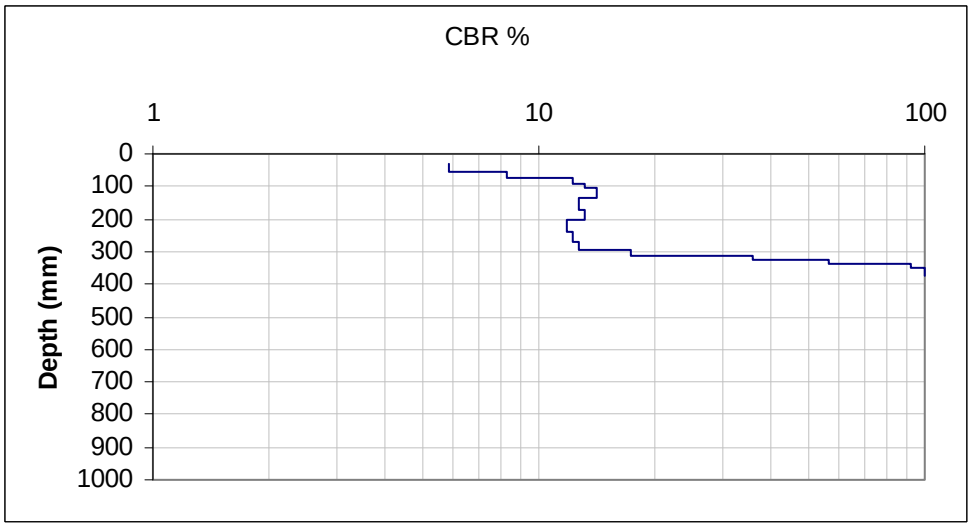
9+30 CL


CBR %
1
10
100
Depth (mm)
0
100
200
300
400
500
600
700
800
900
1000

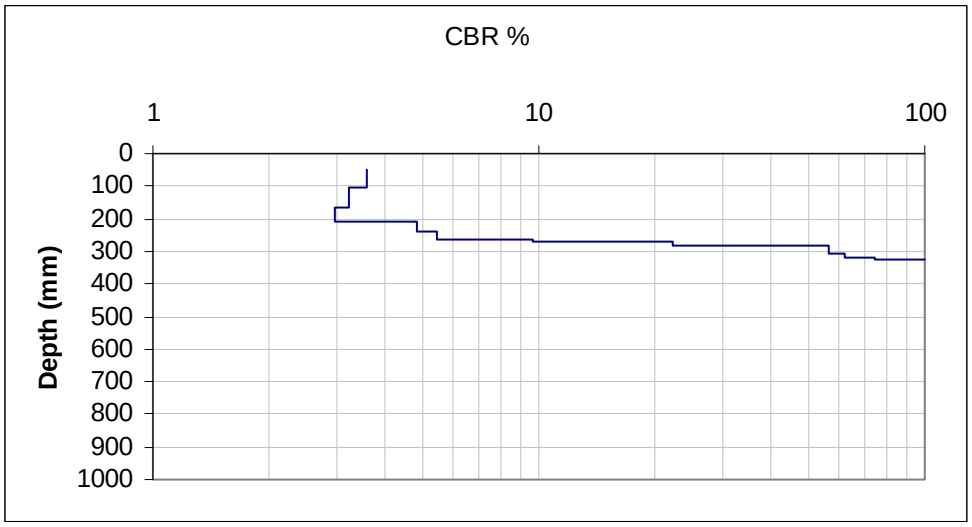
9+30 2N


CBR %
1
10
100
Depth (mm)
0
100
200
300
400
500
600
700
800
900
1000

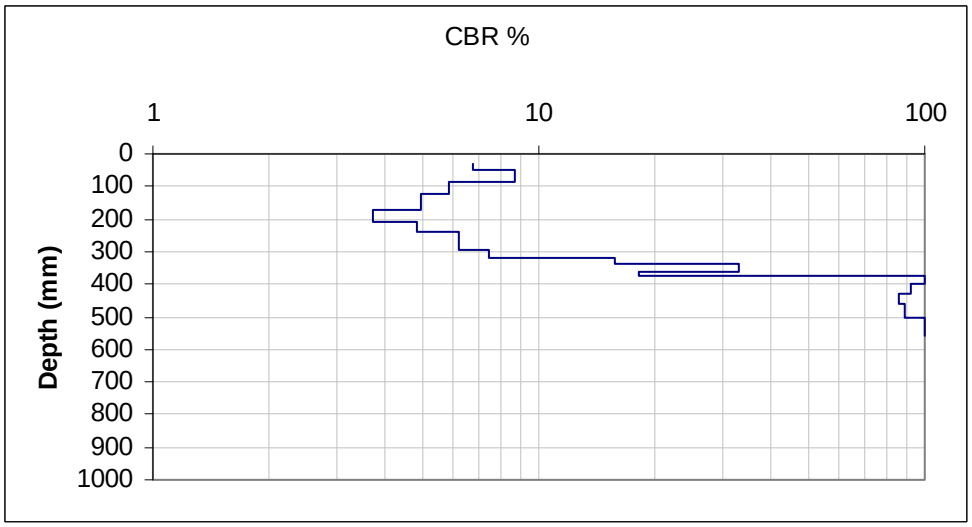
9+30 2S



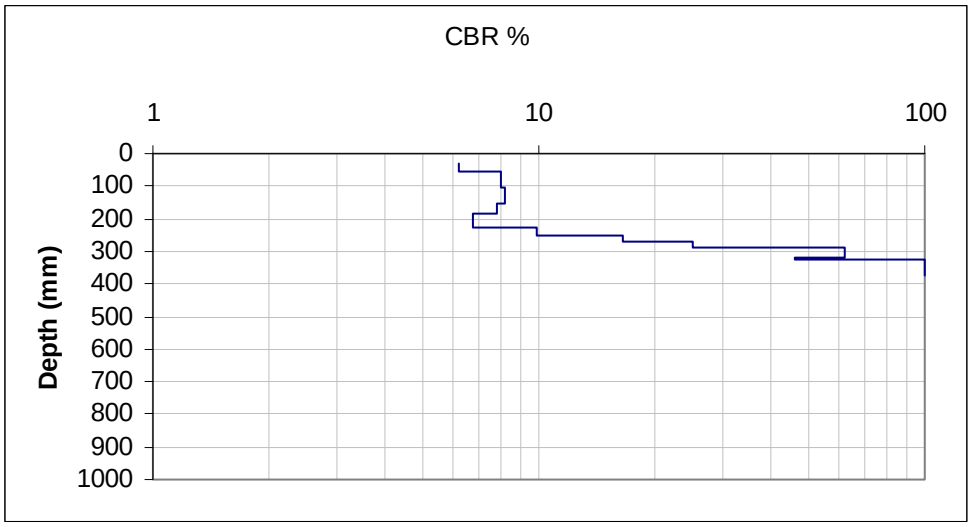
9+30 20N



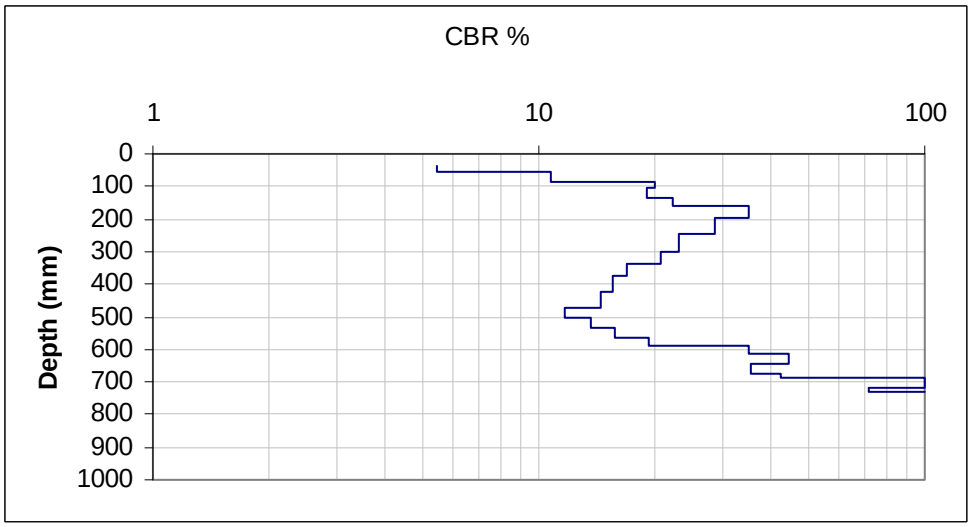
9+30 20S


CBR %
1
10
100
Depth (mm)
0
100
200
300
400
500
600
700
800
900
1000

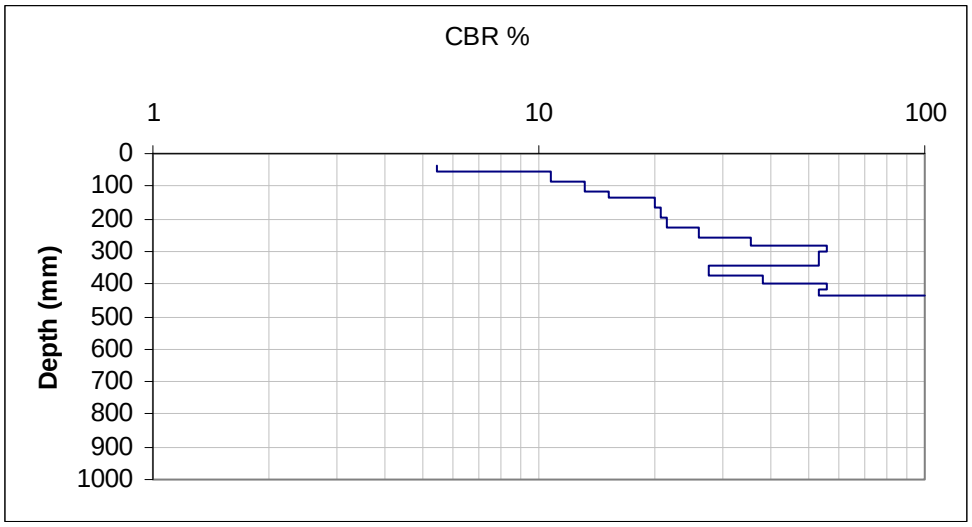
9+70 2N


CBR %
1
10
100
Depth (mm)
0
100
200
300
400
500
600
700
800
900
1000

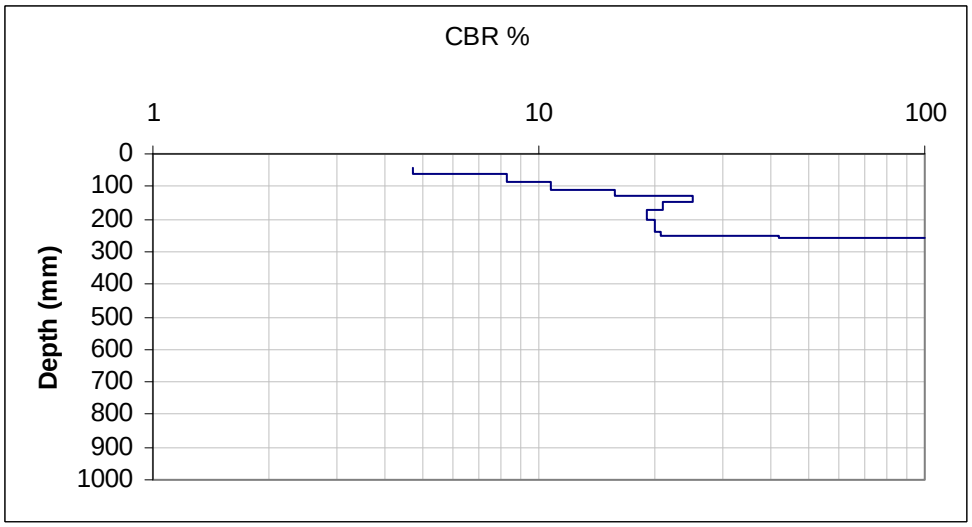
9+70 2S



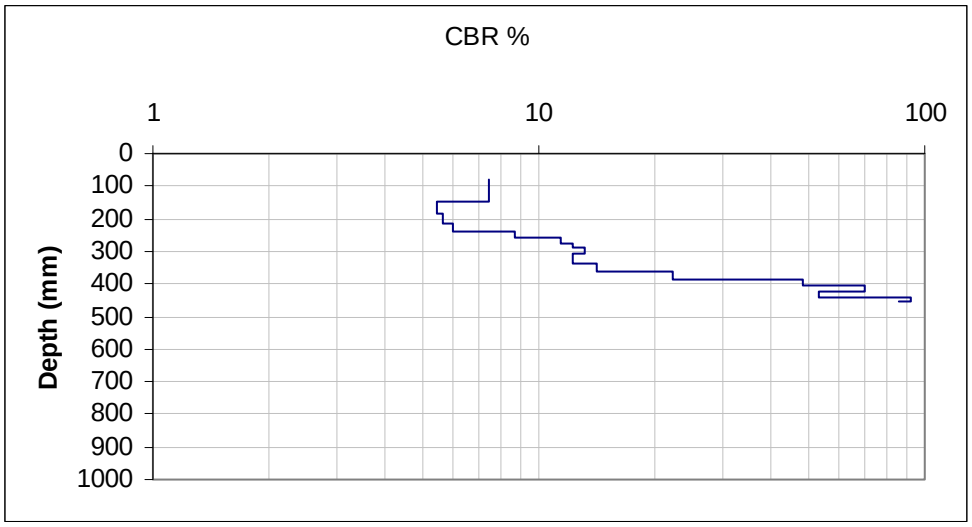
10+10 CL



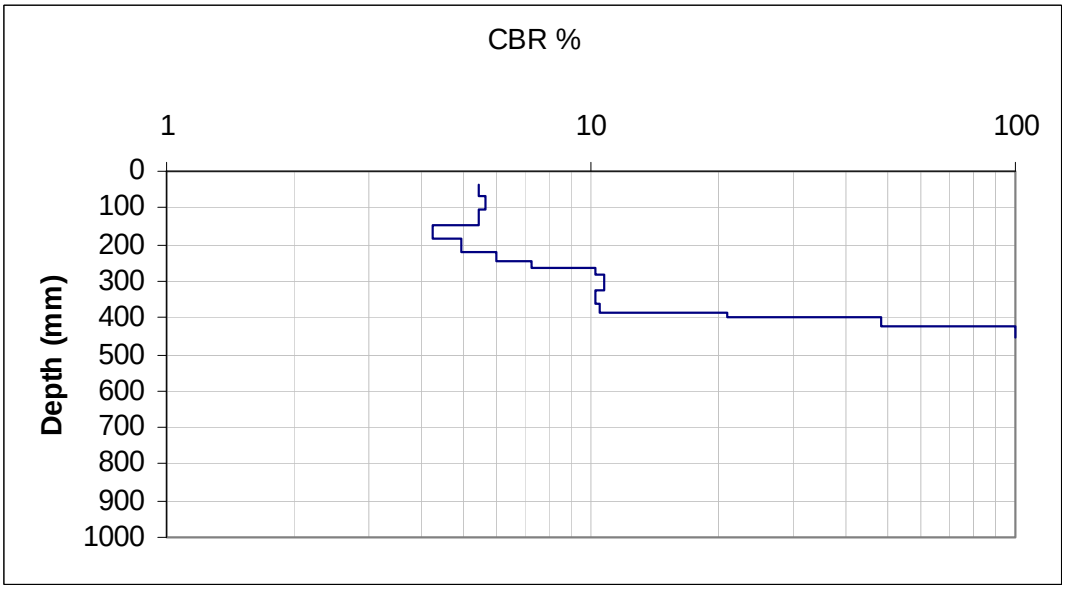
10+10 30N



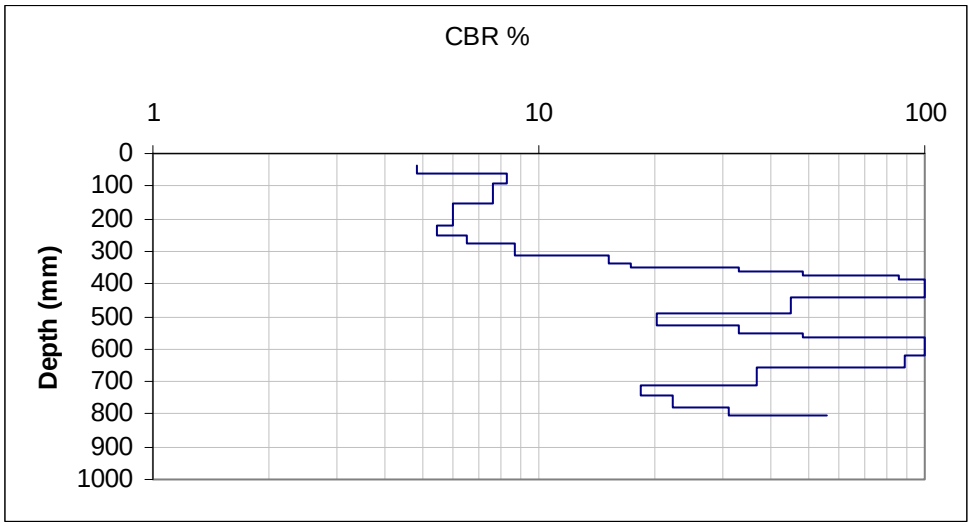
10+10 30S



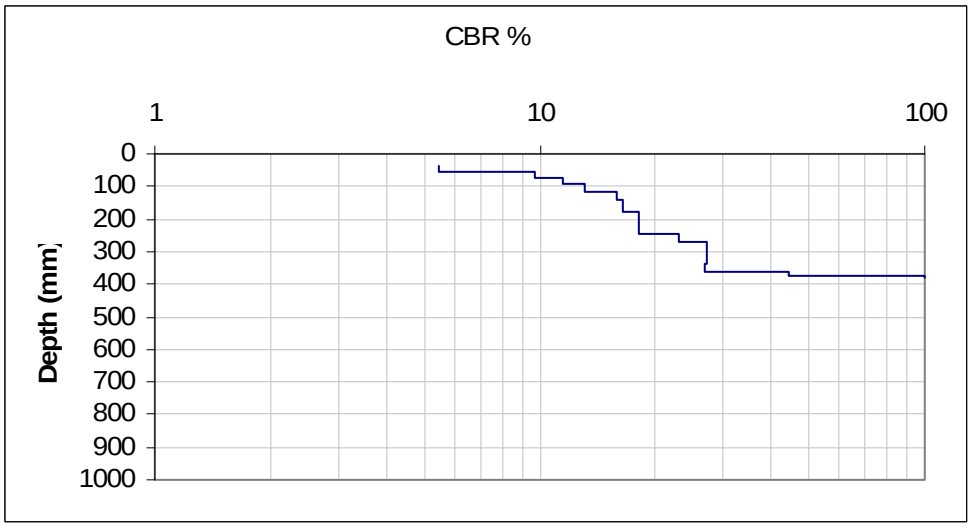
10+70 CL



10+70 CL, second reading

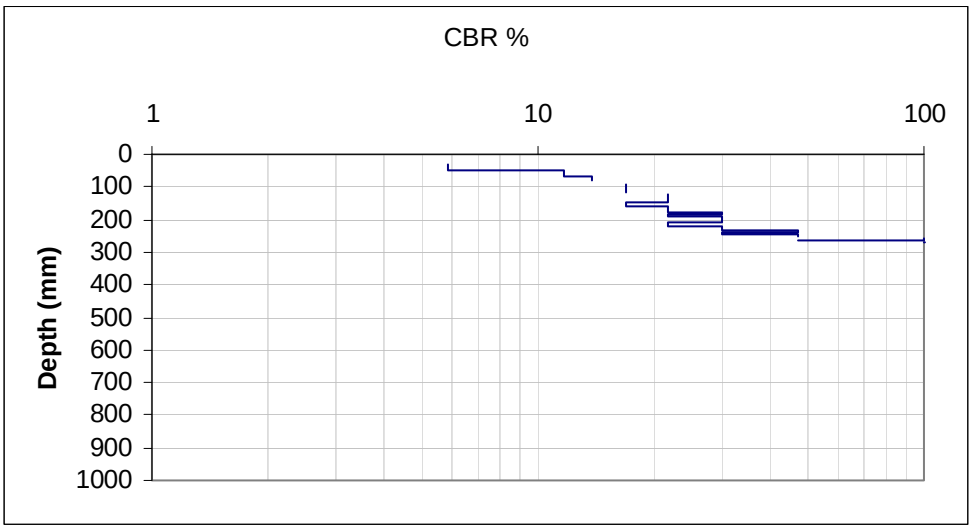


10+70 20N

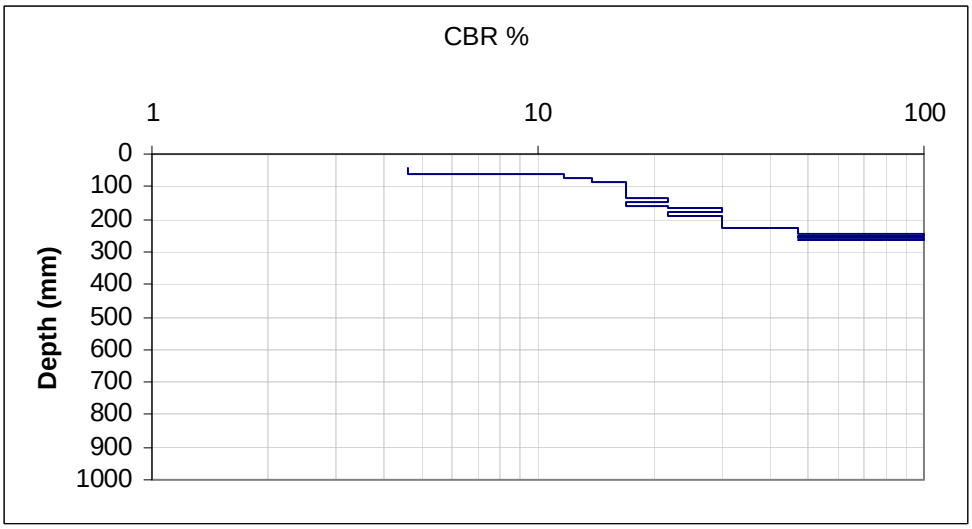


10+70 20S

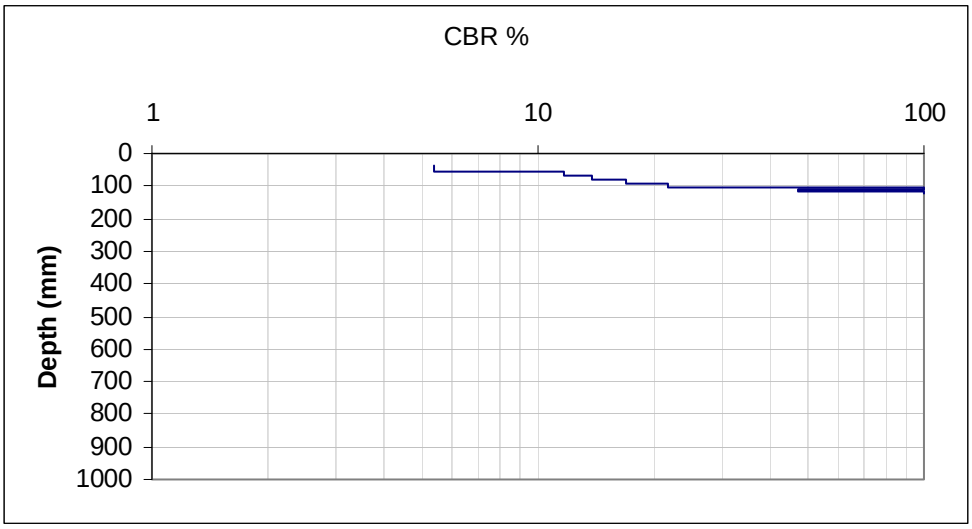
D3. IOP #3, April 20–21, 2006



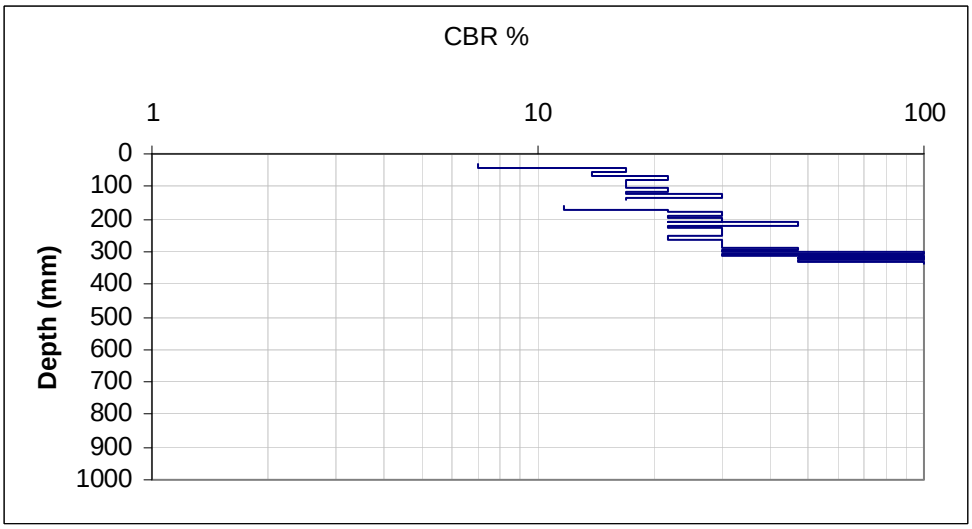
0+40 CL – auto



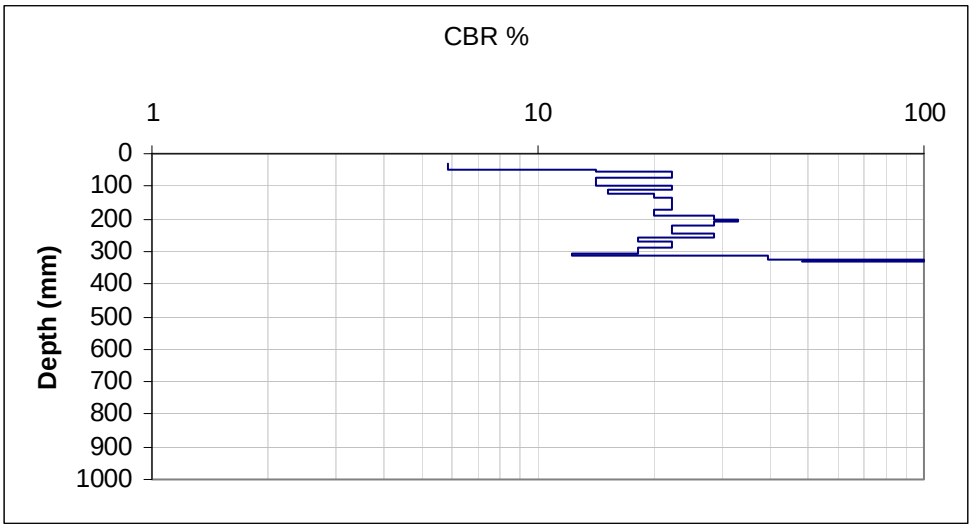
0+90 CL – auto



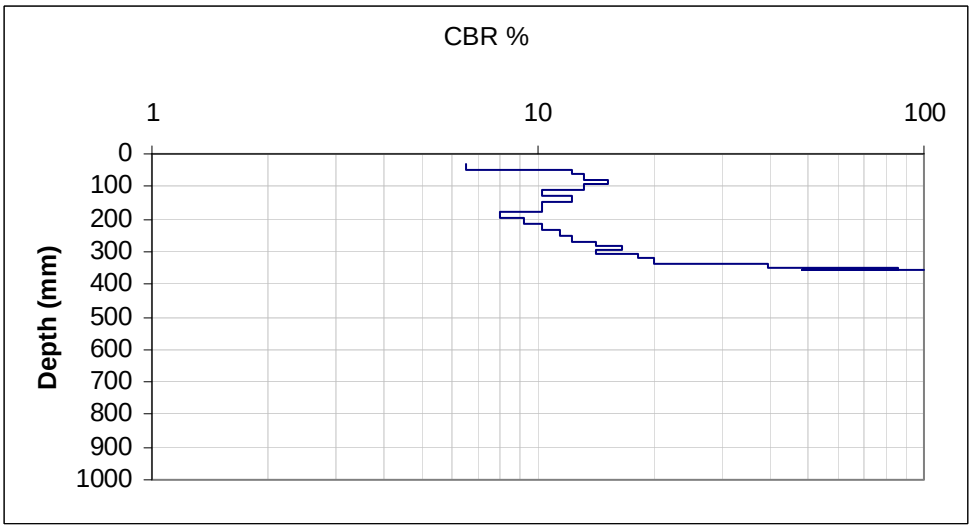
0+90 10S – auto



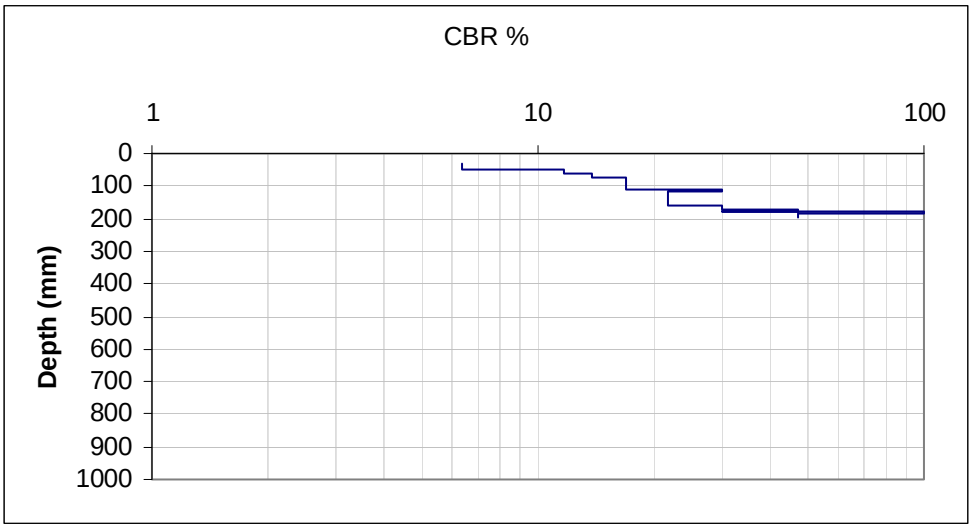
0+90 10N – auto



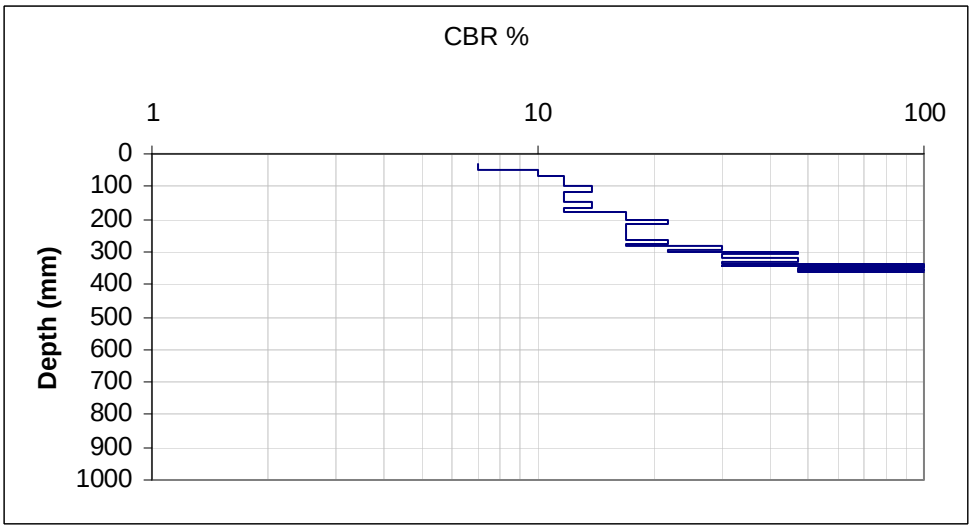
0+90 30N – manual



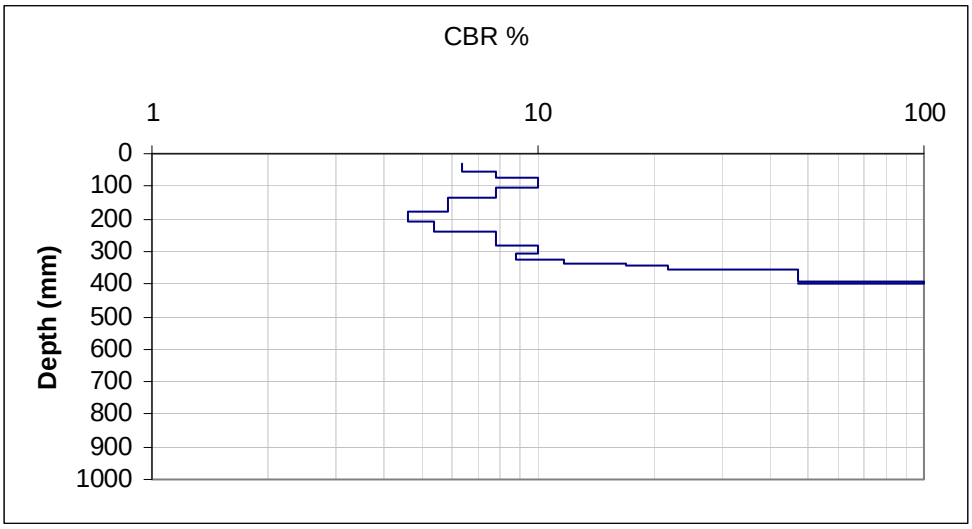
0+90 30S — manual



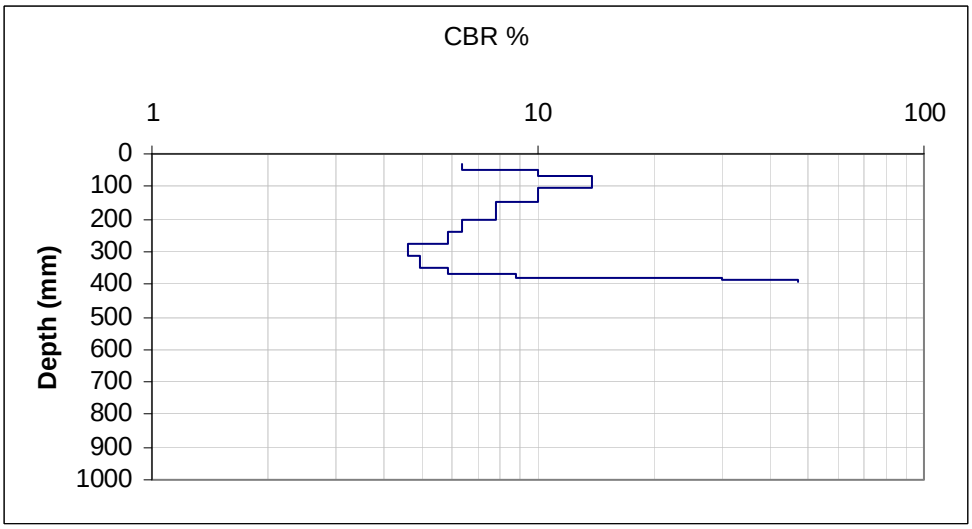
1+30 2N — auto



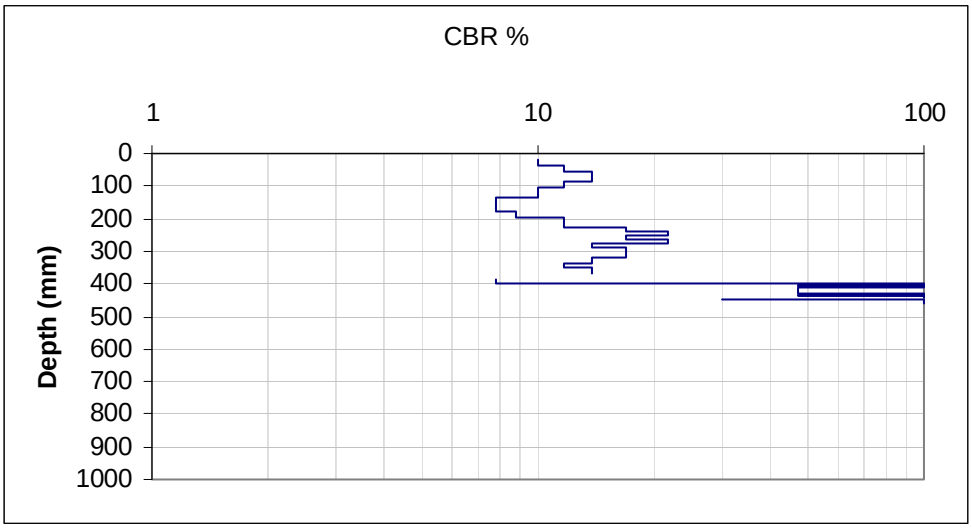
1+30 2S – auto



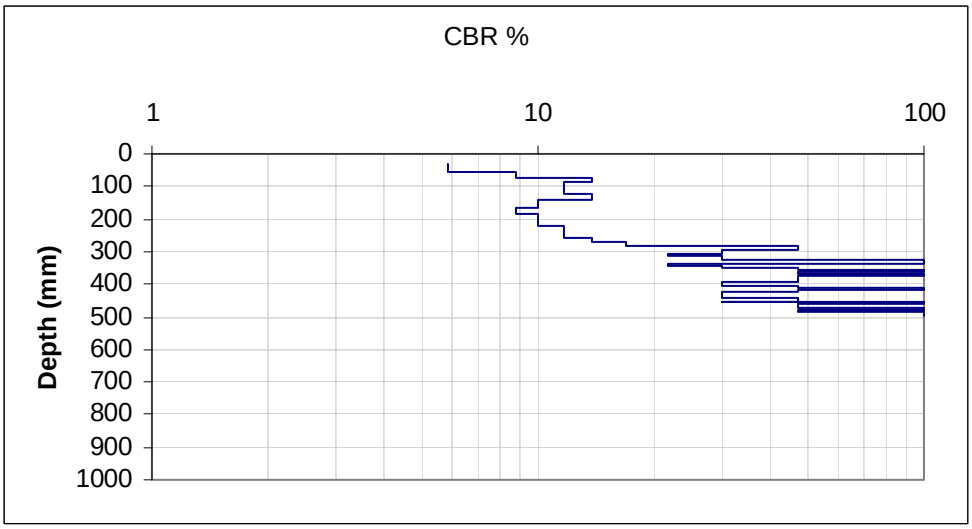
1+70 CL – auto



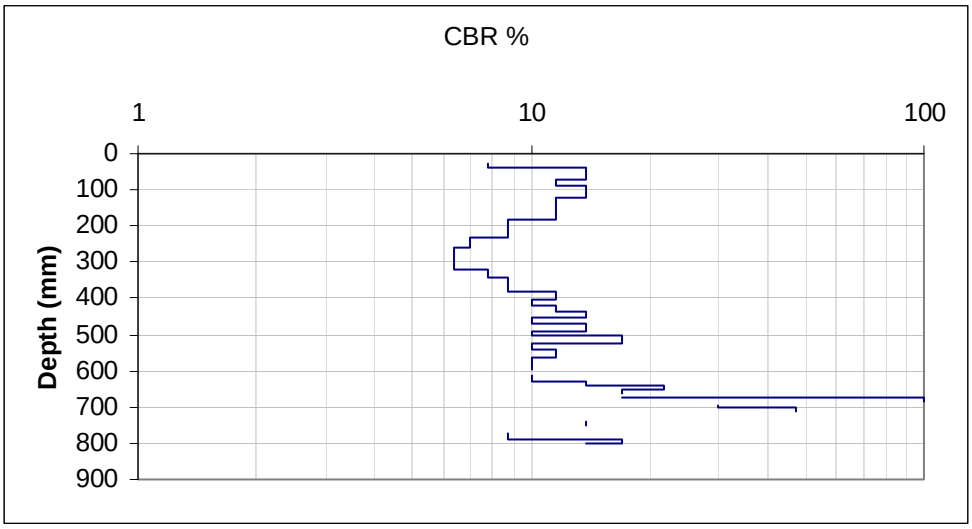
1+70 CL — auto, second reading



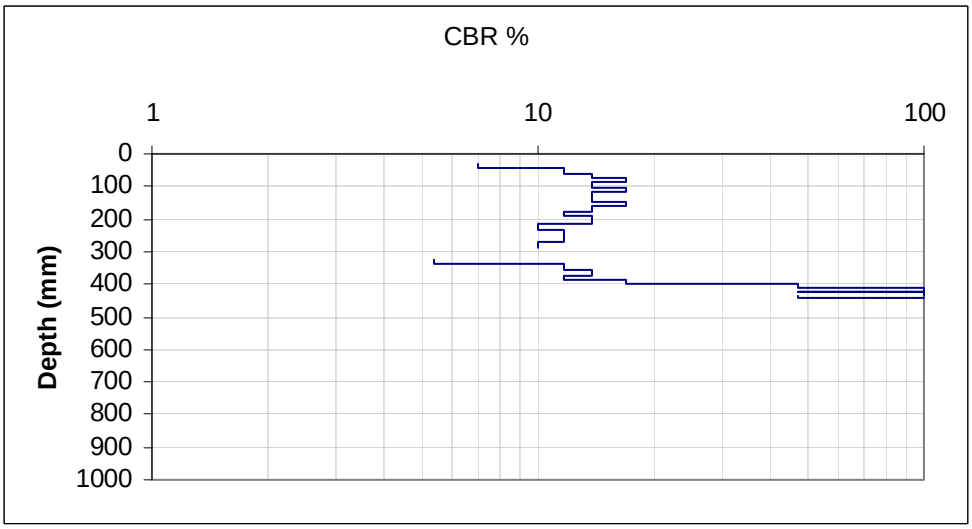
1+70 2N — auto



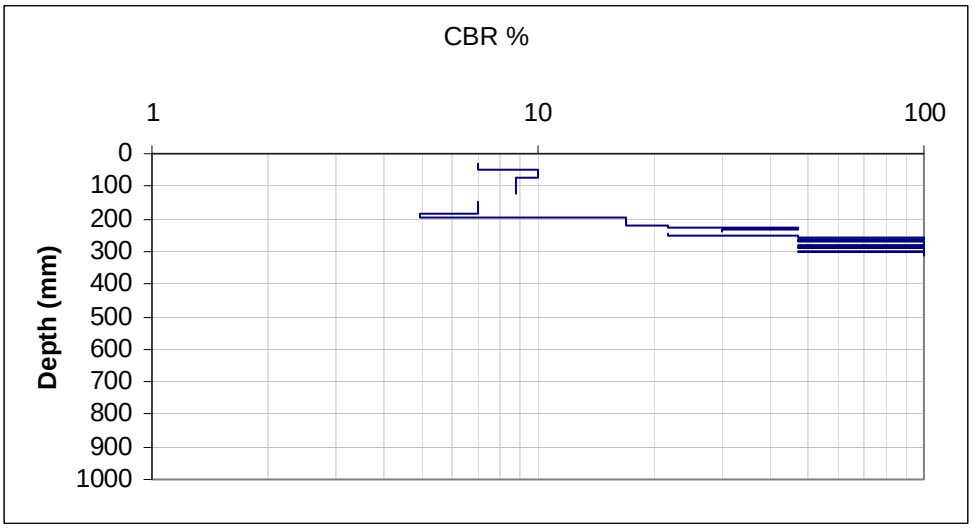
1+70 2S – auto



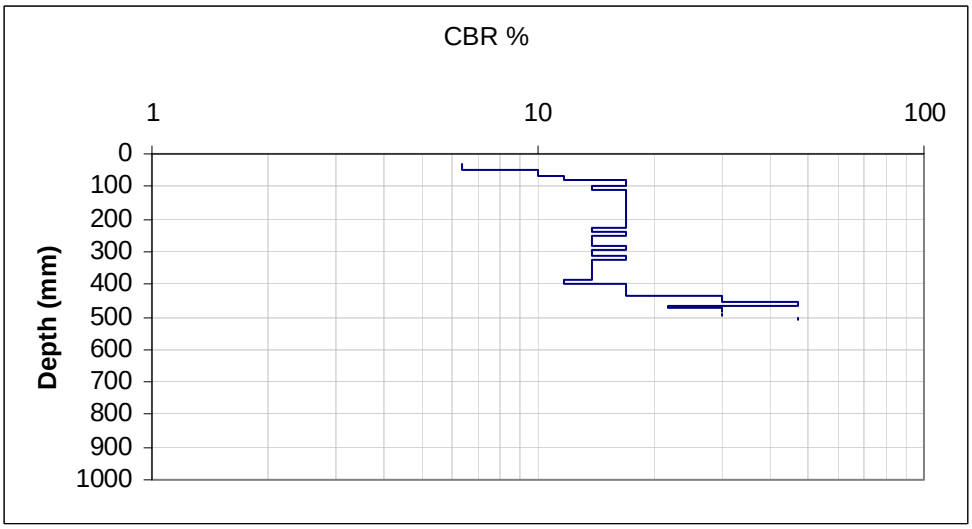
2+10 2N – auto



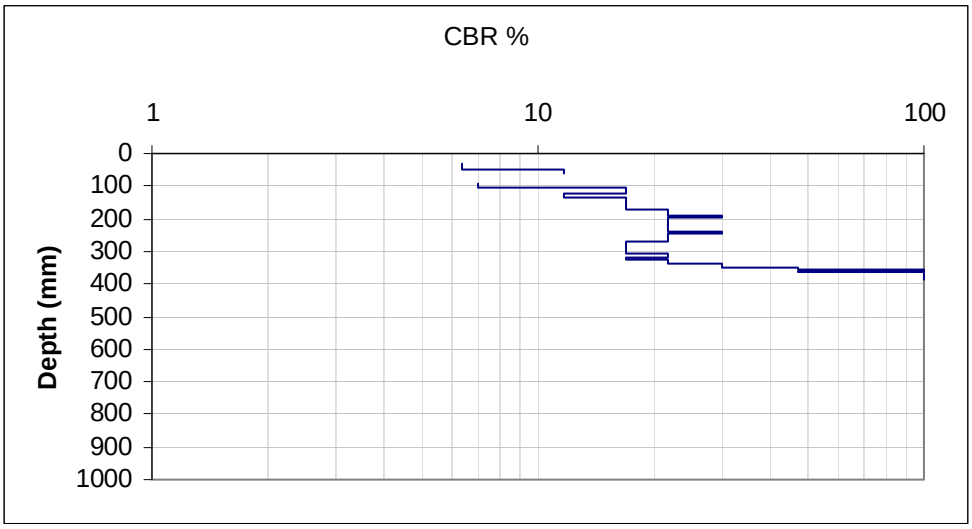
2+10 2S – auto



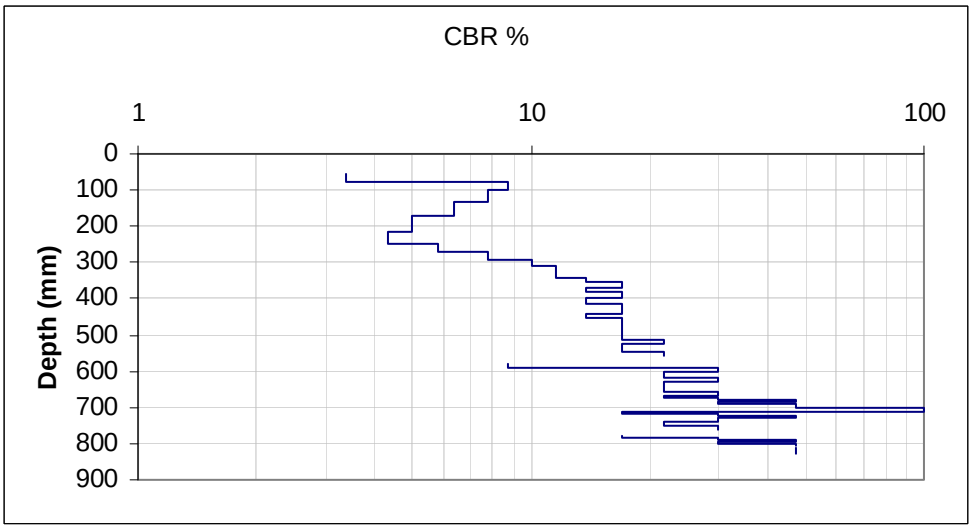
2+50 CL – auto



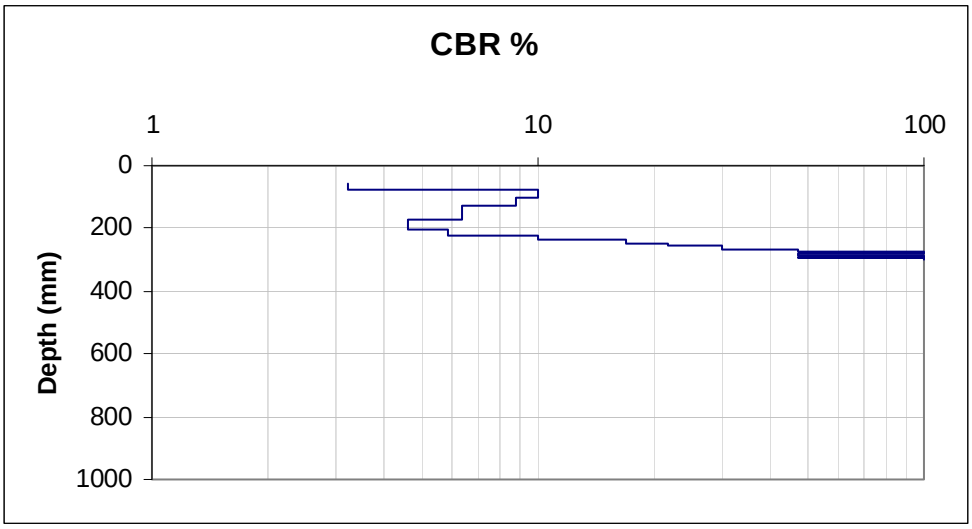
2+50 10S – auto



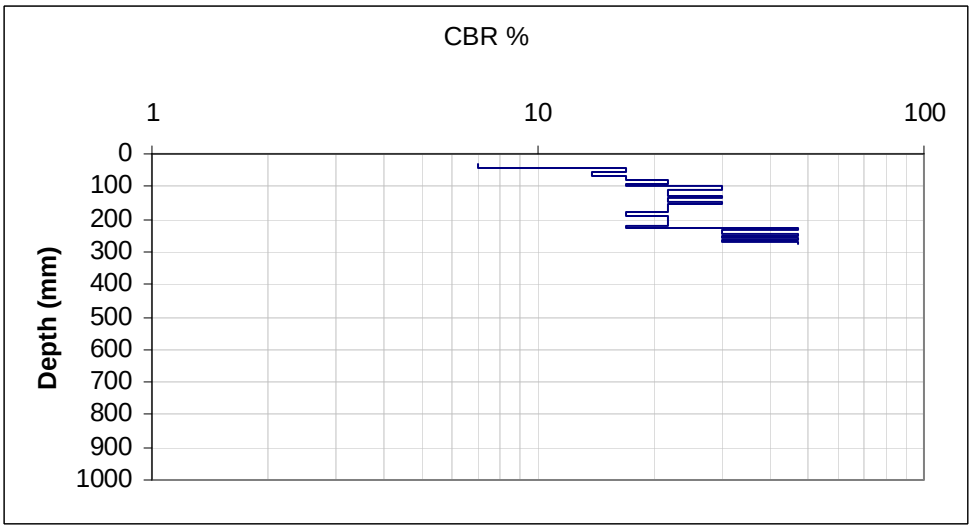
2+50 10N – auto



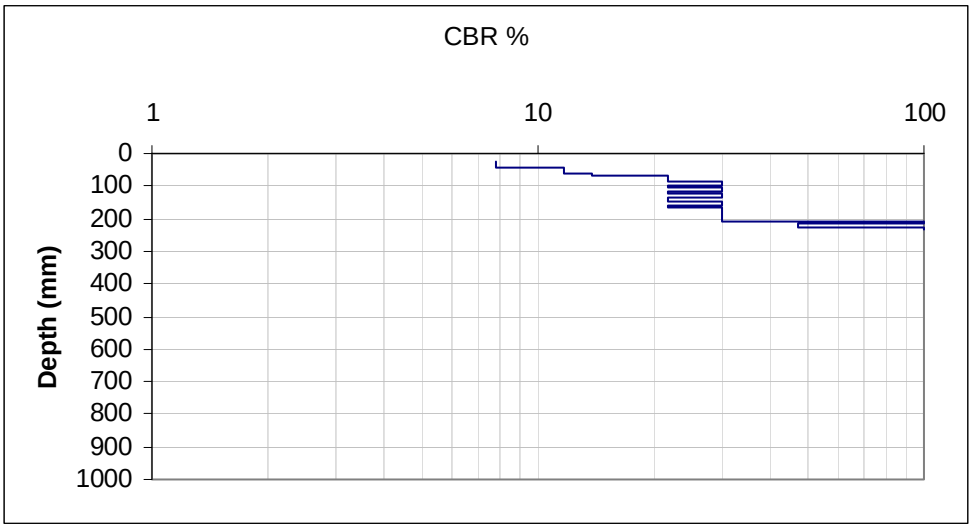
2+80 2N – auto



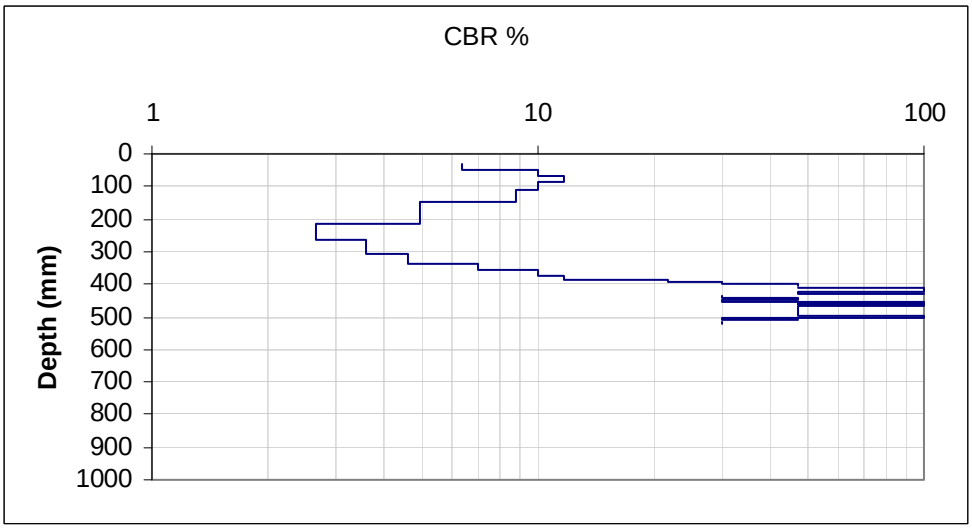
2+80 2S – auto



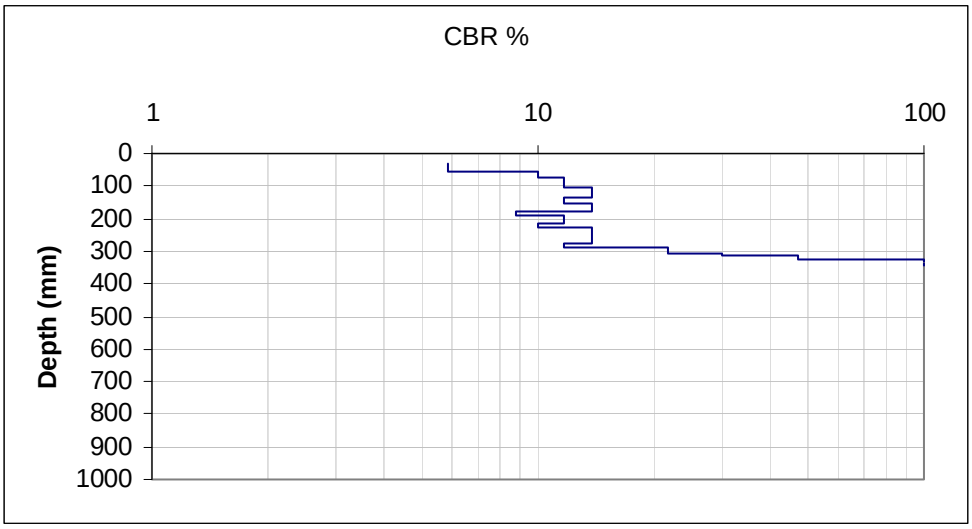
3+30 2S – auto



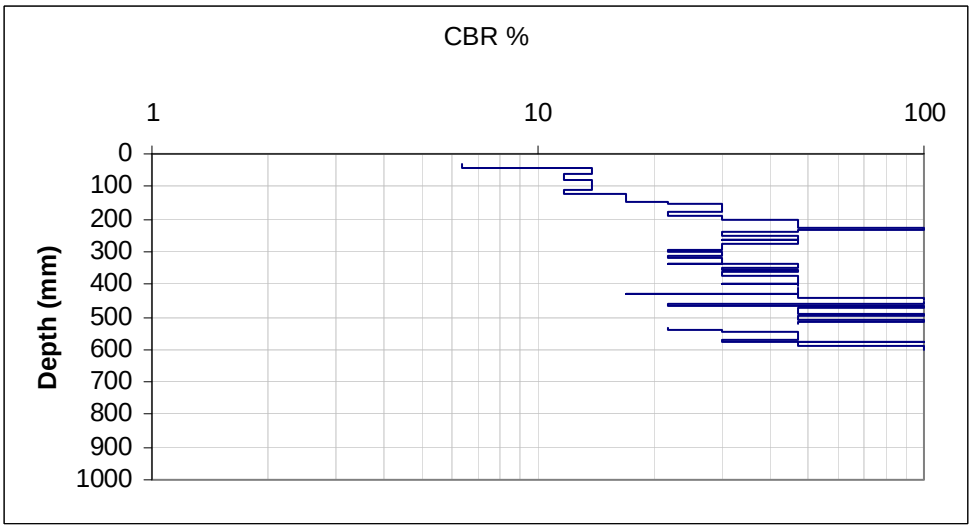
3+30 2N – auto



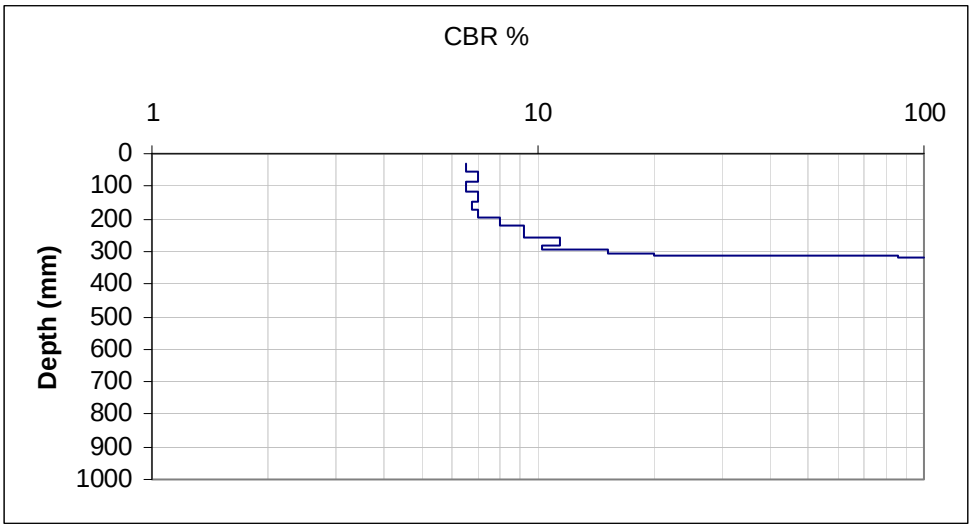
4+00 CL – auto



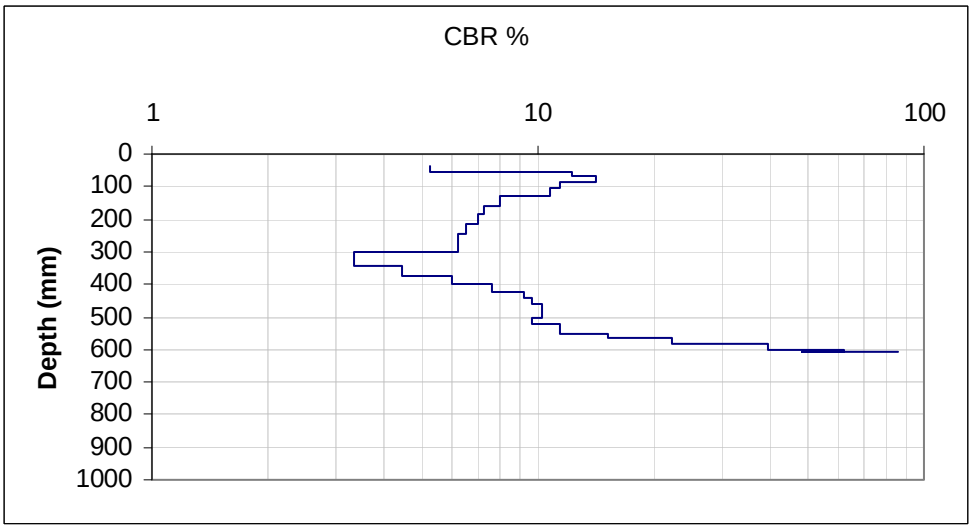
4+00 10S – auto



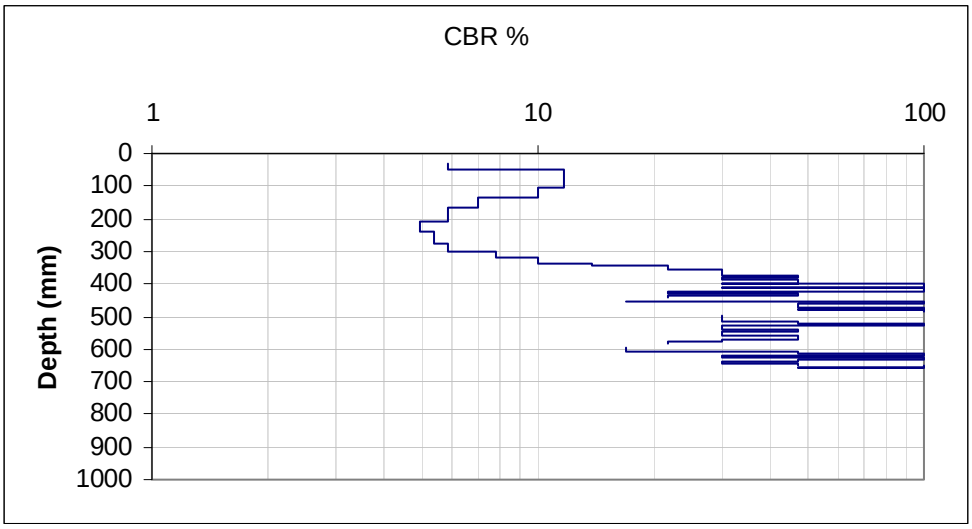
4+00 10N – auto



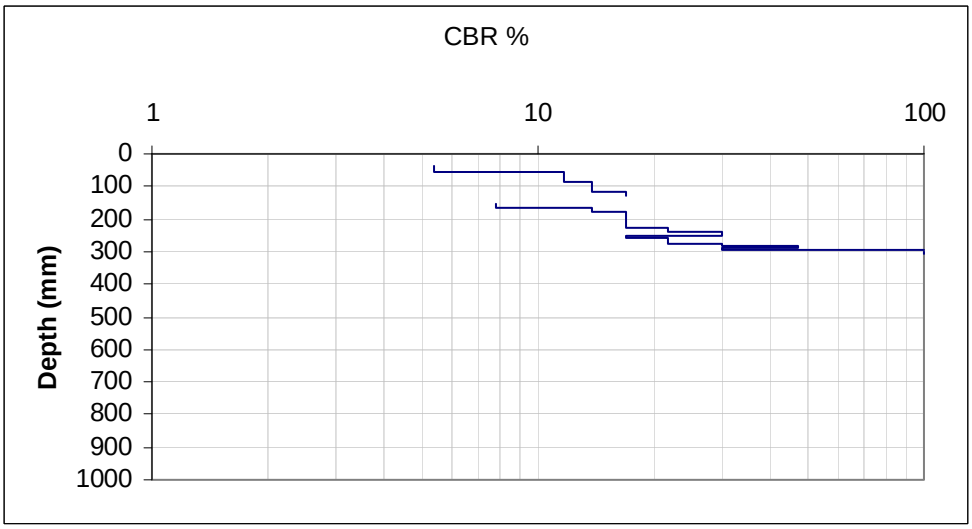
4+00 30N – manual



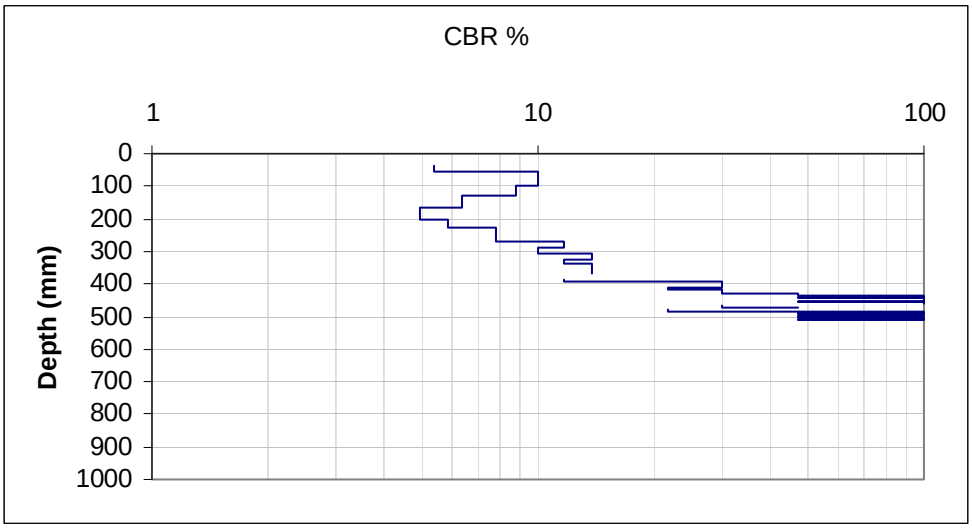
4+00 30S – manual



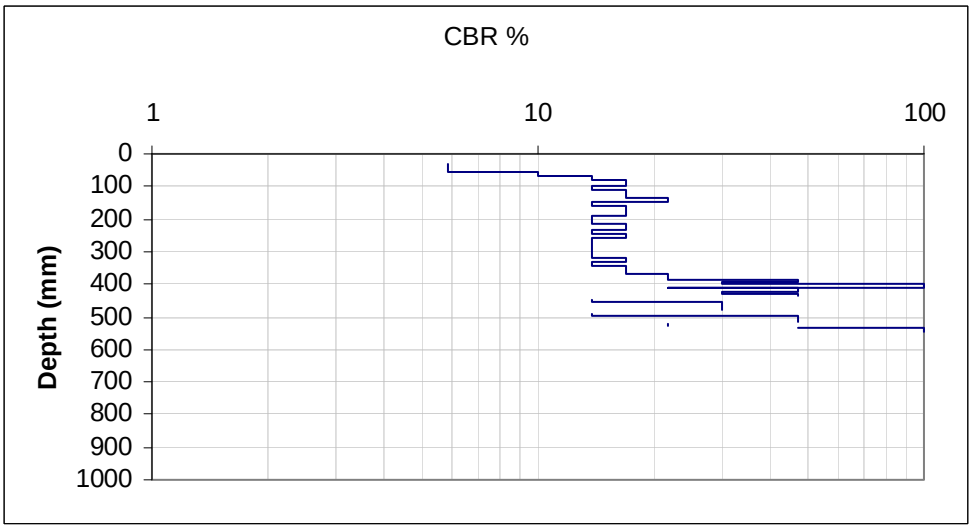
4+70 2N – auto



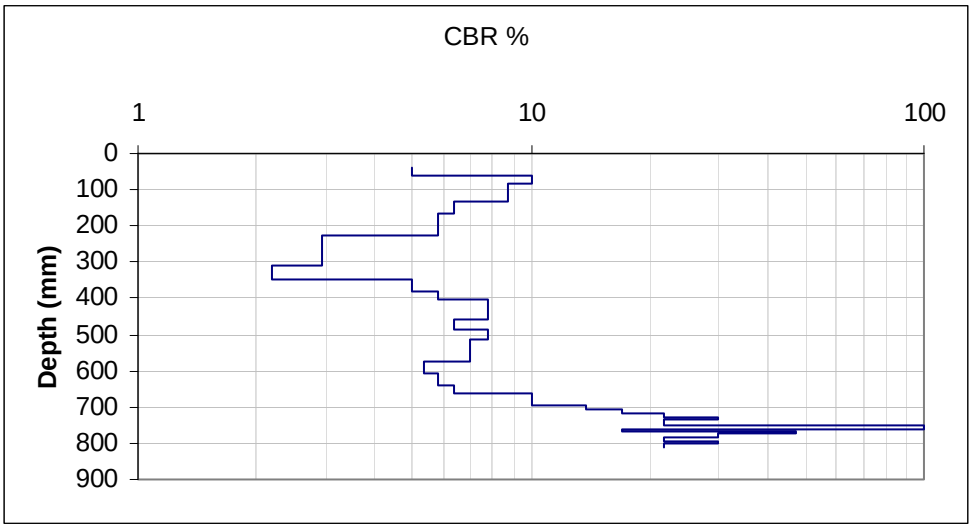
4+70 2S – auto



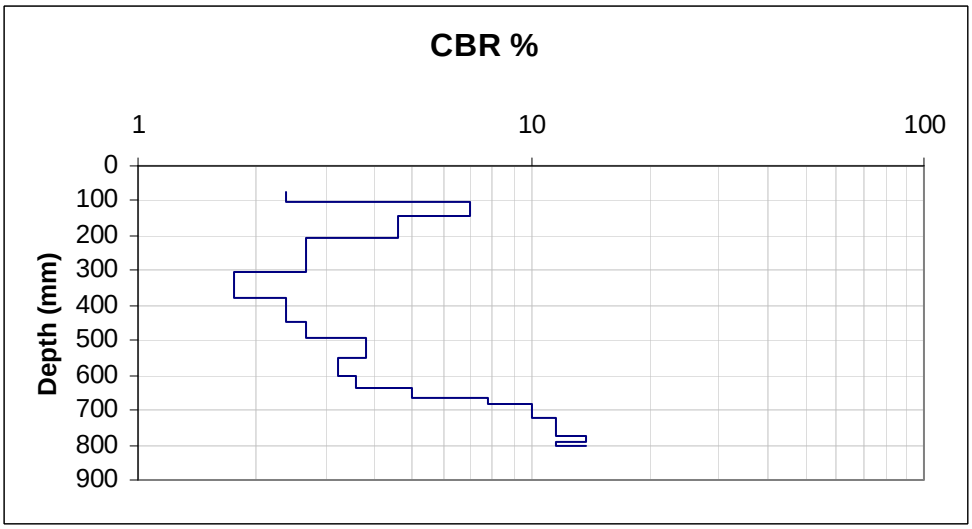
5+20 2N – auto



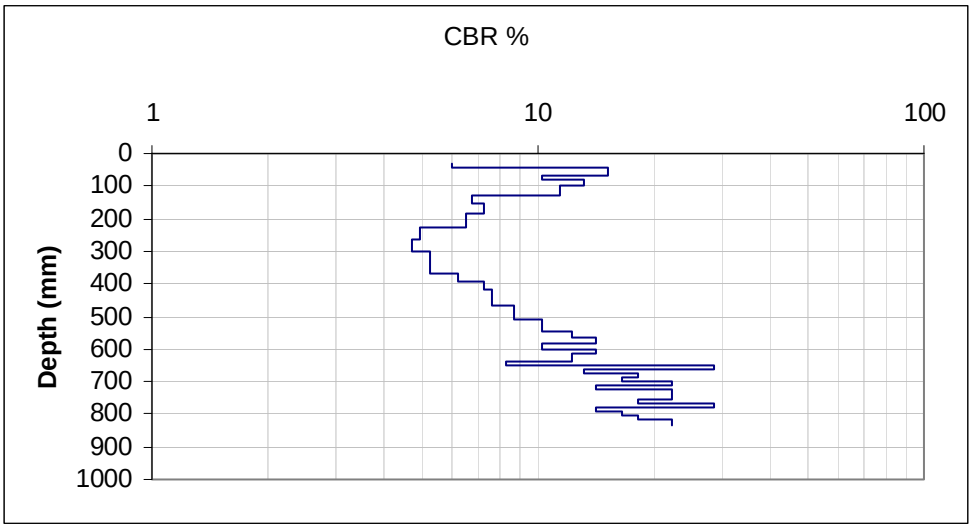
5+20 2S – auto



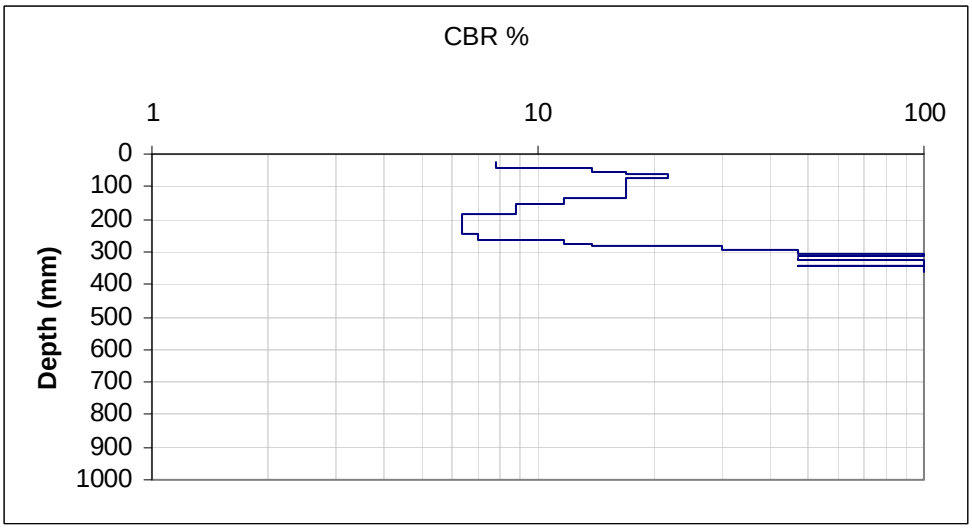
5+50 CL – auto



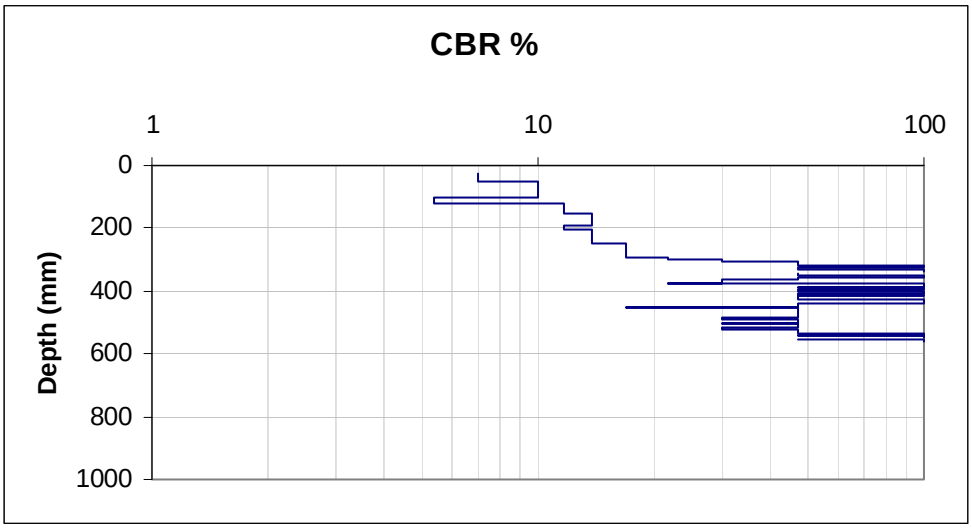
5+50 CL — auto, second reading



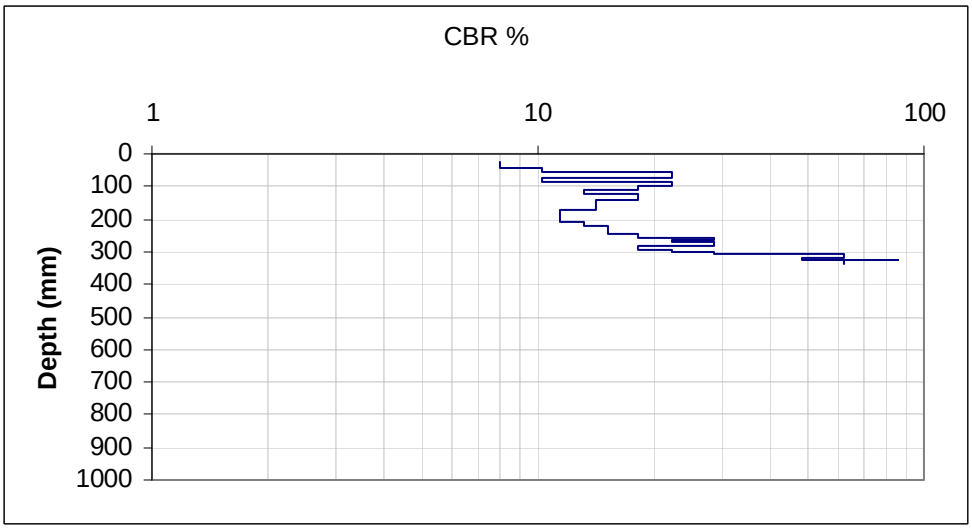
5+50 CL — manual



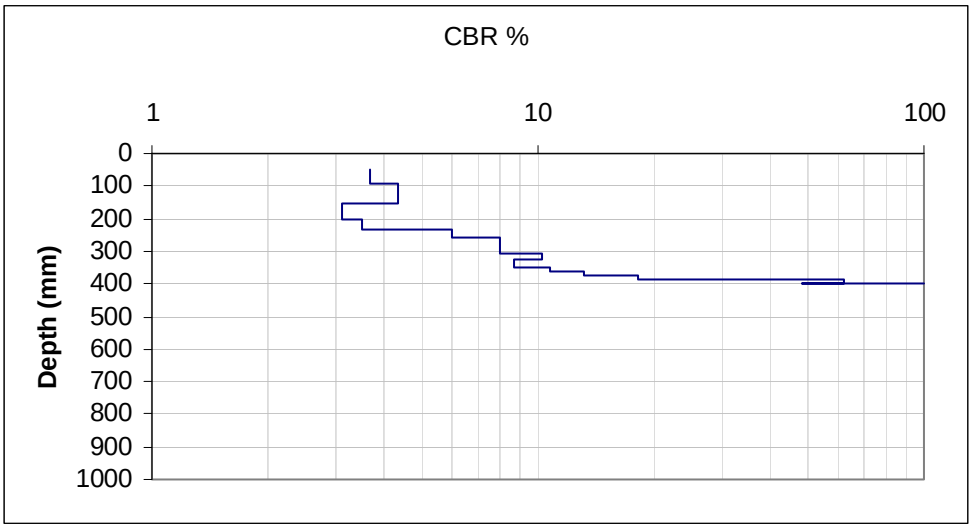
5+50 10N – auto



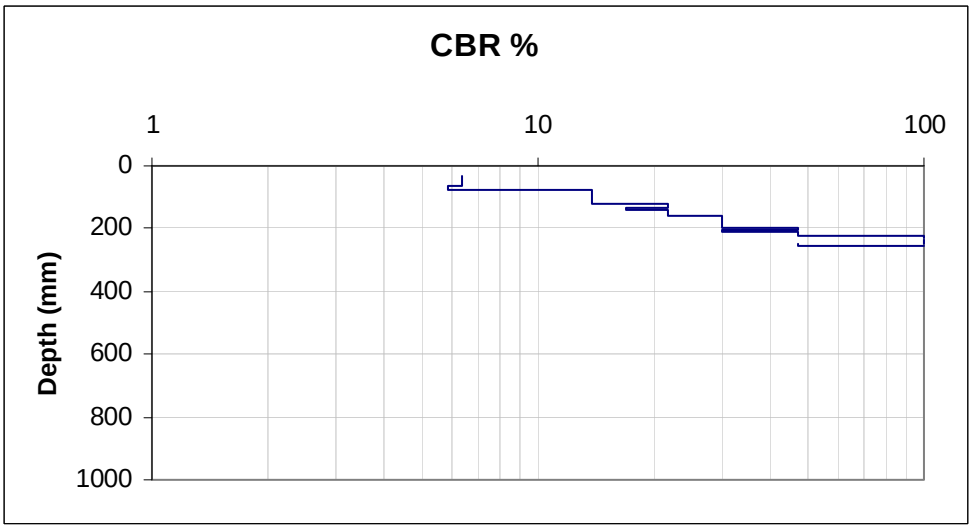
5+50 10S – auto



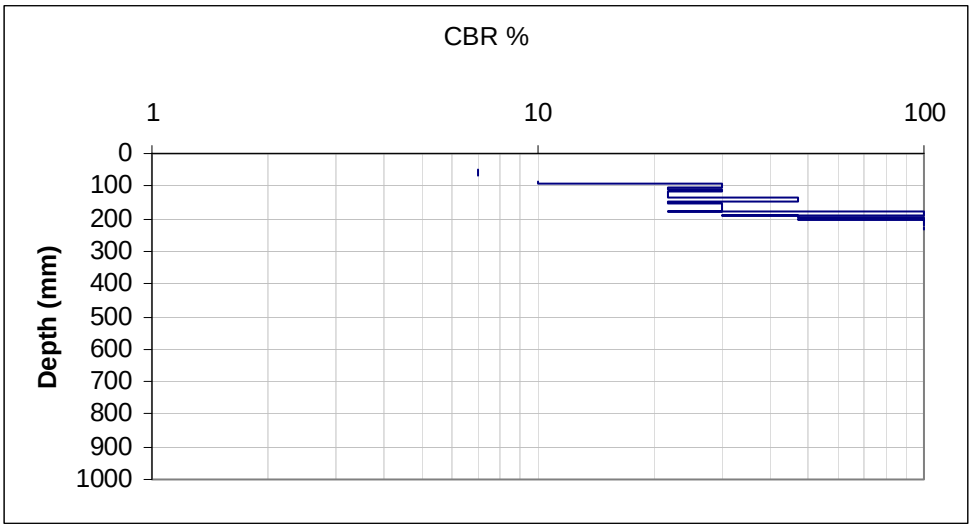
5+50 30N – manual



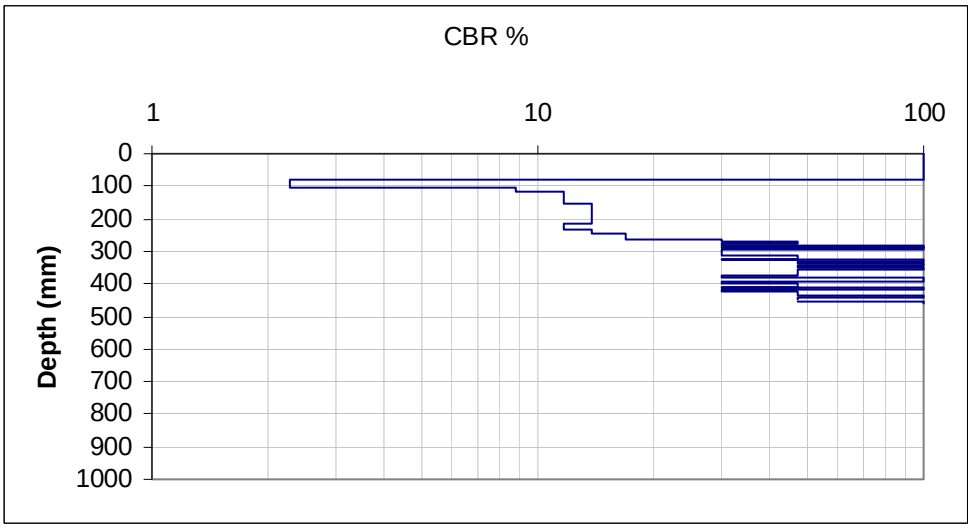
5+50 30S – manual



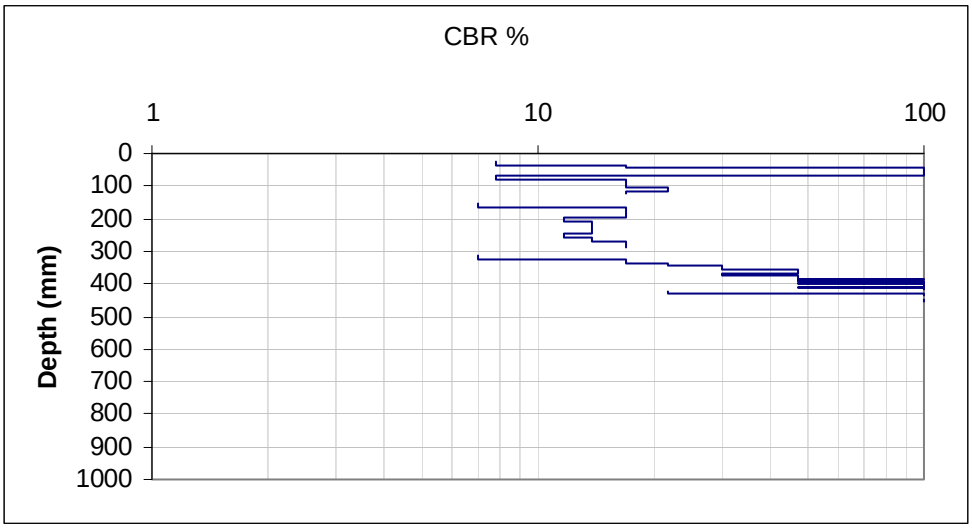
5+80 2S – auto



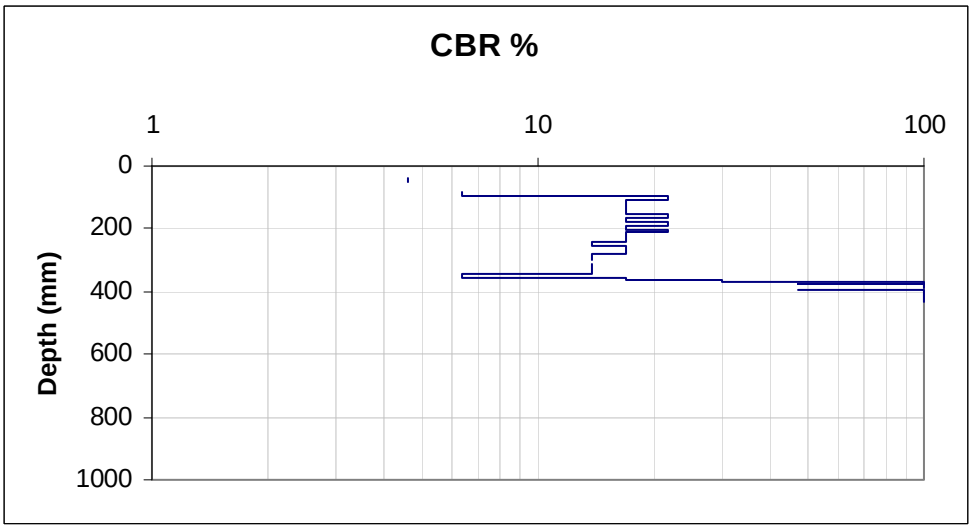
5+80 2N – auto



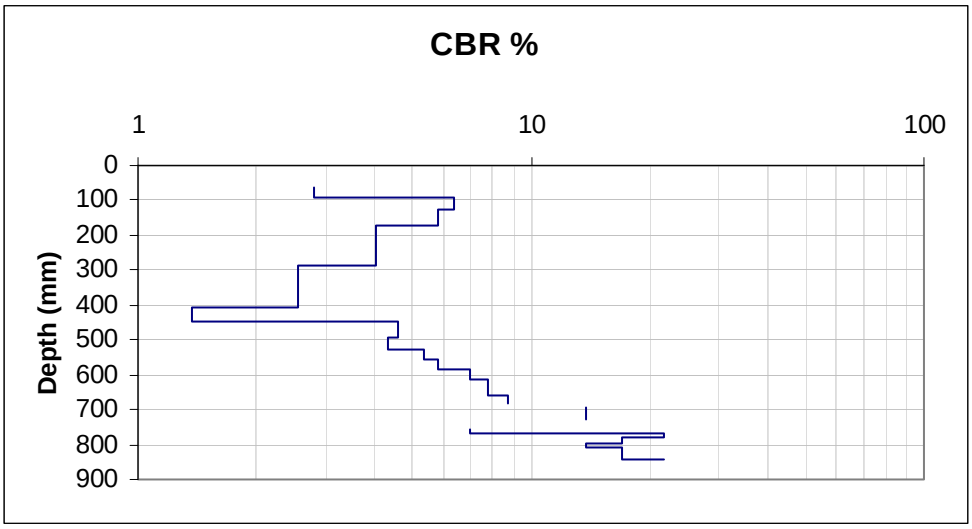
6+30 2N – auto



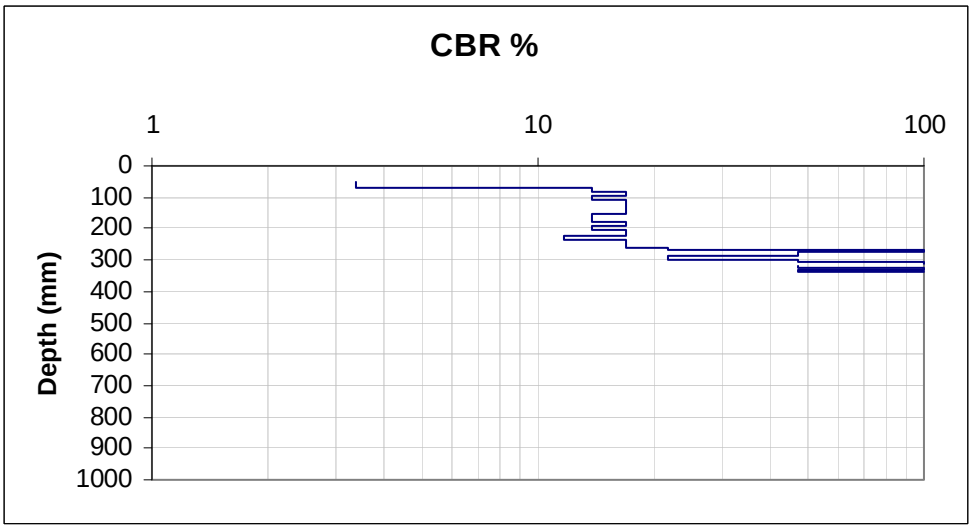
6+30 2S – auto



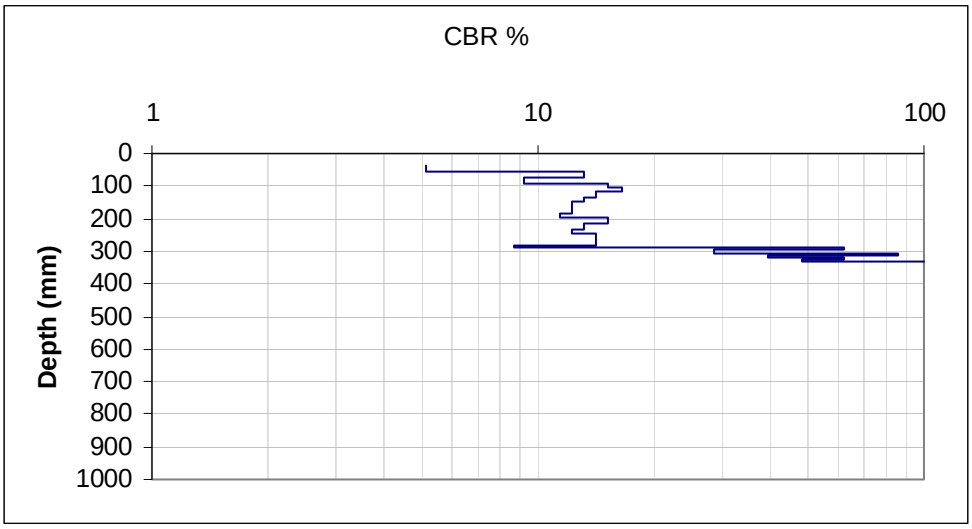
7+00 CL – auto



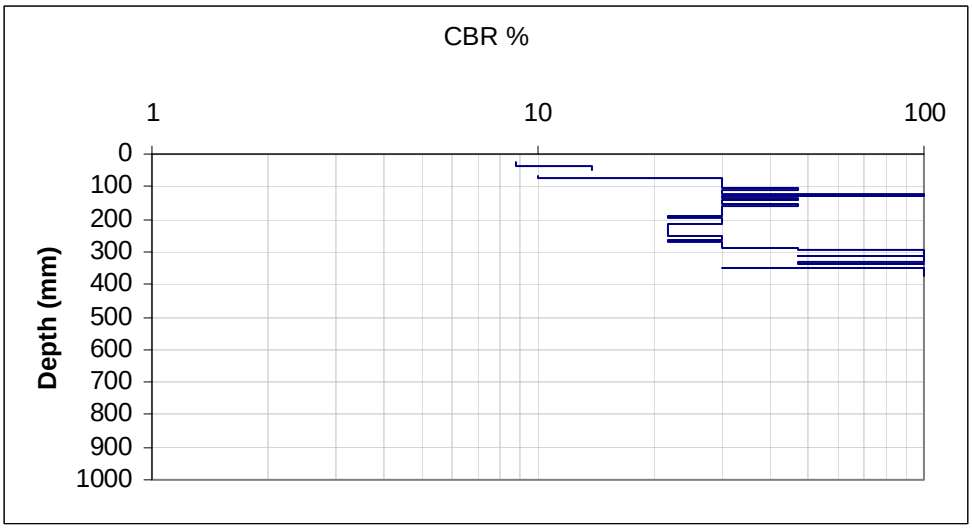
7+00 10N – auto



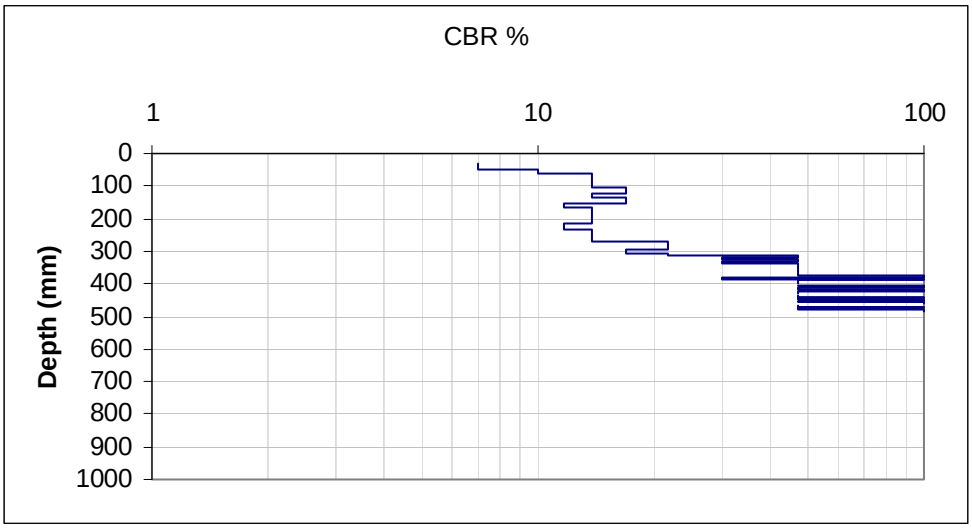
7+00 10S – auto



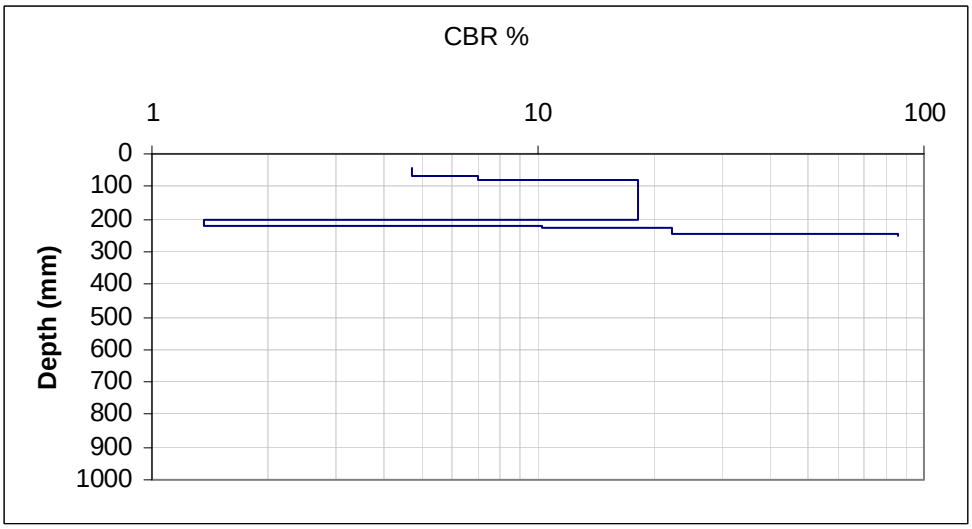
7+00 30S – auto



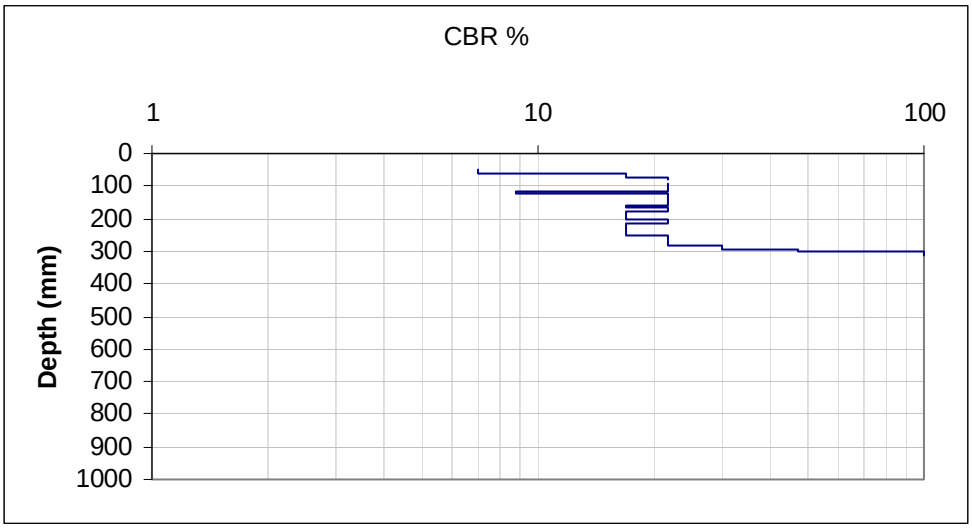
7+70 2S — auto



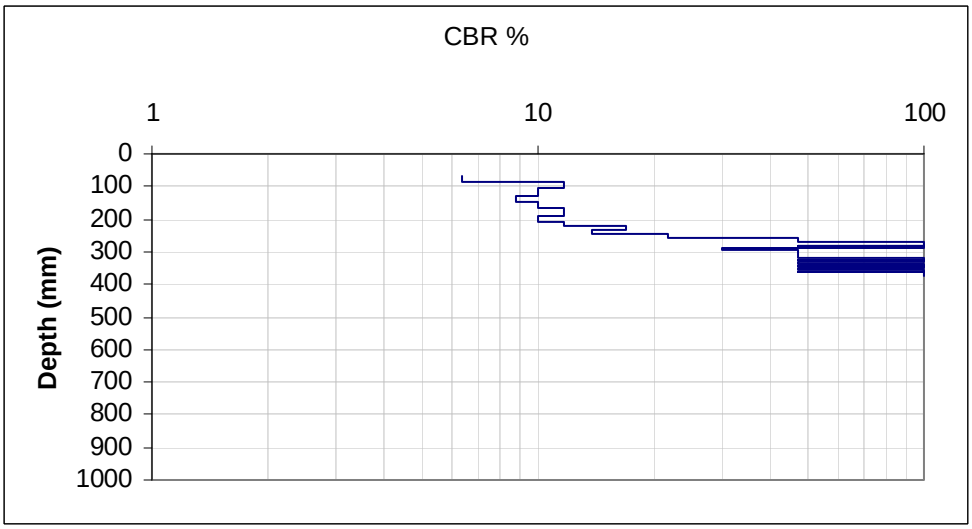
7+70 2N — auto



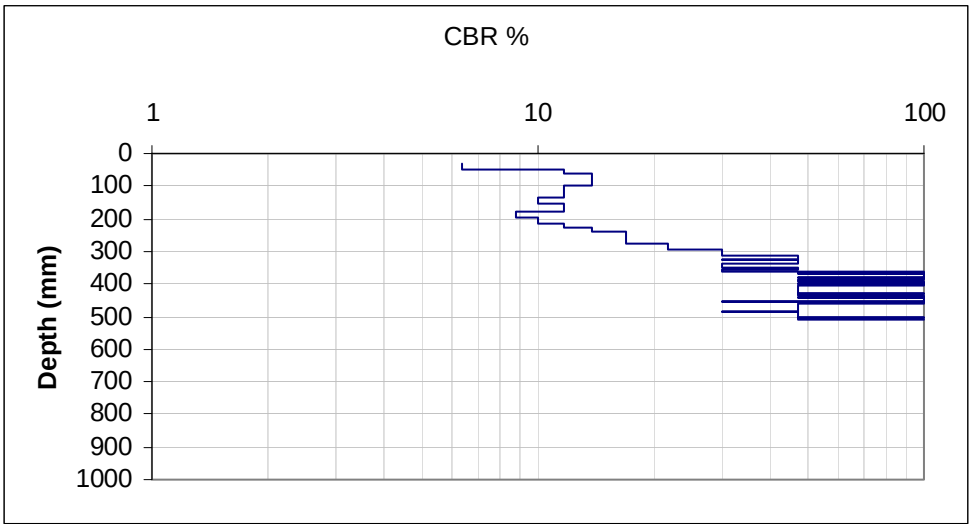
7+70 30N — auto



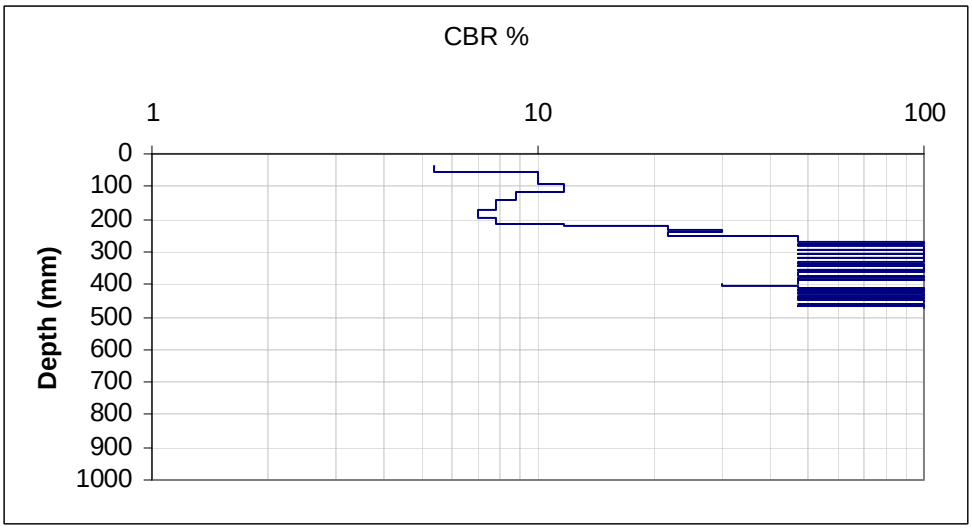
8+20 2N — auto



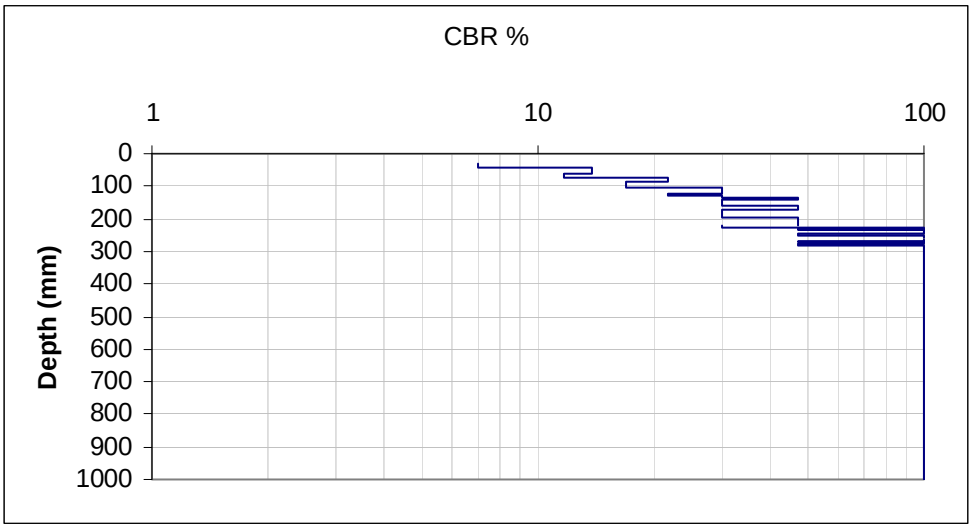
8+20 2S – auto



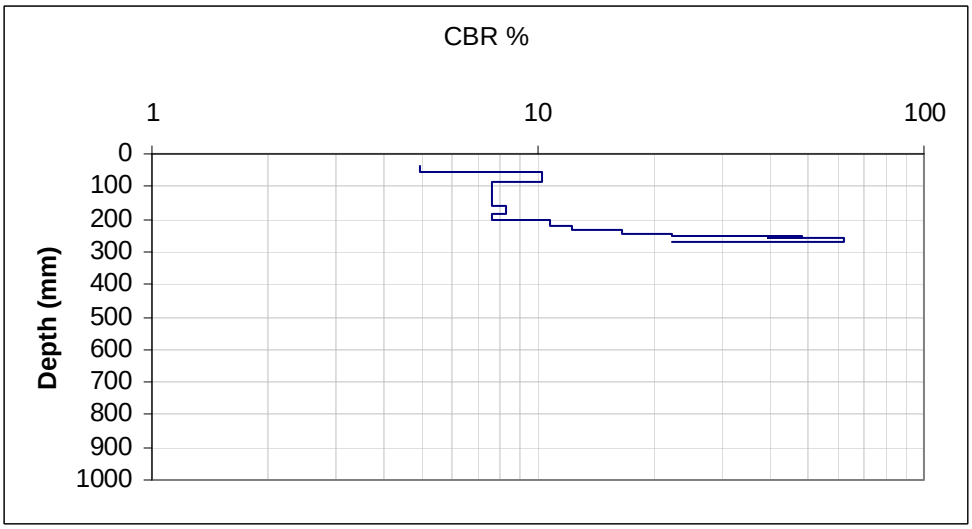
8+50 CL – auto



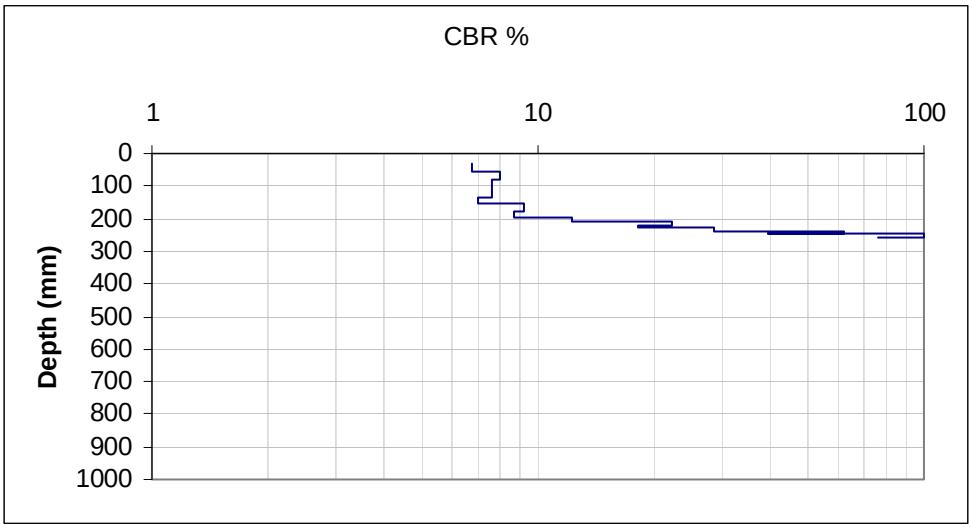
8+50 10S – auto



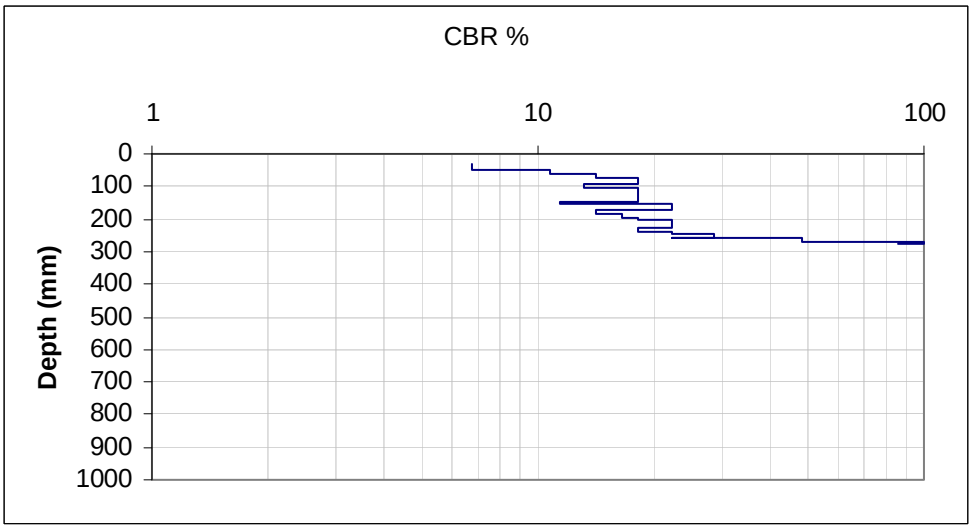
8+50 10N – auto



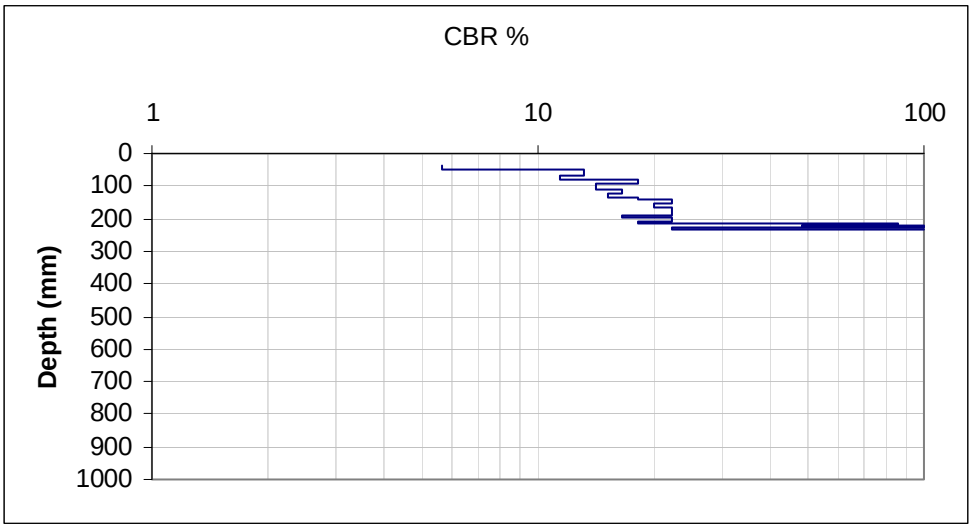
8+90 2N – manual



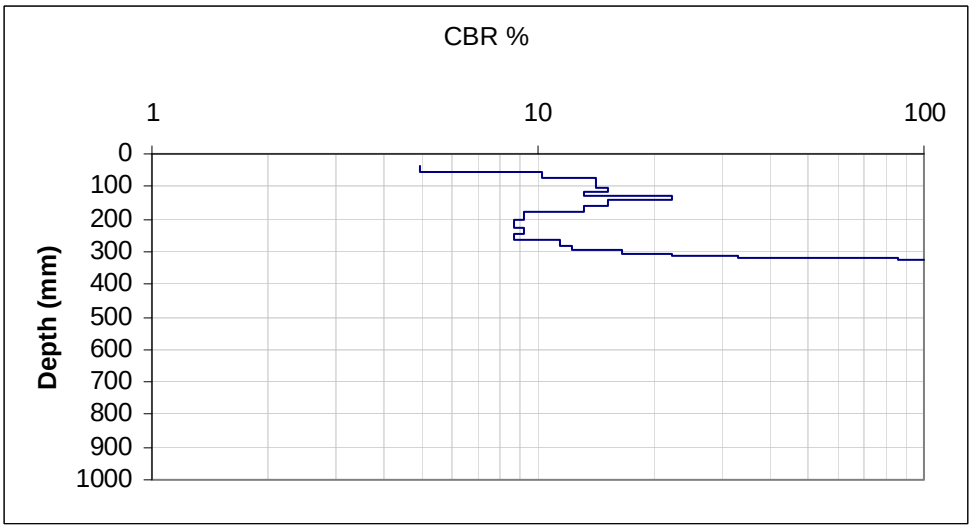
8+90 2S – manual



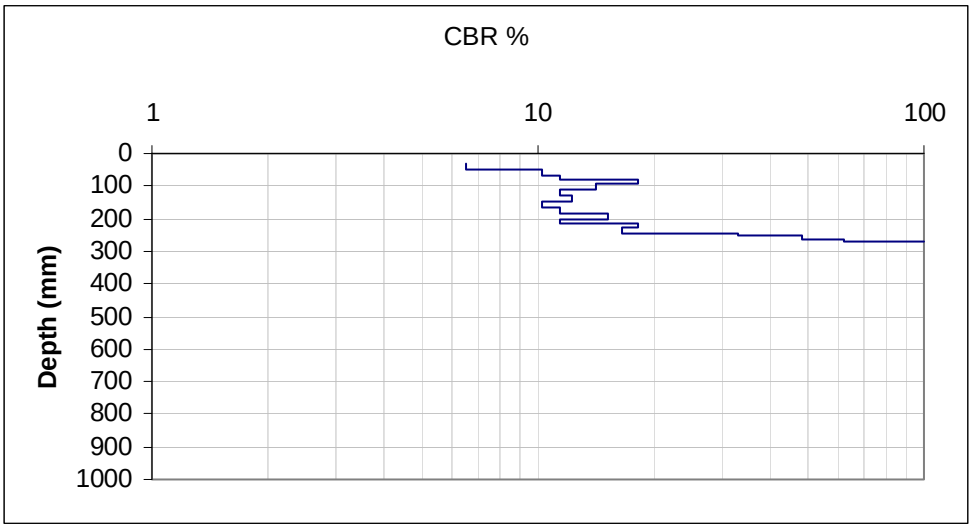
9+30 CL — manual



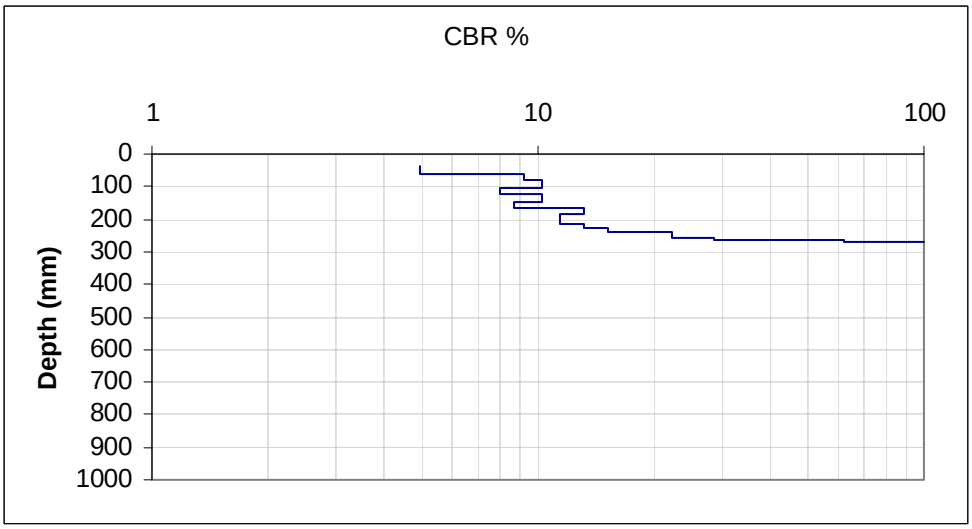
9+30 2N — manual



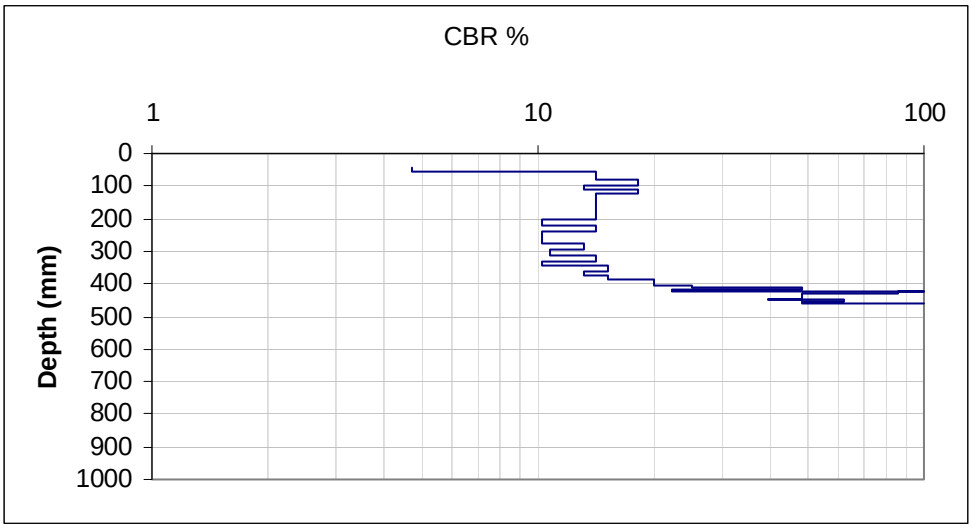
9+30 2S – manual



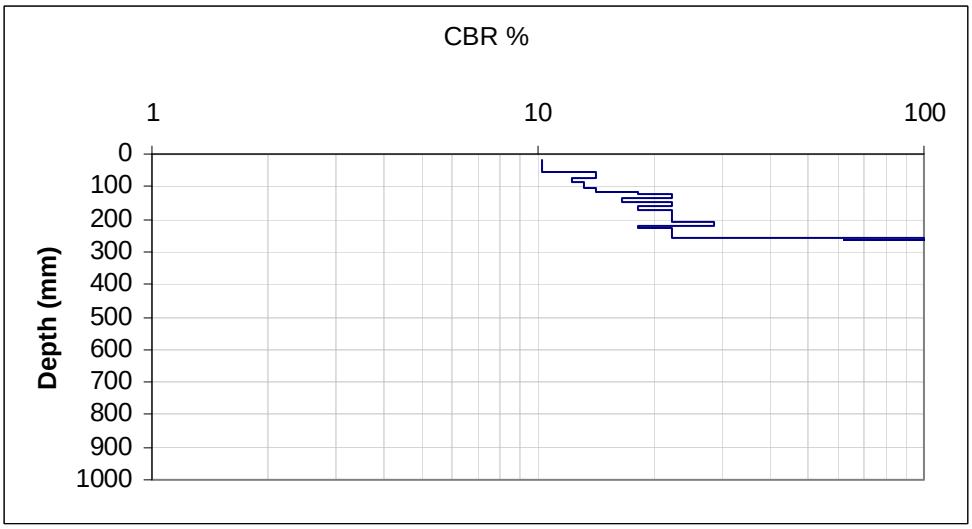
9+70 2N – manual



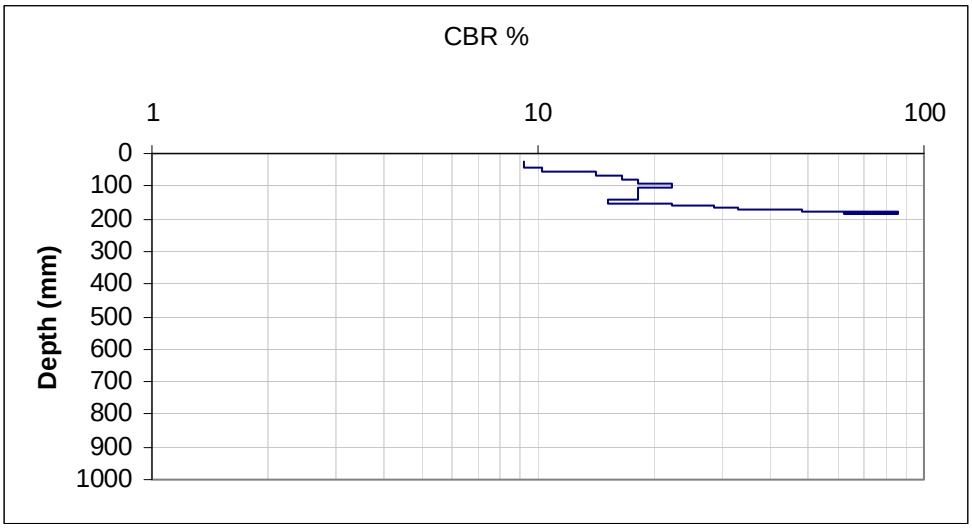
9+70 2S — manual



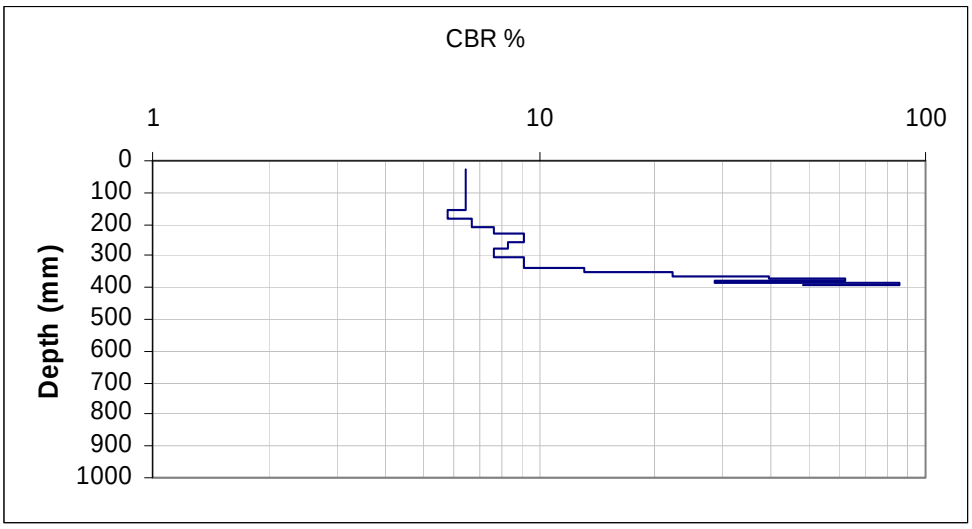
10+10 CL — manual



10+10 30N – manual



10+10 30S – manual



10+70 CL — manual —

REPORT DOCUMENTATION PAGE

Form Approved
OMB No. 0704-0188

Public reporting burden for this collection of information is estimated to average 1 hour per response, including the time for reviewing instructions, searching existing data sources, gathering and maintaining the data needed, and completing and reviewing this collection of information. Send comments regarding this burden estimate or any other aspect of this collection of information, including suggestions for reducing this burden to Department of Defense, Washington Headquarters Services, Directorate for Information Operations and Reports (0704-0188), 1215 Jefferson Davis Highway, Suite 1204, Arlington, VA 22202-4302. Respondents should be aware that notwithstanding any other provision of law, no person shall be subject to any penalty for failing to comply with a collection of information if it does not display a currently valid OMB control number. **PLEASE DO NOT RETURN YOUR FORM TO THE ABOVE ADDRESS.**

1. REPORT DATE *(DD-MM-YYYY)*	2. REPORT TYPE	3. DATES COVERED *(From - To)*
September 2008	Technical Report	

4. TITLE AND SUBTITLE

The Opportune Landing Site Program:
Fort Bliss OLS Suitability Measurement and Analysis

5a. CONTRACT NUMBER

5b. GRANT NUMBER

5c. PROGRAM ELEMENT NUMBER

6. AUTHOR(S)

Rosa T. Affleck, Charles C. Ryerson, Lynette A. Barna, and Keran J. Claffey

5d. PROJECT NUMBER

5e. TASK NUMBER

5f. WORK UNIT NUMBER

7. PERFORMING ORGANIZATION NAME(S) AND ADDRESS(ES)

US Army Engineer Research and Development Center
Cold Regions Research and Engineering Laboratory
72 Lyme Road
Hanover, New Hampshire 03755-1290

8. PERFORMING ORGANIZATION REPORT NUMBER

ERDC/CRREL TR-08-16

9. SPONSORING / MONITORING AGENCY NAME(S) AND ADDRESS(ES)

US Air Force Research Laboratory Air Vehicles Directorate

10. SPONSOR/MONITOR'S ACRONYM(S)

11. SPONSOR/MONITOR'S REPORT NUMBER(S)

12. DISTRIBUTION / AVAILABILITY STATEMENT

Approved for public release; distribution is unlimited.

13. SUPPLEMENTARY NOTES

14. ABSTRACT

The Army's Future Combat System (FCS) relies on agility and speed, including the ability to conduct air transport operations where no runways exist, and where engineers cannot be pre-positioned. One of the most difficult problems is locating large, smooth, flat, and obstruction-free areas that are sufficiently firm to support at least one aircraft operation, and preferably many. The Opportune Landing Site (OLS) program demonstrated the use of remote sensing technology and state-of-the-ground forecast tools to accelerate the process of selecting OLSs. To evaluate the quality of the selected OLSs, ground truth measurements were conducted at Fort Bliss in New Mexico. Before conducting field measurements, several sites identified by OLS software were visually inspected to evaluate and select a suitable OLS for field testing. Evaluation procedures were based on Air Force Civil Engineer Support Agency (AFCESA) recommendations for evaluating airfield pavements. Soil strength and moisture measurements were made at several locations along the OLS, and overall quality was evaluated during three seasons. Assessment software was able to predict an OLS adequate for landing a C-130, but not capable for a C-17. This was true for all three field assessments at Fort Bliss.

15. SUBJECT TERMS

OLS, Opportune Landing Site Program

16. SECURITY CLASSIFICATION OF:			17. LIMITATION OF ABSTRACT	18. NUMBER OF PAGES	19a. NAME OF RESPONSIBLE PERSON
a. REPORT	b. ABSTRACT	c. THIS PAGE			19b. TELEPHONE NUMBER *(include area code)*
U	U	U	U	364	

DEPARTMENT OF THE ARMY
ENGINEER RESEARCH AND DEVELOPMENT CENTER, CORPS OF ENGINEERS
COLD REGIONS RESEARCH AND ENGINEERING LABORATORY, 72 LYME ROAD
HANOVER, NEW HAMPSHIRE 03755-1290

Official Business